

**International
Journal of
Engineering
Technologies
(IJET)**

**Printed ISSN: 2149-0104
e-ISSN: 2149-5262**

**Volume: 3
No: 3
September 2017**

© Istanbul Gelisim University Press, 2017
Certificate Number: 23696
All rights reserved.

International Journal of Engineering Technologies is an international peer-reviewed journal and published quarterly. The opinions, thoughts, postulations or proposals within the articles are but reflections of the authors and do not, in any way, represent those of the Istanbul Gelisim University.

CORRESPONDENCE and COMMUNICATION:

Istanbul Gelisim University Faculty of Engineering and Architecture
Cihangir Mah. Şehit P. Onb. Murat Şengöz Sk. No: 8
34315 Avcilar / Istanbul / TURKEY
Phone: +90 212 4227020 Ext. 221
Fax: +90 212 4227401
e-Mail: ijet@gelisim.edu.tr
Web site: <http://ijet.gelisim.edu.tr>
<http://dergipark.gov.tr/ijet>
Twitter: [@IJETJOURNAL](https://twitter.com/IJETJOURNAL)

Printing and binding:


Anka Matbaa
Certificate Number: 12328
Phone: +90 212 5659033 - 4800571
E-mail: ankamatbaa@gmail.com

International Journal of Engineering Technologies (IJET) is included in:



**Turkish
JournalPark**
ACADEMIC

**International Journal of Engineering Technologies (IJET) is
harvested by the following service:**

Organization	URL	Starting Date	Feature
 The OpenAIRE2020 Project	https://www.openaire.eu	2015	Open Access



INTERNATIONAL JOURNAL OF ENGINEERING TECHNOLOGIES (IJET)
International Peer-Reviewed Journal
Volume 3, No 3, September 2017 Printed ISSN: 2149-0104, e-ISSN: 2149-5262

Owner on Behalf of Istanbul Gelişim University
Rector Prof. Dr. Burhan AYKAC

Editor-in-Chief

Prof. Dr. Mustafa BAYRAM

Associate Editors

Prof. Dr. A. Burak POLAT
Assoc. Prof. Dr. Baris SEVİM
Asst. Prof. Dr. Ahmet AKTAS
Asst. Prof. Dr. Yalcin CEKİC
Asst. Prof. Dr. Ali ETEMADI

Publication Board

Prof. Dr. Mustafa BAYRAM
Prof. Dr. Nuri KURUOĞLU
Prof. Dr. A. Burak POLAT
Asst. Prof. Dr. Ahmet AKTAS
Asst. Prof. Dr. Yalcin CEKİC
Asst. Prof. Dr. Mehmet Akif SENOL

Layout Editor

Asst. Prof. Dr. Ahmet AKTAS

Copyeditor

Res. Asst. Mehmet Ali BARISKAN

Proofreader

Asst. Prof. Dr. Ahmet AKTAS

Contributor

Ahmet Senol ARMAGAN

Cover Design

Mustafa FİDAN
Tarık Kaan YAGAN

Editorial Board

Professor Abdelghani AISSAOUI, University of Bechar, Algeria

Professor Gheorghe-Daniel ANDREESCU, Politehnica University of Timișoara, Romania

Associate Professor Juan Ignacio ARRIBAS, Universidad Valladolid, Spain

Professor Goce ARSOV, SS Cyril and Methodius University, Macedonia

Professor Mustafa BAYRAM, Istanbul Gelisim University, Turkey

Associate Professor K. Nur BEKIROGLU, Yildiz Technical University, Turkey

Professor Maria CARMEZIM, EST Setúbal/Polytechnic Institute of Setúbal, Portugal

Professor Luis COELHO, EST Setúbal/Polytechnic Institute of Setúbal, Portugal

Professor Filote CONSTANTIN, Stefan cel Mare University, Romania

Professor Mamadou Lamina DOUMBIA, University of Québec at Trois-Rivières, Canada

Professor Tsuyoshi HIGUCHI, Nagasaki University, Japan

Professor Dan IONEL, Regal Beloit Corp. and University of Wisconsin Milwaukee, United States

Professor Luis M. San JOSE-REVUELTA, Universidad de Valladolid, Spain

Professor Vladimir KATIC, University of Novi Sad, Serbia

Professor Fujio KUROKAWA, Nagasaki University, Japan

Professor Salman KURTULAN, Istanbul Technical University, Turkey

Professor João MARTINS, University/Institution: FCT/UNL, Portugal

Professor Ahmed MASMOUDI, University of Sfax, Tunisia

Professor Marija MIROSEVIC, University of Dubrovnik, Croatia

Professor Mato MISKOVIC, HEP Group, Croatia

Professor Isamu MORIGUCHI, Nagasaki University, Japan

Professor Adel NASIRI, University of Wisconsin-Milwaukee, United States

Professor Tamara NESTOROVIĆ, Ruhr-Universität Bochum, Germany

Professor Nilesh PATEL, Oakland University, United States

Professor Victor Fernão PIRES, ESTSetúbal/Polytechnic Institute of Setúbal, Portugal

Professor Miguel A. SANZ-BOBI, Comillas Pontifical University /Engineering School, Spain

Professor Dragan ŠEŠLIJA, University of Novi Sad, Serbia

Professor Branko SKORIC, University of Novi Sad, Serbia

Professor Tadashi SUETSUGU, Fukuoka University, Japan

Professor Takaharu TAKESHITA, Nagoya Institute of Technology, Japan

Professor Yoshito TANAKA, Nagasaki Institute of Applied Science, Japan

Professor Stanimir VALTCHEV, Universidade NOVA de Lisboa, (Portugal) + Burgas Free University, (Bulgaria)

Professor Birsen YAZICI, Rensselaer Polytechnic Institute, United States

Professor Mohammad ZAMI, King Fahd University of Petroleum and Minerals, Saudi Arabia

Associate Professor Lale T. ERGENE, Istanbul Technical University, Turkey

Associate Professor Leila PARSA, Rensselaer Polytechnic Institute, United States

Associate Professor Yuichiro SHIBATA, Nagasaki University, Japan

Associate Professor Kiruba SIVASUBRAMANIAM HARAN, University of Illinois, United States

Associate Professor Yilmaz SOZER, University of Akron, United States

Associate Professor Mohammad TAHA, Rafik Hariri University (RHU), Lebanon

Assistant Professor Kyungnam KO, Jeju National University, Republic of Korea

Assistant Professor Hidenori MARUTA, Nagasaki University, Japan

Assistant Professor Hulya OBDAN, Istanbul Yildiz Technical University, Turkey

Assistant Professor Mehmet Akif SENOL, Istanbul Gelisim University, Turkey

Dr. Jorge Guillermo CALDERÓN-GUIZAR, Instituto de Investigaciones Eléctricas, Mexico

Dr. Rafael CASTELLANOS-BUSTAMANTE, Instituto de Investigaciones Eléctricas, Mexico

Dr. Guray GUVEN, Conductive Technologies Inc., United States

Dr. Tuncay KAMAS, Eskişehir Osmangazi University, Turkey

Dr. Nobumasa MATSUI, Faculty of Engineering, Nagasaki Institute of Applied Science, Nagasaki, Japan

Dr. Cristea MIRON, Politehnica University in Bucharest, Romania

Dr. Hiroyuki OSUGA, Mitsubishi Electric Corporation, Japan

Dr. Youcef SOUFI, University of Tébessa, Algeria

Dr. Hector ZELAYA, ABB Corporate Research, Sweden

From the Editor

Dear Colleagues,

On behalf of the editorial board of International Journal of Engineering Technologies (IJET), I would like to share our happiness to publish the eleventh issue of IJET. My special thanks are for members of editorial board, publication board, editorial team, referees, authors and other technical staff.

Please find the eleventh issue of International Journal of Engineering Technologies at <http://ijet.gelisim.edu.tr> or <http://dergipark.gov.tr/ijet>. We invite you to review the Table of Contents by visiting our web site and review articles and items of interest. IJET will continue to publish high level scientific research papers in the field of Engineering Technologies as an international peer-reviewed scientific and academic journal of Istanbul Gelisim University.

Thanks for your continuing interest in our work,

Professor Mustafa BAYRAM
Istanbul Gelisim University
mbayram@gelisim.edu.tr

<http://ijet.gelisim.edu.tr>
<http://dergipark.gov.tr/ijet>

Printed ISSN: 2149-0104

e-ISSN: 2149-5262

International Journal of
Engineering Technologies
IJET

Table of Contents

	<u>Page</u>
<i>From the Editor</i>	<i>vii</i>
<i>Table of Contents</i>	<i>ix</i>
• An Overview of Natural Gas as an Energy Source for Various Purposes / Cenker Aktemur	91-104
• Development of a Face Detection Algorithm Based on Skin Segmentation and Facial Feature Extraction / Jide Popoola, Akintunde Akinola	105-115
• Thermal Stresses on a Reginal Cooling Plate / İbrahim Koç	116-123
• Improving Torsional Rigidity and Seismic Performance of Tunnel Form Building Structures / Can Balkaya, Ihsan Karagoz, Ismihan Gunal	124-134
• Construction Waste Reduction Through BIM-Based Site Management Approach / Burcu Salgın, Atacan Akgün, Nilay Coşgun, Kofi Agyekum	135-142
• Nonlinear Integrated Design of Lattice Domes with Supporting Substructures / Ali Etemadi, Can Balkaya	143-150
• Performance Assessment of Advanced Biological Wastewater Treatment Plants Using Artificial Neural Networks / Harun Türkmenler, Murat Pala	151-156
• Design of Used PET Bottles Crushing Machine for Small Scale Industrial Applications / Aniekan E. Ikpe, Owunna Ikechukwu	157-168
• Performance Evaluation and Modification of an Existing Rice Destoner / Mohammed Gana Yisa, Adeshina Fadeyibi, Kamil Kayode Katibi, O. C. Ucheoma	169-175
• Evaporation Plant for Recycling of Caustic Soda / Emin Taner Elmas	176-185

International Journal of Engineering Technologies, IJET

e-Mail: ijet@gelisim.edu.tr
Web site: <http://ijet.gelisim.edu.tr>
<http://dergipark.gov.tr/ijet>
Twitter: [@IJETJOURNAL](https://twitter.com/IJETJOURNAL)

An Overview of Natural Gas as an Energy Source for Various Purposes

Cenker Aktemur *[‡]

* Department of Mechanical Engineering, Eastern Mediterranean University, G. Magosa, North Cyprus, via Mersin 10, Turkey
(cenkeraktemur_41@hotmail.com)

[‡] Corresponding Author; Cenker Aktemur, Department of Mechanical Engineering, Eastern Mediterranean University, G. Magosa, North Cyprus, via Mersin 10, Turkey, Tel: +90 538 266 0367, cenkeraktemur_41@hotmail.com

Received: 26.03.2017 Accepted: 03.09.2017

Abstract- Energy is gaining great prominence and priority regarding improvement the level of prosperity by completing the economic development of countries. Natural gas is becoming one of the most important energy sources in the world because of the low level of greenhouse gas emissions resulting from the burning of natural gas. For that reason, natural gas consumption is increasing rapidly in the world. Natural gas, which is the main raw material of various chemical products, meets a significant part of the world energy consumption. It is an obvious fact that natural gas is the second most considerable non-renewable fossil fuel-based energy source, after crude oil. This study deals with reviewing natural gas systems considering each aspect. In this context, natural gas as an energy source along with its historical development was briefly given first. Then, status of world natural gas market with regard to geographical distribution of natural gas reserves, consumption, production, lifetime and storage are investigated in all parts of the world. After this exploration of natural gas as primary energy source, pollution caused by natural gas is reviewed since it is utilized in many areas like residential buildings, vehicles and industry. Beside all these, available pipelines delivering natural gas to consumers and planned pipeline projects to be constructed in the near future are reported. Lastly, the use of liquefied natural gas and compressed natural gas as alternative energy source are discussed.

Keywords Natural gas, non-renewable energy, primary energy, fossil fuel.

1. Introduction

Energy is a factor that cannot be ignored in the social and economic development of countries and, therefore, in increasing social welfare, continues to be a considerable issue in all parts of the world. It is extremely noteworthy to obtain energy from continuous, cheap, reliable and clean sources and to utilize it efficiently.

Natural gas is a gas in the fossil-derived gas class which consists of methane gas in large quantities, under the pressure and temperature transformation between the ground layers of the living things of our world living millions of years ago. It is also called H type petroleum gas. Like petroleum, it is found in underground layers in nature. It is made up of methane, less ethane, propane, butane, nitrogen and carbon dioxide gases. Natural gas is a gas mixture of paraffin, carbon, hydrogen in the gaseous state and their percentages depend on the source of the natural gas.

2. Historical development of natural gas

The history of natural gas, which is one of the biggest energy sources of our era, dates back hundreds of years. Statement of the "Sacred Fire" has been used throughout the humanity history. Sanctuaries established before Christianity have retained their importance for centuries in a variety of areas where the gas flames are existed in Azerbaijan. For the first time, natural gas as an energy source was employed for drying salt by Chinese in the reign of Shu Han, after the birth of Chris. In recent history, Chinese have tried to transport natural gas to other places by means of hollowed bamboos.

In Europe, the first natural gas was found in the UK in 1659. There are some documents which shows that natural gas was used for lighting and heating purposes by Northern Italians in this century. Alessandro Volta, who was known especially as a battery finder, declared natural gas as "Flaming Air of Swamps" in 1776. An Italian scientist, Lazzaro Spallanzani, termed as "Natural Gas" in 1795, was

inspired by the gas term created by a Dutch scientist, Jan Baptista Van Helmont, in 1609.

The lighting of the streets and houses benefited largely from natural gas. The first discovery of gas fields was in the vicinity of a salt mine in Charleston city of the U.S. state of West Virginia in 1815. In the following five years, the first commercial gas operations were conducted in state of New York in 1820 by William Hart.

The transportation of natural gas for commercial purposes to a long-distance place was implemented when it is transported to Pittsburgh through pipelines. The total length of pipelines for natural gas distribution reached about 750 km in the same city. On the same date, the total length of other transmission lines within The United States of America borders was just about 40,000 km.

Until Second World War (also known as World War II), natural gas technology was not almost available in the countries outside of the United States. Afterwards, production and consumption of natural gas became widespread with the discovery of prominent sources in Pakistan, the Soviet Union, and North Africa. After the Second World War, there were even more advancements in the production of pipes as well as welding technology, and this led to a significant enhancement in the volume of natural gas transported in the course of time. Canada had an immense amount of natural gas, some of which was exported to America owing to excessive need for natural gas use. In Russia, the gas produced by developing natural gas field was initially shipped to Central Asia, Northern European Russia, and Eastern European countries.

In the mid-1900s, Germany, Italy, France, and Austria were utilizing their existing natural gas potentials. With improvement of the Groningen field in the Netherlands, some potentials here were exported to neighboring countries in 1959. Germany was linked to Groningen gas system in 1964. However, when it comes to rising irretrievable energy demand from internal sources and neighboring countries, natural gas as liquefied was transported by tanker from Algeria, Libya, Brunei, Nigeria, and especially Middle East. In this manner, Japan and the United States of America carried out the transfer of the energy on a vast scale. Natural gas was connected to the system of Western Europe by the Soviet Russia based on the condition that it would start from Germany in 1974 [1].

The first natural gas was detected in Kırklareli / Turkey in 1970. After 6 years, it was utilized at a cement plant in Kırklareli, which was operated under Set Cement Industry and Trade Joint Stock Company. Petroleum Pipeline Corporation (BOTAS in Turkish initials), which will play a very important role in the Turkey natural gas market in the coming years, was established by Turkey Petroleum Corporation (TPAO) in 1974. Natural gas found in the muddy pitch in 1975 was allocated to Mardin Cement Plant in 1982. Electricity generation using natural gas was carried out with domestic sources at Hamitabat Combined Cycle Power Plant in 1985.

When the history of the studies related to natural gas is painstakingly examined in Turkey, it is seen that the first studies pertaining to this topic were the research on "Natural Gas Demand and Supply" carried out by the General Directorate of BOTAS in 1983. This work was carried out with signing of a framework agreement by the Soviet Union with respect to natural gas purchased in 1984. Within 2 years following this agreement, commercial agreement was signed by BOTAS and Sovyet Soyuz Eksport for a 25-year on natural gas imports, which was expected to reach 5 to 6 bcm / year in the 1990s.

This first initiative for the supply of natural gas was made in order to ensure that imports can be carried out effectively. The construction of 842 km long pipeline starts from Malkoclar on Bulgarian border, and then reaches Gemlik-Bursa, Bozuyuk-Eskisehir through Ankara. By the fall of 1988, natural gas was operationalized for the potential use of settlements unit on the route. Along with the construction of this main line, international tenders were launched by the General Directorate of EGO and IGDAS for the construction of natural gas networks among these cities in 1988.

Natural gas was used for the first time in Turkey in residential and commercial sectors in Ankara in October 1988, in Istanbul in January 1992, in Bursa in December 1992, in Izmit in September 1996 and in Eskisehir in October 1996 [2].

3. An outlook of the world natural gas market

Natural gas consumption, which was more local in the 1950s and met only 10% of the world's energy consumption, increased steadily in the following years. The oil crisis that emerged in the 1970s adversely affected the economies and air pollution caused by augmented consumption of coal due to crisis, was one of the most important reasons of this increase. Moreover, the fact that natural gas is cleaner than other fossil fuels has led to an augmentation in its share in international trade.

According to the study done by the International Energy Agency (IEA), it was estimated that world natural gas consumption, which is advanced by an average of 2.1% every year, reached 3.68 tcm in 2015 and would reach 4.78 tcm in 2030. Until 2035, it is anticipated that natural gas will be the only fossil fuel whose proportion will go up in global energy sources. For this reason, natural gas production will boost in all regions except Europe.

In accordance with the New Policy Scenario, world gas demand will reach 4.75 tcm in 2035 and global natural gas consumption is expected to be at the same level with coal consumption in the same year. It was also assumed that 81 % of the increase in natural gas demand would stem from non-OECD (Organization for Economic Co-operation and Development) countries [3].

3.1 World natural gas reserves and geographical distribution

With the commencement of pipeline transport, natural gas has become prevalent in the creation of the increasing energy demand together with evolving technology, and undertaking examinations to reduce reliance on oil as a result of the oil crises experienced throughout the world.

Natural gas reserves have climbed by nearly 56 % in the last two decades. The amount of natural gas reserves, which was 119.9 tcm by the end of 1995, increased in 157.3 tcm in 2005 and 186.9 tcm in 2015. While Europe & Eurasia and Middle Eastern countries accounted for 43.4 % and 30.2 % of the world natural gas reserves in 1990, respectively, the share of Europe & Eurasia reserves diminished by 30.4 % and the Middle East reserves ascended by 42.8 % in 2015 (see Fig. 1). Russian Federation, which ranked first with its proven reserves of 32.3 tcm in 2015, is followed by Iran with 34 tcm and Qatar with 24.5 tcm. The total natural gas reserve of Turkmenistan, which has the largest natural gas reserves and annual production capacity among the Central Asian Republics, is around 17.5 tcm (see Fig. 2).

Today, many producers and consumers are emerging and the share of natural gas in total energy consumption is increasing by slow degrees. As the day goes on, natural gas is expected to meet 21 % of the world's total energy consumption. It is thought to meet approximately 25-30 % in 2030 provided that the technological developments keep going. In addition, it is expected that its share in international trade will develop significantly as it is cleaner than other fuels. When the developments in the international energy market since 1980 are examined, the following three basic factors come to light [4].

- Instead of the traditional oil and gas companies, all of the companies, including the major oil companies, have become an energy company,
- From 2005 onwards, there has been a thought in the world energy consumption that natural gas will get more share rather than oil,
- Instead of purchase and sale in the classic sense of natural gas trade to ensure the safety of the source, the sale is carried out through the sale of the reserve in the production field.

3.1.1 World natural gas reserve lifetime

The natural gas production went down due to the economic crisis experienced in 2009. For that reason, natural gas reserve life increased and the reserve life of 2009 become 62.7 year. Reserves-to-production (R/P) ratios are calculated with the total current reserve (186.9 tcm) divided by the total current production (3.538 tcm); thus, the global reserve life was estimated to be 52.8 years. It is predicted that the US, which has the highest share in world natural gas production, has a reserve life of less than 20 years. However, it is estimated that non-traditional sources of natural gas, which have been produced since the last 10 years in the US, will

extend the reserve life up to 200 years. In the context of the 52.8-year "natural gas reserve life", which is defined in general terms, is the life of the reserves that have been proven to be today's economical production of existing conventional technologies. Approximately half of the reserves of the European Union are made up of the reserves of the Netherlands. It was foreseen that 4.5 years of reserves would remain if the UK continues with its current production [6,7].

3.1.2 World natural gas production

World natural gas production, which was 3463.2 bcm in 2014, increased by 2.2% (3538.6 bcm) in 2015. While natural gas production dropped by 1.5 % in Russian Federation, it rose by 5.4 % in the US, 16.4 % in Myanmar and 5.7 % in Iran. The United States proceeded to be the world's largest natural gas producer with 763.7 bcm. The regions that have the highest increment in natural gas production in 2015 are the Middle East (45.2 %), Asia Pacific (22.6 %) and North America (21.3) [5]. Top 10 countries having the highest total of share in these regions are shown in Fig. 3.

3.1.3 World natural gas consumption

From 1965 to 2015, the use of fossil fuels sustained to grow remarkably and share of energy supply enhanced. Since then, natural gas has been adopted by regions and found itself an important place among fossil fuels even though the consumption quantities have decreased from time to time. The constant increase in natural gas consumption between 2005 and 2008 was followed by a steady increase in the following years after a decline in 2009. Provided that the economic crisis which took place in 2009 is ignored, world natural gas consumption increased by 4.7 % (3051.2 to 3201.4 bcm) when compared to 2008 and 2010 natural gas consumption.

Asia Pacific (20.1 %), North America (28.1 %) and Europe & Eurasia (28.8 %) are regions which witnessed the highest increase in consumption in 2015. From the beginning of 2009 until 2015, natural gas consumption in the US, which is the world's largest natural gas consumer, increased by 20 % (129.3 bcm) whereas natural gas consumption in Russian Federation, which is the world's second largest natural gas consumer, rose nearly by 0.5 % (1.9 bcm). Although consumption in the Europe & Eurasia region, which also includes Turkey, increased by 10 % (3.3 bcm) in 2010 compared to 2009, this consumption amount in 2015 was observed to be lower than consumption amount in 2014. From the beginning of 1965 onwards, natural gas consumption amounts by years are illustrated in Fig. 4.

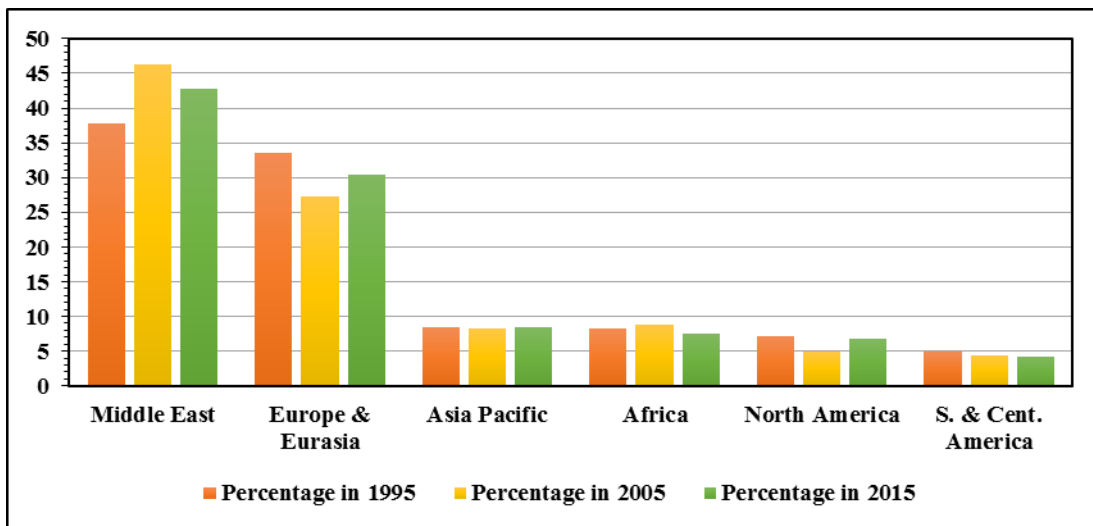


Fig. 1. Distribution of proved natural gas reserves by regions [5].

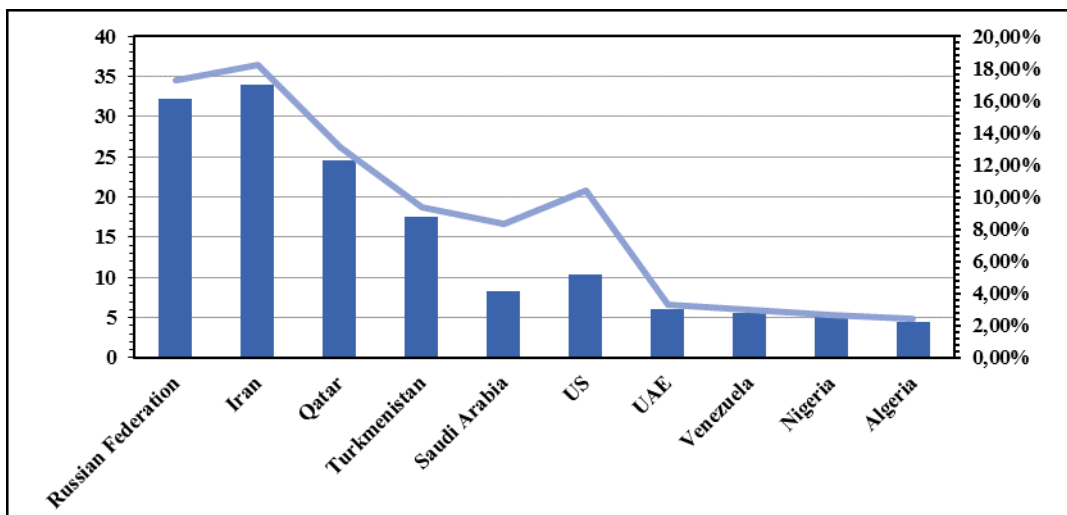


Fig. 2. World proven gas reserves and share of total by 10 countries (tcm) [5].

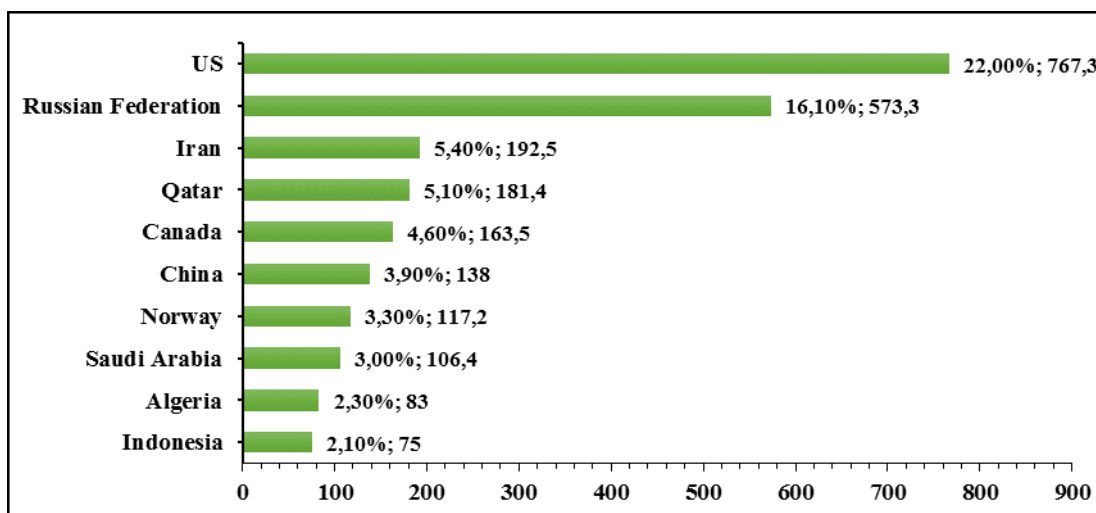


Fig. 3. World natural gas production by ten countries (bcm) [5].

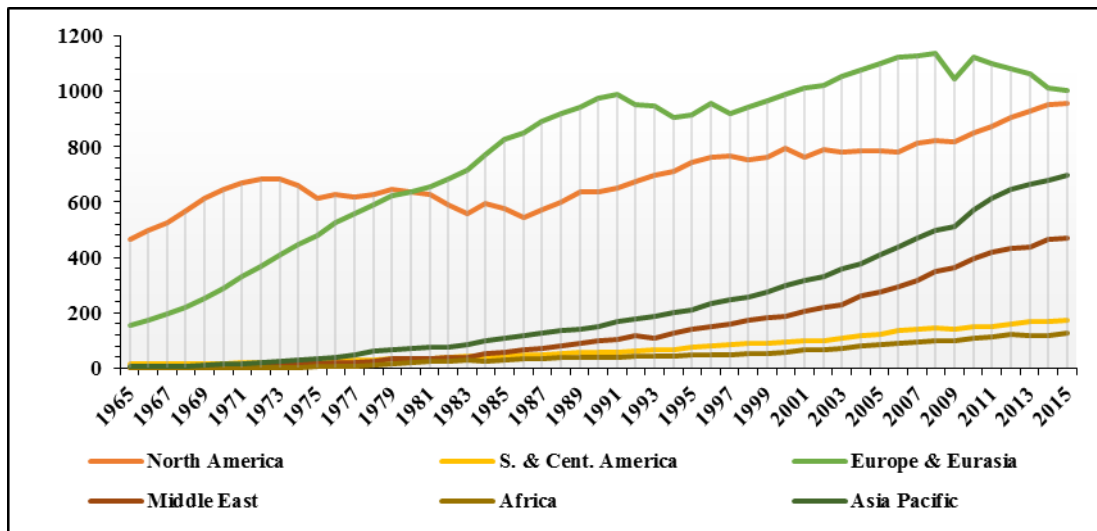


Figure 4. World natural gas consumption by years (bcm) [5].

As depicted in Fig. 4 above, it can be inferred that developed countries consume more natural gas. Developed countries in North America, Europe and Asia regions make up about 80% of the world consumption. The fact that natural gas is a clean fuel, portable and easy to use can be shown as evidence among the reasons for the increase in consumption in these regions.

According to the New Policy Scenario involving IEA's determination in 2011, it is estimated that China's demand for natural gas consumption will rise from 197.3 bcm in 2015 to 500 bcm in 2035. In the light of IEA's determination in 2011, it is pointed out that the world's largest natural gas producer will be Russia's rising natural gas producer with 860 bcm per year and North American natural gas supply-demand will be in balance in 2035 [8].

According to the data in Figure 1, 2, 3 and 4;

- As of 2015, Russian Federation and Iran, which have the largest reserves of natural gas, have roughly 1/3 of the world natural gas reserves.
- The sum of reserves of the Middle East and Europe&Eurasia regions make up almost 75 % of the world natural gas reserves.
- Iran and Qatar in the Middle East, and Russia in Europe&Eurasia are the countries that have the largest reserves of natural gas.
- The total amount of reserves that Iran and Qatar have account for nearly 31 % of total Middle East (42.8 %).
- Around 43 % of the world natural gas production is supplied by Russian Federation, Iran and US.
- While North America region, which has an important share in world natural gas production, is the fifth considering the reserve amount.

3.1.4 Natural gas storage

In the world, underground gas storage was carried out for the first time in a depleted gas reservoir in Canada in 1915, followed by experiments made in New York in 1916 and in Kentucky in 1919. Storage technology between variable demand and fixed supply in natural gas sector, from 1917 to present day, continued to thrive incessantly.

While the total volume of underground natural gas storage working gas capacity was 328 bcm in the world in 2000, it was recorded as 270.6 bcm by the end of 2014. North America has 70 % of world storage facilities with 452 storage facilities, including 402 in the US and 50 in Canada. With the liberalization of natural gas markets and the short-term trade of natural gas, it is hoped that the demand for natural gas storage will increase [9].

Iran, which is one of the largest natural gas producers in the world, operated the first underground natural gas storage facility in the Middle East with the completion of the project carried out by the Iranian Natural Gas Storage Company (NGSC) in May 2011 so that natural gas exports could continue uninterrupted during the winter months. The first step was to expand its capacity from 7.3-9 to 30 million cubic meter.

Immediately after the establishment of the "Underground Storage Coordinatorship" unit within BOTAS in 1988, underground natural gas storage and the reserves of Turkey investigated in order to enable gas storage from the Russian Federation in Turkey. At the end of these examinations salt masses situated in the South of Salt Lake and Northern Marmara gas field were found suitable for use as a warehouse. Silivri natural gas storage facility, which is the only warehouse currently in operation in Turkey, was operated by TPAO and has a total capacity of 2.6 bcm. After completion of additional capacity-building facilities, an excess of 4 bcm of natural gas will be stored in Silivri. It is anticipated that Salt Lake natural gas storage where the

investments are made by Chinese Tianchen Engineering Company will be put into service in 2019 [10].

4. Effects of natural gas on air pollution

In all cities of the world, fossil-based energy sources are being used extensively, either directly or by converting to electricity, in the face of the majority of energy needs. The production and use of fossil-derived energy brings many negative effects on human and environmental health. Air pollution caused by burning varies depending on the amount of fuel burned, the fuel pollution and combustion characteristics, combustion systems and operating conditions, pollutant emissions to atmosphere, and topographic and meteorological conditions.

The most common air pollutants around the city are sulfur dioxide (SO₂), nitrogen oxides (NO or NO₂, often called NO_x), carbon monoxide (CO), ozone (O₃), particulate matter (PM) and lead (Pb). CO₂ emissions are the inevitable product of combustion technology based on the use of fossil fuels, and the amount of CO₂ in the atmosphere increased just about 1.3 times in the last century. In the next 50 years, this amount is likely to increase by 1.4 times. The greenhouse effect caused by CO₂ in the atmosphere enhanced the world average temperature by 0.7 °C over the last century. Particularly in developing regions, pollution has been increasing along with the increase of urbanization and energy consumption.

In turkey the need for heating is supplied by coal, petroleum-based fuels, natural gas, and geothermal sources. While the most consumed energy source is coal, natural gas agreements and investments has been made in recent years and natural gas have begun to be used to meet the significant heating needs. Also, natural gas has been exploited in order to overcome the air pollution arising from intensive urbanization.

Natural gas is a fuel that does not pollute the environment compared to other fuels. The three main polluting factors (SO₂, PM and smut) are not found in natural gas fumes. One of the most important features of natural gas is that it is non-toxic. There is no poisonous and lethal effect in case of natural gas inhalation. However, if there is too much accumulation in the environment, there is a danger of suffocation due to the reduction in oxygen to be inhaled. If the combustion product gases are emitted to the atmosphere, they may poison due to the increase of CO as in other fuels. For this reason, the use of natural gas instead of coal in heating significantly reduces harmful gas emissions [11,12].

As a result of combustion of natural gas which is a cleaner fuel than other fuels due to the emission of pollutants resulting from combustion, CO₂, CO and NO_x are formed. There is no sulfur oxides in it because it does not contain sulfur. It is also an important advantage that it does not form soot and flying ash particles as seen from above table. The lack of carbon monoxide formation, which is described as unburned gas and which is an extremely harmful gas, is another advantage compared to other fuels. NO_x is another

component of combustion products that is harmful to the environment. One of the main reasons for the formation of nitrogen oxides is the high combustion temperature [13].

5. Usage areas of natural gas

The most widely used area of natural gas is energy production area. In addition to ensuring energy demand for natural gas in industrial and residential use, it is also used in cooling systems as well as for improving the performance of the system in thermal power plants, providing better emission values and as a raw material in the industrial sector [14]. Furthermore, natural gas has been utilized an engine fuel in the world. Natural gas motor vehicles that are used in Turkey in recent years are more prevalent.

Around the world, specifically in the 80's, the number of natural gas-producing power plants is increasing due to the fact that natural gas is an environmentally friendly and efficient fuel. It is used in two main forms of electricity generation. According to this, electricity can be produced by turning the steam turbines of water vapor obtained as a result of incineration of natural gas or burning natural gas directly into gas turbines [15]. The reason why natural gas is preferred in electricity generation is the fact that it is more efficient and cost-effective than other sources. According to the UEA's World Energy Outlook 2010 report, the use of natural gas in electricity generation will rise 33 % from 2007 to 2035 [16].

Natural gas is also used in white goods painting, adhesive industry, artificial rubber cutting of metals in industry, heavy industry, making ceramics in ink industry, and obtaining antifreeze.

5.1 Use of natural gas in residential buildings

Energy is a value that is considered to be indispensable for countries that make up the basic input of the social, economic and industrial development of each country. The main objective of countries of the world is to use natural gas in a cost-effective and environmentally friendly manner since natural gas meets a significant proportion of the world's main energy needs. Different factors in the choice of heating systems for buildings can be decisive on the grounds that urbanization and rapid population growth are experienced intensively. These factors include the purpose of the use of the building, the periods of the use of the parts in the building, available and usable fuel types, and the budget of the project.

Alternative heating systems should be considered in order to find a suitable solution for each building in terms of heating technology, economy and environment, and these should be carefully considered. In general, different heating methods may apply to the same building. For example, in residences, central and individual heating systems can be preferred [17].

5.2 Use of natural gas in vehicles

The spread of natural gas as an alternative fuel with low emissions compared to gasoline and diesel vehicles is particularly noticeable in recent years. In spite of the fact that natural gas has rich sources, and has become widespread through the use of pipelines in many countries, the use of natural gas as a fuel in vehicles was slow compared to other applications. The rapid increase in the number of vehicles preventing environmental pollution has become difficult. That is why, European Union countries attach importance to the use of alternative fuels and reduction of emissions on vehicles. In this regard, the use of natural gas is as important as the use of alternative fuels. The studies on natural gas is supported by International Association for Natural Gas Vehicles (IANGV) and European Natural Gas Vehicles Association (ENGVA) institutions, which are known to be leading institutions [18-22].

Detailed studies and research are being conducted for the use of compressed natural gas (CNG) on vehicles in many western countries as it is thought to be an environmentally friendly alternative fuel with low emission amounts. For the sake of giving an example, it is necessary to examine the US, where the greatest number of road transport vehicles are utilized in the world. There are 520 million cars and trucks in the world, 190 million of which are found in this country. It has been determined that an average 50 % of air pollution in the US is caused by exhaust stemming from these vehicles. In order to reduce exhaust emissions in these oil-dependent vehicles, catalytic filters were installed on all gasoline vehicles in the US where various measures were taken, the engine designs of the vehicles were improved, and the gasoline and diesel fuel structures were altered. Since these precautions are not sufficient, The Clean Air Act and The Energy Law, which were adopted in 1990 and 1992, respectively, initiated investigations for alternative fuels [23-25].

Iran is in the forefront in terms of natural gas-powered vehicles, followed by China, Pakistan, and Argentina. The top 10 countries by the number of natural gas-powered vehicles throughout the world are given in Fig. 5. Iran and Argentina are playing leading role in Asia-Pacific and S. & Cent., respectively. The International Association for Natural Gas Vehicles (IANGV) predicted that there would be 65 million natural gas vehicles in all parts of the world in 2020 [26].

For the first time in Turkey, natural gas vehicles produced in TOFAS are exported to many European countries. Doblo and Fiorino, called "Natural Power", are successful examples of natural gas-powered vehicles. With the market which has been created under the leadership of Naturelgaz, as of 2012, the conversion of vehicles to natural gas has begun. CNG conversion systems can be applied to all vehicles including trucks, tractors, trucks, buses, light commercial vehicles and passenger cars. In addition, many leading vehicle manufacturers such as Iveco, Mercedes, MAN, Scania and Volvo have CNG vehicles.

New natural gas-powered buses were used in order to reduce air pollution and fuel costs caused by exhaust gases in public transportation in Kocaeli, Ankara, Kayseri and Istanbul providences, Turkey. Kocaeli Metropolitan Municipality saved about 20 % for 2010 with 45 natural gas buses that were actively commissioned in December 2009 [27].

5.3 Use of Natural Gas in Industry

The use of natural gas, which is easier to obtain than other energy sources and has a lower impact on the environment, is increasingly being used as a primary energy source in the world. Due to the advantages such as high efficiency and short time operation, natural gas-fired combined cycle power plants have been utilizing increasingly in recent years in electric energy production in the world [28].

Gas turbines and steam turbines are used together in combined cycle power plants. In addition to the electric energy obtained from gas turbines using natural gas as fuel, steam generated from the waste heat of the exhaust gases with high temperature from the turbine exhaust and steam turbines provide additional electricity generation. In these plants, combined cycle efficiency can be realized at around 60 % by combining the advantages of high temperature of gas turbine cycles and low temperature of steam turbine cycles. Natural gas-fired combined cycle thermal power plants can be operated in a shorter period of time with lower installation costs than thermal, nuclear and hydroelectric power plants using other fossil-based fuels [29].

Hence, the use of natural gas in electricity increased and now 55 % of the imported natural gas is being used in electricity. At the moment, 45 % of the total electric energy production are obtained from natural gas power plants. The total installed capacity of 277 Natural Gas Power Plants located in Turkey is 22,584.60 MW. In 2015, 98.326.026.435 kilowatt-hours of electricity were produced in natural gas power plants [30].

6. Natural gas pipeline transportation

Transportation of natural gas commenced with small-scale and short-haul routes in the late 19th century. A long-distance transportation of natural gas was brought to Pittsburgh in commercial for the first time in 1883 by way of pipelines. Until the Second World War, natural gas technology was not very common in countries outside the US. After the Second World War, developments in pipe manufacturing and welding technology have resulted in a significant increase in the volume of natural gas transported by allowing pipeline pressures of 25-30 bar to be increased to 60-70 bar and pipeline diameters up to 75 cm. Today, in the international arena, natural gas pipelines can reach up to 150 cm in diameter. In order to facilitate the transportation of natural gas, R&D studies have been continuing in the world and to increase the applicability of new technologies, namely Absorbed Natural Gas (ANG) and Natural Gas Hydrate (NGH) [31].

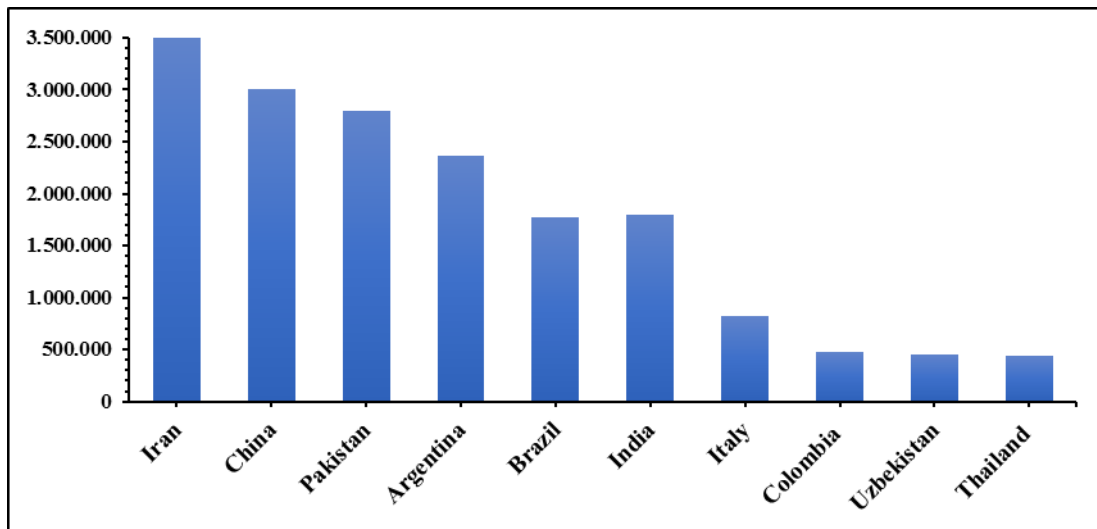


Fig. 5. The number of natural gas-powered vehicles by countries in 2014 [27].

Pipelines are the safest and most efficient way from production sources to demand center with respect to transportation in our globalized world. They, passing through Turkey, are of international vital significance because of the fact that Turkey is positioned at the meeting point of three continents (Asia, Europe and Africa) and therefore serves as a bridge between Asia and Europe accounting for well-nigh 67 % of the world oil reserves and 40 % of the world gas reserves [32]. Turkey supplies natural gas needs from various countries, which are Russian Federation, Iran, Nigeria, Algeria, Azerbaijan, Turkmenistan. While natural gas is supplied via pipelines from Russian Federation, Iran, Azerbaijan, and Turkmenistan, is supplied by tankers in its liquefied form [33].

Natural gas is transported by suitable pipe materials from the source to the consumer at appropriate pressure values. In the Blue Stream Project, the natural gas coming from Russia to Turkey through the Black Sea comes to Turkey within 12 hours with a pressure of 250 bar from Russia. BOTAS is responsible for the distribution of gas in Turkey. Natural gas comes from BOTAS through the RMS (Regulation Measuring Station), zone regulator and service box. Natural gas is transported between cities under high pressure (40-70 bar) through steel pipelines. It is reduced to 14-19 bar at the main pressure reduction stations near the city. This pressure is reduced to 4 bar at certain centers within the city. The natural gas at 4 bar pressure comes to the regulator stations at the residential entrances by way of polyethylene pipes; thus, the pressure is reduced to 21 mbar or to 300 mbar at large consumption points. These installations are carried out by the company which has got the city distribution contract.

6.1 Existing natural gas pipelines in Turkey

It is an obvious fact that Turkey has a growing importance that is growing rapidly in the energy sector. The developing economy and limited natural sources are increasing the energy import requirements of Turkey. Research studies carried out in 2015, report that the total length of natural gas pipeline was 13,276 km 12,963 and 313

km of which was constructed by BOTAS and TPAO companies, respectively, and natural gas supply is ensured to 74 cities.

It is planned to provide natural gas supply to all city centers with the completion of the transmission and distribution line projects which are still going on and will continue after 2015. Turkey currently imports 95-99 % of natural gas that it uses. A variety of natural gas producers in the world are making natural gas purchase agreements with countries. Turkey made the first agreement with the Soviet Union on September 18, 1984 for the supply of natural gas from abroad and has been importing 6 bcm of natural gas per annum since 1987 [34]. The main countries with which Turkey has a natural gas agreement are shown in Table 1.

6.1.1 Russia - Turkey west pipeline

In September 1986, ENKA and its partner Spiecapag (France) signed an agreement with BOTAS for the supply of Russian gas pipeline. The 842 km long Russia-Turkey natural gas main transmission line enters Turkey at Malkoclar at the Bulgarian border and then follows Hamitabat, Ambarli, Istanbul, Izmit, Bursa, Eskisehir route to reach Ankara. Other major works in the agreement encompass 20 MW compressor station, 11 reduction and metering stations, 9 pig stations, 32 line valves, dispatch centers, 3 maintenance centers, telecommunication and telecontrol systems. Natural gas supply capacity of the pipeline to Turkey through Ukraine has an annual 14 bcm under a pressure of 70 bar. This is equal to nearly 75 % of Turkey's current consumption. The project was funded by several export credit agencies such as US Exim, JEXIM, Coface, and ECGD.

Table 1. International natural gas agreements of Turkey [35]

Agreements	Amount (bcm/year)	Signed Date	Status	Expiration
Algeria (LNG)	4,4	1988	In operation	October 2024
Nigeria (LNG)	1,3	1995	In operation	October 2021
Iran	9,6	1996	In operation	July 2026
Rus. Fed. (Blue Stream)	16	1997	In operation	End of 2025
Rus. Fed. (West)	4	1998	In operation	End of 2021
Turkmenistan	15,6	1999	-	-
Azerbaijan (Stage-I)	6,6	2001	In operation	April 2021
Greece	0,75	2003	In operation	End of 2021
Azerbaijan (Stage-II)	0,15	2011	2018	2033

6.1.2 The Russian route pipeline connections (Blue Stream)

Blue Stream project, which is the largest energy project ever applied so far, began with the Intergovernmental agreement signed on 15 December 1997 by Turkey and Russian Federation relating to the shipment of Russian natural gas from the Black Sea to the Republic of Turkey. The pipeline was constructed by the Blue Stream Pipeline B.V., the Netherlands based joint venture of Russian Gazprom and Italian Eni. According to the initial planning, the capacity of line was determined as 16 bcm. Blue Stream project, according to the agreement signed in 1997 by Moscow and Ankara for a 25-year period, foresees to import 16 bcm of natural gas from Russia on a yearly basis. Approximately 380 kilometers of total 1213 kilometers long pipeline carrying natural gas passes under the Black Sea. Pipeline at the bottom of the sea is at the deepest point on Earth, a depth of 2150 meters. Gas transportation agreement officially entered into force on November 17, 2005 [36].

6.1.3 Azerbaijan-Turkey pipeline (Shah Sea)

BOTAS and SOCAR (State Oil Company of Azerbaijan) signed an agreement on March 12, 2001 with the intention of transporting natural gas produced in Azerbaijan to Turkey over Georgia. 1850 km long line starting from Turkgozu village of Ardahan province on Georgian border passes through 20 provinces, including Ardahan, Kars, Erzurum, Erzincan, Bayburt, Gumushane, Giresun, Sivas, Yozgat, Kirsehir, Kirikkale, Ankara, Eskisehir, Bilecik, Kutahya, Bursa, Balikesir, Canakkale, Tekirdag, and Edirne coming to an end in Ipsala district of Edirne on the Greek border [37]. Shah Sea is a giant natural gas field located in the part of Azerbaijan of Caspian Sea. BP (British Petrol) is the main business area since it consists of seven different companies with 28.8 % shareholder in a consortium. 6.6 bcm of gas has been sold to Turkey from Stage 1 project of Shah Sea field since 2007. Development activities began after signed agreements in October 2011 concerning Shah Sea Stage 2 gas sales and transit passes between Azerbaijan and Turkey.

6.1.4 Baku-Tbilisi-Erzurum pipeline (BTE)

Baku-Tbilisi-Erzurum Pipeline is also known as South Caucasus Pipeline or BTE pipeline. BTE gas pipeline, which carries the gas produced from Shah Sea field located in the Caspian Sea of Azerbaijan, is 692 km in length and has a maximum capacity of 25 bcm per annum. As a result of negotiations relating to the supply of gas from Azerbaijan, intergovernmental agreement between Azerbaijan and Turkey for the shipment of Azerbaijani gas to Turkey, and for importation of 6.6 bcm of natural gas sale and purchase agreement was signed by SOCAR and BOTAS on March 12, 2001. The pipeline was constructed between 2005 and 2007, and has been operational since mid-July 2007. Increasing the capacity of portions between territories of Azerbaijan and Georgia in conjunction with production of the Stage 2 of Shah Sea field, BTE was planned to be linked to Trans-Anatolian gas pipeline project on December 17, 2003 [38].

6.1.5 Iran - Turkey pipeline

Natural gas taken from the sources in the East is intended to transport by pipeline to Turkey. Within this framework, natural gas sales and purchase agreement was signed with respect to 9.6 bcm of import of natural gas by National Iranian Gas Company (NIGC) and BOTAS on August 8, 1996 for a 25-year period. Eastern Anatolia gas main transmission line, which provides an amount of 9.6 bcm natural gas transmission from Iran to Turkey annually, is about 1491 km in length. With the completion of the metering station in Bazargan (a city of Iran), natural gas supply from Iran began in December 10, 2001. According to the agreement, the gas flow started at 3 bcm / year and reached 10 bcm / year [39].

6.1.6 Turkey - Greece pipeline

Within the framework of European Commission INOGATE Program (Interstate Oil and Gas Transport to Europe), South European gas ring project has been developed involving interconnection of Turkey and Greece's natural gas network. Intergovernmental agreement relating to supply of natural gas was signed on February 23, 2003. After

being put out to tender by BOTAS on November 25, 2004, natural gas network was started to be constructed in 2005. When its construction was finished on November 17 2007, the total cost of 285-kilometer-long gas pipeline was around 250 million euro. A pipeline starting from Karacabey in Turkey, crossing the Marmara Sea with a distance of 17 km, entering into Greece from Ipsala/Kipi border point and ending in Komotini was envisaged at the Desk Study [40].

6.2 Pipeline projects - incoming pipelines to Turkey

Since 2000, Turkey has been making very important contributions to projects that are closely followed on a global scale. Correspondingly, it has developed a multi-faceted energy policy and played an important role as a powerful regional actor in bringing the West and East together. The projects developed by Turkey are clarified in a comprehensible way below.

6.2.1 Iraq-Turkey pipeline

An integrated project involving field development, production, gas processing and pipeline construction for natural gas fields in Northern Iraq became a current issue with agreements signed by Iraq in 1996. BOTAS began talks with TPAO (Turkish State Petroleum Company) and Shell in the wake of new political developments that took place in Iraq in 2003. The project was named Iraq-Turkey Gas Export Project (ITGEP) by signing a Memorandum of Understanding among the three related above companies above mentioned in the business of natural gas export from Iraq to Turkey in 2008. Potential natural gas exploration and production opportunities for interested parties of Memorandum of Understanding as well as possible links to neighboring countries will form a framework for assessing the natural gas infrastructure in Turkey, and exporting the increased natural gas to Turkey and Europe after negotiating by the internal demands of countries like Iran.

Memorandum of Understanding was signed with respect to the development of natural gas corridor by the Ministry of Energy and Natural Resources and the Iraqi Petroleum Ministry on October 15, 2009. Memorandum of Understanding aims to improve natural gas corridor between the two countries through transport of Iranian natural gas to Turkey and Europe via Turkey [41].

6.2.2 Egypt - Turkey pipeline

Egypt-Turkey natural gas pipeline is also known as Arabian natural gas pipeline. It is a project that emerged after the cancellation of the LNG (Liquefied Natural Gas) project initiated in 1996, resulting from the transfer of 10 bcm of gas from Egypt's pipeline to the Mediterranean Sea. Memorandum of Understanding regarding imports of natural gas from Egypt to Turkey was signed by the Ministry of Energy and Natural Resources and the Egyptian Petroleum Ministry on June 22, 1998.

A framework Agreement was signed by Turkey and Egypt on March 17, 2004 in Cairo, for the import of natural

gas by BOTAS from Egypt Natural Gas Company EGAS and the transit of gas from Egypt to Europe through Turkey. One part of the Arabian natural gas pipeline has been completed and Egyptian gas is currently being provided to Jordan, Syria and Lebanon. When the project is utterly completed for Turkey, Egyptian gas can be an alternative to Russian and Iranian gas. In fact, according to some experts, Egyptian natural gas can be a balancer rather than an alternative, and it should be added to other Arab countries [42].

6.2.3 Transcaspien Turkmenistan-Turkey-Europe pipeline

Natural gas, which is produced in the fields situated in the south of Turkmenistan with Turkmenistan- Turkey-Europe natural gas pipeline project, is intended to be transported to Turkey and to Europe via Turkey with Trans-Caspian gas pipeline. In the context of negotiations, a framework agreement was signed by the Heads of State of Turkey and Turkmenistan in 1998 towards the realization of this project. In accordance with this mutual agreement, Turkmenistan has a total gas of 30 bcm, 16 bcm and 14 bcm all of which will be transported to Turkey and Europe, respectively. A natural gas sale and purchase agreement valid for 30 years was signed on May 21, 1999 by BOTAS and the authorized body for the use of Hydrocarbon Resources of the President of Turkmenistan [43].

6.2.4 Interconnector Turkey-Greece-Italy (ITGI)

Turkey-Greece natural gas pipeline (ITGI) constitutes the first ring of South European gas ring. Intergovernmental agreement of the project was signed in Rome in 2007 by the ministers of countries responsible for energy projects, and it is known as the important projects that will supply natural gas. Intercompany Memorandum of Understanding was signed by BOTAS, DEPA (Public Natural Gas Supply Corporation of Greece) and EDISON (Italian Energy Company) by the General Managers of these companies on June 17, 2010.

Onshore part of the project is 592 km from Komotini (a city in the region of East Macedonia and Thrace) to Adriatic coast, 212 km of which is sea crossing section. Besides this, the maximum depth is estimated to be 1450 m. Within the scope of the project, a total of 11.6 bcm / year gas are planned to be transported through Turkey in the plateau level, 3.6 bcm / year for Greece and 8 bcm / year for Italy of which are supplied from Caspian sources [44].

6.2.5 Trans-Anatolian pipeline (TANAP)

The plan in this pipeline project which is planned to be transferred Azerbaijan natural gas to Europe through Turkey. The main aim of the project was to constitute Southern gas corridor by merging with South Caucasus pipeline (SCP) and Trans Adriatic pipeline (TAP). The seeds of the project were planted at the 3rd Black sea Energy and Economic Forum organized in Istanbul on November, 2011. After a short time, Intergovernmental Memorandum of Understanding was signed by Ministers responsible for energy of the two

countries in Ankara / Turkey on December 24, 2011. After negotiations, an agreement was signed among BP, BOTAS and SOCAR in 2015. The TANAP project is carried out by a consortium led by the SOCAR. The project has a share of SOCAR with 58 %, BOTAS with 30 %, and BP with 12 %.

When its construction is completed, it is intended to be used for the transfer of natural gas extracted from Shah Sea gas facilities. The main line encloses a total of 1850 km, 19 km of which is Marmara Sea crossing. Furthermore, the number and qualifications to be used in the operation of the connection lines in the exit points in Turkey, comprise of above-ground facilities including 7 compressor stations, 4 metering stations, 11 pig stations, 49 block valve stations, and 2 gas outputs to feed into the national gas station network in Turkey.

Within the scope of Shah Sea Stage II, the first step of the line capacity is targeted to be 16 bcm annually, 6 bcm of which will be sold to the Turkish domestic market and the remaining 10 bcm portion will be exported to the European markets. It is expected that the gas will reach Turkey between 2018 and 2020. The capacity of the line has been targeted to reach 16 bcm in 2020, 23 bcm in 2023 and 31 bcm in 2026 [45].

6.2.6 The Nabucco west pipeline

Treaty of the Nabucco West was signed in Vienna with the participation of BOTAS from Turkey on October 11, 2002. The Nabucco pipeline was accelerated with agreement signed by the governments on July 13, 2009. The project was planned to transport natural gas to the EU via Turkey. The main purpose of the project is to supply natural gas by means of Trans-Anatolian gas pipeline project from Shah Sea gas field of West to Europe. The line is also considered to be a part of the EU's Trans-European energy line, and benefited from EU funding for feasibility and engineering studies. According to preliminary calculations, the total cost of the project would be in the range between 4 and 6 billion euro. Thanks to the 1320-kilometer line, 20 bcm of gas would be transported to Central Europe; despite mutual agreements between two countries, the project was officially cancelled in 2013 as a result of disputes [46].

6.2.7 Russia-Turkey-Europe natural gas pipeline (Turkish Stream)

Turkish Stream is the name of the natural gas pipeline project that was planned to transfer from Russia and natural gas to Turkey via the Black Sea. An intergovernmental agreement was signed for the Turkish stream natural gas pipeline project in October 10, 2016. Even though the starting point of the pipeline was determined as the Russkaya compressor station near Anapa, there is no official information on where it would enter Turkey. When the starting point in Turkey is determined, it is expected that Gazprom (a large Russian company) will start works on pipe-laying immediately. The construction of 4 submarine pipelines is planned. In addition, within the scope of the ongoing technical work, a maximum of 63 bcm natural gas

has been considered to be transported on annual basis. It is thought that Turkey will supply about 14 bcm of natural gas per year from this project and the remaining 49 bcm of natural gas will be exported to Europe [47].

6.2.8 Trans adriatic natural gas pipeline (TAP)

After the Nabucco West project was called off, it was replaced by TAP project. It is a natural gas pipeline project initiated by connecting to TANAP in Turkey / Ipsala, with 478 km pipeline from Northern Greece, passing through Albania and then under the Adriatic Sea. The agreement of the project was signed by Shah Sea Consortium on September 19, 2013, and an investment of 35 billion dollars was foreseen. As soon as the construction of the pipeline can be completed at the beginning of 2018, after a very short time from this date, flow of natural gas will put into operation [48, 49].

7. Liquefied Natural Gas (LNG) Transportation

Natural gas is transported by ships when it is not possible to transport through pipelines. In this case, the volume of natural gas is reduced 600 times by refrigerating well below -163 °C and increasing its pressure. LNG is cleaner when compared to natural gas, because contaminants are eradicated during liquefaction. It is then transported by ships equipped with a special way through the methane tanker. The 2000 km long pipeline connecting to Germany natural gas extracted from North Sea is the world's longest natural gas submarine pipeline.

The Government of the Republic of Turkey decided to import 4 bcm of LNG from Algeria with an agreement signed in 1995 for a 26-year period and 12 bcm of LNG from Nigeria with an agreement signed in 1988 for a 36-year period by reason of diversification of supply sources and balance of seasonal burden [50]. Marmara Ereğli LNG Terminal, which is located in an area of 66 hectares, was built between 1989 and 1994. Turkey's second LNG terminal, which was commissioned in the winter of 2006, is situated in Aliaga/Izmir [51].

8. Compressed Natural Gas (CNG) Transportation

Compressors are compressed at a pressure of 206 bar in order to increase the energy density of natural gas, called Compressed Natural Gas (CNG). It is one of the energy types that are likely to become the future fuel. In addition to being used as fuel in vehicles, it meets the needs of consumers by transporting through articulated lorry and special truck in places where the natural gas pipelines are not accessible or reachable. For instance, most of the People's Republic of China's natural gas needs are met by CNG system, and even in Italy, where natural gas pipelines are very common, CNG system is utilized in industrial cities like Genova. In Europe, unlike Italy, it is employed in many countries such as Germany, Holland, France, Austria, Switzerland [52, 53]

Considering that the damage petroleum products used in mass transportation vehicles have given to the environment,

it may be possible to use natural gas as an alternative fuel. The quick increase in the use of individual vehicles, especially in recent years, has accelerated the trend towards more economical alternative fuels and as a result of investments of R & D companies in this area have started to enhance gradually [54-56].

9. Conclusion

The history of natural gas, which is one of the biggest energy sources of our era, dates back hundreds of years. Statement of the "Sacred Fire" has been used throughout the humanity history. For the first time, natural gas utilized as an energy source by Chinese for the salt-drying process has been employed. Subsequently, they transported natural gas to other places by means of hollowed bamboos. Thus, natural gas has begun to spread rapidly in an important manner. It varies depending on usage have been adopted by the majority of people and has expanded gradually for many years over the large parts of the world.

In recent years, especially in the last two decades, the use of natural gas in electricity generation and housing has increased enormously, and the share of natural gas in the developing countries will increase by 4 % per annum by 2030, the share of primary energy resources on natural gas will rise by 23 %. The consumption of countries will enhance by 1.3 % per annum on average, and the augmentation in energy sources and the environment will be decisive.

It will be the most used fossil fuel in the future because of the constant evolution of natural gas and the low carbon emissions it releases. Increasing demand for energy and petroleum expectations indicate that natural gas will be an advantageous position in the future. The development of natural gas in the world is expected to continue with the strengthening of both political and commercial and environmental effects.

References

- [1] J. A. Fagerstrom, "The evolution of reef communities", 1987.
- [2] İ. Atılğan, "Türkiye'nin enerji potansiyeline bakış", Gazi Üniversitesi Mühendislik-Mimarlık Fakültesi Dergisi, vol. 15, 2000.
- [3] S. Shafiee and E. Topal, "When will fossil fuel reserves be diminished?", Energy policy, vol. 37, pp. 181-189, 2009.
- [4] N. H. Afgan, P. A. Pilavachi, and M. G. Carvalho, "Multi-criteria evaluation of natural gas resources", Energy Policy, vol. 35, pp. 704-713, 2007.
- [5] BP Statistical Review of World Energy. BP p.l.c, London, United Kingdom, 64th edition, 2015.
- [6] R. W. Howarth, A. Ingraffea, and T. Engelder, "Natural gas: Should fracking stop?", Nature, vol. 477, pp. 271-275, 2011.
- [7] R. Heinberg and D. Fridley, "The end of cheap coal", Nature, vol. 468, pp. 367-369, 2010.
- [8] M. R. Tek, "Underground storage of natural gas: theory and practice", Springer Science & Business Media, vol. 171, 2012.
- [9] N. A. Afgan, P. A. Pilavachi, and M. G. Carvalho, "Multi-criteria evaluation of natural gas resources", Energy Policy, vol. 35, pp. 704-713, 2007
- [10] M. Balat, "Oil and natural gas transport systems, trade and consumption trends in Turkey", Energy exploration & exploitation, vol. 22, pp. 207-216, 2004.
- [11] M. Balat, G. Ayar, C. Oguzhan and H. Uluduz, Influence of fossil energy applications on environmental pollution, Energy Source, Part B, vol. 2, pp. 213-226, 2007.
- [12] T. Colborn, C. Kwiatkowski, K. Schultz & Bachran, "Natural gas operations from a public health perspective", Human and ecological risk assessment: An International Journal, vol. 17, pp. 1039-1056, 2011.
- [13] K. Bilen, O. Ozyurt, K. Bakirci, S. Karsli, S. Erdogan, M. Yilmaz and O. Comakli Energy production, consumption, and environmental pollution for sustainable development: A case study in Turkey, Renewable and Sustainable Energy Reviews, vol. 12, pp. 1529-1561, 2008.
- [14] T.M. Verhallen and W. Fred Van Raaij, "Household behavior and the use of natural gas for home heating", Journal of Consumer Research, vol. 8.3, pp. 253-257, 1981.
- [15] A. Demirbas, "The importance of natural gas as a world fuel", Energy Sources, Part B, vol. 1, pp. 413-420, 2006.
- [16] M. Balat, "World natural gas (NG) reserves, NG production and consumption trends and future appearance", Energy sources, vol. 27, pp. 921-929, 2005.
- [17] C. S. Weaver, Natural gas vehicles-A review of the state of the art. No. 892133. SAE Technical Paper, 1989.
- [18] M. Ergeneman, C. Sorousbay, and A. G. Goktan, Exhaust emission and fuel consumption of CNG/diesel fueled city buses calculated using a sample driving cycle. Energy Sources, vol. 21, pp. 257-268, 1999.
- [19] H. Engerer and M. Horn, "Natural gas vehicles: An option for Europe." Energy Policy, vol. 38, pp. 1017-1029, 2010.
- [20] N.O. Nylund & A. Lawson, "Exhaust emissions from natural gas vehicles", Issues related to engine performance,

exhaust emissions and environmental impacts, IANGV Emission Report, 2000.

[21] H. Engerer & M. Horn, "Natural gas vehicles: An option for Europe", *Energy Policy*, vol. 38, pp. 1017-1029, 2010.

[22] S. Yeh, "An empirical analysis on the adoption of alternative fuel vehicles: the case of natural gas vehicles", *Energy Policy*, vol. 35, pp. 5865-5875, 2007.

[23] A. Janssen, S. F. Lienin, F. Gassmann & A. Wokaun, "Model aided policy development for the market penetration of natural gas vehicles in Switzerland", *Transportation Research Part A: Policy and Practice*, vol. 40, pp. 316-333, 2006.

[24] P. C. Flynn, "Commercializing an alternate vehicle fuel: lessons learned from natural gas for vehicles", *Energy Policy*, vol. 30, pp. 613-619, 2002.

[25] M. P. Hekkert, F. H. Hendriks, A. P. Faaij & M. L. Neelis, "Natural gas as an alternative to crude oil in automotive fuel chains well-to-wheel analysis and transition strategy development", *Energy policy*, vol. 33, pp. 579-594, 2005.

[26] A. H. Kakaee & A. Paykani, "Research and development of natural-gas fueled engines in Iran", *Renewable and Sustainable Energy Reviews*, vol. 26, pp. 805-821, 2013.

[27] M. Matsumoto, S. Kondoh, J. Fujimoto, Y. Umeda, H. Tsuchiya, K. Masui & H. Y. Lee, "A diffusion model for clean energy vehicles." *Journal of Japan Society of Energy and Resources*, vol. 29, pp. 49-55, 2008.

[28] B. Singh, A. H. Strømman & E. Hertwich, "Life cycle assessment of natural gas combined cycle power plant with post-combustion carbon capture, transport and storage", *International Journal of Greenhouse Gas Control*, vol. 5, pp. 457-466, 2011.

[29] P. A. Pilavachi, S. D. Stephanidis, V. A. Pappas & N. H. Afgan, "Multi-criteria evaluation of hydrogen and natural gas fuelled power plant technologies", *Applied Thermal Engineering*, vol. 29, pp. 2228-2234, 2009.

[30] B. Atilgan & A. Azapagic, "Life cycle environmental impacts of electricity from fossil fuels in Turkey", *Journal of Cleaner Production*, vol. 106, pp. 555-564, 2015.

[31] S. Mokhatab & W. A. Poe, "Handbook of natural gas transmission and processing. Gulf Professional Publishing", 2012.

[32] S. E. Masten & K. J. Crocker, "Efficient adaptation in long-term contracts: Take-or-pay provisions for natural gas", *The American Economic Review*, vol. 75, pp. 1083-1093, 1985.

[33] M. Balat & N. Ozdemir, "Turkey's oil and natural gas pipelines system", *Energy sources*, vol. 27, pp. 963-972, 2005.

[34] H. K. Ozturk & A. Hepbasli, "The place of natural gas in Turkey's energy sources and future perspectives", *Energy Sources*, vol. 25, pp. 293-307, 2003.

[35] BOTAS, Petroleum Pipeline Corporation, 2015, <http://www.botas.gov.tr/>

[36] G. Bacik, "The Blue Stream project, energy co-operation and conflicting interests", *Turkish Studies*, vol. 2, pp. 85-93, 2001.

[37] K. Barysch, "Should the Nabucco pipeline project be shelved?", *Centre for European Reform*, 2010.

[38] T. Babali, "Implications of the Baku-Tbilisi-Ceyhan main oil pipeline project", *Perceptions, Journal of International Affairs (Center for Strategic Research by the Ministry of Foreign Affairs, Turkey)*, vol. 10, pp. 29-59, 2005.

[39] G. Bacik, "Turkey and pipeline politics", *Turkish Studies*, vol. 7, pp. 293-306, 2006.

[40] G. M. Winrow, "Turkey and the East-West Gas Transportation Corridor", *Turkish Studies*, vol. 5, pp. 23-42, 2004.

[41] H. J. Barkey, "Turkey and Iraq: The making of a partnership", *Turkish Studies*, vol. 12, pp. 663-674, 2011.

[42] A. M. Kilic, "Major utilization of natural gas in Turkey", *Energy exploration & exploitation*, vol. 23, pp. 125-140, 2005.

[43] H. K. Ozturk & Arif Hepbasli, "Natural gas implementation in Turkey. Part 2: Natural gas pipeline projects", *Energy sources*, vol. 26, pp. 287-297, 2004.

[44] C. Üstün, "Energy Cooperation between Import Dependent Countries: Cases of Italy and Turkey", *Perceptions*, vol. 16, pp. 71, 2011.

[45] G. M. Winrow, "The southern gas corridor and Turkey's role as an energy transit state and energy hub", *Insight Turkey*, vol. 15, pp. 145, 2013.

[46] A. Sobjak & K. Zasztowt, "Nabucco West—Perspectives and Relevance: The Reconfigured Scenario", *PISM policy paper*, pp. 44, 2012.

[47] M. Hafner & S. Tagliapietra, "Turkish Stream: What Strategy for Europe?", 2015.

[48] N. Sartori, "Energy and politics: behind the scenes of the Nabucco-TAP competition", *IAI WP*, vol. 13, pp. 27, 2013.

- [49] M. MacDonald, "Supplying the EU natural gas market", November, Final Report, Croydo, the United Kingdom, 2010.
- [50] J. J. Zednik, D. L. Dunlavy & T. G. Scott, "Regasification of liquefied natural gas (LNG) aboard a transport vessel", U.S. Patent No. 6,089,022. 18 Jul. 2000.
- [51] B. Kavalov, H. Petric & A. Georgakaki, "Liquefied natural gas for Europe—some important issues for consideration", Joint Research Centre of the European Commission Reference Report, 2009.
- [52] A. Demirbas, "Fuel properties of hydrogen, liquefied petroleum gas (LPG), and compressed natural gas (CNG) for transportation", *Energy Sources*, vol. 24, pp. 601-610, 2002.
- [53] S. Thomas & R. A. Dawe, "Review of ways to transport natural gas energy from countries which do not need the gas for domestic use", *Energy*, vol. 28, pp. 1461-1477, 2003.
- [54] J. Ally & T. Pryor, "Life-cycle assessment of diesel, natural gas and hydrogen fuel cell bus transportation systems", *Journal of Power Sources*, vol. 170, pp. 401-411, 2007.
- [55] M. J. Economides, K. Sun & G. Subero, "Compressed natural gas (CNG): an alternative to liquefied natural gas (LNG)", *SPE Production & Operations*, vol. 21, pp. 318-324, 2006.
- [56] R. A. B. Semin, "A technical review of compressed natural gas as an alternative fuel for internal combustion engines", *Am. J. Eng. Appl. Sci.*, vol. 1, pp. 302-311, 2008.

Development of a Face Detection Algorithm Based on Skin Segmentation and Facial Feature Extraction

Jide J. Popoola*[‡], Akintunde Akinola*

*Department of Electrical and Electronics Engineering, Federal University Technology, P.M.B. 704, Akure, Ondo State, Nigeria

(jidejulius2001@gmail.com, akinolatunde11@gmail.com)

[‡]Corresponding Author; Jide J. Popoola, Department of Electrical and Electronics Engineering, Federal University of Technology, P.M.B. 704, Akure, Ondo State, Nigeria. Tel: +234803 413 1860,

jidejulius2001@gmail.com

Received: 27.03.2017 Accepted: 23.08.2017

Abstract- This paper presents a face detection algorithm capable of detecting face(s) without prior training as a face classifier. The technique employed in developing the algorithm is based on skin segmentation and facial feature extraction of the two eyes and mouth. Skin segmentation was done in the red, green, blue color space. White balance correction was employed to correct the change in image temperature that occurs due to change in lighting conditions at the point of acquiring image. Morphological operations and bounding box were employed to search and extract face region from the segmented skin region. Facial feature, eyes and mouth, were extracted for final verification of the sensed face using the Laplacian of Gaussian filter and the isosceles triangle matching rules. The extracted features were used to develop the face detection algorithm. The developed algorithm was evaluated using random images taken under different lighting conditions. Furthermore, the efficiency of the developed face detection algorithm was evaluated using a standard face detection image database. The result obtained shows that the developed face detection algorithm performed satisfactorily well with 81.37% detection accuracy. Furthermore, the results obtained from the performance evaluation of the developed face detection for this study has shown it clearly that accuracy detection of dissimilar faces in images with complex background is possible and attainable.

Keywords Face detection, face detection methods, skin segmentation, morphological operations, isosceles triangle matching.

1. Introduction

In image processing, in image processing, one of the current research areas is automatic face detection. Interest in automatic face detection is increasing on daily basis because of countless applications that require the application of automatic face detection as a cornerstone for series of applications revolving around automatic facial image analysis [1]. For instance, as reported in [2], it is being used in applications such as authentication, attendance system and electronic passport. In addition, as reported in [2], it has also been used in a new naked-eye auto-stereoscopic display which requires accurate human face and eye locations. According to [1], face detection is also the initial step towards most of the modern vision-based human-computer and human-robot interaction systems. Basically, face detection in real-world is one of the visual tasks that human beings can do effortlessly. However, in computer vision,

human faces detection is a challenging task for computers. This is because human faces are not easy to model as face modeling according to [3] requires accounting for all possible appearance variations caused by changes in scale, location, orientation, pose, facial expression, lighting conditions and partial occlusions.

Tactically, the main task of face detection system or algorithm is to determine whether or not a face exists in a given image. Hence, according to [4], face detection is defined as a process of determining whether a face is present or not in a scanned or digitalized photo, an image or a video, and reporting the location of each face(s) if there are any. It is the first step of automatic system that analyzes the information contained in faces. Face detection plays an important role in success of any face processing system. Often, face recognition systems work by applying a face

detector to locate the face, and then apply a separate recognition algorithm to identify the face [5].

Basically, process of automatic human face recognition is one of the most difficult and important areas in computer vision and pattern recognition. It is as a security mechanism being used in replacing metal key, plastic card, and password or PIN number. However, most face recognition systems or algorithms require the input face to be free of background, that is, to be separated from the entire image. Therefore, a successful face detection process is essential in enabling successful face recognition task. If we do not have a successful face detection method, we cannot develop a successful face recognition system [6]. Therefore, face detection process should not be treated merely as a preprocessing of a face recognition system or other computer vision process; rather, it should be treated with the same importance as the other computer vision problems.

Conventionally, according to [7-10] face detection techniques or methods are classified into four classes: knowledge-based methods, feature invariant methods, template matching methods, and appearance-based methods. In knowledge-based methods, human knowledge of typical face geometry and arrangement of facial features are usually employed. In this method, facial features in an input image are first extracted, which aids face candidate's identification based on coded rules. On the other hand, in feature invariant methods, structural features that exist in the face, such as facial local features, texture, shape, and skin color, are usually targeted and use to locate faces [5]. In template matching methods, a standard face pattern is usually parameterized by a function. Hence, this method involves computation of the correlation values between the standard pattern and an input image. While face detection algorithms based on template matching methods depend on a pre-defined template to function, appearance-based face detection algorithms learn from examples in images. In this face detection method; face detection is usually view as a pattern classification problem with two subsets: face and non-face.

Based on these four methods, a lots of face detection algorithms have been developed. Similarly, in detecting face, various skin color based algorithms have been developed. The adoption of skin color based algorithm is based on the fact that color is an important feature of human faces [11]. According to [11], using skin color as a feature for locating a face has diverse advantages. One of these advantages, according to [12], is the fact that color processing is faster than other facial features processing. In this paper, a skin color segmentation based on feature invariant face detection approach to extract the skin areas in single image was employed. The method works by checking the pixels in order to categories pixels into skin and non-skin. The rule governing the pixel's classification employed is stated in Section 3. For sequential and logical presentation of the study presented in this paper, the rest of this paper is structured as follows. Section 2 presents review on related work on face detection algorithms. In Section 3, detailed information on the procedures involved in developing the face detection algorithm for this study is presented. The

performance evaluations result of developed face detection algorithm for this study is presented and discussed in Section 4. The paper is finally concluded in Section 5.

2. Related Work

There are many researches on face detection using different methods that have been carried out over the years. Those that were centered on skin segmentation in detecting faces in images are reviewed in this section. In [13], skin like pixel was detected using evolutionary agents. In the study face like regions were segmented from the skin-like pixel by activating the evolutionary behavior of the agents. Then wavelet decomposition was applied to each region to detect the possible facial features and a three-layer back propagation neural network (BPNN) was used to detect eyes among the features. Similarly, in [11], facial feature was used to detect faces. Skin like region was first segmented using a combination of color space. Eyes and mouth were then extracted using principal component analysis on the detected skin like region. Likewise, in [14], segmented skin like region with the Hue saturation value color space were employed. Feature vector of the segmented skin like region was calculated with two dimensional discrete cosine transform. BPNN was used to classify the feature vectors that belong to skin like regions. Similarly, authors of Reference [15] also performed skin color segmentation for skin like regions using the Luminance-Blue Chroma Difference Red Chroma Difference (YCbCr) color space and possible faces were found using Linear Support Vector Machine (SVM). For final verification of face, eyes and mouth are verified using the information gotten from Cb and Cr. They found eye and mouth via the difference in value of Cb and Cr. For eye region; $Cb > Cr$ and for mouth region; $Cb < Cr$, where Cb is the value of Blue Difference Chroma and Cr is the value of Red Difference Chroma. Likewise, authors of Reference [16] also performed segmented skin like regions using the Luminance-Blue Luminance Difference-Red Luminance Difference (YUV) color space to decrease computational time when using the window scanning technique. The window just scans the segmented region instead of scanning the whole image. The segmented skin like regions is sent to BPNN to find face candidates. The authors in [16] carried out the final verification of face using Bayesian Decision

Aping *et al* (2010), [17], modeled skin color in the elliptical region using Cb and Cr channel in YCbCr color space. Skin like regions are segmented if the color values are clustered inside the elliptic region. Face is verified by using template matching. Li *et al* (2010), [18], performed skin color segmentation with the threshold values of Cb, Cr, normalized r and normalized g. Faces are then selected from the skin like region based on the following criteria; bounding box ratio, ratio of area inside and area bounding box, and minimum area of the region. The final verification is done by combining the results from skin like region with AdaBoost.

In most of these algorithms, two profound costly assumptions are usually made by the developers [19]. The first assumption according to [19] is to assume the availability of frontal faces of similar sizes, which in reality

is not generally true due to varied nature of face appearance and environmental conditions. The second assumption usually made by those developers has observed by [19] is that the exclusion of background in their images is necessary for reliable face detection. However, in most situations, a face could occur in a complex background hence making this assumption invalid. Similarly, most of the developed face detection algorithms described requires the algorithms to be trained first as a face classifier. This training takes several hours or even days to obtain accurate result. Although some face detector or algorithms only needs to be trained once to obtain the trained data, if the trained data is lost or damaged this time consuming training process have to be carried out all over again. These observed disadvantages necessitate the development of the face detection algorithm developed in this study using feature invariant approach. The method employed in this study detects faces without prior training of the developed face detection algorithm as a face classifier. This is done to save time that would have been consumed in training the algorithm as well as reducing the algorithm computational complexity. The step-by-step approach in developing the face detection algorithm for this study is presented in next section.

3. Developed Face Detection Procedural Stages

In developing the face detection algorithm for this study, whose goal is to detect the presence of faces in an image, the activities involved were divided into: white balance correction performance, segmentation of skin color in the red, green, blue (RGB) color space, logical 'and' operations, morphological operations and application of bounding box, face detection verification by extracting the facial feature of eyes and mouth, and application of isosceles triangle matching rules. The flow of the all activities in the framework is shown in Fig. 1. Detailed information on each stage involved in developing the face detection algorithm for this study as well as the results obtained in some stages, where appropriate, are presented and discussed for more clarification in the following subsections.

3.1 White Balance Correction

This is the first stage involved in developing the face detection algorithm for this study. The white balance correction was performed to correct variation in white balance of the image as a result of differences in illumination conditions of the environment where an image is acquired, which might cause some non-skin region look like skin region. Therefore, it is important to correct the white balance of input image before segmentation is performed. Also, it is important to carry out white balance correction process before segmentation because it enhances the production of good output of skin color and improves the overall detection rate.

The white balance correction was performed as follows: The average value of red channel (R_{av}), green channel (G_{av}), and blue channel (B_{av}) of image is first obtained. The average gray value of the image is then calculated from the obtained

channel values information using the mathematical expression presented in [20];

$$Gray_{av} = \frac{K(R_{av} + G_{av} + B_{av})}{3} \quad (1)$$

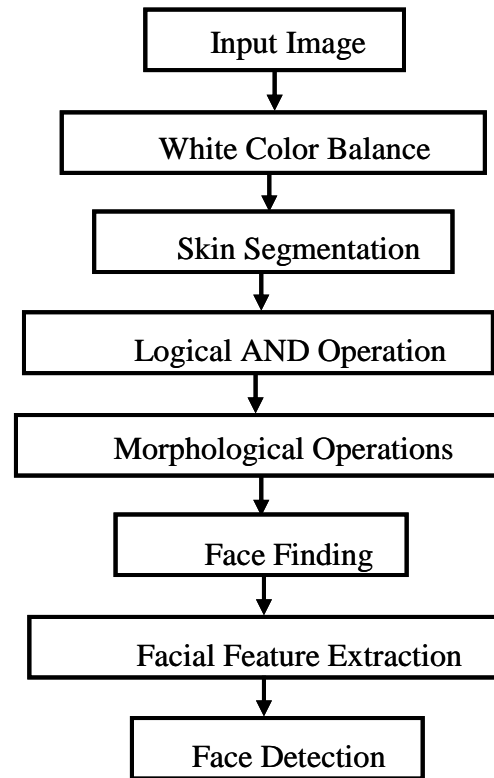


Fig. 1. The framework of the developed face detection.

The obtained average gray value is then used to calculate an adjustment parameter for each color channel using the following relationships;

$$KR = \frac{Gray_{av}}{R_{av}} \quad (2)$$

$$KG = \frac{Gray_{av}}{G_{av}} \quad (3)$$

$$KB = \frac{Gray_{av}}{B_{av}} \quad (4)$$

where KR , KG and KB are the adjustment parameters for red, green and blue channels respectively. The adjustment parameter that is obtained is used to generate a new image, $New(I)$, from original image, $Org(I)$, using the relationships presented in [20];

$$New(R) = KR \times Org(R) \quad (5)$$

$$New(G) = KG \times Org(G) \quad (6)$$

$$New(B) = KR \times Org(B) \quad (7)$$

Typical original input image and the resulting image after white balance correction in this study is shown in Fig. 2a and Fig. 2b respectively.



(a)

Fig. 2a. Original input image.



(b)

Fig. 2b. White balance correction image.

3.2 Skin Segmentation

Skin color segmentation is the second step involved in developing the face detection algorithm for this study. This

step is important because only the segmented skin region is searched while searching for face. It therefore helps in reducing computational time in face detection algorithm development. In developing the face detection algorithm for this study, the RGB color space technique was used in describing skin color. The skin segmentation was performed based on the rules for skin segmentation in RGB space reported in [5,21], which is defined as;

$$pixel = \begin{cases} \text{skin,} & \begin{cases} R > 95 \text{ and } G > 40 \\ \text{and } B > 20 \text{ and} \\ \max\{R, G, B\} - \\ \max\{R, G, B\} > 15 \end{cases} \\ \text{non-skin} & \begin{cases} |R - G| > 15 \text{ and } R > G \\ \text{and } R > B \\ \text{otherwise} \end{cases} \end{cases} \quad (8)$$

The parameters R, G and B are the red, green and blue channel value of the color pixel of image. If the pixel satisfies the conditions stated in (Eq. 8), it is regarded as skin color and binary image is formed, thus the algorithm moves to the next stage.

3.3 Logical AND Operation

The logical 'AND' operation is the third stage involved in developing the face detection algorithm for this study. The stage is essential for two reasons: (i) to eliminate generated unwanted skin color like region that occasionally occurs during white balance correction from both the segmented original image and segmented; and (ii) to extract the final skin image. Fig. 3 shows the final skin image obtained from the logical AND operation performed on the original and white balance corrected image in this study.

3.4 Morphological Operations

Morphological operations are the fourth stage involved in developing the face detection algorithm for this study. Morphology, according to [22], is a broad set of image processing operation that process images based on shapes. Its objective is to transform the images into simpler ones by removing irrelevant information while essential shapes of the images are reserved. Thus, it helps in enhancing the image so as to make face finding in the image easy. The morphological operation applied at this stage in this study is the morphological closing operation. The closing operation merges gaps and fills holes. The morphological closing operation is achieved by applying dilation and erosion operation using the same structural element. According to [23], while dilation adds pixels to the boundaries of objects in an image, erosion removes pixels on object boundaries. After the successful completion of the stage, the face finding stage was carried out.



Fig. 3. Segmented skin region image.

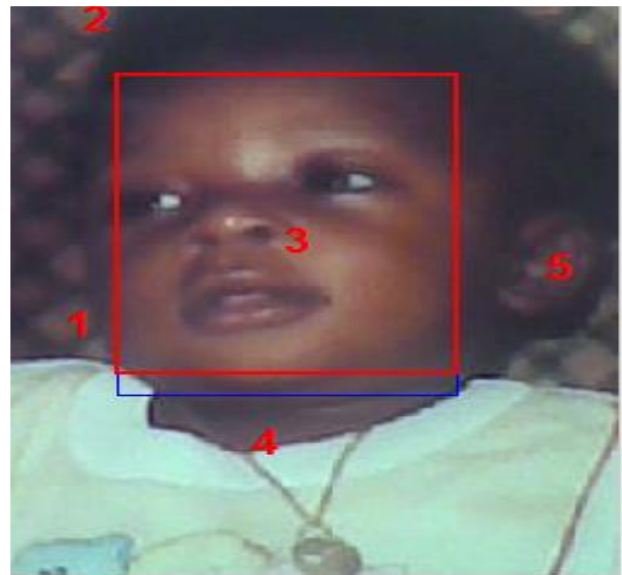


Fig. 4a. Bounding box on the face region.

3.5 Face Finding

Face finding is the fifth stage in the development of face detection for this study. The stage is the next stage after morphological operations, which is to analyze all the skin regions to determine if it is a face region or not. Every skin region is labeled as shown in Fig. 4a. On each label two conditions are considered to select a region to be a face region. The first condition is the ratio of bounding box covering each label. This ratio, which is defined as the width over the height of the bounding box, must lie between 0.6 and 1.2. This is in accordance with [24] that states that the ratio of width to height of the region of interest is usually 1. The other condition is to cover some gaps inside the region in order to distinguish the face from the other body part such as hand as segmentation on hand will have no gaps which makes it different from face. Based on these two conditions, the face region is selected and is extracted from the input image with the bounding box as shown in Fig. 4b. The extracted face is then sent to the facial feature extraction stage for final verification of face.

3.6 Face Feature Extraction

This is the sixth and last stage of the algorithm development. Facial features are significant features of the face. Examples of facial features are eyes, eyebrows, nose, lips, mouth, cheek, etc. In this study, the facial features that were extracted are the two eyes and the mouth. Laplacian of Gaussian (LoG) filter was applied to enhance the image. The essence of the filtering process is to define the features to be extracted as well as detecting edges so as to properly separate the region of interest from the background.



(b)

Fig. 4b. Face region from bounding box.

The Laplacian of Gaussian combines Gaussian filter with Laplacian for edge detection. The Laplacian detects the edge point of the image by finding the zero crossing of the second derivative of the image intensity. However, because the second derivatives are very sensitive to noise, there is the need for Gaussian filter to swipe away noise before filtering. Since LoG filter is linear, the two constituent filters (Gaussian and Laplacian) can be applied separately. The operation can be performed by convolving the image with a Gaussian smoothing filter and then computing the Laplacian of the result using mathematical expression in (Eq. 9);

$$L(x, y) \otimes G(x, y) \otimes f(x, y) \tag{9}$$

where L, G and f are the Laplacian, Gaussian and Image respectively. The result of the filtering operation of a found face region is shown in Fig. 5.

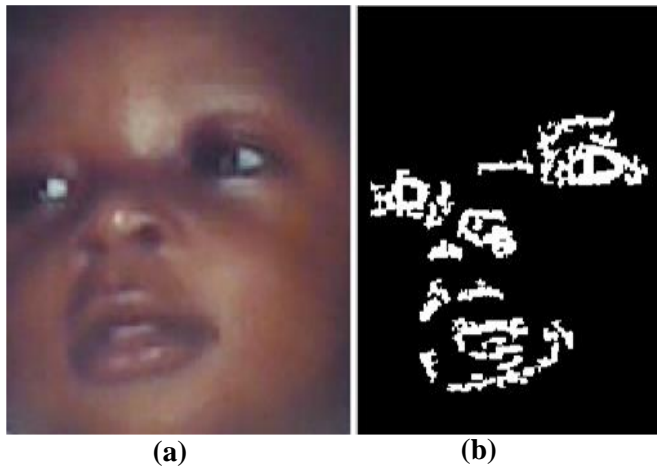


Fig. 5. (a) Found face region (b) LoG filtered image.

The application of the LoG filter helps to define facial features properly. With this, the facial feature of eyes and mouth can be extracted. The image resulting from the LoG filter is divided into three regions of right (R), left (L) and down (D) regions as shown in Fig. 6. The right eye is detected in the right region and the left eye in the left region by using the following criteria according to [25];

- (i) The X position of right eye should be in region of $0.125 \times width$ to $0.405 \times width$;
- (ii) The X position of left eye should be in region of $0.585 \times width$ to $0.865 \times width$;
- (iii) The Y position of left eye and right eye should be less than $0.5 \times height$;
- (iv) Area should be greater than 100 pixel square; and
- (v) Bounding box ratio of label should be in the region of 1.2 to 4

where *width* in the criteria denotes the width of the face image and *height* denotes height of face image [25].

If a label in the right region satisfies criteria (i), (iii), (iv) and (v), it is selected to be a right eye. Similarly, if a label in the left region satisfies criteria (ii), (iii), (iv) and (v) then it is selected to be the left eye. If right eye and left eye is selected successfully, mouth can be selected using the isosceles triangle matching rule. According to [26], the two eyes and mouth generate an isosceles triangle and also the distance between the two eyes and the midpoint of the eyes to mouth are equal. Any component of the down region can pass for mouth candidate. Therefore, to find mouth the following steps were taken.

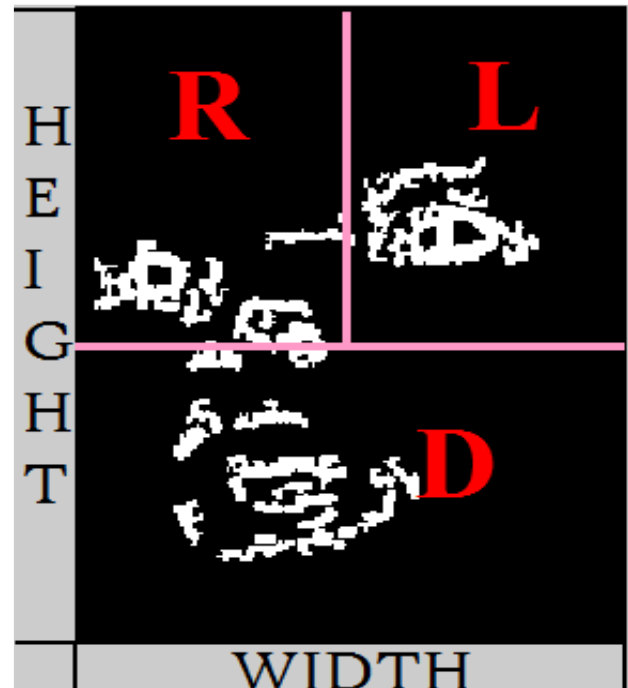


Fig. 6. Division of filtered image into three regions.

If a label in the right region satisfies criteria (i), (iii), (iv) and (v), it is selected to be a right eye. Similarly, if a label in the left region satisfies criteria (ii), (iii), (iv) and (v) then it is selected to be the left eye. If right eye and left eye is selected successfully, mouth can be selected using the isosceles triangle matching rule. According to [26], the two eyes and mouth generate an isosceles triangle and also the distance between the two eyes and the midpoint of the eyes to mouth are equal. Any component of the down region can pass for mouth candidate. Therefore, to find mouth the following steps were taken.

Euclidean distance of right eye to a possible mouth (R_x) and Euclidean distance of left eye to a possible mouth (L_x) is calculated. Euclidean distance between the midpoint of eyes and the possible mouth (M_x) is calculated and lastly Euclidean distance between the two eyes (E_x) is also calculated. From the calculated distance, the mouth was found by determining the absolute difference between R_x and L_x and the absolute difference between E_x and M_x . The sum of the two differences is used in determining the total error T_e using the mathematical expressions in (10), (11) and (12) respectively.

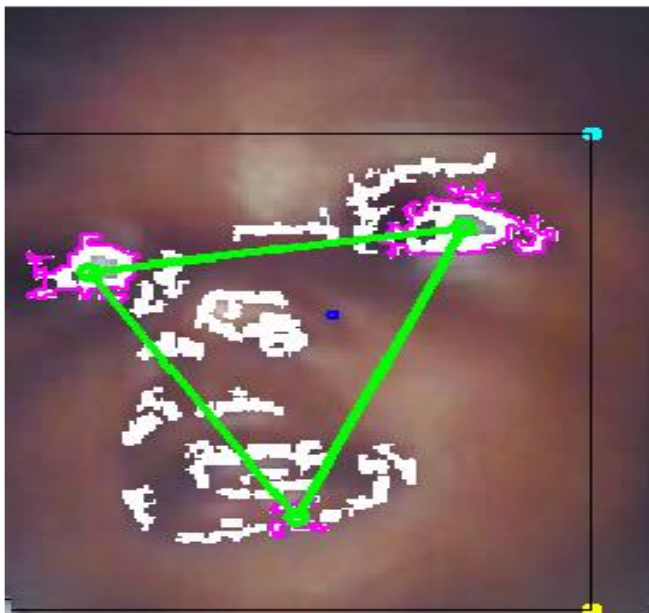
$$d_1 = |R_x - L_x| \tag{10}$$

$$d_2 = |E_x - M_x| \tag{11}$$

$$T_e = d_1 + d_2 \tag{12}$$

where d_1 and d_2 are the absolute differences between $|R_x \text{ and } L_x|$ and $|E_x \text{ and } M_x|$ respectively. If the values of d_1 and d_2 are less than 0.25 of the Euclidean distance between the two eyes $K(E_x)$, then the component is possibly a mouth. The component with the minimum total

error $K(T_e)$ is selected as mouth. If mouth is found it means the facial features, eyes and mouth which are the required features to be extracted has been found. On the basis of the found facial features, verified face image is extracted. Fig. 7a and Fig. 7b show the isosceles matching of the two eyes and mouth on the image and the extracted final image obtained respectively.



(a)

Fig. 7a. Extraction of facial feature.



(b)

Fig. 7b. Detected face image.

4. Developed Face Detection Algorithm Performance Evaluation

After the successful development of the face detection algorithm, its performance evaluation was carried out. In order to present and discuss the performance evaluation of the developed face detection algorithm satisfactorily, this section is divided into two subsections. In the first subsection, the actual detection accuracy of the algorithm was evaluated using three different performance indices. In the second subsection, the comparative performance evaluation of the developed algorithm was carried out by comparing its result with other related studies in the surveyed literature.

4.1 Developed Algorithm Detection Accuracy Evaluation

The developed algorithm's detection accuracy performance evaluation was conducted using the Bao face database. The database contains a total of 370 color images. 149 of the images contain just one person while the remaining 221 contain more than one person. The primary purpose of the database is for measuring face detection algorithm. Images in this database were taken under uncontrolled conditions; i.e. uncontrolled illumination, varying pose, different facial expression for both outdoor and indoor images. From this database 102 images were selected randomly to evaluate the performance of the algorithm. Images were also selected randomly to test the performance of the algorithm using the following parameters: true positive (TP), which are the total numbers of faces correctly detected as faces, true negative (TN), which are the total numbers of non-faces correctly detected as non-faces and false positive (FP), which are the total numbers of non-faces wrongly detected as face. The performance indices employed in evaluating the developed algorithm are the correct detection rate (CDR), miss rate (MR) and false detection rate (FDR). In estimating the performance indices, the mathematical expression used are as follows;

$$CDR = \frac{TP}{TF} \times 100\% \quad (13)$$

$$MR = \frac{TN}{TF} \times 100\% \quad (14)$$

$$FPR = \frac{FP}{TF} \times 100\% \quad (15)$$

where TF is the total number of faces. The result of the measured detection accuracy for the developed algorithm is presented in Table 1.

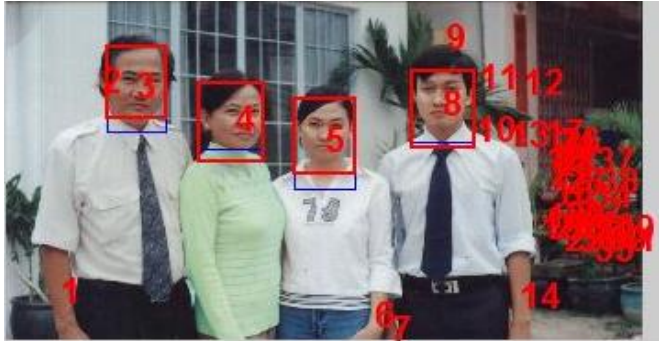
Table 1. Detection rate accuracy result

Image used	Number of image	Without white balance correction			With white balance correction		
		CDR (%)	MR (%)	FPR (%)	CDR (%)	MR (%)	FPR (%)
Bao-Database	102	71.57	28.43	2.94	81.37	18.62	2.94
Selected Random Image	15	73.33	26.67	0.00	80.00	20.00	0.00

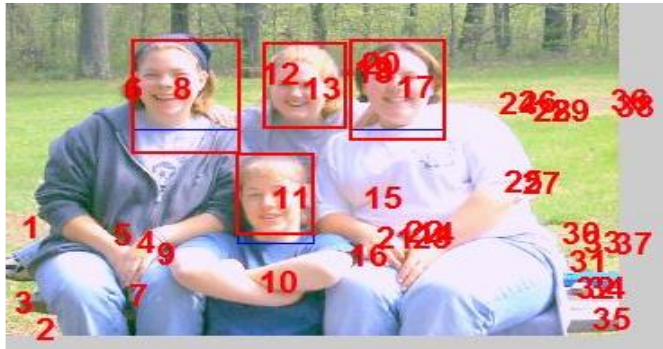
Table 1 shows the correct detection rate, miss rate and false positive rate for the developed algorithm with and without white balance correction. The Table shows that with white balance correction, the detection rate of the algorithm improves from 71.57% when there was no white balance correction to 81.37% when there was white balance correction for the Bao database. Similarly, for the images taken at random, there was an increase in detection rate from 73.33% to 80% when there was no white balance correction and when there was white balance correction respectively. The overall result shows that the developed algorithm performs satisfactory well with an average correct detection rate that is over 70.0% with and without white balance correction.

In addition, the detection accuracy of the developed algorithm for this study was further evaluated using a group photograph from Bao-database that consists of dissimilar frontal face sizes as well as complex background as shown in Fig. 8a and Fig. 8b. The obtained results of the face finding and face feature extraction analyses and typical isosceles checking as well as some typical faces detected when Fig. 8a and Fig. 8b were used to evaluate the performance of the developed algorithm are shown in Fig. 9a-d. Three out of the images in Fig. 8a and Fig. 8b were selected for final analysis in Fig. 9c and Fig. 9d because of space.

The results show that the developed algorithm is able to detect each of the faces despite the fact that they are of dissimilar frontal face sizes. Similarly, critical analysis of Fig. 9a and Fig. 9b show that the developed algorithm is capability of distinguishing faces from non-faces in an image with complex background. This capability also shows that occurrence of face(s) in a complex background has no negative impact on the detection accuracy of the developed face detection algorithm for this study.



(a)
Fig. 9a. Face finding result for Fig. 8a.



(b)
Fig. 9b. Face finding result from Fig. 8b.

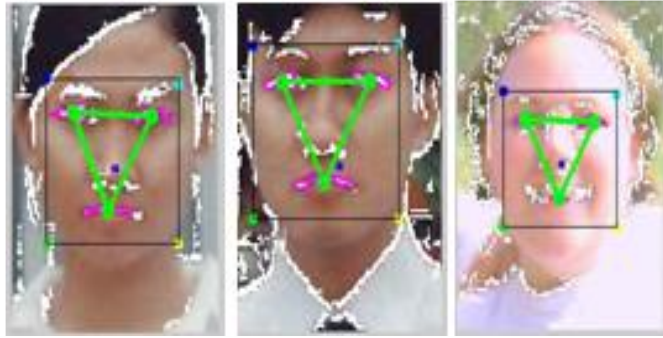


(a)



(b)

Fig. 8. Original images with complex background.



(c)

Fig. 9c. Some selected face feature results from Fig. 9a and Fig. 9b.



(d)

Fig. 9d. Some Detected faces Fig. 9c.

4.1 Developed Algorithm Comparative Performance Evaluation

In order to further evaluate the performance of the developed face detection algorithm, results obtained from it were compared with similar face detection algorithm developed using the same Bao database for testing. The direct comparison of the present work with other similar studies in the surveyed literature is presented in Table 2. The choice of the reference studies, [9,27,28] were characterized by using the same Baodatabase for the evaluation however, the reference studies employed different features and methods. The result of the comparative performance evaluation shows that only two out of the three studies used

in the comparative performance evaluation outperform the present work while the present work outperforms the third reference study. Comparing the detection rate of the developed algorithm in this study with corresponding detection rates in the reference studies show that the algorithm developed in this study performs relatively well with similar studies in the surveyed literature

Furthermore, the performance of the developed algorithm for this study was further evaluated by comparing its computational time with other similar studies in literature. The results of the computational time taken for another three different algorithms on face detection in literature were compared with the computational time taken for the algorithm developed in this study. Although, the processors and the memories of the systems used in running those algorithms differ, the result of the computational time taken presented in Table 3 shows that the algorithm developed in this study has a lesser computational time taken of 2.46 seconds. The comparative computational time taken result shows that the algorithm developed for this study outperforms others despite the fact that it has the largest image size compared with reference studies in literature. This significant advantage is as a result of the fact that the algorithm for this study does not work as a classifier.

Table 2. Comparative detection result of the present work and other published studies

Reference Author(s)	Feature and method employed	Testing Database	Detection rate (%)
Erdem <i>et al</i> (2011) [9]	Haar features and skin colour base classifier	Bao database	88.48
See <i>et al</i> (2013) [27]	Skin segmentation and edge detection	Bao database	84.70
Khammari and Chemesse (2013) [28]	Neural Network and Gaussian model	Bao database	77.47
Developed Algorithm	Skin segmentation and facial feature extraction	Bao database	81.37

Table 3. Comparative result of computational time of the present work and others

Author(s)	Method Applied	Image Size Range	Average Time (second)
Rowley <i>et al</i> (1999) [29]	Neural Network Based Face Detection	320 by 240	5.00
Garcia and Delakis (2002) [30]	Skin segmentation and edge detection	352 by 288	4.00
Mohammed <i>et al</i> (2008) [31]	Neural Network and Gaussian model	63 by 180 to 200 by 219	5.00
Developed Algorithm	Skin segmentation and facial feature extraction	189 by 219 to 320 by 408	2.00

5. Conclusion

In this paper, we have successfully developed a face detection algorithm that utilizes skin segmentation and facial feature extraction method to decrease high FDR in face detection algorithms. Similarly, we also employed white balance correction to correct any change in image temperature at the point of acquiring image in order to

improve the result of skin segmentation and the overall detection rate of the algorithm. In addition, the face detection algorithm for this study was developed without being trained as a classifier, which has considerably, reduces the computation complexity of the developed face detection algorithm in this study. Furthermore, the performance evaluation of the developed algorithm using Bao database, which is a standard face image detection database, shows

that the developed algorithm performs satisfactorily well with relatively high CDR. Typical results of the performance evaluation of the developed algorithm shows that the developed algorithm performed satisfactorily well with 81.37% detection rate. Furthermore, the comparative performance evaluation test carried out on the developed algorithm shows that the developed algorithm performs favorably well with other algorithms in literature with better computational time.

References

- [1] S. Zafeiriou, C. Zhang, and Z. Zhang, "A survey on face detection in the wild: past, present and future", *Computer Vision and Image Understanding*, vol. 138, pp. 1-24, 2015.
- [2] J. Jin, B. Xu, X. Liu, Y. Wang, L. Cao, L. Han, B. Zhou, and M. Li, "A face detection and location method based on feature binding" *Signal Processing: Image Communication*, vol. 36, pp. 179-189, 2015.
- [3] H. Pan, Y. Zhu, and L. Xia, "Efficient and accurate face detection using heterogeneous feature descriptors and feature selection", *Computer Vision and Image Understanding*, vol. 117, pp. 12-28, 2013.
- [4] G. Onder, and A. Kayacik, "Multiview face detection using Gabor filters and support vector machine", *Technical Report, IDE0852, Bachelor Thesis in Computer System Engineering, School of Science, Computer and Electrical Engineering, Halmsted University, Sweden, 2008.* Online [Available]: <https://www.diva-portal.org/smash/get/diva2:239370/FULLTEXT01.pdf>. Accessed on October 17, 2016.
- [5] D. Ghimire, and J. Lee, "A robust face detection method based on skin color and edges", *Journal of Information Process System*, vol. 9, no. 1, pp. 141-156, 2013.
- [6] C. Lin, and K-C. Fan, "Triangle-based approach to the detection of human face", *Journal of Pattern Recognition*, vol. 34, no. 6, pp. 1271-1284, 2001.
- [7] M.R Mahmoodi, and S.M. Sayedi, "A face detection based on kernel probability map", *Computers and Electrical Engineering*, vol. 46, pp. 205-216, 2015.
- [8] Y. Ban, S-K. Kim, S. Kim, K-A. Toh, and S. Lee, "Face detection based on skin color likelihood", *Pattern Recognition*, vol. 47, pp. 1573-1585, 2014.
- [9] C.E. Erdem, S. Ulukaya, A., Karaali, and A.T. Erdem, "Combining HAAR feature and skin colour based classifier for face detection", *In Proceedings of IEEE International Conference on Acoustic Speech and Signal*, Prague Congress Centre, Prague, Czech Republic, pp. 1497-1500, 22-27 May 2011.
- [10] M-H. Yang, D.J. Kriegman, and N. Ahuja, "Detecting faces in Images: A survey". *IEEE Transactions On Pattern Analysis and Machine Intelligence*, vol. 24, no. 1, pp. 34-58, 2002.
- [11] S.K. Singh, D.S. Chauhan, M. Vasta, and R Singh., "A robust skin colour based face detection algorithm", *Tamkang Journal of Science and Engineering*, vol. 6, no. 4, pp. 227-234, 2003.
- [12] H-J. Lin, S-Y. Wang, S-H. Yen, and Y-T. Kao, "Face detection based on skin color segmentation and neural network", *In proceedings of IEEE International Conference on Neural Networks and Brain*, Beijing, China, pp. 1144-1149, 13-15 October 2005.
- [13] Y. Wang, and B. Yuan, "A novel approach for human face detection from colour images under complex background", *Pattern Recognition*, vol. 34, no. 10, pp. 1983-1992, 2001.
- [14] M. Tayyab, and M.F. Zafar, "Face detection using 2D-discrete cosine transform and back propagation neural network", in *Proceedings of IEEE Conference on Emerging Technologies*, Islamabad, Pakistan, pp. 35-39, 19-20 October 2009.
- [15] J. Ruan, and J. Yin, "Face detection based on facial features and linear support vector machines", *In Proceedings of the International Conference on Communication Software and Networks*, Chengdu, Sichuan, China, pp. 371-375, 27-28 February 2009.
- [16] X. Liu, G. Geng, and X. Wang, "Automatically face detection based on bp neural network and bayesian decision", in *Proceedings of 6th IEEE International Conference on Natural Computation*, Yantai, China, pp. 1590-1594, 10-12 August 2010.
- [17] C. Aiping, P. Lian, T. Yaobin, and N. Ning, "Face detection technology based on skin color segmentation and template matching. *IEEE 2nd International Workshop on Education Technology and Computer*. Wuhan, China, pp. 708-711, 6-7 March 2010.
- [18] Z. Li, L.Xue, and F. Tan, (2010). "Face detection in complex background based on skin color features and improved adaboost algorithms", *IEEE International Conference on Progress in Informatics and Computing*, Shanghai, China, pp. 723-727, 10-12 December 2010.
- [19] E. Hjelmas, and B.K. Low, "Face detection: A survey", *Computer Vision and Image Understanding*, vol. 83, pp. 236-274, 2001.
- [20] H. Zhu, S. Zhou, J. Wang, and Z. Yin, "An algorithm of pornographic image detection", in *Proceedings of the 4th IEEE International Conference on Image and Graphics*. Chengdu, Sichuan, China, pp. 801-804. 22-24 August 2007.
- [21] M.J. Taylor, and T. Morris, "Adaptive skin segmentation via feature-based face detection", in *Proceedings of International Society for Optics and Photonics, (SPIE Photonics) Brussels, Belgium, 14-17 April 2014.* Online [Available]: http://www.cs.man.ac.uk/~tmorris/pubs/AdaptSS_SPIE.pdf. Accessed on 17 October 2016.
- [22] R.C. Mat, S. Azmi, R. Daud, A.N. Zulkifli, and F.K. Ahmad, "Morphological operation on printed circuit board (PCB) reverse Engineering using MATLAB", in *Proceedings of Knowledge Management International*

- Conference and Exhibition*, Legend Hotel Kuala Lumpur, Malaysia, pp. 529-533, 6-8 June 2006.
- [23] D. Chudasama, T. Patel, and S. Joshi, "Image segmentation using morphological operations", *International Journal of Computer Applications*, vol. 117, no. 18, pp. 16-19, 2015.
- [24] A. Khanparde, S. Reddy, and S. Ravipudi, "Face detection using color based segmentation and morphological processing – a case study", in *Proceedings of the International Symposium on Computer Engineering and Technology*, Mandi Gobindgarh, Punjab, India, pp. 147-151, 19-20 March 2010.
- [25] C. Gürel, "Development of a face Recognition System", *A Master of Science Thesis at the Atilim University, Ankara, Turkey*, p. 81, 2011. Online [Available]: <http://docplayer.net/2761592-Development-of-a-face-recognition-system-a-thesis-submitted-to-the-graduate-school-of-natural-and-applied-sciences-atilim-university-cahit-gurel.html>. Accessed on October 20, 2016.
- [26] H. Rahman, and J. Afrin, "Human face detection in colour images with complex background using triangular approach", *Global Journal of Computer Science and Technology Graphics and Vision*, vol. 13, no. 4, pp. 45-50, 2013.
- [27] Y.C. See, N.M. Noor, and A.C. Lai, "Hybrid face detection with skin segmentation and edge detection", in *Proceedings of 3rd IEEE International Conference on Signal and Image Processing Applications*. Melaka, Malaysia, pp. 406-411, 8-10 October 2013.
- [28] M. Khammari, and B. Chemesse, "Face detection in complex background of colour images using mixture gaussian model and neural network", *International Conference on System and Processing Information.*, Guelma, Algeria, 12 – 14 May 2013. Online [Available]: https://www.researchgate.net/profile/Chemesse_ennehar_Bencheriet/publication/257945701_Face_Detection_in_Complex_Background_of_Color_Images_Using_Mixture_Gaussian_Model_and_Neural_Network/links/02e7e53314aca3ee57000000.pdf. Accessed on October 17, 2016.
- [29] H. Rowley, S. Baluja, and T. Kanade, "Neural network-based face detection", *IEEE Transactions on Pattern Analysis and Machine intelligence*, vol. 20, no. 1, pp. 23–38, 1998.
- [30] C. Garcia, and M. Delakis, "A neural network architecture for fast and robust face detection", *IEEE 16th International Conference on Pattern Recognition*, Quebec City, Canada, vol. 2, pp. 44-47, 11-15 August 2002.
- [31] A. Mohamed, Y.W. Weng, J. Jiang, and S. Ipson, (2008). Face Detection Based Neural Networks Using Robust Skin Segmentation. In *Proceedings of the 5th IEEE International conference on Multi-Systems, Signals and Devices*. Amman, Jordan, pp. 1-5, 20-22 July 2008.

Thermal Stresses on a Reginal Cooling Plate

Ibrahim Koc*[‡]

*Department of Aircraft Fuselage-Engine Maintenance, School of Applied Sciences, Istanbul Gelisim University, 34215 Istanbul, Turkey

(ibkoc@gelisim.edu.tr)

[‡]Corresponding Author; Ibrahim Koc, Department of Aircraft Fuselage-Engine Maintenance, School of Applied Sciences, Istanbul Gelisim University, 34215 Istanbul, Turkey, Tel: +90 212 422 7020, Fax: +90 212 422 7401, ibrahimkoc4951@gmail.com

Received: 14.04.2017 Accepted: 21.07.2017

Abstract- In this study, stresses and strains that occur on the surface of material are investigated for a flat plate that is made cooling as numerically and analytically. The cooling blowing ratios applied to the surface vary between 0.5 and 1.75. The cooling injection angle is 30 degrees with the horizontal. Plexiglas plate were used in experiments which done for analytical solution and numerical modelling studies. Air was injected to cooling zone at 57 °C and 77 °C. The results show that the cooling surface size varies with the blow ratio. In addition, the sizes of thermal stresses and displacements of surface set out that they are indicators of cooling.

Keywords Cooling, thermal stress, cooled plate.

1. Introduction

Generally, the formation of any temperature gradient along the wall of a container causes thermal stress. Detailed thermal stress analysis for spherical and cylindrical containers is given [1-4].

Composite materials, which are made of ceramics and metals, are already used in heat resistant parts, such as pistons. Functionally gradient materials (FGM) are composite materials. They reduce the thermal stress and they are resistant to super high temperature. In order to support the design of FGM, the computer programs that analyses the transient heat transfer and the transient thermal stress of FGM have developed [5]. The finite element method is used in this study.

Application of Taylor transformation to the thermal-stresses in isotropic annular fins presents the stresses distribution in a perfectly elastic isotropic annular fin. The stresses distribution is integrated obtain the results. The thickness of the fins is assumed sufficiently small so as to have a state of plane stress and one-dimensional heat conduction [6]. "A coupled heat transfers and thermal stress analysis is developed for a thin-film high T_c superconductor device" [7]. The stress fields in the adhesive layer and the composite members of two tee joints bonded to a rigid base and a flexible plate were investigated [8].

In this study, the inclined jet was applied on the Plexiglas plate. Stress and strain in the material were investigated numerically and analytically.

2. Experimental Apparatus and Procedure for Analytical Solution

A schematic view of wind tunnel used in the experiments which done for analytical solution is presented in Figure 1. The test set up consists of a fan, heater, orifice, plenum chamber, Plexiglas plate, thermocouple, hot-wire anemometry, miniature wire probe (55P15), probe support for single-sensor probe, traverse system and computer. The test section is 460 mm wide, 460 mm high and 610 mm long. The blowing ratios are 0.50, 0.75, 1.0, 1.25, 1.50, 1.75 and the injection angle with respect to the horizontal plane is 30°.

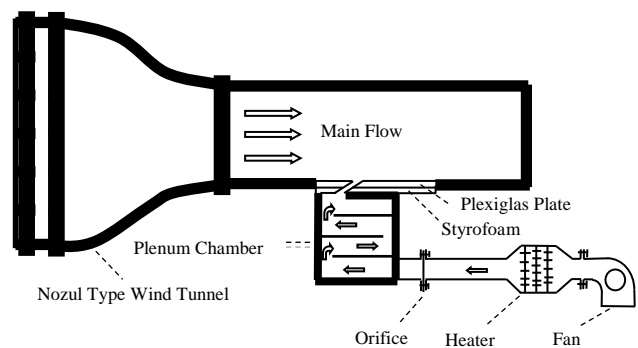


Fig. 1. Schematic view of test facility.

In the experiments, a transparent Plexiglas plate with a small conduction coefficient is used. A plenum chamber is used to supply a steady injection. The orifice made of Plexiglas was designed to measure the flow rate of injected

air. Centrifugal fan for injection of air from out to the test chamber and the heater for getting up the ambient temperature to 330 K and 350 K and a rheostat for controlling the power of heater are used. The heater has two resistances and both of them are 1000 W. Oblique manometer for calculating mass flux of air, which is injected, and the insulation material which is 5 mm thickness for preventing the heat losses from Plexiglas surface to the surroundings are used. In addition, digital thermometer and the thermocouples which are K (Chromel-Alumel) type for measuring of temperature also the cardboards for getting different mass fluxes in experiments are used.

Eleven injection holes in a single row are located on a Plexiglas plate for thermal stress and strain investigation. The hole's cross-section diameters are 8.5 mm. All of the hole geometries in the model are cylindrical and they have the same cross-section area value. The injection angles are 30° to the surface and main flow. Measurements were made for cylindrical holes at the exit of the sixth hole. Schematic view of cylindrical holes is presented in Figure 2. The place of the coordinate axes was considered as out of the sixth hole.

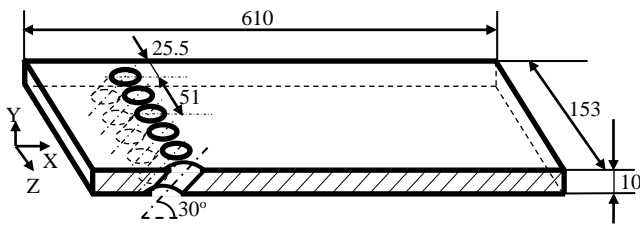


Fig. 2. Schematic view of cylindrical holes with a row.

Plexiglas plate was fastened the wind tunnel test room's surface as shown Figure 3. In order to measure the temperature of Plexiglas surface, thermocouples were fitted to the surface. The position of the thermocouples, K type, is shown Figure 3.

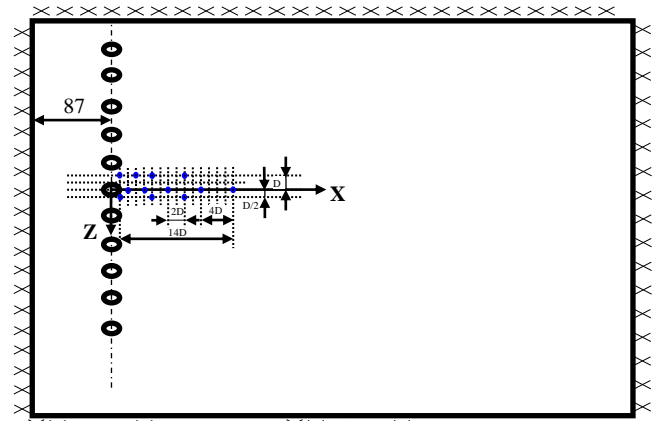


Fig. 3. The position of thermocouples on the Plexiglas plate.

In the experiments, the warmer air from the main flow air is injected into the wind tunnel at an angle of 30 degrees. The main flow velocity is measured by using hot wire probe 55P11 (Dantec hot-wire probe). The injection velocities are used for the calculations of blowing ratios. These velocity values were found by using orifice. The suitable velocities were regulated by using the cardboards that are attached on the fan. Hot-wire anemometry is used for the measurement of velocity in single dimension. This device is also called Constant-Temperature Anemometer (CTA). The measurement probe is calibrated in the wind tunnel before the measurement of velocity is experimented. The velocity values, 0, 5, 10, 15, 20, 25 and 30 m/s, were considered for calibration. The traverse system is used for moving the probe to a known point. The computer is used for analyzing the data obtained from the hot wire anemometry.

Measurements were done for cylindrical holes. The air is injected 57 °C and 77 °C. The blowing ratios are 0.50, 0.75, 1.00, 1.25, 1.50 and 1.75. The injection velocity is used for the calculation of blowing ratio. This velocity value was found by using orifice. Data used in measurements are given in Table 1.

Table 1. The values used to measure blowing ratio

Hole geometry	The injection air				The main flow characteristics				
	$T_j(K)$	$V_j(m/s)$	$\rho_j(kg/m^3)$	$\dot{m}(kg/s)$	$T_\infty(K)$	$V_\infty(m/s)$	$\rho_\infty(kg/m^3)$	M	I
Cylindrical		6.17		0.0041	298.5		1.1845	0.50	0.295
		9.26		0.0061	296.4		1.1943	0.75	0.659
	330	12.34	1.0516	0.0082	298.5	10.70	1.1845	1.00	1.180
		15.43		0.0102	297.3		1.1901	1.25	1.837
		18.51		0.0123	298.9		1.1826	1.50	2.660
		21.60		0.0143	296.9		1.1920	1.75	3.470
		6.35		0.0039	298.6		1.1840	0.50	0.317
		12.69		0.0079	298.9		1.1826	1.00	1.271
	350	15.86	0.9980	0.0099	298.2	10.34	1.1859	1.25	1.979
		19.04		0.0119	298.2		1.1859	1.50	2.853
	22.21		0.0138	298.2		1.1859	1.75	3.882	

The mainstream air velocity and the injected air velocity ratio are determined according to the blowing ratio:

$$M = \frac{\rho_j V_j}{\rho_\infty V_\infty} \quad (1)$$

Where M is the blowing ratio, ρ_j is the injected fluid density, V_j is the injected fluid velocity, ρ_∞ is the main flow density and V_∞ is the main flow velocity. The injected cooling air temperature was selected as 330 and 350 K.

One of the parameters that affect the flow field is the momentum flux ratio. The momentum flux ratio is used as some physical justification for choosing the blowing ratio. It is well accepted that the key parameter of jet penetration in a cross flow is the momentum flux ratio, shown in equation 2. In the experiments, the different momentum fluxes are obtained by changing the temperature of the injected air. The momentum flux ratio is determined by as follows [9]:

$$I = \frac{\rho_j V_j^2}{\rho_\infty V_\infty^2} \quad (2)$$

Where I is the momentum flux ratio. The values of momentum flux ratio are given in table 1.

The hot air which is 330 K is injected into the main flow which is about 10.70 m/s velocity. The hot air which is 350 K is injected into the main flow which is about 10.34 m/s velocity. In experiments, the temperatures on the Plexiglas plate were measured for the second hole in different mass fluxes by using thermocouples. The thermal stress and strain was calculated from measuring temperatures.

The ambient temperature is heated in the heater and then it is forwarded to the plenum chamber and it is exerted to pressure in plenum chamber and it is injected into the main flow for injection holes which are 30° to the main flow.

The temperature of the air which is injected from holes and the temperature of main flow should be known for calculations of thermal stress and strain. Therefore, one piece number thermocouples are located to the entering of Plexiglas in the wind tunnel.

In analytical solutions, the thermal stresses and strains variations on cooled plate which is made of Plexiglas material are investigated for the different blowing ratios which are defined in top. The 2D thermal stress field was calculated for different blowing ratios at flat surface. The thermal stress was calculated from temperatures using the following equation:

$$\sigma = \alpha \Delta T E \quad (3)$$

$$\alpha = \frac{1}{L} \frac{\Delta L}{\Delta T} \quad (3.1)$$

Where σ is the stress, α is the coefficient linear thermal expansion, ΔT is temperature difference, E is the modulus of elasticity, L is the length of material and ΔL is the elongation. In the analytical solution and numerical study the modulus of elasticity (E) and the coefficient linear thermal

expansion (α) were taken $3.102 \cdot 10^3 \text{ N/mm}^2$ [10] and $7.5 \cdot 10^{-5}$ [11] respectively.

3. Numerical Investigation

Computations are performed to simulate thermal stresses over the cooled plate. The 3D computational domain is shown in Figure 4. GAMBIT software [12-15] was used to create the geometry and related mesh for the domain. A commercial CFD code based upon finite element volume, FLUENT 5.4 [12-15] has been applied to the flow simulation.

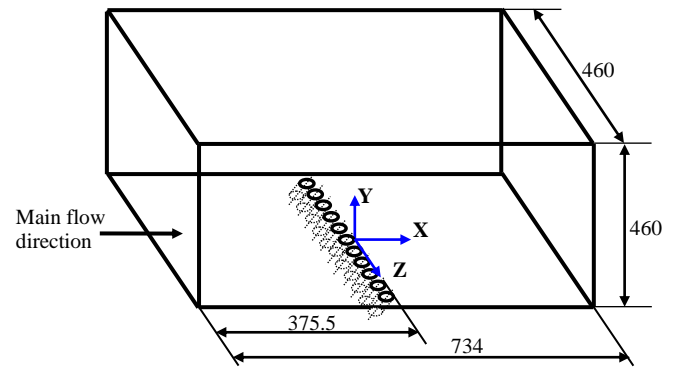


Fig. 4. Schematic view of the wind tunnel model.

Tetrahedral mesh for the injection holes and hexahedral mesh for the rest of the domain were used. The injection holes were finer meshed compared to other sections. Standard k-ε turbulence model [16] and standard wall function [17] are employed. The standard k-ε model is a semi-empirical model and it is based on model transport equations for the turbulent kinetic energy (k) and its dissipation rate (ε). The model transport equation for k is derived from the exact equation, while the model transport equation for ε is obtained using physical reasoning and bears little resemblance to its mathematically exact counterpart. In the derivation of the k-ε model, it was assumed that the flow is fully turbulent and the effects of molecular viscosity are negligible. The wall function is used between the turbulent zone and the wall. Therefore, the distance from the wall at the cells adjacent to the wall was determined by considering the range over which the log law is valid.

The distance, which is between the best adjacent mesh and the surface, was considered. Non-dimensional numbers were defined [18]:

$$y^+ = \frac{Y u^*}{\nu} \quad (4)$$

$$u^* = \frac{U}{u^+} \quad (4a)$$

$$u^+ = \frac{1}{\kappa} \ln E y^+ \quad (4b)$$

In equation (4), u^* is frictional velocity, is non-dimensional length, is non-dimensional velocity, U is the flow velocity and κ is von Karman constant, where κ is 0.4

and E is 9. y^+ is less than 10 value in the laminar zone. The turbulence models are not used at this zone. In generally, is recommended from 20 to 50 values. The suitable y^+ value was selected from 30 to 40 in numerical study.

The assumptions were as follows in numerical study. Heat loss from the injection holes' surfaces is not there and the system is steady state. The air is an ideal gas and it is compressible. In addition, radiation and conduction are neglected. The turbulence intensity for the main stream, for the jets entering the computation domain and for backflow is taken as 1 per cent.

In numerical study, the injected cooling air velocity and related temperature, the mainstream air velocity and related temperature were taken from the experiments.

4. Results and Discussion

The following results are found for the effects of blowing ratios and temperatures on the thermal stresses and the displacements of surface as analytical and numerical. The experiments which done for analytical solution were done at the injection temperature that are 330 and 350 K and the main flow temperature, which is ambient temperature. The experiments were carried out for with the blowing ratios and temperatures. The stress in main flow direction were evaluated for $z/D = 0$ at 330 K (Figures 5-10) and 350 K (Figures 11-15).

When the figures are investigated, the stress is high value in low-blowing ratios (Figures 5-10). The biggest stress is 0.5 in the present blowing ratios as shown in Figures 5-10. For example, in Figure 5, the stress is 4.4290 N/mm² for the numerical study at $X/D = 1$ at the 0.5 blowing ratio and in Figure 6 and Figure 7 and Figure 8 and Figure 9 and Figure 10, the stresses are 3.9342 N/mm² and 3.0555 N/mm² and 2.4912 N/mm² and 1.9171 N/mm² and 2.0474 N/mm² at the 0.75 and 1.00 and 1.25 and 1.50 and 1.75 blowing ratio in the same point, respectively. For the analytical study at $X/D = 1$ at the 0.5 blowing ratio, the stress is 3.7464 N/mm² in Figure 5. In Figure 6 and Figure 7 and Figure 8 and Figure 9 and Figure 10, the stresses are 3.4672 N/mm² and 3.1414 N/mm² and 2.2572 N/mm² and 2.7109 and 2.5248 N/mm² at the 0.75 and 1.00 and 1.25 and 1.50 and 1.75 blowing ratio in the same point, respectively. A similar situation can be seen in the figures in different points (Figures 5-10). From these results, the cooling surface is better at the 0.5 blowing ratio.

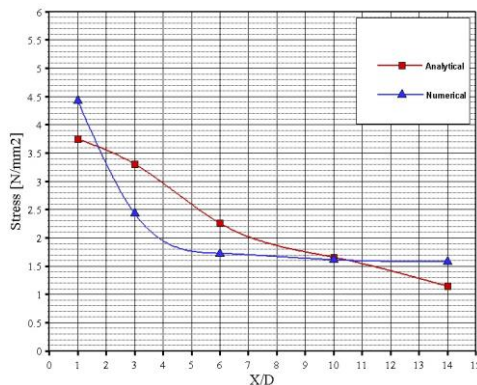


Fig. 5. The stress in the main flow direction for M=0.5(Z=0)

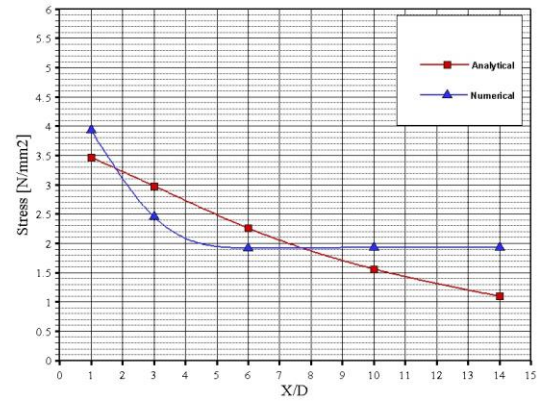


Fig.6. The stress in the main flow direction for M=0.75(Z=0)

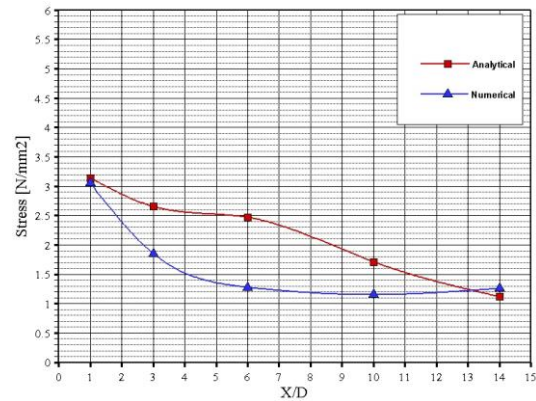


Fig.7. The stress in the main flow direction for M=1.00(Z=0)

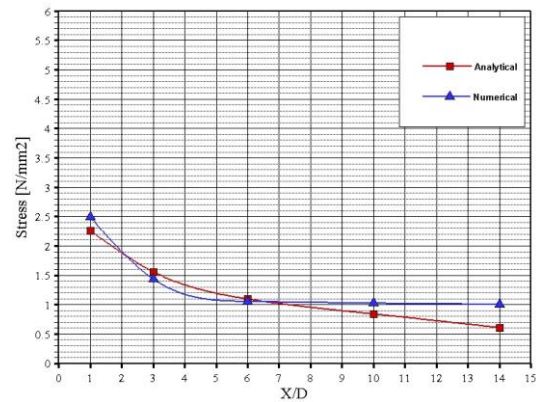


Fig.8. The stress in the main flow direction for M=1.25(Z=0)

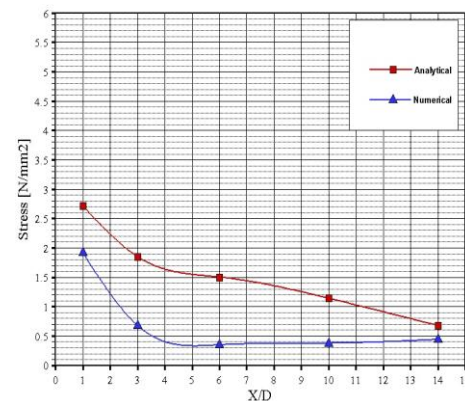


Fig.9. The stress in the main flow direction for M=1.50(Z=0)

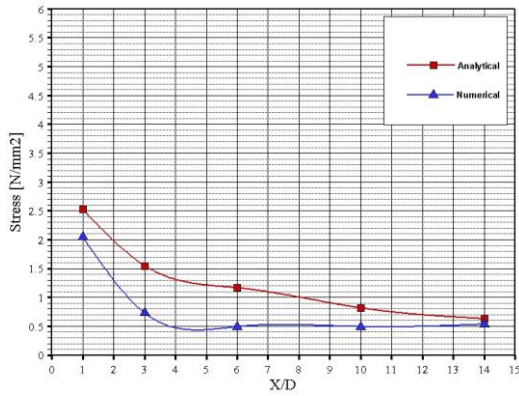


Fig.10. The stress in the main flow direction for M=1.75(Z=0)

When the differences between the injection temperature and main flow temperature are increased the stress increases for the same blowing ratios in mainstream direction (Figures 11-15). For example, in Figure 5, while the stress is 4.4290 N/mm² and 3.7464 N/mm² for 330 K injection temperature at X/D = 1 at the 0.5 blowing ratio, in Figure 11, the stress is 8.0220 N/mm² and 5.9105 N/mm² for 350 K injection temperature in the same point and the same blowing ratio.

Especially, this situation is seen in the high-blowing ratios as shown in Figure 10 and 15. For example, the maximum stress values are 2.0474 N/mm² and 2.5248 N/mm² for 1.75 blowing ratio at 330 K injection temperature (Figure 10) but they are 3.6360 N/mm² and 4.1420 N/mm² for the same blowing ratio at 350 K injection temperature (Figure 15).

The results of numerical and analytical studies were given for blowing ratios as similar comparing from figure 5 to figure 15. When the blowing ratio is increased, the stress decreases in both numerical and analytical studies for the main flow direction (Figures 5-15).

When the analytical and numerical studies were investigated their results are in good agreement each other as seen in Figures 5-15. The deviations of the numerical studies can result from the insufficiency of turbulence modelling in mixture part and from the wall function and from the assumptions.

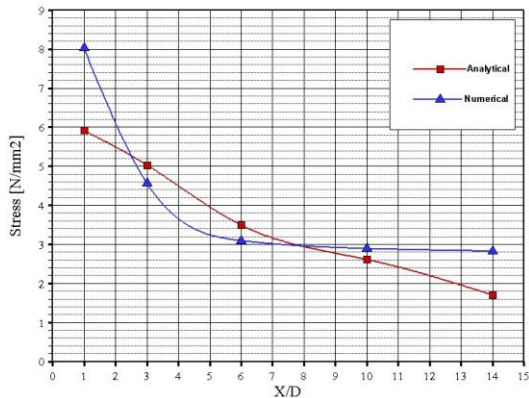


Fig.11. The stress in the main flow direction for M = 0.5 (Z=0)

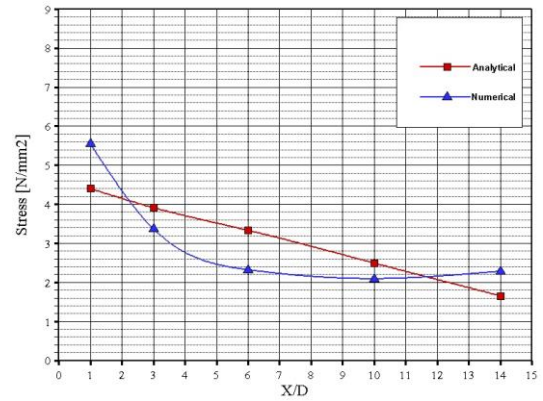


Fig.12. The stress in the main flow direction for M=1.00(Z=0)

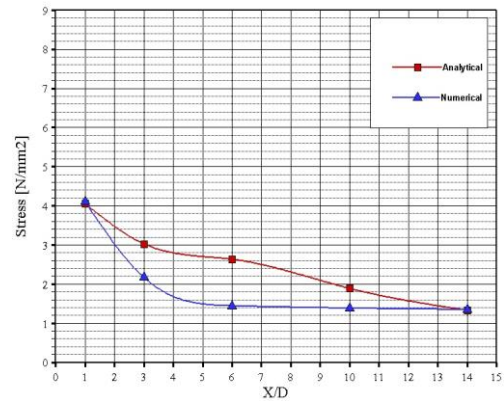


Fig.13. The stress in the main flow direction for M=1.25(Z=0)

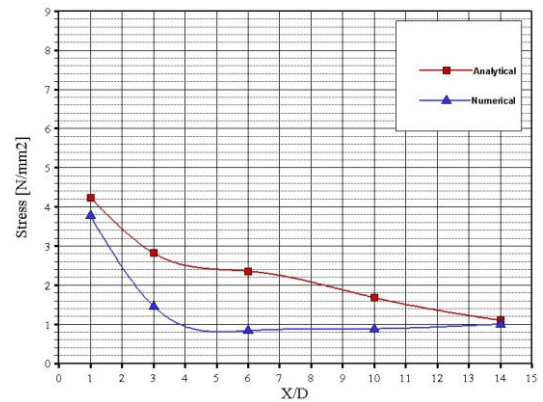


Fig.14. The stress in the main flow direction for M=1.50(Z=0)

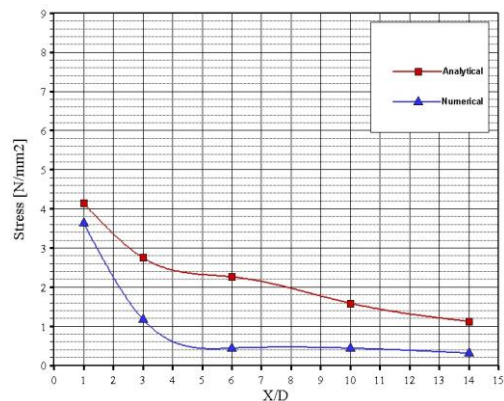


Fig.15. The stress in the main flow direction for M=1.75(Z=0)

The results of measuring of strain on the flat surface show that the value of strain is bigger in the low blowing ratios (Figures 16-21). It is difficult to bend the injection coming from holes at the high blowing ratios. Moreover, there are more separations from the surface at the high blowing ratios. Therefore, the high strain exists near the hole regions for the low blowing ratios.

For example, in Figure 16, the strain is 856.50 μm for the numerical study at $X/D = 1$ at the 0.5 blowing ratio and in Figure 17 and Figure 18 and Figure 19 and Figure 20 and Figure 21, the strains are 760.81 μm and 590.89 μm and 481.76 μm and 370.73 μm and 395.93 μm at the 0.75 and 1.00 and 1.25 and 1.50 and 1.75 blowing ratio in the same point, respectively. For the analytical study at $X/D = 1$ at the 0.5 blowing ratio, the strain is 724.50 μm in Figure 16. In Figure 17 and Figure 18 and Figure 19 and Figure 20 and Figure 21, the strains are 670.50 μm and 607.50 μm and 436.50 μm and 524.25 μm and 488.25 μm at the 0.75 and 1.00 and 1.25 and 1.50 and 1.75 blowing ratio in the same point, respectively. A similar situation can be seen in the figures in different points (Figures 16-21). From these results, the strain on the cooling surface is bigger at the 0.5 blowing ratio.

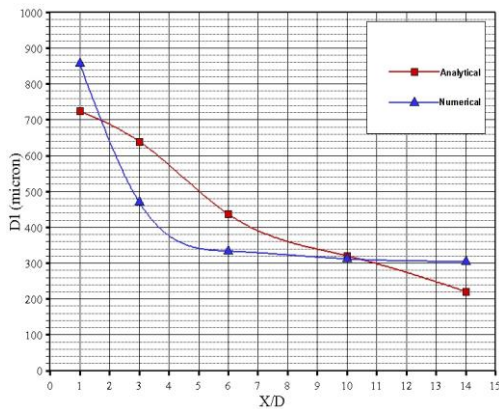


Fig.16. The strain in the main flow direction for M = 0.50 (Z = 0)

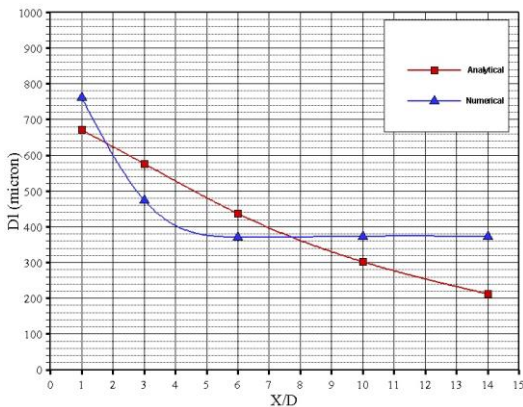


Fig.17. The strain in the main flow direction for M = 0.75 (Z = 0)

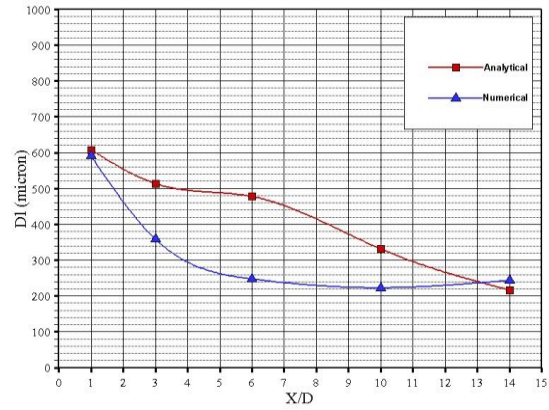


Fig.18. The strain in the main flow direction for M = 1.00 (Z = 0)

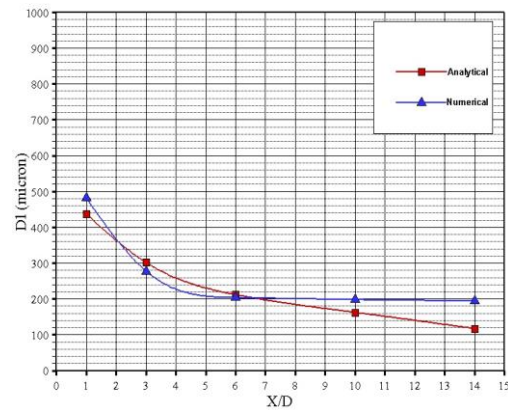


Fig.19. The strain in the main flow direction for M = 1.25 (Z = 0)

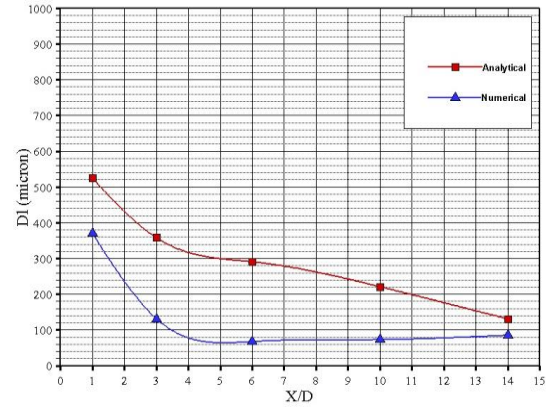


Fig.20. The strain in the main flow direction for M = 1.50 (Z = 0)

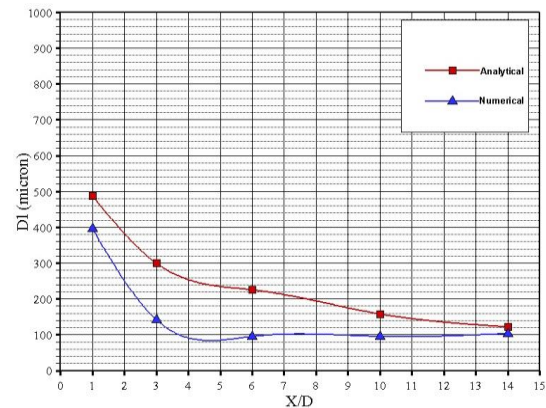


Fig.21. The strain in the main flow direction for M = 1.75 (Z = 0)

When the differences between the injection temperature and main flow temperature are increased the strain increases for the same blowing ratios in mainstream direction (Figures 16, 22). For example, in Figure 16, while the strains are 856.50 μm and 724.50 μm for 330 K injection temperature at $X/D = 1$ at the 0.5 blowing ratio, in Figure 22, the strains are 1551.32 μm and 1143.00 μm for 350 K injection temperature in the same point and the same blowing ratio.

The results of numerical and analytical studies were given for blowing ratios as similar comparing from figure 22 to figure 26. When the blowing ratio is increased, the strain decreases in both numerical and analytical studies for the main flow direction (Figures 22-26).

When the analytical and numerical studies were investigated their results are in good agreement each other as seen in Figures 22-26. The deviations of the numerical studies can result from the insufficiency of turbulence modelling in mixture part and from the wall function and from the assumptions.

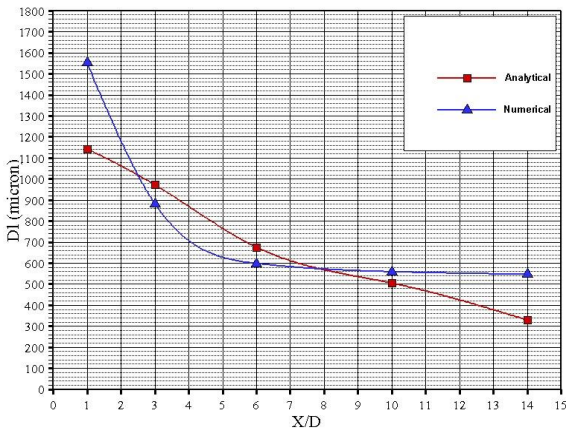


Fig.22. The strain in the main flow direction for $M = 0.50$ ($Z = 0$)

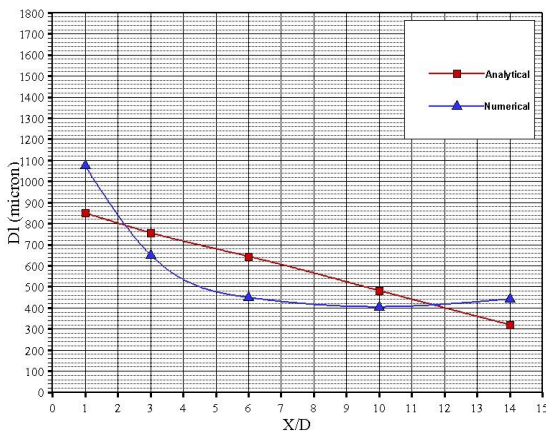


Fig.23. The strain in the main flow direction for $M = 1.00$ ($Z = 0$)

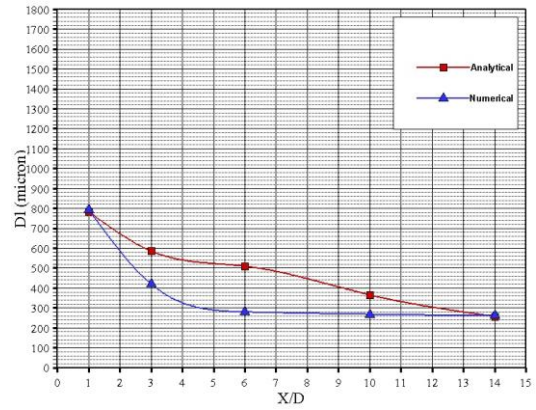


Fig.24. The strain in the main flow direction for $M = 1.25$ ($Z = 0$)

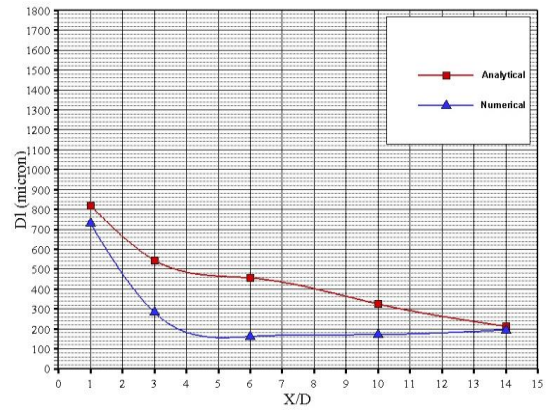


Fig.25. The strain in the main flow direction for $M = 1.50$ ($Z = 0$)

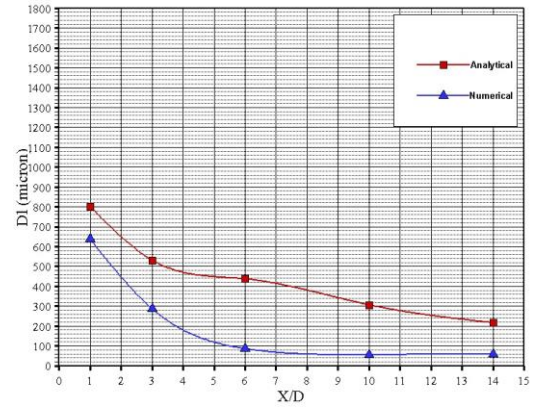


Fig.26. The strain in the main flow direction for $M = 1.75$ ($Z = 0$)

5. Conclusion

In this study, stresses and strains which occur on the surface of material are investigated for a flat plate which is made cooling as numerically and analytically. As on conclusions following results are found:

- the blowing ratio and injection temperature affect the stress and strain on cooled flat;
- the stress and strain are reduced in main flow direction;
- for stress and strain, the biggest values are blowing ratio 0.5 in the main flow direction;

- when the blowing ratio is increased the stress and strain decrease in main flow direction;
 - when the difference between the injection and main flow temperature is increased the stress and strain increase in main flow direction;
 - the value of cooling effectiveness is better in the low blowing ratios;
 - the stress and strain are higher in the region close to the hole because of the jet impact;
 - the penetration of the jets which have low blowing ratios into the main flow is better than the others;
- the stress and strain decrease away from the jet holes.

References

- [1] S. Timoshenko and J.N. Goodier, *Theory of Elasticity*, McGraw-Hill, New York, 1951.
- [2] B. A. Boley and J. Fr. Weiner, *Theory of Thermal Stresses*, Wiley, New York, 1960.
- [3] W. Nowaki, *Thermo-Elasticity*, Pergamon Press, Oxford, 1965.
- [4] W. Johnson and P.B. Mellor, *Engineering Plasticity*, Ellis Harwood, London, 1983.
- [5] T. Fuchiyama and N. Noda, "Analysis of Thermal Stress in a Plate of Functionally Gradient Material", *The Society of Automotive Engineers of Japan*, vol. 16, No.3, pp. 263-268, 1995.
- [6] L.T. Yu and C.K. Chen, "Application of Taylor Transformation to the Thermal Stresses in Isotropic Annular Fins", *J. Therm. Stresses.*, vol.21, No.8, pp. 781-809, 1998.
- [7] B. Gu, P.E. Phelan and S. Mei, "Coupled Heat Transfer and Thermal Stress in High-t-c Thin-Film Superconductor Devices", *Cryogenics*, vol. 38, No.4, pp. 411-418, 1998.
- [8] M.K. Apalak, Z.G. Apalak and R. Gunes, "Thermal and Geometrically Nonlinear Stress Analyses of an Adhesively Bonded Composite Tee Joint with Double Support", *J. Thermoplast. Compos.*, vol. 17, No.2, pp. 103-136, 2004.
- [9] R.J. Goldstein, E.G.R. Eckert and F. Burggraf, "Effects of Hole Geometry and Density on Three-Dimensional Film Cooling", *Int. J. Heat. Mass. Tran.*, vol. 17, pp. 595-607, 1974.
- [10] Altuglas International Arkema Inc., *Exceptional Grade for Broad-Range Applications*. Altuglas International Arkema Inc. 100 PA Rt. 413 Bristol, PA 19007, 2015, www.altuglasint.com
- [11] Evonik Industries, *PLEXIGLAS® GS/PLEXIGLAS® XT Product Description*, Evonik Röhm GmbH, Kirschenallee, 64293 Darmstadt, Germany, 2015, www.evonik.com
- [12] Fluent Incorporated (1998a), *Gambit: Tutorial Guide*, Fluent Incorporated, Lebanon, NH.
- [13] Fluent Incorporated (1998b), *Gambit: User's Guide*, Fluent Incorporated, Lebanon, NH.
- [14] Fluent Incorporated (1998c), *FLUENT 5 User's Guide*, Fluent Incorporated, Lebanon, NH.
- [15] Fluent Incorporated (1998d), *FLUENT Tutorial Guide*, Fluent Incorporated, Lebanon, NH.
- [16] B.E. Launder and D.B. Spalding, *Lectures in Mathematical Models of Turbulence*, Academic Press, London, 1972.
- [17] B.E. Launder and D.B. Spalding, "The numerical computation of turbulent flows", *Computer Methods in Applied Mechanics and Engineering*, vol.3, pp. 269-89, 1974.
- [18] C-J. Chen and S-Y. Jaw, *Fundamentals of Turbulence Modelling*, Taylor & Francis, Washington, DC, 1998.

Improving Torsional Rigidity and Seismic Performance of Tunnel Form Building Structures

Can Balkaya*[‡], Ihsan Karagoz** , Ismihan Gunal***

*Department of Civil Engineering, Faculty of Engineering and Architecture, Istanbul Gelisim University, Istanbul, Turkey.

**Department of Civil Engineering, Faculty of Engineering and Architecture, Beykent University, Istanbul, Turkey.

***Department of Civil Engineering, Faculty of Engineering, Suleyman Demirel University, Isparta, Turkey.

(cbalkaya@gelisim.edu.tr, ihsankaragoz@beykent.edu.tr, igunal@gelisim.edu.tr)

[‡]Corresponding Author; Can Balkaya, Department of Civil Engineering, Istanbul Gelisim University, Istanbul, Turkey,

Tel: +90 212 422 7020, Fax: +90 212 422 7401, cbalkaya@gelisim.edu.tr

Received: 21.04.2017 Accepted: 11.09.2017

Abstract- Tunnel form buildings, which have shear-wall dominant structural systems, are usually built in countries exposed to substantial seismic risk and very commonly used because of its fast construction technique and low cost. Very limited research has been directed to their experimental studies on 3D behavior, seismic performance, load capacities, collapse mechanisms, and crack propagations. Previous studies indicate that most of the time the first period of the structure is torsion due to construction techniques outer faces is open to take the tunnel forms to out by cranes. This will cause less torsional rigidity, whereas for strong earthquakes, torsional rigidity has to be increased. Four different strengthening techniques, i.e., steel braces, reinforced concrete (RC) infill shear wall, precast concrete shear wall, and RC shear wall at the façade, were applied to improve torsion rigidity. Experimental studies and 3D nonlinear finite element analysis (FEA) were performed on models. The analytical model results, the economy and applicability of construction techniques suggest that steel bracing is the most suitable and practical method to improve torsional rigidity as well as seismic performance. Three-story scaled existing and strengthened experimental models are tested under pushover loads, and the results are compared with 3D nonlinear finite element analysis.

Keywords Tunnel form building, shear wall, experimental study, torsional rigidity, seismic performance, pushover loading.

1. Introduction

Tunnel form buildings, which have shear-wall dominant structural systems, are usually built in countries exposed to substantial seismic risk and very commonly used in Turkey. They are composed of vertical and horizontal panels set at right angles (Fig. 1), and all wall and floor elements are utilized as primary load-carrying members. Unlike conventional reinforced concrete (RC) structures, tunnel form buildings contain no beams and columns because they can be constructed rapidly and economically. However, despite the abundance of such structures, three-dimensional (3D) experimental studies on 3D behavior, seismic performance, load capacities, collapse mechanisms, and crack propagations have been limited. 3D behavior and

seismic performance of the tunnel form structures are previously studied [1–4] by nonlinear finite element analysis (FEA) and modeling. Balkaya and Kalkan [5] indicated that the first period is usually torsion due to construction techniques (Fig. 1) that leave the outer faces open; thus, tunnel forms can be placed and removed using cranes. The result is decreased torsional rigidity, whereas for strong earthquakes, torsional rigidity needs to be increased. The proposed method in this study can be used during new construction after tunnel form construction, or it can be used to increase the existing torsional rigidity and seismic performance of tunnel form buildings by retrofitting. To improve torsional rigidity also increase the seismic performance of the building due to additional rigidities in x and y directions.



Fig. 1. Tunnel form construction and formwork system.

In previous experimental studies, two four-story scaled building with one span specimens were tested under quasi-static cyclic lateral loading in longitudinal and transverse directions [6]. Yuksel SB [7] tested a full-scale shear wall using a test specimen that was designed to represent the lower stories of structural walls in high-rise tunnel form buildings.

In this study, four strengthening techniques were evaluated to determine if they increased torsional rigidity and seismic performance of shear-wall dominant tunnel form buildings. First, 3D nonlinear FEA was performed using SAP2000 for proposed models. The best strengthening method was selected. Then, for the selected steel brace method the results were compared with experimental tests. 3D and 1/3-scale three-story models of existing and strengthening tunnel form building with steel braces were tested under pushover loading to observe their seismic behavior and performance, torsional behavior, load capacities, and crack propagations. The concrete quality was C20 (20 MPa). The reinforcement and welded wire fabric was StIII (420), and the steel profile quality was St37. In

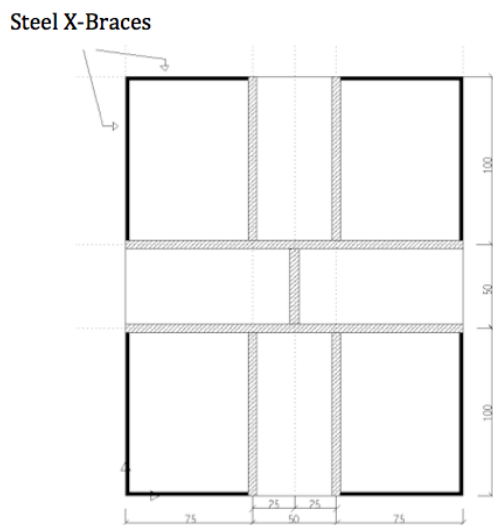
walls and slabs, $\varnothing 5/10$ StIII reinforcements were used in both directions.

2. Strengthening Techniques for Torsional Rigidity

Four strengthening techniques, i.e., steel braces, RC infill shear wall, precast concrete shear wall, and RC shear wall at the façade, were studied as shown in Fig. 2b, Fig. 2c, Fig. 2d. These techniques addressed the key consideration of closing the gaps due to tunnel form construction techniques.

2.1. Steel Brace

Fixing the steel brace at the upper and lower parts of layers within the axis and on the edges of the tunnel form shear walls was intended to increase the rigidity of the building’s corner points under lateral loads. Fig. 2a shows the plan view (i.e., $2.0 \times 2.5 \text{ m}^2$) of the existing tunnel formwork structure, and the steel profiles at the corner box sections are shown in Fig. 2b. The steel profiles are at the corner box sections of $45 \times 45 \times 2$ and the others $40 \times 40 \times 2$ with steel type St37.



(a) Plan view

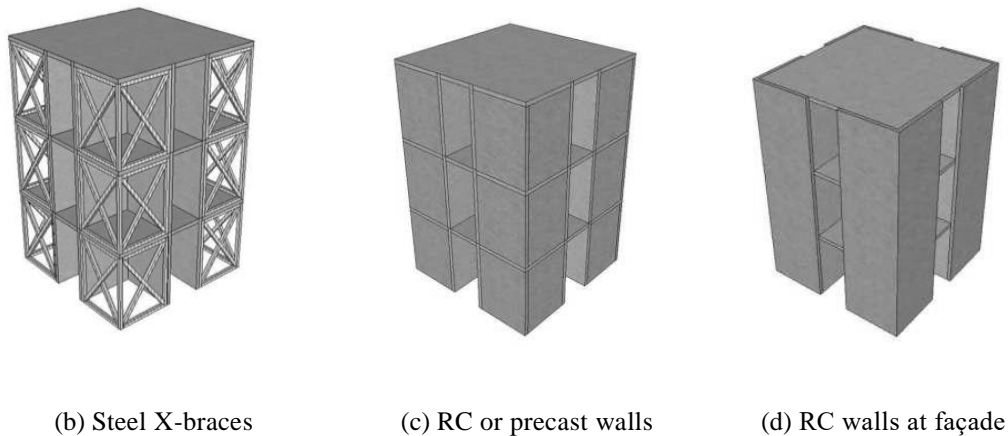


Fig. 2. Plan and 3D views of alternative strengthening models.

2.1. RC Infill Shear Walls

RC infill shear walls were mounted on the inner axes of the building within the floor-wall axis (Fig. 2c). The partition section was the same as in the existing tunnel formwork building. For constructing shear walls, which could not be constructed because the tunnel formworks were removed at the outer faces, RC infill shear walls were constructed within the edges using anchorages.

2.2. Precast Concrete Shear Walls

As it is easy to replace precast concrete shear wall, it was considered as an alternative to RC infill shear wall. The precast concrete shear wall showed the same characteristics as the RC infill shear wall (Fig. 2c) in terms of structural behavior.

2.3. RC Shear Wall at the Façade

The RC shear wall at the façade was designed to replace the RC infill and the precast concrete shear walls. It is anticipated that the RC shear wall at the façade will be easier to construct since it will be constructed through a climbing form on an existing RC building constructed with a tunnel formwork system (Fig. 2d). The anchorages for

the climbing form would be prepared before construction. The tunnel formwork would be prepared after the structure was completed.

3. 3D Nonlinear Finite Element Analysis of Models

3D nonlinear FEA was performed on the four strengthening techniques using SAP2000 structural analysis software. For the non-linear FEA, the shear walls and slabs consisted of shell components. The Mander model was used for concrete C20 nonlinear material modeling. Nonlinear material properties of concrete, anchorages, and steel profiles (St37) are shown in Fig. 3. In the analysis, in accordance with the loading experiment model, incremental loads were applied at the connection points between the shear walls and floors as P at the second floor and 2P at the top floor. The first dynamic period of the existing structure was torsion ($T = 0.04$ s), as shown in Fig. 4. This result indicates that a typical tunnel form building structure model is low torsion-resistant. The 3D behavior, load capacities, collapse mechanisms, crack propagations, and seismic performance of experimental modeling of the existing structure and retrofitted structure models are explained in Section 3.2. The deformed shapes and first periods are shown for steel X-braces and RC/precast walls in Fig. 5a and Fig. 5b, respectively.

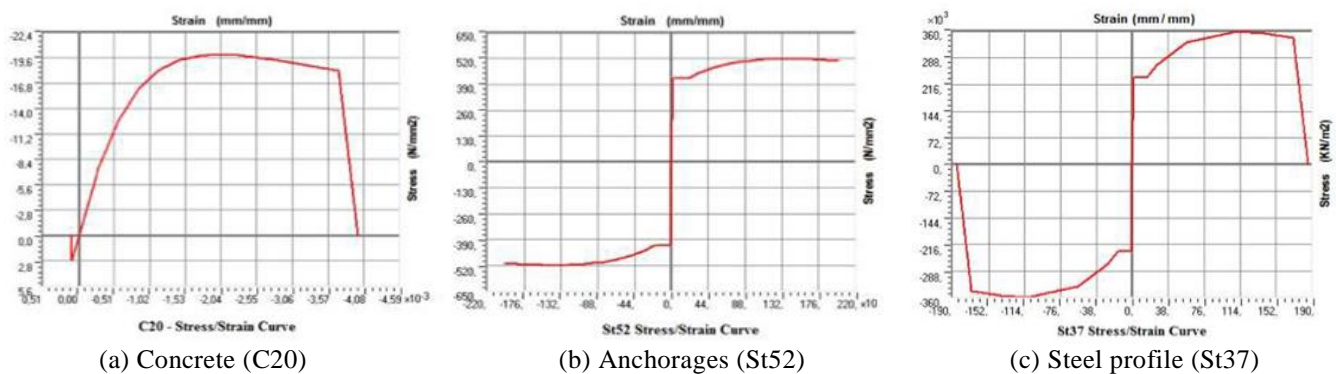


Fig. 3. Nonlinear material properties.

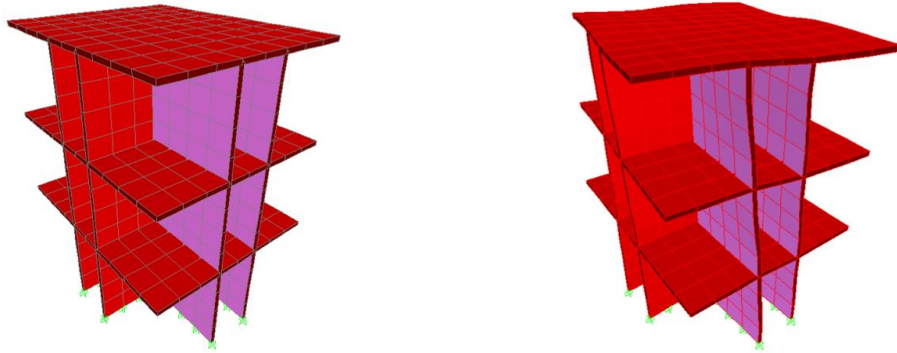
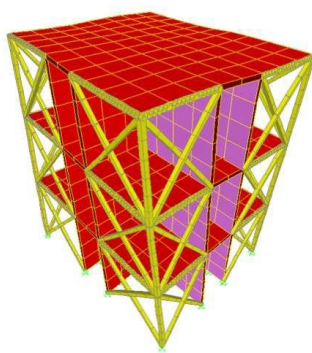
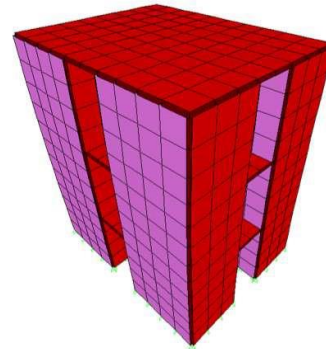


Fig. 4. Existing structure model and first period (torsion (T) = 0.04 s).



(a) Steel X-braces (T = 0.25 s)



(b) RC or precast walls (x direction, T = 0.007 s)

Fig. 5. Deformed shapes and first periods of structures with steel braces and RC/precast walls.

The results indicate that strengthening with steel X-braces doubles the torsional rigidity of the existing structures. In addition, the steel braces are easy to mount, economical, and add very little structural load on the system. Based on these results, seismic performance experiments were conducted to consider existing tunnel form building structures equipped with steel bracing at the corners.

4. Experimental Studies

Experimental studies were performed to observe the impact of strengthening techniques on the torsional rigidity and seismic performance of tunnel form building structures. The 3D behaviour of existing tunnel form buildings with and without strengthening were observed under earthquake loads, and their lateral load capacities, crack patterns, and collapse mechanisms were obtained. Models were constructed, as outlined in Section 2. The tunnel form building plan dimensions were $2.0 \times 2.5 \text{ m}^2$ (Fig. 6).

4.1. Existing Tunnel Form Building Model

4.1.1. Existing Experimental Model

The existing RC building modelled in this study was constructed and tested in the Earthquake Research Laboratory of Suleyman Demirel University in Isparta, Turkey. The model of the existing three-story tunnel form building had a wall and floor thickness of 5 cm. Based on the actual tunnel form building structures material quality, C20 was used as the concrete mixture. StIII class Ø5 ribbed rebar was used as reinforcement for the RC walls, making a net with 5 cm intervals. Q131/131 mesh reinforcement, produced by welding the Ø5 steel bars at 5 cm intervals, was used for floors (Fig. 7), and Ø5 reinforcement was added at 15 cm intervals where the structural bearings emerged. Since the model was created to represent the tunnel formwork building that consisted of walls and slabs as box structure, the depth of concrete cover was 5 mm, and the amount of fine aggregate was increased considering the placement of the concrete. At the base, the reinforcement was Ø12 placed at 15 cm interval in both directions. To eliminate the base movement in the laboratory, the anchorage spaces were set at 50 cm intervals, as shown in Fig. 8. The anchorages were mounted tightly in the experimental model structures' basement.

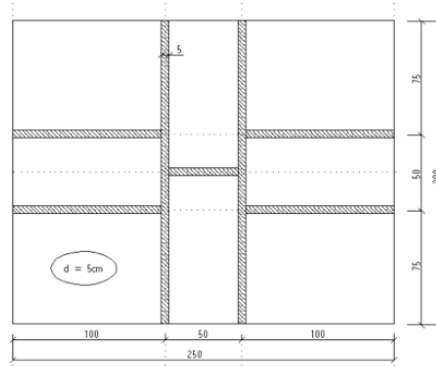


Fig. 6. Experimental tunnel form building model plan (dimensions: 200 × 250 cm²), (Wall and floor thickness are 20 and 5 cm, respectively).

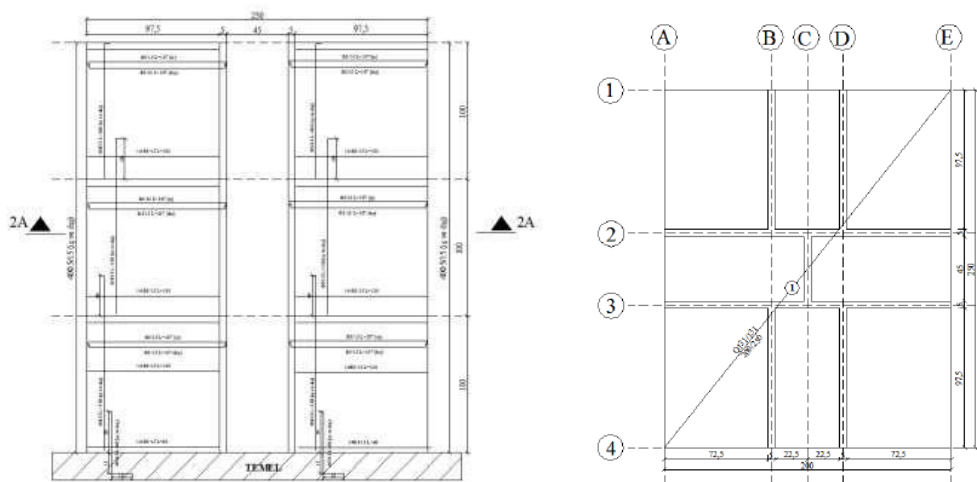


Fig. 7. Tunnel form building shear wall and floor mesh reinforcement.

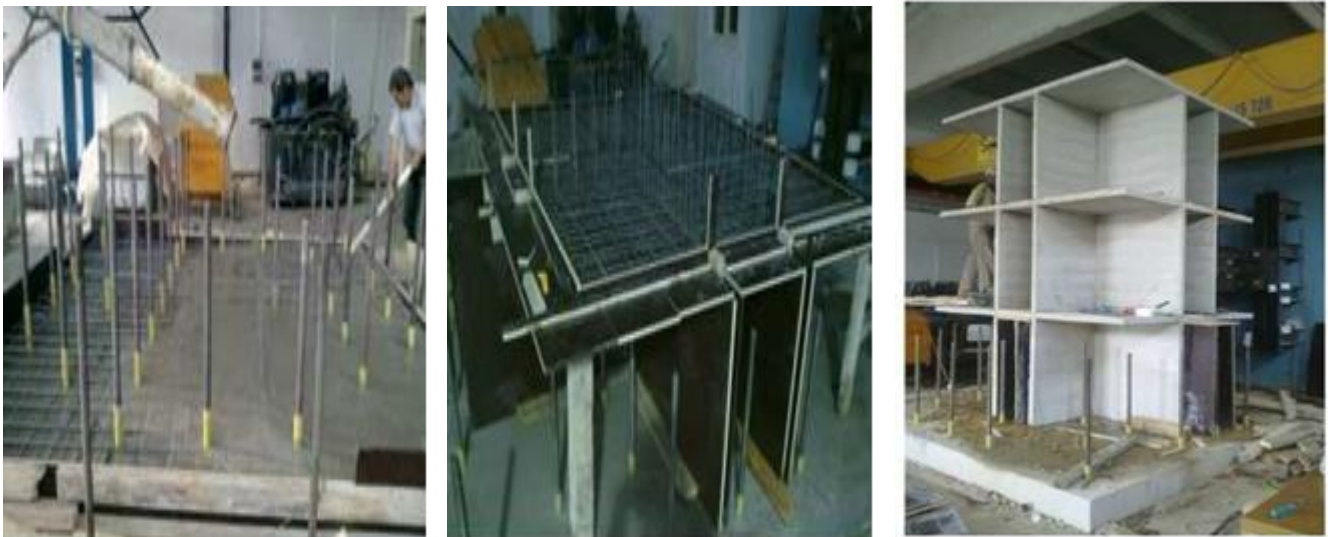


Fig. 8. Construction of 3D model of existing tunnel form building.

4.1.2. Loading

As the loading wall in the laboratory was unilateral, the experimental apparatus for the 3D model of the existing tunnel form building (Fig. 9) was designed to exert pull and push forces for cycling loading on the model by providing a plate and four tie bars on floor levels at the back of the structure, as shown in Fig. 9. Seismic loads were applied as pushover loading, and a load cell platform was arranged to transfer the load to the top two floors by pushing the 2/3 ratio to the upper floor level and the 1/3 ratio to the second floor level.

Before applying pushover forces, 50 kg/m² loading was applied on each floor slab as additional vertical load using cement bags. Linear variable differential transformers were placed on each floor, including rotation and foundation movements, to measure the basic displacements corresponding to the pushover loads. Horizontal seismic loads were applied to the structure in the form of cyclic pushover loading. Loads were applied to the model until the structure collapsed.

Pushover loads were gradually increased by considering the linear and nonlinear behavior of the structure.



Fig. 9. Pushover loading platform.

4.1.3. Crack Propagation and Damages

During loading, cracks were marked according to load cycle number, color, and crack propagation. If cracks

occurred due to push forces, they were marked in blue. If cracks occurred due to pull forces, they were marked in red. Crack patterns on the existing tunnel form building model before collapse are shown in Fig. 10.





Fig. 10. Crack patterns on the existing tunnel form building model before collapse.

Crack propagations and the cracks emerging after the collapsing force and mechanisms were separately drawn for the shear walls in the direction of force. In addition, the cracks vertical to the direction of force according to the names of shear walls is shown in Fig. 11. To show the 3D effects, the entire shear wall in that direction is shown in Fig. 11. Furthermore, to show the emergence of the cracks in both the surfaces of the shear systems of tunnel formwork, the surfaces are drawn separately in the longitudinal (loading) direction for the P1 and P2 walls (Fig. 11).

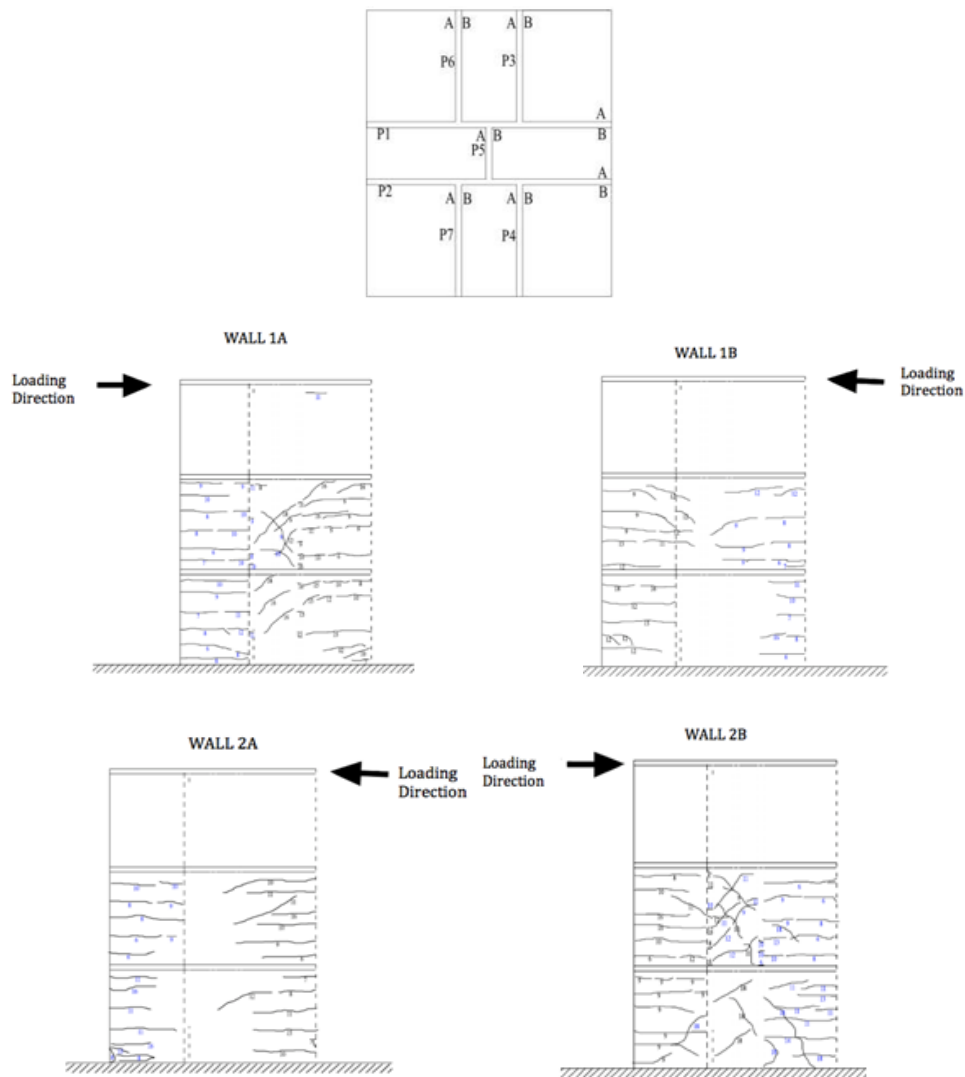


Fig. 11. Wall numbering and crack propagations corresponding to loading steps (step numbers are indicated on the cracks).

The first cracks were observed as hair cracks at connection points less than 12.9 tons of tensile force. Similar cracks were observed under compressive force. Then cracks emerged in the direction of loading between the first and second floors under 14.9 tons of tensile force. The detailed drawings of other cracks under tensile and compressive forces are shown in Fig. 11. CODA software was used to convey the data from measurement devices in experiments.

4.1.4. Load Capacity of the Existing Model

A load–displacement curve of existing tunnel from building experiment model is shown in Fig. 12. The existing structure load capacity is determined under 31.0 tons of force.

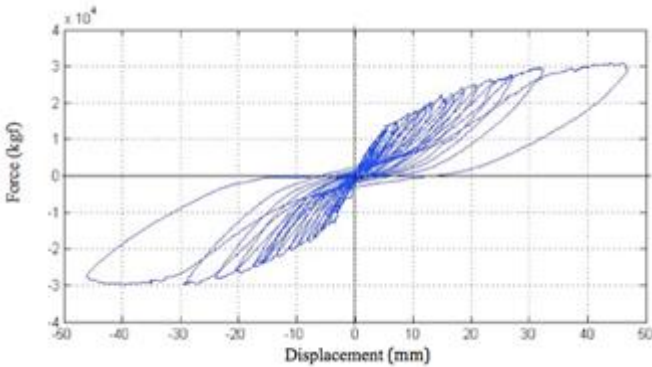


Fig. 12. Load–displacement curve of existing tunnel form building structure model.

4.2. Strengthened Tunnel Form Building Model

4.2.1. Strengthened Experimental Model

For the torsional rigidity strengthening experimental study, models were constructed in the laboratory and steel X-braces strengthening techniques were applied, as

outlined in Section 2. Steel braces were located at the corners of the buildings (Figs. 13 and 2b). The St37 steel material was utilized, as shown in Fig. 3c. To prevent any problems with unilateral loading, the steel frame dimensions were revised to 30 × 30 × 2, the box and cross-components were revised to a 30 × 30 × 2 box profile, and the steel in the columns at the edges were replaced with 40 × 40 × 3 steel profiles.



Fig. 13. Experimental model strengthened with X-braces.

4.2.2. Loading

The loading platform and vertical loads and instrumentation and wall numbers (Figs. 9 and 11, respectively) that were used in the existing model were used in the strengthened model. Table 1 lists the pushover loading steps.

4.2.3. Crack Propagation and Damages

Crack propagations for the strengthened experimental model are shown in Fig. 14.

Table 1. Pushover loading steps.

Lateral Push-Over Loadings		
	Tension (ton)	Compression(ton)
Step 1:	5.00	5.00
Step 2:	10.00	10.00
Step 3:	15.00	15.00
Step 4:	17.00	17.00
Step 5:	19.00	19.00
Step 6:	21.00	21.00
Step 7:	23.00	23.00
Step 8:	25.00	25.00
Step 9:	28.00	28.00
Step 10:	31.00	31.00
Step 11:	34.00	34.00
Step 12:	37.00	37.00
Step 13:	38.00	

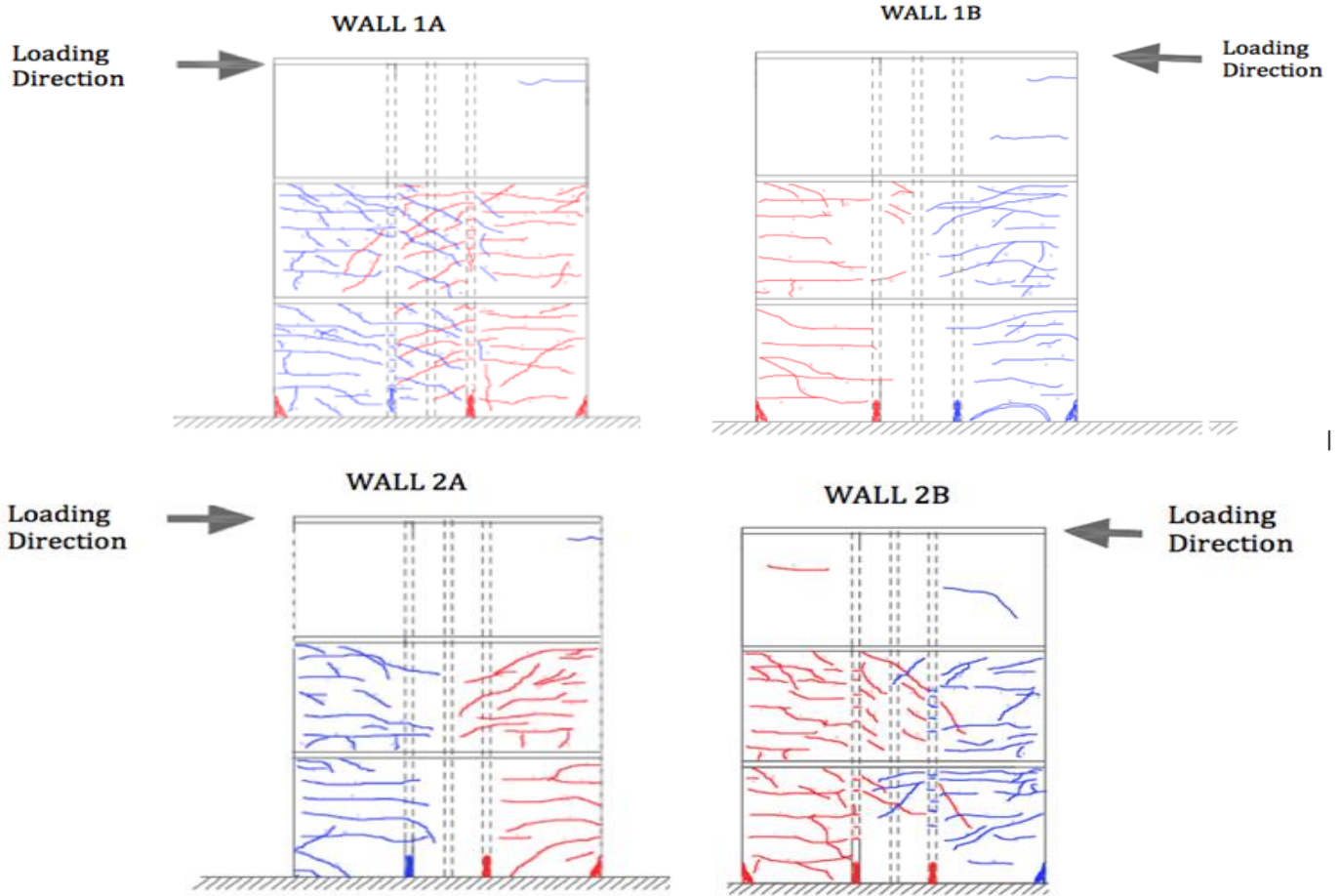


Fig. 14. Crack propagations for strengthened experimental model.

The first cracks were observed as hair cracks on the lower shear wall in the direction of loading under 17.0 tons of compressive force. In Step 5 and 6, cracks developed in walls vertical to the direction of loading under 19.0 tons of compressive and 21.0 tons of tensile forces, respectively. In Step 9, under 28 tons, noticeable cracks were observed

between the basement and shear wall connections. Major damage was observed at first-story shear walls and brace connections at the foundation level (Fig. 16) due to tension-compression coupling effects [3] before the collapse.



(a) Cracks on second-story shear walls



(b) Cracks on first-story shear walls



(c) Damage at wall and steel brace connections at the foundation level

Fig. 15. Damage in strengthened model before the collapse.

4.2.4. *Load Capacity of the Strengthened Model*

As shown in Fig. 16, the capacity of the strengthened model was 38.0 tons.

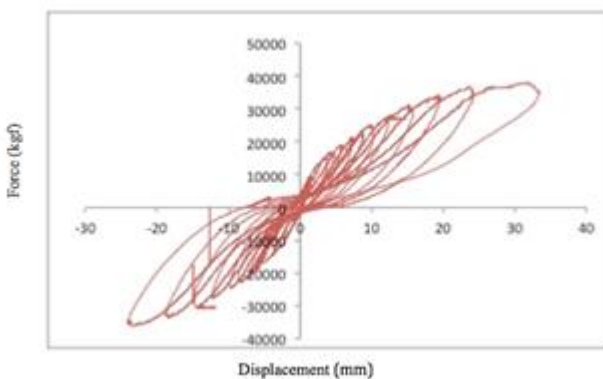


Fig. 16. Load–displacement curve of strengthened tunnel formwork structure model.

5. **Results and Discussion**

3D nonlinear FEA of the existing and strengthened structures was performed using SAP2000 structural analysis software. Material properties, dimensions, and all other information are provided in Section 3. In nonlinear FEA, the shear walls and slabs were modeled as shell components. Considering the rigidity of the load-bearing system, no diaphragm assumption was made for the floors. According to the modal analysis results, the first three modes of the existing structure were determined to be torsion, x direction, and y direction. Experimental model studies are performed for the selected steel X-braces strengthening method. In the strengthened steel brace model, the torsion rigidity gradually increased. The system passed from torsion to deflection mode. Pushover loading, in accordance with the loading experiment model, was incrementally applied at the junction points between shear walls and floors. Because of nonlinear FEA, the earthquake performance of the existing and strengthened models was determined to be 32 and 40 tons, respectively.

6. Conclusions

The steel X-braced strengthened tunnel form building model collapsed in the deflection phase rather than the torsion phase, and the crack pattern of the structure differed from that of the existing structure due to the steel bracing components used at the edges. Through strengthening, both the torsional rigidity and the earthquake performance of the structure were improved. In testing the existing experimental model in the laboratory, the collapse load of the strengthened structure was 38 tons, while that of the existing model was 31 tons. In experiments and FEA, the system was removed from the undesired mode of torsion, and increase in torsional rigidity and earthquake performance was observed.

The first natural periods of the structures are generally torsion due to tunnel form construction technique and may lead to damage in major earthquakes. The practical applicability and economy of the method outlined here is essential for both earthquake performance and retrofitting the tunnel formwork structures damaged in earthquake.

The experiments show the earthquake behaviors and collapse mechanisms of the existing tunnel form building structures and strengthened structures. Buildings constructed with a tunnel formwork system first dynamic mode may appear torsion, this situation occurs because of removing the mold in the tunnel formwork systems and transporting it to the upper floor.

The systems developed in this research are recommended for improving the torsional rigidity and earthquake performance of both new construction and retrofitting.

Acknowledgements

Turkish National Science Foundation (TUBITAK) supported this research, Industrial R&D Project No 3100355.

References

- [1] Balkaya C, Schnobrich WC. "Nonlinear 3D behavior of shear-wall dominant RC building structures", *Structural Engineering Mech* 1993; 1:1-16.
- [2] Balkaya C, Kalkan E. "Nonlinear seismic response evaluation of tunnel form building structures", *Comput Struct* 2003b; 81: 153-65
- [3] Balkaya C, Kalkan, E. "Three-dimensional effects on openings of laterally loaded pierced shear walls", *ASCE, Journal of Structural Engineering* 2004b; 130: 1506-1514.
- [4] Balkaya C, Kalkan E. "Estimation of fundamental periods of shear-wall dominant building structures", *Earthquake Engineering Structural Dynamics* 2003a; 32: 985-98.
- [5] Balkaya C, Kalkan E. "Seismic vulnerability, behavior and design of tunnel form building structures", *Engineering Structures* 2004a; 26: 2081-2099.
- [6] Yuksel SB, Kalkan E. "Behavior of tunnel form buildings under quasi-static cyclic lateral loading", *Structural Engineering Mechanics* 2007; 27: 99.
- [7] Yuksel SB. "Structural behavior of lightly reinforced shear walls of tunnel form buildings", *IACSIT International Journal of Engineering Technology* 2014; 6:34-37.

Construction Waste Reduction Through BIM-Based Site Management Approach

Burcu Salgın*[‡], Atacan Akgün*, Nilay Coşgun**, Kofi Agyekum****

*Department of Architecture, Faculty of Architecture, Erciyes University, 38030, Kayseri, Turkey

** Department of Architecture, Faculty of Architecture, Gebze Technical University, 41400, Kocaeli, Turkey

*** Department of Building Technology, Kwame Nkrumah University of Science and Technology, Kumasi, Ghana

(bsalgin@erciyes.edu.tr, atacan@erciyes.edu.tr, nilaycosgun@gtu.edu.tr, agyekum.kofi1@gmail.com)

[‡]Corresponding Author; Burcu Salgın, Department of Architecture, Erciyes University, 38030, Kayseri, Turkey

Tel: +90 352 437 5282, Fax: +90 352 437 6554, bsalgin@erciyes.edu.tr

Received: 22.05.2017 Accepted: 30.08.2017

Abstract- Today, construction practices with potential damages to the environment are carried out uncontrollably to respond to the rapidly growing population needs. In the construction sector, which is one of the leading sectors closely following technological developments, steps must be taken to protect the world's ecologic balance. The goal of the professionals is not only to put up a building in accordance with its design but also to comply with environmental requirements in a respectful way. Different parameters such as erroneous design decisions, inadequate work schedules, sudden weather oppositions, defects in product supply can directly or indirectly affect the construction process, resulting in the generation of construction waste on the construction site. These wastes negatively affect the living and non-living environment. It is not technically possible to completely eliminate construction wastes generated during the construction process, but it is possible to control and recover these wastes. For this reason, innovative applications are important in the construction sector. This study examines the potential of BIM applications in preventing/reducing wastes in the construction process. For this purpose; articles that talk about the reasons of waste generation in the construction sector and the relationship between BIM technology and construction waste management practices were examined, and the findings obtained were evaluated. BIM applications are being proposed to be developed to prevent/reduce wastes on the construction site.

Keywords C&D Waste, Building Information Modelling, Construction Site Management

1. Introduction

The definition of waste includes all types of materials which exist as solid, liquid or gas, which arise as a result of production and usage activities, and which, when disposed of directly or indirectly, have the potential to harm human health or the natural environment.

Waste may be classified as medical, domestic, industrial, agricultural, mineral and construction & demolition (C&D). The various types of wastes may pollute air, water and soil, and may negatively affect the topography of the land. Pollution of the natural environment, such as air, water and soil, has a wide range of negative effects. This may take the form of visual pollution of a landscape, or biological or

ecological effects on living organisms, including humans, plants and animals, and may lead to various diseases. Although the primary focus is on addressing the environmental damage caused by such waste streams, they also represent considerable economic losses. In this context, the effective management of these wastes in order to minimize their environmental and economic impacts is one of the most important issues of the 21st century. This is because waste prevention/reduction is the most beneficial, most economical and most environmentally sustainable approach within the waste management hierarchy. Consumption of natural resources and increasing production of waste require solutions to protect the quality of the natural and built environments. For these solutions to be effective,

waste management models must be developed and it is important to reduce waste at the source.

Increased construction activities along with the increasing population in the world lead to growing environmental problems, because buildings and the users of buildings generate waste throughout the building life processes (construction, usage and demolition). Various interpretations and definitions of waste can be found in construction waste related literature. The European Waste Framework Directive 2008/98/EC define waste as “any substance or object which the holder discards or intends or is required to discard” [1]. Ekanayake and Ofori [2] defined construction waste as “any material, apart from earth materials, which needs to be transported elsewhere from the construction site or used within the construction site itself for the purpose of land filling, incineration, recycling, reusing or composting, other than the intended specific purpose of the project due to material damage, excess, non-use, or non-compliance with the specifications or being a by-product of the construction process”. Mossman [3] defined material waste as anything that is not needed to generate value for the end-user. Waste can also be defined as an excessive use or carelessness of material [4]. Several studies have categorized the major sources of waste on construction sites to include reworks/repairs, defects, material waste, delays, waiting, poor material allocation, and unnecessary material handling [5, 6, 7, 8, 9]. Waste may also occur as a result of natural

disasters like earthquakes and tornadoes. As can be inferred in the definitions, there are several kinds of construction wastes and they occur at different stages of a building’s life cycle. To prevent economic and ecological loses, it is important to prevent/reduce construction waste on construction sites. With this aim, many site management strategies are developed all around the world. One of them is using BIM in construction site management. Although it is quite a new approach, it is gradually gaining recognition among construction professionals. This paper is therefore aimed at reviewing literature on the reduction/prevention of construction waste using BIM-based construction site management approach.

2. Origins of Construction Waste on Site

This section of the study adopted a similar methodology used by Nagapan et al. [10] to conduct their study. It involved a two-stage methodology which included: identifying the cause of waste generation through literature review and categorization of the major factors. Generally, waste may occur as a result of series of events and may not be due to a remote aspect [11]. Mapping of the factors in Table I gives a preliminary idea on what past researchers had discovered about the factors that contribute to construction waste generation on sites.

Table 1. Causes of waste generation on construction sites identified in literature

		References													
		Bossink & Brouwers [12]	Garas et al. [13]	Alwi et al. [14]	Alwi et al. [15]	Ekanayake & Ofori [16]	Poon et al. [17]	Polat & Ballard [18]	Poon et al. [19]	Tam et al. [20]	Wang et al. [21]	Wan et al. [22]	Wahab & Lawal [23]	Lu et al. [24]	Najatpoor et al. [25]
Causes of Waste Generation															
Designing	Last minute changes	•	•	•	•	•	•	•	•	•	•	•	•	•	
	Designers' lack of knowledge	•	•	•	•	•	•	•							
	Design errors	•		•	•	•		•		•		•			
	Complicated design					•	•	•							
	Poor design quality				•						•				
	Lack of environmental awareness						•				•				
Com.	Lack of coordination among parties		•		•			•				•			
	Lack of communication among designers		•					•	•						
Materials	Poor material handling		•		•	•		•	•	•		•	•	•	
	Ordering errors	•	•			•	•	•	•	•			•	•	•
	Poor quality of materials	•			•	•			•	•			•	•	•
Planning	Wrong material storage	•	•		•				•	•	•	•	•	•	•
	Poor site management		•			•		•			•	•	•	•	
	Poor planning	•			•	•		•				•			
	Lack of waste management plans	•	•					•							
Labouring	Workers' mistakes	•	•			•		•	•	•	•			•	
	Damage during transportation on site	•	•			•	•				•		•	•	
	Lack of knowledge		•				•				•				
	Lack of experience				•									•	
	Shortage of skilled workers				•			•							
External Factors	Effect of weather	•		•	•	•		•		•		•			
	Accidents	•				•		•		•					
	Theft	•	•			•									
	Vandalism		•										•		

This matrix analysis identifies findings from past researchers around several parts of the world. Fourteen scholarly research papers were deemed significant for this study. From these papers, 24 factors that lead to waste generation on construction sites were identified. These factors are grouped into 6 categories as; design, communication, materials, planning, laboring and external factors. Table I shows the mapping of the various causes of waste against the studies that identified such wastes.

Table I shows that the factor with the highest frequency is the last-minute changes in design. This factor was identified in 13 out of the 14 articles considered in this study. This significant factor is in the category of designing which has six factors. The significant factors for all categories are shown in Table II. These six factors are the most frequent ones in literature, so they are described. However, all the other factors may also be very important in the generation of waste on construction sites as well.

Table 2. Categorization of major factors that contribute to waste generation

Categorization	Major factor determined
Designing	Last minute changes
Communication	Lack of coordination among parties
Materials	Ordering errors
Planning	Wrong material storage
Labouring	Workers' mistakes
External Factors	Effect of weather

A. Last Minute Changes

The ‘last minute changes’ was found to be the most frequent factor that generates construction waste among other factors. These problems occur because of some of the changes requested by clients, especially in the last minute. This becomes a problem because of the inadequate communication between parties to the contract during the design stage of a building. At the design stage, the client and the designer must agree on the design and they should make the final decision together before the contractor starts the construction. If this is not done, changes may occur during the construction, when problems are encountered in the drawings.

B. Lack of Coordination Among Parties

If the parties (contractors, designers and the clients) who are involved in construction projects do not have good communication among themselves, there probably will be defects in the design. At the end, it is possible to have waste on construction sites because of the poor coordination. A good communication among team members can help avoid such wastes.

C. Ordering Errors

It is always important to order the materials in their right quantity to avoid delivering the materials in excess that may lead to wastage. This can be achieved through the proper estimation of materials prior to the start and during the execution of the project [26].

D. Wrong Material Storage

Another factor that contributes to materials wastage on site is wrong material storage which is always connected with an inappropriate protection strategy. Inadequate stacking and insufficient storage can result in waste. When materials are stacked without pallets, are wrongly stored at any open space without proper protection -such as bricks/blocks or bags of cement-, bad weather conditions -such as rain- can cause wastage of such materials. Proper storage of materials is very necessary to avoid waste generation on construction sites.

E. Workers' Mistake

Inadequate knowledge in handling materials on the part of the workers is also one of the major causes of waste on construction sites. Skoyles and Skoyles [27] highlighted the significance of human mistakes in waste minimization. According to Lingard et al. [28], for the 3Rs (i.e. reduction, reuse and recycling) to be achieved, managers should learn to work on the behavior of construction workers concerning how to handle materials. Teo et al. [29] added that the behavior of the labor forces is likely to affect the generation of waste at all levels on construction sites, hence, the need to address such issues. Tam and Tam [30], in their study revealed that when the staff were offered incentives and rewards, an estimated 23% waste reduction was recorded. As a result of that, it is important for company policies to focus on educating staff on waste reduction. The policies should also create awareness and encourage contractors to adopt waste minimization measures in their activities. The implications of such policies will be very significant to the construction industry, and help improve its performance towards sustainability [31].

F. Effect of Weather

Changes in the weather is one of the factors that cannot be controlled by human because it is a natural effect. Weather changes are caused by unforeseen circumstances. Hence, good management skills should be applied to reduce wastage that result from such occurrences [32].

3. Construction Waste Reduction Approaches on Construction Sites

Waste reduction is a major component in waste management. ‘Waste reduction’ can be defined as any activity that can reduce the quantity, supply and the environmental impact of waste. The benefits derived from waste minimization include the following [33]:

- Reducing the amount of landfill spaces,
- Saving natural resources,
- Saving energy,
- Minimizing pollution.

To achieve these benefits, there are several approaches which have been adopted worldwide. Key amongst such approaches is the use of BIM-based site management approach. Professionals within the construction sector are generally enthusiastic and propose that BIM can provide better project construction outcomes, reduced errors,

omissions and conflicts. Although limited in literature, studies regarding the use of BIM in construction site management for construction waste prevention/reduction suggests promise and potential.

4. Building Information Modelling

One of the dynamic sectors where technological developments are put into practice as quickly as possible is undoubtedly the construction sector, although it is still slow compared to some sectors where industrialized production is carried out. The results of the race to follow innovations in order to make a difference in the competitive conditions of the world are followed with interest in architecture and construction world. BIM is one of the technological developments that have been increasingly seen in the recent years in the acceleration of adoption by construction project stakeholders, which are closely related to the construction industry. As the most comprehensive of the existing conditions, BIM can be thought of as a new project management concept that allows all participants to simulate all aspects of a construction project in a digital environment and share data on a single model.

A. Definition of BIM

Some of the definitions of BIM encountered in the literature survey conducted within the scope of this paper are as follows:

- BIM is a modeling technology that integrates all the processes (design, manufacturing, communication, analysis, etc.) involved in the life cycle of structures and inseparably interrelated [34].
- BIM is a parametric component-based, three-dimensional reference structure modeling system created using file formats that allow all disciplines involved in the project life cycle to exchange their data. In the broader context, BIM is a new approach to design and construction beyond modeling [35].
- BIM is a system that allows visualization of the entire process from the construction of a building to its physical construction [36].
- Beyond being a software, technology and / or tool, BIM is the whole set of processes in which all data defining the life cycle of a building is produced and managed. The 'master builder' designation, which indicates that architects have assumed all responsibility for the structure in the ancient times, evolved as a 'master of digital architecture' for BIM in today's design and construction World [37].
- BIM is a complex form of management of social and technical resources that make sense of the concepts of complexity, cooperation and interrelation, which are the most important actors of today's building world. The focus of this management system is to locate the right

information at the right time and in the right place [38].

- BIM is a vehicle that continues to develop rapidly in the construction sector and is used in the construction of healthy communication among all project stakeholders and continues to develop in the construction sector [39].

According to the definitions obtained as a result of the literature survey, BIM in its comprehensive form; is an interdisciplinary point of view designed to shorten the standard of the architectural and construction sector in the short term, designed to maximize the organizational scheme at the highest level, redefining the content of the project participants' definition and meeting the users' requirements at every level of the project life cycle and at every level of detail.

B. Building Life Cycle and BIM Usage

One of the most important differences of BIM's existing technologies in the design and construction sector is that it has a potential to accommodate all participants and processes involved in the project life cycle [40], not a single discipline or process. It is believed that BIM, which is thought to have an infrastructure that can be used efficiently during the pre-design feasibility stage and post-construction operation and maintenance processes, is adapted to the successive progressive and chain reaction characteristics of all stages constituting the project life cycle.

It is foreseen that the area in which the technology can be used throughout the life cycle of the project must be well determined so that the value added of the BIM can meet the expectations of the employer and the contractor. In Figure 1, the project is divided into four sections as planning, design, construction and operation in the BIM utilization chart, which is produced by Penn State University Computer Integrated Research Program, interviews with leading names of the construction industry, Process, the components for which BIM can be used, the order of distribution of these components in terms of phases, and the use of BIM [41].

PLAN	DESIGN	CONSTRUCT	OPERATE
Existing Conditions Modeling			
Cost Estimation			
Phase Planning			
Programming			
Site Analysis			
Design Reviews			
Design Authoring			
Energy Analysis			
Structural Analysis			
Lighting Analysis			
Mechanical Analysis			
Other Eng. Analysis			
LEED Evaluation			
Code Validation			
3D Coordination			
Site Utilization Planning			
Construction System Design			
Digital Fabrication			
3D Control and Planning			
Record Model			
Maintenance Scheduling			
Building System Analysis			
Asset Management			
Space Management / Tracking			
Disaster Planning			

Fig. 1. Use of BIM throughout the project life cycle [41].

5. Previous Researches Related to Construction Waste Prevention/Reduction by Bim-Based Construction Site

Through a thorough review of literature, it was revealed that there are various studies that relate to BIM in construction activities but limited studies that relate to BIM-based construction site management (BCSM).

A literature searches for the last ten years -from 2007 to (February)2017- was conducted using the key words; Building Information Modeling (BIM), Construction Site Layout Planning (CSLP), Construction Site Waste Management (CSWM), Construction Waste Management (CWM), and Construction Waste Reduction (CWR). This part of the study is an integrative review that seeks to answer the following research questions:

- **Q1.** Does BCSM help to reduce/minimize construction waste?
- **Q2.** What features of BIM could be used to prevent/reduce construction waste on site?
- **Q3.** What are the benefits of using BCSM to reduce construction waste?
- **Q4.** What are the barriers to the use of BCSM to reduce construction waste?
- **Q5.** What are the current applications of BCSM to reduce construction waste?

In all, over approximately 50 papers and texts were consulted, of which six were primary research studies [42, 43, 44, 45, 46, 47] that detailed BIM-Based Construction Site Management for C&D Waste Prevention/Reduction. The answers to the questions asked in this section were derived from the limited studies consulted and they are discussed to include the following:

Q1. Does BCSM help to reduce/minimise construction waste?

Lu et al. [42] shared the aspect of The UK's Construction 2025 Strategy. As part of the strategy, it was revealed that "BIM has the potential to reduce/minimise construction waste during design and construction stages of projects". According to Lu et al. [42], many professionals in the industry, such as architects, engineers and surveyors, take this a step further by considering BIM to be a major actor in the battle against construction waste. The rhetoric tries to show the potential benefits of BIM, such as clash detection and on-site coordination. Partly owing to these potential benefits, BIM has been advocated as a solution to CWM. It provides virtual and computational environment to ponder on assorted design possibilities and construction schemes, with a view to minimizing waste before it is generated on site.

Won et al. [43] also postulated BIM as an effective means to reduce the amount of C&D waste through improving the quality and accuracy of design and construction, and minimising design errors, rework, and unexpected changes. It is a possible solution for eliminating the major causes of construction waste that arise during both the design and construction stages.

According to Cheng et al. [44], people have tried and succeeded in using BIM to reduce improper design, residues of raw materials, unexpected changes in building design and improve procurement, site planning, and material handling in construction management.

Ahankoob et al. [45] stated that a relatively new methodology which people in the construction industry are using to minimise the generation of waste in the design and pre-construction phase is the use of BIM.

Ahankoob et al. [45] and Rajendran and Gomez [46] introduced the potential use of BIM technology to minimize construction waste, but these efforts were limited to the design phase and did not discuss the specific methods to utilize BIM for C&D waste minimization. However, the study did not propose specific methods to minimize and manage C&D waste.

Furthermore, the UK Construction 2025 Strategy recognised that BIM has the potential to reduce construction waste during design and construction stages [48]. Unfortunately, no efforts have been made to develop BIM aided CWM design decision making tools and methodologies to date. Also, there is inadequate research on the development and review of tools and methodologies that use BIM to support CWM decision making during the design phase of projects. Additionally, there are no research attempts to relate the use of BIM to construction waste causes [47].

Q2. What features of BIM could be used to prevent/reduce construction waste on site?

Lu et al. [42] described the potential benefits of BIM, such as clash detection and on-site coordination, with the assumption that they will automatically become a reality. BIM is a potential tool that can be utilized in a virtual computational environment within which designers and contractors can employ different design and construction options with a view to minimizing construction waste.

According to Won et al. [43], the uses of BIM like validation of designs, quantity take-off, phase planning, site utilization planning, amongst others were proposed for the reduction of construction waste. BIM can also enable us to minimize the amount of C&D waste by improving quality and accuracy of design and construction, thereby reducing design errors, rework, and unexpected changes. Use of BIM can reduce improper design, residues of raw materials, and unexpected changes in building design and improve procurement, site planning and material handling in construction management.

Ahankoob et al. [45] listed the basic BIM solutions for waste reduction to include conflict, interference and collision detection, construction sequencing and construction planning, reducing rework, synchronizing design and site layout, detection of errors and omissions (clash detection) and precise quantity take-off.

Q3. What are the benefits of using BCSM to reduce construction waste?

BIM provides a level ground for less expensive, virtual,

graphical, and computational environment to enable stakeholders deliberate on various design options and construction schemes, which have a significant impact on construction waste minimization [42]. It is stated in Lu et al.'s [42, pp.589], study that "A less than well-thought-out construction scheme may cause problems in the delivery of a project, including excessive construction waste generation. BIM allows modelling of entire construction process and prior accounting of the waste-generation risks of alternative strategies. With detailed 3D models of buildings in the BIM component library, it is a 3D model of a construction project can be generated rapidly. Waste generation can be computed instantaneously and presented graphically on a dashboard along with other project performance metrics".

Consequently, validation of designs can minimize the amount of waste generated on site since such wastes are mainly generated due to improper design and unexpected changes during the design and construction phases [43]. According to Cheng et al. [44], BIM uses can also reduce different kinds of waste that can be removed by lean construction.

Q4. What are the barriers to the use of BCSM to reduce construction waste?

BIM has benefits on construction waste minimization on sites, nevertheless, as the digital representation of a physical facility, BIM itself cannot manipulate information to allow informed decision-making for CWM; and for this purpose, it relies on algorithms [42]. Lu et al. [42], Ahankoob et al. [45], Rajendran and Gomez [46] and Liu et al. [47] introduced the potential use of BIM technology to minimize construction waste, but these efforts were limited to the design phase and did not discuss the specific methods to utilize BIM for C&D waste minimization.

Q5. What are the current applications of BCSM to reduce construction waste?

Lu et al. [42] cited Porwal and Hewage's [49] paper which they conducted a BIM-enabled analysis to minimize the waste rate of structural reinforcement. BIM was selected as the hub for communicating project information among the various design teams. The findings from the study revealed that construction waste generation can be determined at both the design and construction stages of projects, and this could be achieved by developing a system dynamics (SD) model to estimate waste generation in relation to different design and construction combinations [42].

According to Lu et al. [42, pp.589] "neither commercial BIM solutions nor academic studies have sufficiently extended BIM to perform CWM, despite widespread calls to do so". Moreover, there has not been any technique or tool available that explores BIM as a platform to reduce C&D waste [44].

6. Conclusion

In this study, the articles that deal with the relationship between BIM technology and construction waste management practices were examined in detail. The methods investigated the use of BIM technology related to

construction waste reduction on construction sites. This study only focused on the construction process, however, design and post-production phases that are located in the project life cycle were excluded.

The common idea that emerges in all the articles examined is that BIM technology is a technological development that can be very useful in construction waste management. However, the study did not find any existing BIM based site management laid down procedures to construction waste reduction. This is mainly due to the fact that BIM is an emerging technology, and it is thought that the plug-ins to support construction waste management have not been developed yet.

It is envisaged that the construction waste that is generated consciously and / or unconsciously during the construction process can be minimized by the possibilities of technology. At this point, it is thought that BIM technology, which can create the whole project on the digital interface, can be utilized with a systemic approach.

References

- [1] Waste Framework Directive 2008/98/EC, (2008). [Online]. Available: <http://eur-lex.europa.eu/LexUriServ/LexUriServ.do?uri=OJ:L:2008:312:0003:0030:EN:PDF>
- [2] L. L. Ekanayake and G. Ofori, "Construction material source evaluation", Proceedings of the 2nd Southern African Conference on Sustainable Development in the Built Environment, Pretoria, 2000.
- [3] A. Mossman, "Creating value: a sufficient way to eliminate waste in lean design and lean production", *Lean Construction Journal*, pp. 13-23, 2009.
- [4] L. E. Chandler, *Materials Management on Building Sites*, England: The Construction Press Ltd., 1978.
- [5] S. H. Lee, J. E. Diekmann, A. D. Songer and H. Brown, "Identifying Waste: Applications of Construction Process Analysis", Proceedings of the Seventh Annual Conference of the International Group for Lean Construction, USA, 1999.
- [6] L. F. Alarcon, *Training Field Personnel To Identify Waste And Improvement Opportunities In Construction*, L. F. Alarcon, Ed. *Lean Construction*, Rotterdam: A. A. Balkema, Rotterdam, Brookfield, 1997, pp. 402-413.
- [7] S. Alwi, "The Relationship Between Rework and Work Supervision of Upper Structure in The Reinforced Concrete Building Structure", M. S. Thesis, University of Indonesia, Jakarta, 1995.
- [8] L. Koskela, "Lean Production in Construction", *The 10th International Symposium on Automation and Robotics in Construction (ISARC)*, Elsevier, USA, pp. 47-54, 1993.

- [9] C. J. Robinson, *Continuous Improvement in Operations; A systematic Approach to Waste Reduction*, Productivity Press, Cambridge, Mass., 1991.
- [10] S. Nagapan, I. A. Rahman, A. Asmi, "A Review of Construction Waste Cause Factors", *Asian Conference of Real Estate: Sustainable Growth Managing Challenges (ACRE 2011)*, Johor Bahru, Malaysia, 2011
- [11] E. R. Skoyles and E. J. Hassey, "Wastage of materials", *Building Research Establishment Current Paper 44/74*, 1974.
- [12] A. G. Bossink and H. J. H. Brouwers, "Construction waste: quantification and source evaluation", *Journal of Construction Engineering and Management*, ASCE, Vol. 122(1), pp. 55–60, March 1996.
- [13] L. G. Garas, R. A. Anis and E. A. Gammal, "Material Waste in the Egyptian Construction Industry", *Proceedings of the 9th Annual Conference of the International Group for Lean Construction*, National University of Singapore, Singapore, 2001.
- [14] S. Alwi, K. Hampson and S. Mohamed, "Non Value-Adding Activities in Australian Construction Projects", In *Proceedings International Conference on Advancement in Design, Construction, Construction Management and Maintenance of Building Structure*, Bali, Indonesia, 2002.
- [15] S. Alwi, K. Hampson and S. Mohamed, "Waste in the Indonesian construction projects", In *Proceedings 1st International Conference of CIB W107 - Creating a sustainable Construction Industry in Developing Countries*, South Africa, pp. 305-315, 2002.
- [16] L. L. Ekanayake and G. Ofori, "Building Waste Assessment Score: Design-Based Tool", *Journal of Building and Environment*, Vol. 39, pp. 851-861, 2004.
- [17] C. S. Poon, A. T. W. Yu and L. Jaillon, "Reducing Building Waste at Construction Sites in Hong Kong", *Construction Management and Economics*, Vol. 22, pp. 461–470, 2004.
- [18] G. Polat and G. Ballard, "Waste in Turkish Construction: Need for Lean Construction Techniques", *Proceeding 12th Annual Conference of the International Group for Lean Construction (IGLC-12)*, Elsinore, Denmark, pp. 488-501, 2004.
- [19] C. S. Poon, A. T. W. Yu, S. W. Wong and E. Cheung, "Management of Construction Waste in Public Housing Projects in Hong Kong", *Journal of Construction Management and Economics*, Vol. 22, pp. 675–689, September 2004.
- [20] V. W. Y. Tam, L. Y. Shen, I. W. H. Fung and J. Y. Wang, "Controlling Construction Waste by Implementing Governmental Ordinances in Hong Kong", *Journal of Construction Innovation*, Vol. 7(2), pp. 149-166, 2007.
- [21] J. Y. Wang, X. P. Kang and V. W. Y. Tam, "An Investigation of Construction Wastes: An Empirical Study in Shenzhen", *Journal of Engineering, Design and Technology*, Vol. 6(3), pp. 227-236, 2008.
- [22] K. M. S. Wan, M. M. Kumaraswamy and D. T. C. Liu, "Contributors to Construction Debris from Electrical and Mechanical Work in Hong Kong Infrastructure Projects", *Journal of Construction Engineering and Management*, Vol. 135(7), 2009.
- [23] A. B. Wahab and A. F. Lawal, "An evaluation of waste control measures in construction industry in Nigeria", *African Journal of Environmental Science and Technology*, Vol. 5(3), pp. 246-254, March 2011.
- [24] W. Lu, H. Yuan, J. Li, J. J. L. Hao, W. Mi and Z. Ding, "An Empirical Investigation of Construction and Demolition Waste Generation Rates in Shenzhen City, South China", *Journal of Waste Management*, Vol. 31, pp. 680-687, 2011.
- [25] A. A. Najafpoor, A. Zarei, F. Jamali-Behnam, M. Vahedian-Shahrودي and A. Zarei, "A Study Identifying Causes of Construction Waste Production and Applying Safety Management on Construction Site", *Iranian Journal of Health Sciences*, Vol. 2(3), pp. 49-54, 2014.
- [26] Clackmannanshire Council, (2011). *Guidance on Construction Site Waste Management*. [Online]. Available: <http://www.clacksweb.org.uk/environment/constructionsitewastemanagement/>
- [27] E. Skoyles and J. R. Skoyles, *Waste prevention on site*, London: Mitchell, 1987.
- [28] H. Lingard, G. Gilbert and P. Graham, "Improving Solid Waste Reduction and Recycling Performance Using Goal Setting and Feedback", *Construction Management and Economics*, Vol. 19(8), pp. 809-817, 2001.
- [29] M. M. M. Teo, M. Loosemore, M. Masosszeczy and K. Karim, "Operatives Attitudes Towards Waste on a Construction Project", *Annual Conference – ARCOM 2000*, Vol. 2, pp. 509-517, 2000.
- [30] V. Tam and C. Tam, "Waste reduction through incentives: a case study", *Building Research & Information*, Vol. 36(1), pp.37-43, 2008.
- [31] R. A. Begum, C. Siwar, J. J. Pereira and A. H. Jaafar, "Attitude and behavioral factors in waste management in the construction industry of Malaysia", *Resources, Conservation and Recycling*, Vol. 53(6), pp. 321-328, 2009.
- [32] T. O. Adewuyi and I. A. Odesola, "Factors affecting material waste on construction sites in Nigeria", *Journal of Engineering and Technology*, Vol. 6(1), 2015.
- [33] R. J. Camm and P. M. Nuttall, "Waste Minimization: Incentives and Barriers", in *Waste Minimization through Process Design*, A. P. Rossiter, Ed, New York: McGraw-Hill International Book Company, 1995, pp. 29-42.
- [34] C. Eastman, P. Teicholz, R. Sacks and K. Liston, *BIM Handbook*, 2nd Edition, New Jersey, Wiley, 2011.

- [35] R. Crotty, *The Impact of Building Information Modelling: Transforming Construction*, Spon Press, London, 2012.
- [36] B. Hardin and D. McCool, *BIM and Construction Management: Proven Tools, Methods, and Workflow*, 2nd Edition, John Wiley & Sons, 2015.
- [37] R. Deutsch, *BIM and Integrated Design: Strategies for Architectural Practice*, John Wiley and Sons INC., New Jersey, 2011.
- [38] F. E. Jernigan, *Big BIM Little BIM*, 4Site Press, Salisbury, Maryland, 2007.
- [39] E. Krygiel and B. Nies, *Green BIM: Successful Sustainable Design with Building Information Modelling*, Wiley Publishing Inc., Indianapolis, Indiana, 2008.
- [40] C. Bylund and A. Magnusson, *Model Based Cost Estimations: An International Comparison*, Lund University Faculty of Engineering, LTH, Lund, 2011.
- [41] PSU, *BIM operate. construct.design.plan. Project Execution Planning Guide*, The Pennsylvania State University, The Computer Integrated Construction Research Group, 2010.
- [42] W. Lu, C. Webster, K. Chen, X. Zhang and X. Chen, "Computational building information modelling for construction waste management: Moving from rhetoric to reality", *Renewable and Sustainable Energy Reviews*, Vol. 68, pp. 587–595, 2017.
- [43] J. Won, J. C. P. Cheng and G. Lee, "Quantification of construction waste prevented by BIM-based design validation: Case studies in South Korea", *Waste Management*, Vol. 49, pp. 170–180, 2016.
- [44] J. C. P. Cheng, J. Won and M. Das, "Construction and demolition waste management using BIM technology", *23rd Ann. Conf. of the International Group for Lean Construction*, Perth, Australia, pp. 381-390, 29-31 July 2015.
- [45] A. Ahankoob, S. M. Khoshnava, R. Rostami, C. Preece, "BIM perspectives on construction waste reduction", *Management in Construction Research Association (MiCRA) Postgraduate Conference*, pp. 195–199, 2012.
- [46] P. Rajendran and C. P. Gomez, "Implementing BIM for Waste Minimization in the Construction Industry: A Literature Review", *The 2nd International Conference on Management*, Malaysia, pp. 557-570, 2012.
- [47] Z. Liu, M. Osmani, P. Demian and A. Baldwin, "A BIM-aided construction waste minimisation framework", *Automation in Construction*, Vol. 59, pp. 1–23, 2015.
- [48] HM Government, *Construction 2025: Industrial Strategy: government and industry in partnership*. (2013). Available: https://www.gov.uk/government/uploads/system/uploads/attachment_data/file/210099/bis-13-955-construction-2025-industrial-strategy.pdf 2013
- [49] A. Porwal and K. Hewage, K., "Building Information Modeling-Based Analysis to Minimize Waste Rate of Structural Reinforcement", *Journal of Construction Engineering and Management*, Vol. 138(8), pp. 943-954, 2012.

Nonlinear Integrated Design of Lattice Domes with Supporting Substructures

Ali Etemadi*, Can Balkaya**‡

*Department of Civil Engineering, Faculty of Engineering and Architecture, Istanbul Gelisim University, Istanbul, Turkey.

** Department of Civil Engineering, Faculty of Engineering and Architecture, Istanbul Gelisim University, Istanbul, Turkey.

(aetemadi@gelisim.edu.tr , cbalkaya@gelisim.edu.tr)

‡Corresponding Author; Can Balkaya, Department of Civil Engineering, Istanbul Gelisim University, Istanbul, Turkey,

Tel: +90 212 422 7020, Fax: +90 212 422 7401, cbalkaya@gelisim.edu.tr

Received: 14.06.2017 Accepted: 21.07.2017

Abstract- This paper investigates the response interaction between reinforced concrete substructure and steel raised lattice roofing. The viewpoint of dynamic stability and nonlinear seismic behavior are considered as both geometrical and material nonlinearity. In particular, dynamic stability performance of single layer Diamatic domes located on peripheral reinforced concrete columns is investigated under vertical loads and seismic excitation. Different supporting structures with rigidity and reinforcement detailing of the circular peripheral columns are considered in the integrated design. The vibration modes for the lattice dome with and without substructure effects are studied. Results show that high capacity substructure or fixed supporting assumption may lead to unsafe stability performance as well as uneconomical designs. The integrated design of composite system, RC supporting substructure and upper lattice roof could be provided superior dynamic stability performance when compared to the design without supporting substructure.

Keywords Integrated design, Lattice dome, Dynamic instability, Budiansky-Roth criterion, Mander model, PEEQ, Supporting substructure

1. Introduction

Lattice domes are a popular kind of space structures use for covering large sporting and cultural areas as sports centers, halls, gymnasiums, theaters, hangars, exhibition centers and other wide span roofs. Likewise, being lightweight, having a high degree of indeterminacy, high rigidity, satisfactory seismic vulnerability, being simple to produce, being fast to assemble, being fully prefabricated, which means there is no need to weld on site are the main reasons that may be outlined for widespread use of lattice roof shells. From the perspective of seismic vulnerability, lightness and spatial load distribution mechanisms that result in lower internal forces may be underlined in less damage of lattice shells when exposed to when compared to neighbor conventional buildings.

Steel lattice shells are usually supported by peripheral columns, reinforced concrete (RC) frames and wall substructures to provide architectural requirements and increase usable capacity of buildings. In design practice, upper lattice roofs are modeled with fixed boundary supports and the dynamic response interaction effects between the roofs and supporting substructure are not

taken into account. Whereas it is known that failure modes are well correlated with dynamic interaction of both parts of structure, which may bring about significantly different results compared to fixed support case. This is particularly valid when system passed elastic ranges. We learned from past earthquakes that a weak point of lattice shells located at the vicinity of anchor supporting. From this perspective, the seismic assessment of supporting substructures on dynamic responses of whole system is crucial and need more detailed studies.

Several studies are carried out investigating the influence of rigidity or/and flexibility of boundary support on dynamic behavior of raised lattice roofs (Moghaddam, 2000; Hazrati and Chenaghloou, 2007; Takeuchi et al., 2004; Cao et al., 2004; Wang et al., 2008). Moghadam (2000) examined the seismic response of double-layer barrel vault roofs, with and without the sub-columns, with an emphasis on post buckling behavior of roof elements. Hazrati and Chenaghloou (2007) investigated dynamic effect of rigid and flexible supporting substructures. The support reactions and the effective frequency content are other issues that were discussed.

Cao et al. (2004) compared dynamic responses of three different raised cylindrical lattice shell models (model with concrete supporting substructures, hinged supports and elastic supports) to obtain an appropriate analytical model. In this way, the performance of combined system and influence of some structural parameters, including height and strength capacity of columns are investigated.

It was found that an interaction between lattice roof and substructure may lead to unsafe results and cannot be overlooked. Wang et al (2008) examined seismic response of the elevated single layer oval shell sit on peripheral RC columns, in the case where, some regular roof parts of lattice roof replaced by Buckling-Restrained-Braces (BRBs). Recently, J. Sun et. al (2014) and J. Yan et.al (2016) also emphasized the important role of the substructure in the design.

Despite many new achievements of accomplished studies in most of them, only an elastic behavior of supporting substructures is incorporated into dynamic analysis. While, feasible roof nonlinearity and unexpected failure mode of supporting structure as well as unrealistic large seismic forces of roof members at the vicinity of boundary supports as well as overestimate forces of connections are some consequences those could be outlined, can be affected from linear assumption of supporting substructures. In this study, it is intended to achieve more realistic seismic behavior of inelastic composite system by considering both the geometrical and the material nonlinearity of supporting substructure.

The integrated design of the composite system in the presence or absence of supporting structures is examined. It is planned to clarify the overview appropriate design methodology to consider the integrated design elevated lattice domes supported by peripheral columns. However, in most cases steel domes are designed and constructed with fixed supported assumptions like dome is stayed on the ground. But this assumption is doing not represent the real behavior.

2. Modeling and Method of Analysis

The geometry of the analytical models is built up using the FORMIAN platform (Nooshin and Disney, 2001). The program has been developed on the basis of the Formex algebra that enables one to form different geometrical surfaces of lattice shells very easily through changing of some control parameters. Several single layer spherical domes with Diamatic configuration in the presence or absence of peripheral columns are generated. The output of the Formian model is converted into an input file of the ABAQUS (Karlsson and Sorensen 1999) analyzer to perform dynamic instability analyses. The geometry and surface configuration for both types of dome models are shown in Fig. 1. The openings of domes are 40 m and raise-span (f/L) ratios are $1/5$. Likewise, the sweep angle is $A=40$, frequency, $m=7$; number of sectors, $n=6$; and joint's form of dome members are rigid connections.

The moment resistance substructure frames that including pipe member columns being supported by pin connections is considered. The tension ring is circled around the lattice dome and the connecting links between the tension ring and the supporting substructure are pin joints. The requirements for simplifying principal modes are clarified and distributions of maximum acceleration in both horizontal and vertical directions are introduced through the simple expression as a function of their own period ratio and mass proportion of dome and supporting substructure. The pipe sections with size of $\text{Ø}160 \times 6.5$ mm are used for peripheral ridge components. Remaining components of domes, including the rib members are orbital with $\text{Ø}114 \times 3$ mm diameter in size.

The structural RC substructure models are designed for combined gravity and seismic effects, in compliance with the Turkish seismic code specifications (TEC, 2007). The supporting RC columns are prepared and detailed according to the Turkish standard for design and construction of reinforced concrete structures (TS-500, 2000).

The supporting substructures composed of twenty-four RC columns with $H=6.0$ m height and flexural stiffness, that arranged around the dome, periphery. Each column placed under the peripheral ridge nodes one among. The column heights are 6 m and are located at a distance of the 5.22 m. The diameters of circular sections and in turn reinforcement details varied to cover the full range of support conditions, from rigid to flexible in comparison to those of the upper domes. The RC column diameter changed in range of 50 cm to 90 cm, which symbolized through D50 to D90 at an acronym of models.

In first stage, the single dome restrained by fixed supports, is analyzed (Fig. 1.a). The mechanical properties and reinforcement detail of supporting ring columns are changed to adjust both rigidity and strength capacity ratio of the substructures and upper domes given in Table 1. The notation shown in Table 1 defined geometry of the composite structure, for example, the "G5H6D50" symbolizes the model with raise-span ratio equal to $1/5$ and peripheral supporting columns with 6 m height and circular section of the 50 cm diameter. The "G5" notation denotes the lattice dome without supporting substructure.

The transverse reinforcement of all columns are $\text{Ø}10/10$ mm stirrups. It is assumed that concrete compressive strength equal to 30 MPa (C30). The yield strength of both longitudinal and transversal reinforcement is considered equal to 420 MPa. The Poisson's ratio is $\nu=0.3$. The longitudinal reinforcement arrangement of the D60 model is shown in Fig. 2.

The comparison made between dynamic performances of the steel lattice dome located on the RC supporting structures with different rigidity and strength capacity ratio towards the dome shell.

2.1 Elements Used for Simulation and Material Properties

The lattice domes tabular beams and peripheral RC columns are modeled using the Pipe-31 and Beam-31 elements from ABAQUS element library. The constitutive relation of mild steel tubular member material (Q235) is assumed an elastic-perfectly plastic model. The other mechanical characteristics of the steel tubular members are: $\sigma_y=235 \times 10^6 \text{ N/m}^2$, $E=2.06 \times 10^{11} \text{ N/m}^2$, $\nu=0.3$, $\rho=7850 \text{ kg/m}^3$. The mechanical properties of RC sub-columns are: C30, $E=2.5 \times 10^{10} \text{ N/m}^2$, $\nu=0.2$, $\rho=2500 \text{ kg/m}^3$ and the specified compressive strength is $f_{ck} = 30 \text{ MPa}$. In as much as the Beam 31 element cannot incorporate post-yielding degradation properties, stiffness softening, strength deterioration and concrete confinement characteristics due to reinforcement into the calculations. The Mander confined RC model is used and developed in "MATLAB" in order to incorporate post yielding properties of substructure columns into analysis through updating input file of whole model in the ABAQUS analyzer software.

It is assumed that an inelasticity of RC columns initiate when an internal compression force reaches to 40

% of the concrete compressive strength ($0.4f_c$) and upon passing this limit, the behavior curve, followed predefined Mander strain-stress envelope (Mander, 1988). Other post yielding properties of cross sections such as; tension stiffening; and failure criteria are defined in to the input file in a similar way. An example of stress-strain relationship (G5H6D60 column model) is shown in Fig. 3.

2.2 Gravitational Loads and Ground Motion Data

The roof load was taken as 1.47 kN/m^2 . All loads and self-weight of structures were treated as lumped masses and concentrated at roof nodes. For this purpose, roof nodes were defined as a mass element with an amount equal to 12.68 kN . The analyses were conducted in two steps. In first step, the dome was allowed to deform under the dead loads, then given ground motion record was applied in to model. The ground motion recorded at the "EL-CENTRO- Imperial Valley, Irrigation District" in 1940 was adopted to quake the system. The record selected has impulsive pulses in the beginning of time series, which could be led to severe structural damages by transmitting high energy to structure. That is why, the first ten second of tri-axial ground motion were adopted in following dynamic performance assessments.

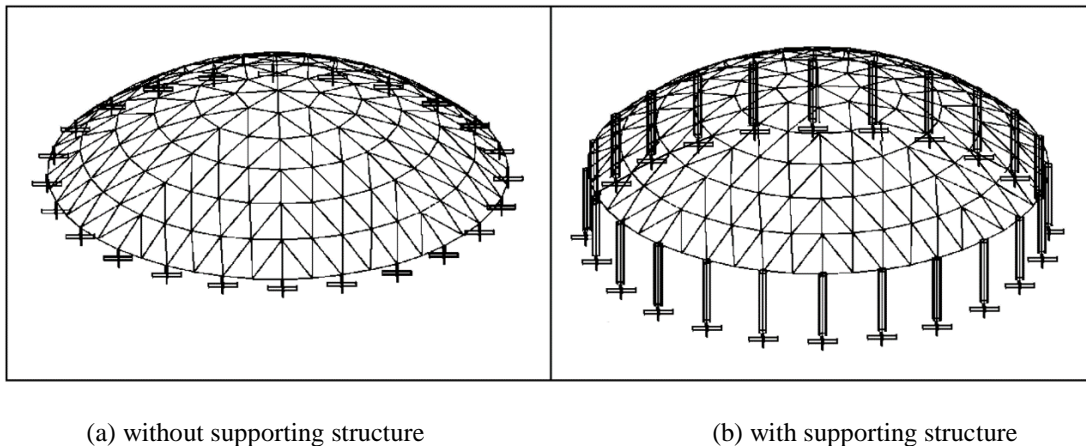


Fig. 1. Geometric models of the Diamatic domes.

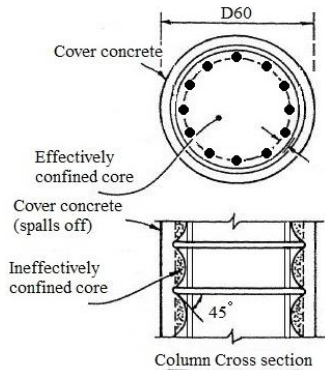


Fig. 2. Reinforcement detailing of substructure.

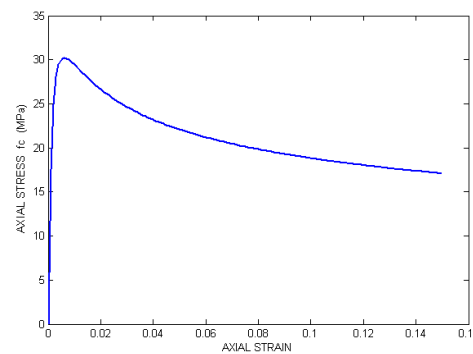


Fig. 3. Mander model stress-strain curve for circular column of D60 model ($f_{ck}=30 \text{ MPa}$).

Table 1. Cross-section and material properties of substructure peripheral columns

Models	Diameter (cm)	Rebars	Flexural Stiffness Kc (kN/m)
G5H6D50	D50	10Φ26	1065.2
G5H6D60	D60	12Φ28	2208.9
G5H6D70	D70	16Φ30	4092.3
G5H6D75	D75	16Φ32	5392.9
G5H6D80	D80	2x16Φ24	6981.3
G5H6D85	D85	2x16Φ25	8897.2

3. Dynamic Analysis of Integrated Dome Structures with Supporting Substructure

The dominant natural frequencies and mode shapes with greater mass participation factor are determined through the modal analysis. The dominant frequencies are required to create the Rayleigh’s coefficient in assembling

a damping matrix. Contrary to conventional buildings, where first few modes dedicated large percentage of mass participation, the spatial type structures have many vibration modes with significant mass participation factor ratio. The reason may be coming from the high degrees of freedom and wide spreading of masses throughout roofs. The Eigen frequencies ordinates for different supporting structure models and without supporting structure case are plotted in Fig. 4.

It is seen that frequencies ordinates corresponding to lower modes, which mainly belongs to prevailing horizontal movement, for domes with supporting substructures are less than those of single dome structures. Likewise, the natural frequencies are almost the same after the fifth mode. The reason underlying such similarity may be due to the high axial stiffness of columns in all cases and its ineffectiveness while vertical movements are prevailing. The higher modes of space structures are effective as well. The frequencies of lower dominant vibration modes are tabulated in Table 2.

Table 2 Comparison of free vibration frequencies (Hz) for some lower modes

Order of Frequency		1	3	5	7	10
No Substructure	G5	3.657	4.062	4.087	4.182	4.188
	Ø50	1.638	2.222	3.67	3.69	3.84
Domes with substructure (Column Sections)	Ø60	2.143	2.928	3.713	3.781	3.859
	Ø70	2.606	3.723	3.745	3.884	3.902
	Ø75	2.794	3.763	3.898	3.899	4.001
	Ø80	2.948	3.783	3.916	3.944	4.019
	Ø90	3.170	3.825	3.950	3.963	4.11

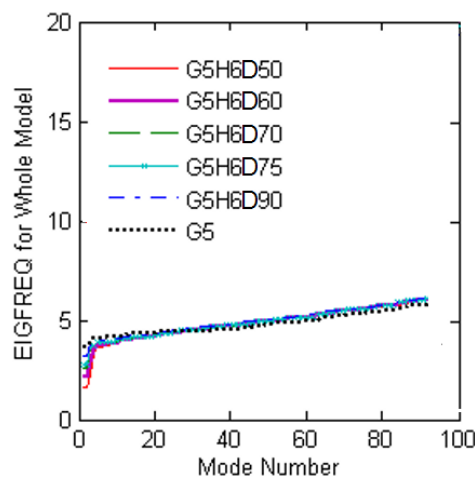


Fig. 4. Frequencies corresponding to mode numbers obtained from modal analysis.

The upper steel lattice roof and the supporting RC substructure composed of two structural materials, which in turn lead to different energy loss mechanisms at different parts of structural system, for this reason distribution of damping forces will not be similar to distribution of the inertial and elastic forces and in turn, damping matrix will be non-proportional (Clough and Penzien 2003). To construct the non-proportional damping

matrix, firstly proportional matrix is developed for each distinct part of the structure and then the damping matrix is formed through direct assembly. The modal damping of steel upper lattice dome is taken two percent of critical damping while those of the concrete supporting substructure would be five percent. In this way, the Rayleigh's coefficients are introduced to the analyzer for each part of models, individually.

To create a damping matrix with Rayleigh's method, the damping matrix coefficients (α and β) should be in hand. The mode shapes #2 with supporting substructure columns G5H6D90 model and dome with unsupported substructure model (G5) are illustrated in Fig. 5. As shown in Fig. 5, the second mode shapes for both models that exhibit lateral motion are compared. Lattice dome supported with columns has higher period value. Also P-

Delta effect will be playing an important role for the dynamic response of structure with sub-columns as well as the support conditions at substructure and upper dome connections. The local displacement is higher in the dome without substructure case as compared to the elevated dome because of the part of energy dissipated in the substructure peripheral columns.

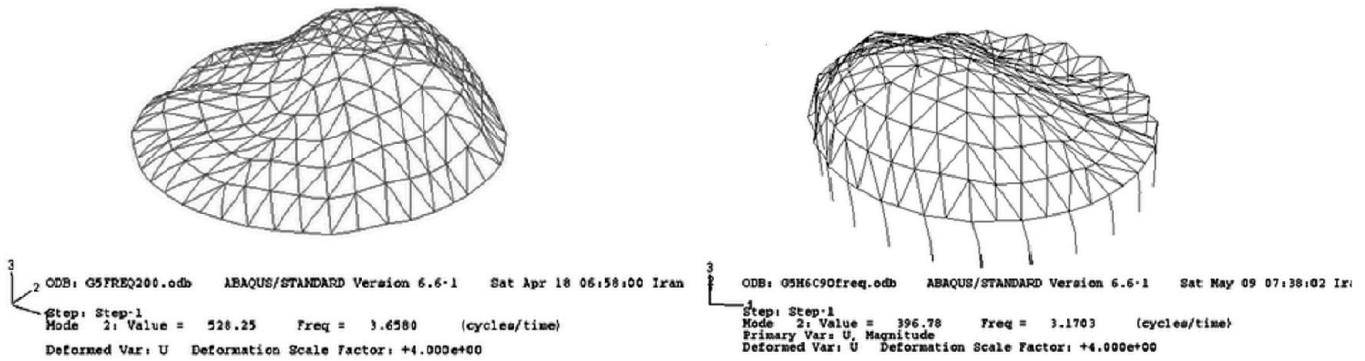


Fig. 5. Dominant mode shapes of model D90 with and without supporting substructure .

4. Discussion of Integrated Design Results

To evaluate dynamic performance, the structural model (see Table 1) are subjected to given ground motion at different intensities, such that the peak ground acceleration is increased stepwise and dynamic stability of the whole system are examined. Supporting substructures with different strength and rigidities in addition to a fixed boundary support (single dome) are considered as detailed in Table 1. More than a hundred nonlinear time history analyses are carried out. The dynamic buckling Lyapunov's Budiansky-Roth (1962) criterion was adopted to evaluate dynamic resistance loss of systems. The Budiansky-Roth criterion firstly applied by Budiansky and Roth to understand critical conditions for a pressure-loaded, clamped, shallow, thin, spherical shell. Using this method, the govern equations of motion solved for several values of loading parameter, i.e. starting from a small quantities and incrementing its severity.

The equivalent plastic strain (output variable PEEQ) parameter is examined and the maximum vertical displacements of apex node of domes are adopted as reference point to represent dynamic performance of systems. The PEEQ used to evaluate the yield condition of the beam element tube section. It is the total accumulation of plastic strain to define the yield surface size and obtained by integrating the equivalent plastic strain rate over the history of the deformation. Essentially it is a scalar measure of all the components of equivalent plastic

strain at each position in the model, somewhat like Von Mises stress that is a scalar measure the shear stress at a point and for loading with reversals. The zero values of the PEEQ represent that there is no plastic yielding in the cross section, so that it always grows with development of plastic deformations.

The nonlinear dynamic analysis is performed in stepwise. Firstly, the model with a high capacity substructure (G5H6D90) is exposed to stepwise incrementing uniaxial signal. Then analysis is repeated with increasing the peak ground acceleration amplitudes. The peak displacements of reference apex node platted corresponding to the peak ground acceleration intensities. The displacement time series of the dome apex node are shown in the Fig. 6 and the displacement response graphs of the vertex node corresponding to the peak ground acceleration for the G5H6D90 model is illustrated in Fig. 7.

The results show that, the structure remains stable until ground motion intensity increased up to 800 gals (0.8g). the structural components performed well in elastic range and small changes in response displacement exhibited. The peak displacement response of reference node raised abruptly once acceleration intensity reach to 900 gals (0.9g), plasticization of roof components initiated and in turn dynamic resistance of structure are lost (see Fig. 7). Therefore, the dynamic instability factor tolerated by this method based on the Budiansky-Roth criteria, determined as 900 gals (0.9g).

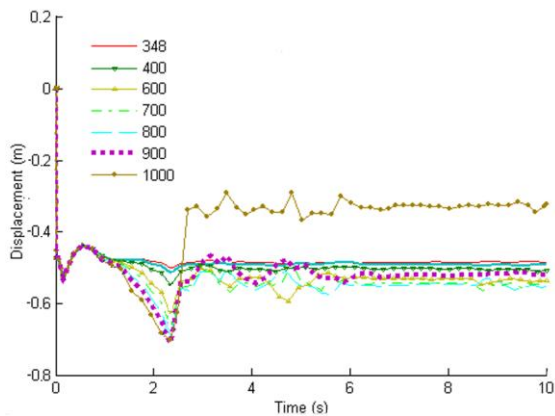


Fig. 6. The displacement time history of the apex node under given ground motion with different intensities.

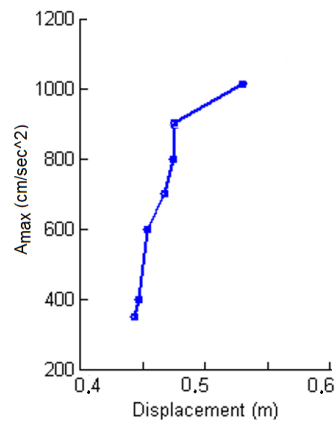
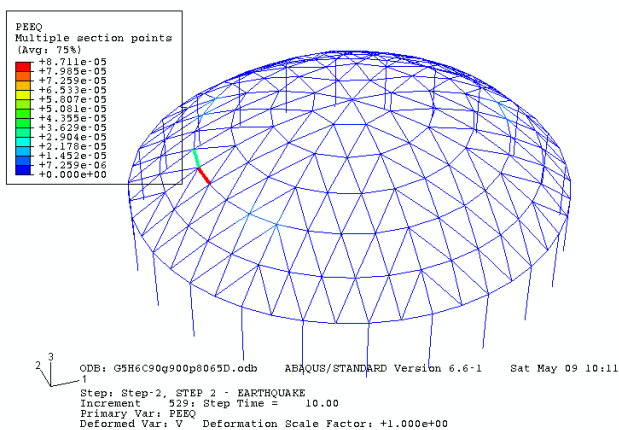


Fig. 7. The maximum displacement response of the dome apex node (G5H6D90 model).

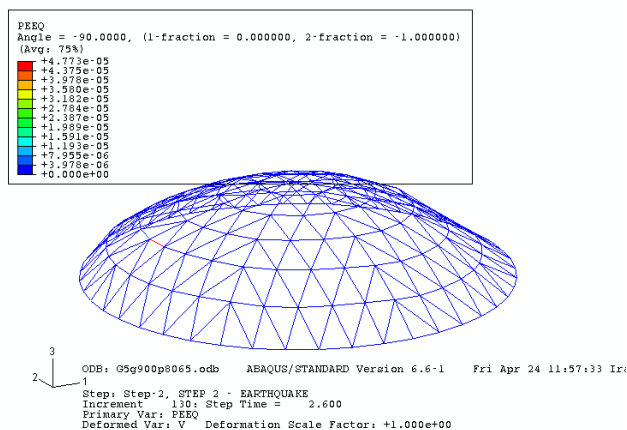
Fig. 8 shows the dynamic failure mechanism of high capacity supporting substructure model. The failure mode is similar to that of single lattice dome, i.e., the supporting peripheral columns do not affect the yield mechanism pattern and plasticization location. A similar procedure repeated for the rest of structural models. Both uniaxial and tri-axial ground accelerations of El Centro earthquake are applied to evaluate dynamic failure of the combined systems. Later, the section dimension and reinforcement

details of peripheral circular RC columns are modified to reach weaker supporting substructure.

Result shows that reduction of the cross section from Ø75 cm diameter (G5H6D75 model) to Ø70 cm (G5H6D70 model) influence failure mechanics. The failure mechanism and location of yielding shifted from an upper dome to supporting substructure. The yielding mechanism pattern for both the G5H6D75 and the G5H6D70 models seen in Fig. 9.



(a) Model G5, single dome



(b) Model G5H6D90

Fig. 8. The location of plasticization beginning for the rigid supporting substructures.

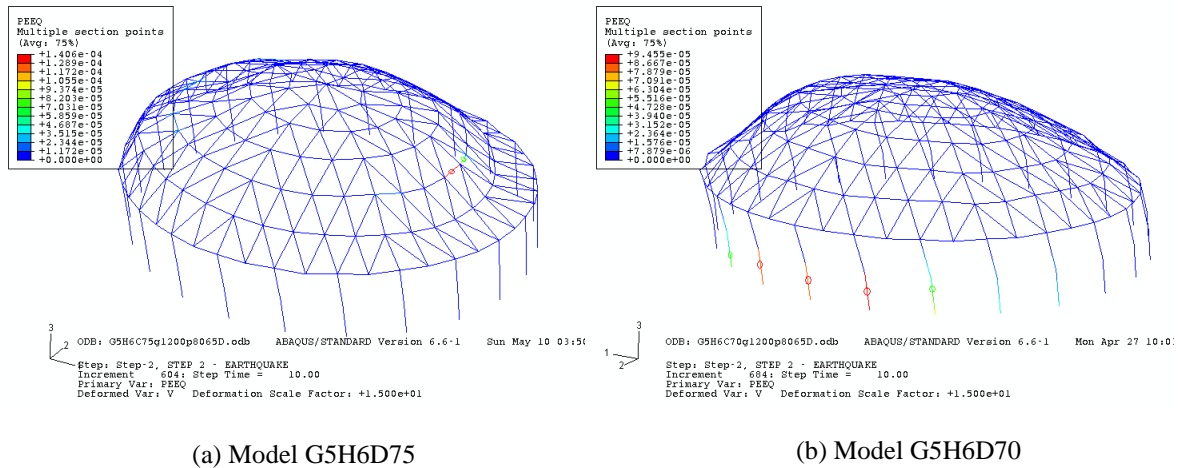


Fig. 9. The location of failure occurrence for weak substructures.

The dynamic instability levels under the uniaxial 1D (NS component) and triaxial 3D ground motions are shown in Fig. 10. Each chart represents rate of dynamic instability factor in term of peak ground acceleration intensity. The highlighted column charts in denote systems those dynamic failures initiated from roof members and distributed over the surface and the light color columns belong to structural systems that the failure mechanism generated from supporting ring columns.

A comparison of two graphs (Fig. 10) shows that, the dynamic resistance located at a higher altitude for uniaxial excitation, than corresponding tri-axial excitation scenarios. Graphs demonstrated that uniaxial excitation may leads to an underestimated evaluation of dynamic stability level for such structural complexes. It seems employing all three components of ground motion is necessary for more realistic estimation of dynamic resistance performance of raised lattice roofs.

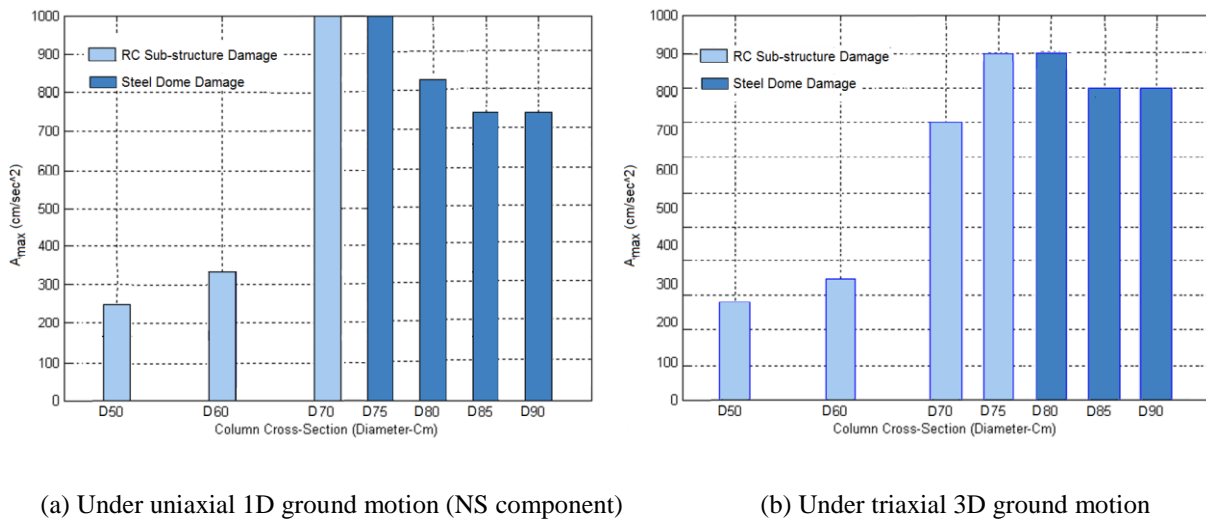


Fig. 10. Corresponding acceleration amplitude of dynamic failure resistance of structural models with supporting columns.

Furthermore, it is observed that seismic performance of upper dome may be affected by supporting substructure responses. That is to say, when substructures strength is higher than those of upper domes, the dynamic stability performance becomes similar to fixed support roofs. Likewise, it is seen that the proportional rigidity ratio of the upper dome and substructure improves dynamic instability, provided that the structural components of supporting substructure behave in elastic limits. The proportional rigidity ratio of both part of system result in constructive and beneficial interaction between them in

terms of internal force distribution and ductility of system, regardless of failures occurring in the upper roof or the peripheral sub-columns.

It is clear that, poor performance of peripheral columns disturbed serviceability, and the system loose service capabilities even in moderate ground motions. For instance, in Fig. 10 both systems undergo to ground motion at same hazard level, the G5H6D80 model shows the upper dome failure mode. In contrast, failures initiating from the sub-columns in the G5H6D75 model. It is observed that regulating the ratio of strength capacity of

supporting substructures with upper roof structures makes that initial forces of roof members are partly reduced, particularly at vicinity of the connecting locations to a supporting substructure. The most vulnerable places of lattice roof damages generally seen at support or roof members those close to boundary supports, that it is observed in the previous earthquakes.

5. Conclusions

An analysis results suggest in general, that:

- The lattice domes have a high dynamic resistance with respect to common building structures such that under moderate ground motions, lattice roofing elements remain in inelastic range. The lightweight of lattice roofs as well as its spatial load distribution mechanism is the main reason underlying satisfactory seismic performance.
- It is desired to use triaxial seismic excitation when evaluate the dynamic stability performance of raised lattice roofs. Applying uniaxial excitation may result in overestimate stability performances.
- Owing to high axial rigidity of the supporting sub-columns, vertical movement modes and corresponding frequencies are almost the same for all structural models, whereas dominant horizontal movement modes and related frequencies are varied, depending on the rigidity of the supporting substructure that seen at lower frequencies.
- Lattice dome supported with columns has higher period value. Thus, such a flexible system will have higher energy dissipating capacity through the higher deformation ability.
- P-Delta effect will be playing an important role for the dynamic response of structure with sub-columns as well as the support conditions at substructure and upper dome connections.
- The local displacement is higher in the dome without substructure case due to the part of energy dissipated in the substructure peripheral columns.

Regardless of the fact that failure mechanisms initiate from upper or supporting substructure, the proportional rigidity ratio between them give rise to better dynamic performance of the whole system in comparison to the fixed support model without supporting substructure model. The weak columns affect serviceability level due to yielding of the supporting substructure prior to reaching ultimate dynamic resistance of the upper domes.

It seems that considering the fixed supports or highly resistant substructure assumption will be unsafe and uneconomical designs. Thus, integrated design will be necessary for real nonlinear behavior considering seismic load effects due to the elevated height and composite interaction effect at the connections. In practice, there is needed for further investigation to reveal dynamic response interaction between both parts of such composite structural systems.

References

- [1] Budiansky B. and Roth R. S. (1962), "Axisymmetric dynamic buckling of clamped shallow spherical shells," (NASA TN D-1510), collected papers on Instability of Shell Structures.
- [2] Cao Z., Xue S.D. and Zhang Y.G. (2004), "Analytical model and vibration control for shells", IASS Symposium, Montpellier.
- [3] Clough R.W. and Penzien J. (2003), "Dynamics of structures", Computers and Structures, Inc. PP.242-245, Third Edition
- [4] Fan F. and Shen S. Z. (2004), "Study on the dynamic strength failure of reticulated domes", IASS Symposium, Montpellier.
- [5] Hazrati Y. and Chenaghlou M. R. (2007), "Effect of rigid and flexible support to seismic behavior of double layer barrel vaults," 2th National conference of spatial structures, Tehran, Iran.
- [6] Karlsson H. and Sorensen (1999), ABAQUS/Post Manual, Version 5.8, Pawtucket, RI, USA.
- [7] Mander J., Priestley M. and Park R. (1988), "Theoretical stress-strain model for confined concrete," American Society of Civil Engineering (ASCE).
- [8] Moghaddam H. (2000), "Seismic behavior of space structures", International Journal of Space Structures, Vol. 15, No. 2, pp. 119-135.
- [9] Nooshin H. and Disney P. (2001), "Formex configuration processing 2", International Journal of Space Structures, Vol. 16, No. 1.
- [10] Sun J., Li H., Nooshin H. and Parke Gerard A.R. (2014), "Dynamic Stability Behavior of Lattice Domes with Substructures", International Journal of Space Structures.
- [11] Takeuchi T., Ogewa T., Nakagawa M. and Kumagai T. (2004), "Response evaluation of medium-span lattice domes with substructures using response spectrum analysis", IASS Symposium, Montpellier.
- [12] Turkish Earthquake Code (TEC, 2007). Specification for buildings to be built in seismic zones, Ministry of Public Works and Settlement Government of Republic of Turkey.
- [13] TS-500 (2000). Requirements for design and construction of reinforced concrete structures. Turkish Standards Institute.
- [14] Wang X., Chen J. and Wu Ch (2008), "Dynamic analysis of single layer lattice shell with BRBs", Proceedings of the 6th International Conference on Computation of Shell and Spatial Structures, IASS-IACM, Cornell University, Ithaca, NY, USA.
- [15] Yan J., Qin F., Cao Z., Mo Y.L. (2016), "Mechanism of coupled instability of single-layer reticulated domes", Engineering Structures, 158-170.

Performance Assessment of Advanced Biological Wastewater Treatment Plants Using Artificial Neural Networks

Harun Türkmenler*[‡], Murat Pala**

*Department of Environmental Engineering, Faculty of Engineering, Adıyaman University, Adıyaman, Turkey

**Department of Civil Engineering, Faculty of Engineering, Adıyaman University, Adıyaman, Turkey

(hturkmenler@adiyaman.edu.tr, pala@adiyaman.edu.tr)

[‡]Corresponding Author; Harun Türkmenler, Department of Environmental Engineering, Adıyaman University, Adıyaman, Turkey, Tel: +90 416 223 3800, Fax: +90 416 223 3809, hturkmenler@adiyaman.edu.tr

Received: 29.06.2017 Accepted: 22.09.2017

Abstract- In this study, the application of Artificial Neural Network (ANN) techniques was used to predict the performance of wastewater treatment plant. The ANN-based model for prediction of effluent biological oxygen demand (BOD) concentrations was formed using a three-layered feed forward ANN, which used a back propagation learning algorithm. Based on the mean absolute percentage error (MAPE), the sum of the squares error (SSE), the absolute fraction of variance (R^2), the root-mean-square (RMS), the coefficient of variation in percent (cov) values, and ANN models predicted effluent BOD concentration. The R^2 values were found to be 94.13% and 93.18% for the training and test sets of treatment plant process, respectively. It was found that the ANN model could be employed successfully in estimating the daily BOD in the effluent of wastewater biological treatment plants.

Keywords Artificial neural network, Biological oxygen demand, Modeling, Performance assessment, Wastewater treatment plant

1. Introduction

Biological Oxygen Demand (BOD), Chemical Oxygen Demand (COD) and Suspended Solid (SS) parameters, design and operating of the treatment systems, checking of whether wastewater discharge limits are suitable for the receiving environment are important parameters used to evaluate the performance of the treatment systems. That the number of treatment plants and the importance of are increasing day by day makes it necessary to apply for new methods in first prediction then in analysis of pollutant parameters.

That the influent parameters of wastewater treatment plants show great changes makes it difficult to run these plants with an optimum performance. Several tools have been tried to be developed to run the plants at optimum performances especially for the last 10 to 15 years. Among these tools, the most commonly used one is a mathematically developed active sludge models, employing differential equations in a form of matrices. Although active sludge models have been being developed through IAWQ

(International Association of Water Quality) since 1987, these models still have some weaknesses and disadvantages. Thus, as an alternative to these developed mathematical models, artificial intelligence technics which are based on neural networks and have more common usage area have been lately started to be used and successful results have been achieved [1].

Traditional modeling techniques used in bioprocesses are based on balance equations together with rate equations for microbial growth, substratum consumption and formation of products. Also, since microbial reactions coupled with environmental interactions are non-linear, time variable and a complex nature [2] of traditional deterministic and empirical modeling have shown some limitations [3]. Moreover, predicting the plant operational parameters using conventional experimental techniques is time consuming and is an obstacle in the way of efficient and effective control of such processes. The ANN-based models were found to provide an efficient and a powerful tool to predict WWTP performance [4].

However, in the studies mentioned above, ANN models were configured as single or multiple input and single (or two) output(s). For instance, Wen et al. predicted BOD [5], Choi et al. modeled Total Nitrogen (TN) [6], Mjalli et al. grouped the input–output data in two vectors (one input and one output) for the first approach and four vectors (three inputs and one output) for the second approach [7]. Most of the studies so far have aimed the prediction of overall treatment plant performance or performance of a particular process, but none of these have considered the consecutive subsections (primary and secondary treatment units) in the whole WWTP. Models considering the main treatment units separately and estimating multiple parameters have not been sufficiently developed yet. It is stated by Mingzhi et al. that there is still no all-inclusive procedure or method to design such intelligent controllers by far because of its semi-empirical nature in spite of some successful practical applications [8]. So, studies carried out so far are mostly based on two or three parameters input and single output.

The ANN model is very effective in representing the relationships between input and output variables in nonlinear and complex systems. Moreover, ANN models have been widely applied to address problems in process forecasting and control in water and wastewater treatment [9, 10].

In this study, the most critical operation parameters most commonly used in declaration of the pollution level of the wastewater and checking of the performance of the wastewater treatment have been selected as influent-effluent control parameters of the model. These parameters are BOD, COD and SS, TN, Total Phosphorus (TP) and the flow rate. ANN model was developed for the prediction of effluent BOD. The model was performed to the influent and final effluent streams in the Atakoy Advanced Biological Wastewater Treatment Plant (AABWWTP).

2. Material and Methods

2.1. General Description of Advanced Biological Wastewater Treatment Plant

The objective of the plant is to collect the wastewater from Bakırköy, Bahçelievler and Bağcılar districts completely and Küçükçekmece and Gaziosmanpaşa districts partially, which are currently discharged to Ayamama and Tavukcu Rivers, and therefore polluting the Marmara Sea, through collectors, to convey such wastewater to the AABWWTP, where the wastewater is treated in advanced level, and finally, to discharge the treated wastewater to the environment harmlessly. The treatment plant treats the wastewater produced by a population of 1 600 000 people, by removing carbon, nitrogen and phosphorus with a capacity of 400 000 m³/day. Fig. 1. shows the process flow diagram of AABWWTP. The sludge produced by the plant is made environmentally harmless in the driers.

Data was taken from the database of AABWWTP of Istanbul/Turkey a period of 306 daily records of the year 2012. This period was satisfactory as it covers all probable seasonal variations in the studied variables. To construct the model structure, totally 6 critical wastewater quality

parameters were selected as input variables. The output of the ANN model includes BOD. Total 306 data are used and from this 276 for training and 30 for testing.

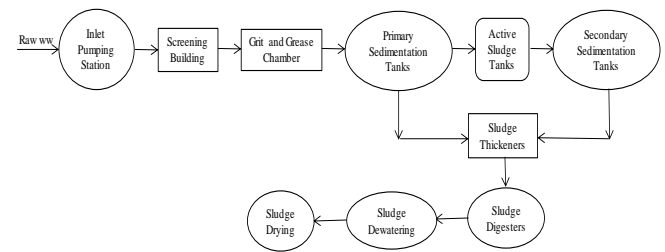


Fig. 1. Process flow diagram of AABWWTP.

2.2. ANNs

The ANNs are computer systems developed to automatically fulfil the aim of producing new knowledge by learning and skills like exploring which are exclusive to human brain. It is either extremely difficult or impossible to achieve these skills with traditional computer methods. Therefore, It can be said for artificial neural network to be a computer science branch concentrating on adaptive data processing for cases for which programming is either impossible or extremely difficult [11].

Mjalli et al. has successfully made the predictions of key parameters like BOD, COD and SS values in the effluent in an urban wastewater treatment plant [7]. Cinar monitored the performance of a domestic wastewater treatment plant in terms of BOD, SS and fecal coliform parameters and successfully predicted the effluent parameters with an ANN model [12]. By using a 10-month BOD and SS data of a domestic wastewater treatment plant, Hamed et al. showed that performance could be predicted correctly based on these parameters after a few stages of training [4].

When the interactions between the inputs and outputs of a target events that a neural network is wanted to learn are non-linear, Multilayer Perceptron (MLP) Model can be utilized. Since the pollution level coming into the treatment plant isn't constant and the correlation between parameters can't be stated through equations, the multilayer perceptron model has been used [11].

Economical and easy operation of these wastewater treatment plants at present is an important subject through the utilization of the data that is obtained as the plant is operated in the prediction of the data that will be obtained in the future. It has today been possible to control the plants through modelling in computers by the prediction of operation parameters numerically in advance. ANNs are a data processing system that has a parallel scattering and is composed of many processing units and connections. The ability of ANNs to learn and make generalizations over the relations of the experimental inputs and outputs without a need of any assumption or suggestion provides a big contribution to the studies in this field.

ANN model was developed to predict effluent BOD concentration for the AABWWTP. ANN is an information processing system inspired by the way such as biological nervous systems e.g. brain. The aim of a neural network is to compute output values from input values via some internal calculations [13].

There are many various kinds of training algorithms. Back Propagation Algorithm (BPA) is one of the most common classes of training algorithms for Feed Forward Neural Networks (FFNNs) [14].

To solve complex problems in many different fields of application such as pattern recognition, identification, classification, speech, vision, and control systems, ANNs have been employed successfully. Today, ANNs can be trained to solve problems which are difficult for conventional computers or human beings. Moreover, one of the plus points of ANNs, different from the conventional approach, is that it extracts the desired information directly from the data. A neuron is the fundamental processing element of a neural network. A biological neuron is based on input from other sources and perform in a way that a general non-linear process on the result of combining them and give the final result. An input layer, some hidden layers, and an output layer usually compose the network [15].

A MLP is the most basic and commonly used ANN. This includes at least three or more layers, including an input layer, an output layer, and a number of hidden layers. Each neuron in one layer is connected to the neurons in the next layer, and there are no connections among the units of the same layer. Depending on the problem, the number of neurons in each layer may change (Fig. 2.). The relationship between inputs and outputs can be represented in an easier way using biases network. Generally, a transfer function including algebraic equations may be linear or non-linear [16].

In context of this study, the influent values of the pollution parameters of the wastewater treatment plant have been tried to be taught to the network. Since the network is to make predictions based on the values of the network, Multilayer Perceptron Model has been chosen. In this network, values are supplied to the network on entrance layer, and after they pass through sub-layers, they go to the output layer, where the answer of the network to the input data is served to the world outside.

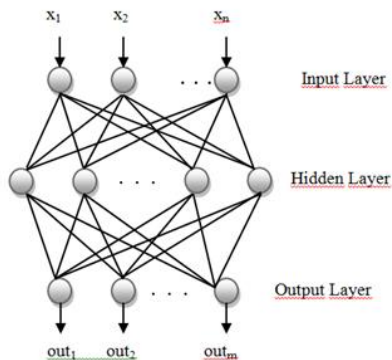


Fig. 2. A typical MLP neural network.

Neural networks are formed by input data vectors, neurons and output functions. Input data to the neuron are transformed by means of a base function and leave by an activation function [17] connection between input and output data and neurons is made by weight factors, which determine the effect of the input variable on the neuron.

The weighted sum of input components is calculated as

$$Net_j = \sum_{i=1}^n w_{ij} x_i \tag{1}$$

where Net_j is the weighted sum of the j th neuron for the input received from the preceding layer with n neurons, w_{ij} is the weight between the j th neuron and the i th neuron in the preceding layer, and x_i is the output of the i th neuron in the preceding layer. The output of the j th neuron, out_j , is calculated using a sigmoid function as follows:

$$out_j = f(Net_j) = \frac{1}{1 + \exp(-kNet_j)} \tag{2}$$

where k is a constant that is used to control the slope of the semi linear region. Non-linear Sigmoid activates in each layer except the input layer [18].

Through a particular training pattern in which it adjusts the weights by a small amount at a time, the BPA, as one of the most famous training algorithms for the MLP, is a gradient descent technique to minimise the error. The conjugate gradient algorithm (CGA) and the scaled conjugate gradient algorithm (SCGA) as several adaptive learning algorithms have newly been explored. In CGA, to determine an appropriate step size, which makes the CGA faster than BPA, a search is made in each iteration along the conjugate gradient direction. SCGA is more effective than BPA and CGA [19]. By using a step size scaling mechanism, SCGA avoids a time-consuming line search per learning iteration [20].

3. Results and Discussion

3.1. ANNs in Certain Formulation of Treatment Process

In this study, ANN is used to develop a formula based on the logistic sigmoid (logsig) transfer function. The data used for training and testing ANN was obtained from AABWWTP. The result of using the normalization values shown in the Table 1, inputs and outputs are normalized in the (0–1) range. In Table 1, the maximum and minimum values of inputs and outputs are also showed. There are six input parameters in the input layer, namely the Q_w , BOD_{in} , COD_{in} , SS_{in} , TN_{in} , and TP_{in} and the output parameter is BOD_{out} (Fig. 3). The range of inputs and outputs in the trained network is given in Table 1.

With a binary sigmoidal transfer function, the chosen network architecture was 6-9-1 (Fig. 3); SCG was the learning algorithm used. 10 000 iterations were performed in order to find out the optimum result.

Table 1. The range of input and output parameters and normalization values

Parameters	Range of values	Normalization value
Q _w (m ³ /sn)	5,52-0,99	6,9
BOD _{influent} (mg/L)	560-120	700
COD _{influent} (mg/L)	2.352-325	2940
SS _{influent} (mg/L)	1.744-148	2180
Total-N _{influent} (mg/L)	132-26	165
Total-P _{influent} (mg/L)	25,50-4,20	31,88
BOD _{effluent} (mg/L)	37-4	46,25

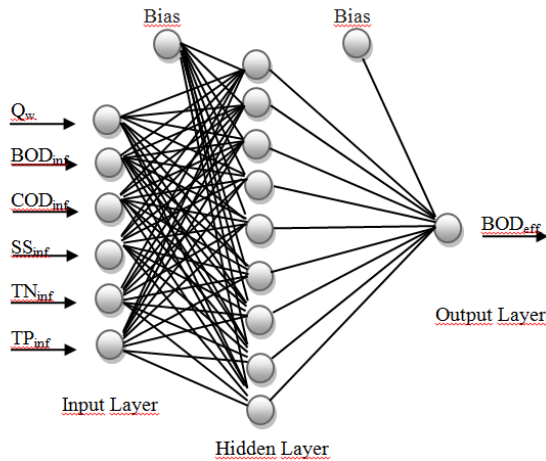


Fig. 3. The architecture of proposed backpropagation neural network.

The network uses the default SCG algorithm for training. The application randomly divides input vectors and target vectors into two sets as follows: 90% is used for training; 10% is used to validate that the network is generalizing and to stop training before over-fitting.

For effluent BOD of the training errors are ensured below. Results showed that errors for each condition were quite satisfactory. Thus, the trained Artificial Neural Networks was shown good results quite satisfactory. The performance of training and test sets and the trained ANN statistical parameters are shown in Figures 4 and 5, and in Table 2, respectively. As shown in Figures 4 and 5, and in Table 2, the correlation factor, for any two sets, a pretty high proof of the correctness of trained ANN model.

Table 2. Statistical parameters of the ANN formulation.

	Training set	Test set
MAPE	23.8079	24.3268
SSE	2.3666	0.3334
RMS	0.0929	0.1037
cov	0.2569	0.2743
R ²	0.9413	0.9318

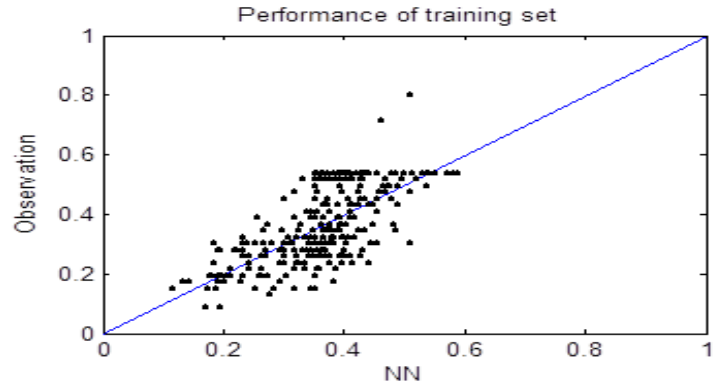


Fig. 4 The performance of the training set.

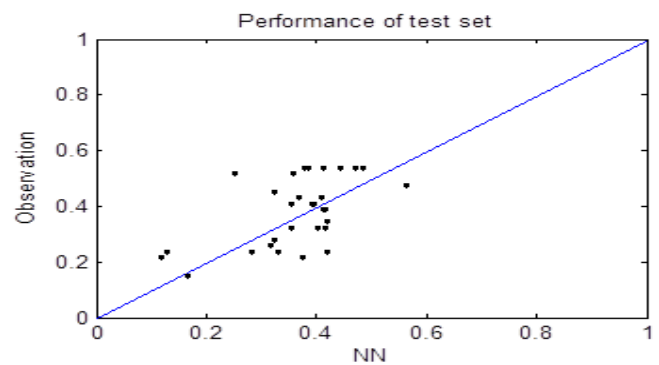


Fig. 5 The performance of the test set.

The MAPE, SSE, R², RMS, and the cov are defined as follows, respectively:

$$MAPE = \left(\frac{o-t}{o} \right) * 100 \tag{3}$$

$$SSE = \sum_j (o_j - t_j)^2 \tag{4}$$

$$R^2 = 1 - \left(\frac{\sum_j (t_j - o_j)^2}{\sum_j (o_j)^2} \right) \tag{5}$$

$$RMS = \left((1/p) \sum_j |t_j - o_j|^2 \right)^{1/2} \tag{6}$$

$$cov = \frac{RMS}{o_{mean}} * 100 \tag{7}$$

where o is the output value, p is the pattern, o_{mean} is the mean value of all output data, and t is the target value.

The maximum MAPEs were found to be 23.8079% and 24.3268% and the R² values to be approximately 0.9413 and 0.9318 for the training and test sets for the effluent BOD model, respectively. In this case, the network response is satisfactory, and simulation can be used for entering new inputs.

ANN models predicted the dynamic behavior of BOD concentrations with good accuracy and provided a very good fit to the training data and the testing data (Figs. 4 and 5). The proposed neural networks can satisfactorily describe the behavior of the process. As a result, the predicted effluent

BOD rates matched the observed concentrations based on the relatively low SSE, MAPE and very high R^2 values, suggesting good prediction performance of the models. When considering the high level of complexity of these biological processes, the broadness of the data range and the computed error values, it is seen that the method successfully predicts the target output.

ANN method is an economical and useful method which can be used in prediction of effluent values and efficiency as the experimental work is both costly and time-consuming. As a consequence of the studies carried out, it has been seen that MLP model, which has been modelled through the data used

from the AABWWTP values had a great match with the real data.

3.2. Certain Formulation of Effluent BOD

By using the parameters (inputs, weights, normalization factors) of the proposed ANN model, the certain formulation of effluent BOD is derived. From the trained ANN, all necessary parameters are gated, and from the weights of the trained ANN model, the certain expression is formed. In Tables 3 and 4, the weights and bias values in the derivations of ANN based formulations are given. Each input is multiplied by a connection weight.

Table 3. Weight and bias values between input and hidden layers.

Weights	Number of hidden layer neurons (i)								
	1	2	3	4	5	6	7	8	9
w_{1i}	-22,088	-25,193	-24,737	-12,696	5,5185	-8,3588	16,211	21,819	-76,642
w_{2i}	-13,351	-15,793	21,3465	-1,1106	-6,2143	25,6021	-12,314	-19,088	25,8532
w_{3i}	-1,0371	2,9238	-17,403	-1,2963	-6,135	-0,1825	-1,7067	17,7272	56,167
w_{4i}	1,5861	0,59	-38,798	4,5001	-15,806	18,0896	13,325	29,2159	-20,066
w_{5i}	3,6185	5,8039	28,1283	-18,064	12,3541	-25,636	-7,3943	-21,79	-56,363
w_{6i}	-7,3057	-9,3036	16,6211	4,632	9,5572	13,19	8,0006	-11,485	0,3147
Bias	19,2864	21,6877	-6,5005	8,8204	5,3474	-6,8099	-0,5591	4,0212	34,5093

Table 4. Weight values between output and hidden layers.

Weights	Number of hidden layer neurons (i)								
	1	2	3	4	5	6	7	8	9
w_i	18,8592	-16,273	13,5517	-4,3086	-9,6423	1,0393	-5,6049	16,8257	1,0551

In a simple manner, to generate a result first of all products and biases are simply gathered, then transformed through a transfer function (logistic sigmoid), and finally outputs are obtained more easily. Inputs and outputs are normalized prior to the learning process of artificial neural networks. Normalization values to obtain a correct result from the proposed formulas have to be thoroughly considered in this study. Proposed formulation as input parameters obtained from the Table 1 between the maximum and minimum values should be noted that current [21]. -2.8380 is bias value between hidden layer and output.

4. Conclusions

In wastewater treatment plants, important parameters of the effluent, BOD, COD, SS, TN and TP, have to be monitored. When these modelling practices are compared to the traditional ones the formers have a lot of advantages. The most important of them is getting the result correctly and quickly. So, by means of using past data for more than one parameter or component predictions can be done toward future and experimental practice need can be minimized and thus, operation costs of the plant can be greatly reduced. Another important advantage of ANNs is that due to their fast-learning ability they can solve a question that they have never encountered before. Therefore, usage of ANNs in

modelling practices of wastewater treatment plant has become more common. This paper reveals that estimation of effluent BOD for wastewater treatment process using ANN verifies to be a better technique than conventional mathematical modeling. ANN gives very satisfactory results for the proposed model.

This study confirms the ability of the artificial neural network modeling to forecast the performance of AABWWTP. The proposed certain formulation in the present study will be of help to make this procedure short in a more effective manner than experimental works.

Through the knowledge of the parameters affecting the efficiency of the treatment, new and theoretic output and efficiency values can be produced by means of using trained and tested ANN analysis without doing further experimental studies. As a result, ANN is an effective method in prediction of the effluent BOD concentrations of AABWWTP and the efficiency values based on those.

It is concluded that, ANN provides an effective analyzing and diagnosing tool to understand and simulate the non-linear behavior of the treatment process, and is used as a valuable performance assessment tool for plant operators and decision makers.

Acknowledgements

The author would like to thank to the Istanbul Water and Sewerage Administration (İSKİ), Istanbul, Turkey, for providing the AABWWTP process data used in this study.

References

- [1] Cinar O, Yilmaz A., "Application of Artificial Neural Network Method on Operation of Wastewater Treatment Plant: An Example Study", *KSU. Journal of Science and Engineering*, 8(2): 48-52, 2011.
- [2] Lee D S, Park JM., "Neural network modeling for on-line estimation of nutrient dynamics in a sequentially-operated batch reactor", *Journal of Biotechnology*, 75: 229–239, 1999.
- [3] Cote M, Grandjean B P, Lessard P, Yhibault J., "Dynamic modeling of the activated sludge process: improving prediction using neural networks", *Water Research*, 29: 995–1004, 1995.
- [4] Hamed M, Khalafallah M G, Hassanein E A., "Prediction of wastewater treatment plant performance using artificial neural network", *Environmental Modeling and Software*, 19: 919–928, 2004.
- [5] Wen C. H., Vassiliadis C. A., "Performing hybrid artificial intelligence techniques in wastewater treatment", *Engineering Applications of Artificial Intelligence*, 11: 685-705, 1998.
- [6] Choi D., Park H., "A hybrid Artificial Neural Network As A Software Sensor for Optimal Control of A Wastewater Treatment Process", *Water Res.*, 35: 3959-3967, 2001.
- [7] Mjalli F. S., Al-Asheh S., Alfadala H. E., "Use of artificial neural network black-box modeling for the prediction of wastewater treatment plants performance", *J. Environ. Manage.*, 83: 329-338, 2007.
- [8] Mingzhi H., Ma Y., Jinquan W., Yan W., "Simulation of a paper mill wastewater treatment using a fuzzy neural network", *Expert Systems with Applications*, 36: 5064-5070, 2009.
- [9] Zhang Q., Stanley SJ., "Real-time wastewater treatment process control with artificial neural network", *J Environ Eng. ASCE*, 125: 153–160, 1999.
- [10] Yu RF., Cheng WP., Chu ML., "On-line monitoring of wastewater true color using digital image analysis and ANN", *J Environ Eng. ASCE*, 131: 71–79, 2005.
- [11] Oztemel E., "Artificial Neural Networks", Papatya Publication, İstanbul, 2003.
- [12] Cinar O., "New tool for evaluation of performance of wastewater treatment plant: Artificial neural network", *Process. Biochem.*, 40: 2980–2984, 2005.
- [13] Delgrange V. N., Cabassud N., Cabassud M., Durand-Bourlier L., Laine J. M., "Neural networks for prediction of ultrafiltration transmembrane pressure: application to drinking water production", *Journal of Membrane Science*, 150: 111–123, 1998.
- [14] Demuth H., Beale M., Hagan M., "Neural Network Toolbox 5: Users Guide", Natick. MA The MathWorks Inc., 2007.
- [15] Kalogirou S. A., "Applications of artificial neural-networks for energy systems", *Applied Energy*, 167: 17–35, 2000.
- [16] Lu W., "Neural network model for distortional buckling behaviour of coldformed steel compression members", Ph.D. thesis, Helsinki University of Technology, 2000.
- [17] Machon I., López H., Rodríguez-Iglesias J., Marañón E., Vázquez I., "Simulation of a coke wastewater nitrification process using a feed-forward neuronal net", *Environmental Modelling and Software*, 22: 1382–1387, 2007.
- [18] Pala M., "A new formulation for distortional buckling stress in cold-formed steel members", *Journal of Constructional Steel Research*, 62: 716–722, 2006.
- [19] Berke L., Patnaik S. N., Murthy P. L. N., "Optimum design of aerospace structural components using neural networks", *Computers & Structures*, 48(6): 1001–1010, 1993.
- [20] Kang H. T., Yoon C. J., "Neural network approaches to aid simple truss design problems", *Microcomputers in Civil Engineering*, 9: 211–218, 1994.
- [21] N., Pala M., Elmas M., Eryılmaz D. M., "A new approach to determine the base shear of steel frame structures", *Journal of Constructional Steel Research*, 65: 188-195, 2009.

Design of Used PET Bottles Crushing Machine for Small Scale Industrial Applications

Ikpe Aniekan E.*[‡], Owunna Ikechukwu**

*[‡]Department of Mechanical Engineering, University of Benin, Nigeria

**Department of Mechanical Engineering, University of Benin, Nigeria

(ikpeaniekan@gmail.com, ikechukwu.owunna@uniben.edu)

[‡]Corresponding Author: Ikpe Aniekan, Room 142, Mechanical Engineering Department, University of Benin, Nigeria,

Tel: +2349024773812, E-mail: ikpeaniekan@gmail.com

Received: 07.07.2017 Accepted: 22.09.2017

Abstract- In this study, PET bottles crushing machine was designed to convert used PET bottles into shreds readily available for recycling. Preliminary tests and mechanical factors were extensively evaluated on the conceptual designs to ensure that the concept with optimal performance and efficiency is selected. Experimental test was conducted to determine the power required to overcome the shear stress of the PET bottles and it was found out that 10hp was the power required. With a set of crushing forces ranging from 1000-3000N, Finite Element Analysis (FEA) was performed for five different scenarios on the 201 Annealed Stainless Steel cutting blade to inspect the material response to stresses and corresponding deformations. The maximum von Mises stress was $2.089e+006\text{N/m}^2$. The material yield strength was found to be $2.92e+008\text{ N/m}^2$, and applying a force of 3000N on the cutting blade produced a maximum displacement of $2.220e-003\text{ mm}$. This therefore imply that the material will not deform or fail under a force equal to or below the material yield strength value. Tests carried out on the final machine design indicated efficiency of 82.2% which is only 6% less than the efficiency of existing ones.

Keywords: PET bottles, Crushing, Design, Machine, non-biodegradable, Environment.

1. Introduction

One of the prevalent environmental problem encountered in most developing countries is Solid Waste Management (SWM). Waste has been defined as any material that is of no value to the owner, and therefore disposed as waste [1]. Municipal solid waste (MSW) also known as urban solid waste is defined as non-air and sewage emissions generated within and disposed by the municipality. These includes household waste, commercial refuse, construction and demolition debris, dead animals and abandoned vehicles [2]. MSW is mainly characterized by paper, vegetable matter, plastics, textiles, metals, rubber and glasses [3]. MSW management is gradually becoming a plague that requires immediate attention for optimum protection of public health and environment. This is as a result of increasing population growth, high rate of consumption, urbanization, lack of effective waste management plan etc. [4]. In recent times, studies have shown that apart from the environmental

pollution and contamination of ground water by organic waste, plastic waste such as polyethylene terephthalate (PET) bottles is one of the waste management problems hampering the developmental and aesthetical state of our environment as a result of its indiscriminate disposal.

Polyethylene terephthalate is a polyester made from terephthalic acid (a di-carboxylic acid) and ethylene glycol (a di-alcohol) through the process of polymerisation. Since the introduction of PET bottles over 60 years ago, it has been a means of packaging water, juices, carbonated soft drinks, edible oil, liquor, chemicals etc. However manufacturers as well as consumers have grown increasing interest in the use of PET bottles due to a number of reasons [5].

In attempt to prevent sharing of drinking cups and maintain hygiene, PET bottles became widely acceptable because they are disposable, cheap, lightweight and made of durable materials which can readily be moulded into different

shapes and sizes relevant to a wide range of applications [6]. As a result of the world's increasing population which is about 7 billion people, there has been a high tendency for empty PET bottles to increase. The global PET packaging market was worth \$48.1 billion in 2014, amounting to almost 16 million tons according to a new market report. Demand for PET packaging is expected to increase by an average of 4.6% annually over the next five years, and will amount to 19.9 million tons, worth \$60 billion by 2019. With overall PET packaging consumption of 15.4 million tons in 2013, PET bottles for beverages accounted for over 80% of overall sales at 12.5 million tons (up to 3.7% on 2012). In 2013, bottle water became the largest category for PET packaging; sales of PET water bottles grew by 7.3% reaching 5.45 million tons [7]. This statistic poses a great environmental risk as a result of the fact that bottles made of polyethylene terephthalate (PET) material is non-biodegradable and can spend millions of years in the ground with little or no decomposition [8]. The huge quantities of PET bottles currently being marketed and consumed possibly find their way into waste dumpsites [9], and this creates serious environmental problems.

However, indiscriminate disposal of PET bottles and other non-biodegradable materials end up clogging drainage systems during raining season, causing flood and waterlog in residential areas which consequently serve as breeding ground for vectors such as mosquitoes. The inert nature of PET bottles renders them resistant to bio-degradation which leads to an increase in the amount of PET bottle wastes in dump sites [14, 15]. Moreover, the presence of plastic wastes in the environment is considered hazardous due to their potentials to catch fire easily. It also has negative effect on arable soil especially for farming purpose. Consequently, action should be taken to promote recycling of plastic bottles. According to Oseni [10], plastics which typically exemplifies PET bottles are more or less non-biodegradable as they remain undecomposed in the ground for several thousands of years.

Recycling is an aspect of environmental engineering that deals with the development of technically reasonable solutions to environmental problems which may involve designing a sustainable approach that can convert waste materials to useful items, thereby, avoiding the use of virgin raw materials which depending on the production process may constitute high level of environmental pollution, require high energy input and huge cost of production [11]. According to Tukur [5], manufacturing of PET bottles from virgin raw materials require high energy input with increasing CO₂ emission, and since plastics are not degradable materials, its accumulation after use contributes significantly to the prevalent problems bedeviling sustainable environmental protection practices. Recycling of PET bottles is bound to realize a lot of saving in

production costs, conserve limited resources, and alleviate environmental pollution [12].

PET bottles crushing machine is that which performs the function of crushing PET bottles or plastic materials into granules or shreds for recycling and production of new products rather than using virgin raw materials for production [13]. This study is focused on the design of a crushing machine for handling of used PET bottles. From the aforementioned points of view, crushing of PET bottles for recycling is cheaper than manufacturing the bottles from virgin raw material, and can also help in controlling the waste disposal problems ravaging the environment particularly in developing countries. For this reasons, there is a need for expansion of plastic recycling programs as well as cheaper machines to handle the problems associated with plastic waste management particularly PET bottles which has a wide range of application worldwide.

2. Methodology

To design the PET bottle crushing machine, two design concepts were considered as shown in Fig 1 and 2. The functional requirements considered included cost, safety, functionality, performance and reliability as presented in the decision matrix shown in Table 1. Experimental test was carried out in the workshop using a guillotine equipment to determine a set of forces required to crush empty PET bottles into shreds. Using SOLIDWORKS 2017 version, detailed computer aided design of the selected design concept was represented and stress analysis was carried out on the crushing blade to determine its integrity in actual service conditions.

2.1. Design Concept one (Simple Crank Mechanism)

Crank Mechanism as the name implies uses a simple crank mechanism to perform its crushing operation. The mechanism generally consists of a crank wheel connected to a reciprocating arm which usually terminates in a sliding piston. The crank is connected to the power source, while the reciprocating arm converts the rotary motion of the crank to reciprocating motion which is transferred to the piston where work is done. This is the prevailing mechanism in motor vehicles and reciprocating compressors. The major parts of the machine were fabricated using mild steel, this is because it is easy to join among all other metals. Above all, it is a very versatile metal, necessitating its use by many industrial applications. Apart from its versatility, it is also very cheap and readily available for use. Fig. 1 shows isometric skeletal view of design concept one (Simple Crank Mechanism).

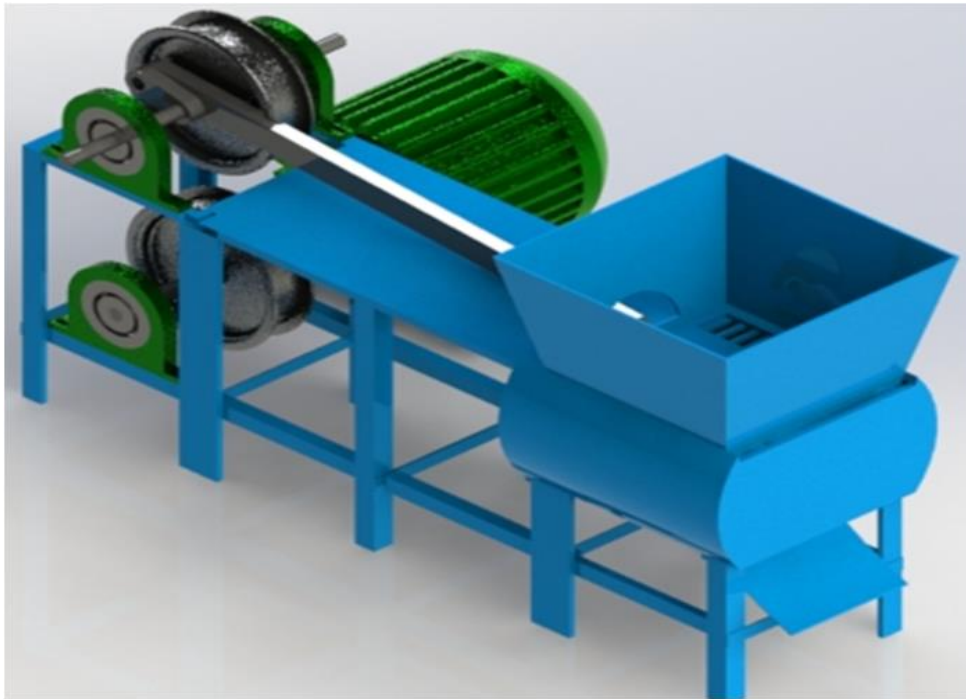


Fig. 1. Isometric view of a Simple Crank Mechanism.

The machine comprises of a motor at the base and a table with the hopper on the opposite end. Compressed or flattened bottles are loaded through the hopper. Power is generated by a motor at the base of the machine and thus, transmitted to the blade shaft through a belt to the pulley located at the blade shaft. The crank is attached to the pulley through the crank pin. A reciprocating arm is connected from the crank pin through the side into the base of the hopper. The end of the arm ends in a blade which slides in the hopper thus carrying out the shredding action. The crushing compartment is separated from the collection unit by a mesh which helps to control the size of pellets at the output of the machine. The large size particles remain in the crushing compartment for crushing.

2.2. Design concept two (Rotary blade against a fixed blade)

Design concept two applies the action of a rotational blade against a fixed blade in the hopper to crush PET bottles

contrary to the reciprocating action of the slider crank. The machine consists of a hopper and a frame made from angle bars. The hopper which has a voluminous inlet through which the PET bottles are fed into the machine, is mounted directly over the blades and the crushing compartment. They are secured to the frame by bolts and nuts. The rotary blade which is fixed to a shaft is designed with 201 Annealed Stainless Steel (SS) due to its good corrosion and wear resistance properties. The collector unit consist of a perforated curved plate to serve as a mesh for size control. During crushing action, the PET bottles are loaded into the machine through the hopper. The shaft rotates the loaded PET bottles into the space between the fixed blades, this allows the blade to exert enough force to overcome the shear resistance of the bottles. The fixed blade is bolted to the frame and cuts across the crushing compartment. The main important components of the machine are the frame, hopper, fixed and rotary cutters, pulleys, electric motor, bearing, perforated barrel as shown in Fig. 2.

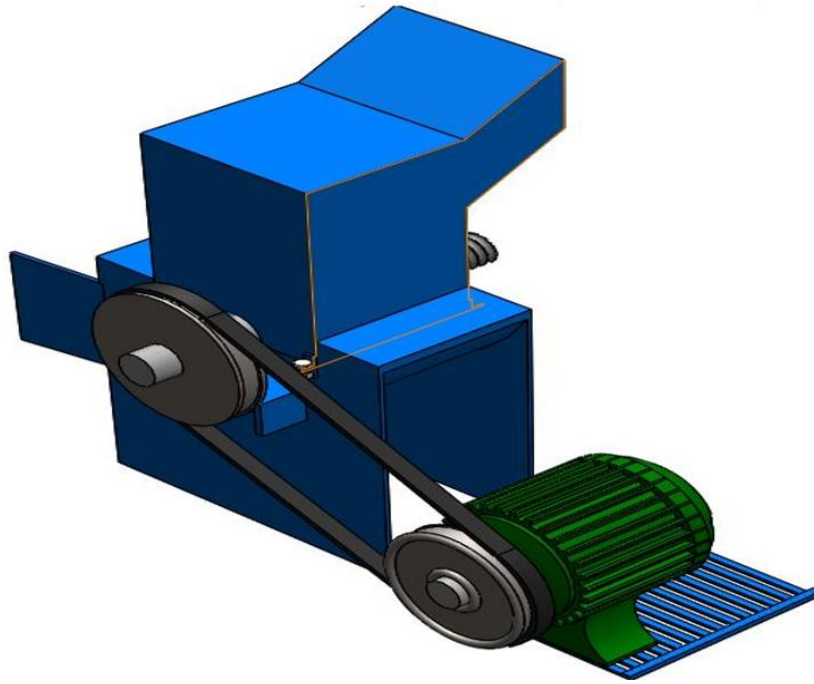


Fig. 2. Isometric view of design concept two Second (Rotary blade against a fixed blade).

The frame also guides, supports and holds in accurate alignment all the moving members of the operating machine. The barrel that houses the cutting chamber is perforated with a hole of 5mm so that the crushed PET bottles can pass through it into a collecting trough. The machine is also powered by electric motor via belt drive connected to the main shaft that turns the rotary cutters. Bulk of the parts in the machine were fabricated using mild steel due to its high strength, toughness, and weldability as a result of low carbon content, but however not readily tempered. PET bottles are fed into the hopper inlet without material preparation. The empty PET bottles settle down in the barrel that has in it fixed and rotary cutters made of high carbon steel. The rotary cutters are set into motion by switching on the 10 horse power electric motor that runs at 1440rpm. Also, there is a clearance between the fixed and rotary cutters where the PET bottles drop as they are loaded from the hopper inlet and are constantly being

smashed by the rotary cutters repeatedly until they are crushed. The crushed particles in the perforated barrel drops under gravity through the perforations of about 5mm and collected underneath with a trough.

2.3. Selection of Suitable Design Concept

Decision matrix was used to select the best concept for detailed design and fabrication. A decision matrix is a list of values in rows and columns that allow engineers to analyze and rate the performance relationship between a set of values and information. Each category is assigned a weighing factor based on the design characteristics which measure its relative importance (Norton, 1999). The design decision matrix proposed for the two concepts in this study is presented in Table 1.

Table 1. Decision matrix

Functional Requirement	Functionality	Performance	Reliability	Safety	Cost	RANK
Ratings	0.30	0.25	0.20	0.15	0.10	1.0
First Design Concept	6	2	4	2	4	3.8
	1.8	0.5	0.8	0.3	0.4	
Second Design Concept	5	9	8	9	9	7.6
	1.5	2.25	1.6	1.4	0.9	

Based on the ranking, the second design concept was selected for detailed design and fabrication. However, the first design concept was not considered due to material loss as a result of friction between rubbing surfaces such as the sliding parts and the frame as well as the space occupied by the machine. However, Design concept 2 was selected for its cost, portability, safety, functionality, reliability and above all, its ranking in the design decision matrix shown in Table 1.

3. Experimental Design Theories

The shearing forces required to cut the PET bottles were determined using a guillotine equipment represented in Fig. 3.

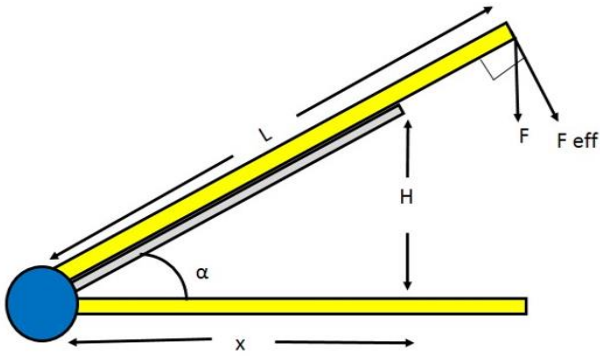


Fig. 3. Analysis of a guillotine equipment.

Where,

F_{eff} is the effective cutting force required (applied normal to the Handle)

L is the length of the force from the pivot

x is the horizontal length of the gutting blade from the pivot

H is the height of the blade from the Base

F is the cutting force applied to the Handle

α is the angle Between the blade and the base

Lb is the length of the cutting blade

Now if a force F is applied at the handle, the equation for the effective force is given by:

$$F_{eff} = F \cos \alpha \tag{1}$$

Fig. 4 represents the schematic diagram of forces acting at the handle of the guillotine equipment.

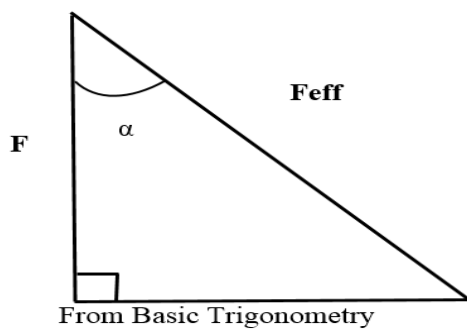


Fig. 4. Schematic of Forces acting at the Handle.

$$\cos \alpha = \frac{x}{Lb} \tag{2}$$

$$F_{eff} = \frac{mgx}{Lb} \tag{3}$$

We know that torque is the turning force of the blades

$$\text{Stress} = \frac{F_{eff}}{\text{Area}} \tag{4}$$

Where,

Area =

$$\text{Thickness of blade} * \text{Length in contact with bottle} \tag{5}$$

Therefore the equation for Power is given by

Power (p) =

$$\text{Torque (T) x Angular speed of motor } (\omega) \tag{6}$$

$$P = T \times \frac{2\pi N}{60} \tag{7}$$

$$\text{Where } \omega = \frac{2\pi N}{60} \tag{8}$$

$$T = F \times r \tag{9}$$

Where r = radius of the blade. The expression shown in equations 10, 11 and 12 were considered for the determination of the shaft speed.

$$\frac{D_1}{D_2} = \frac{N_2}{N_1} \tag{10}$$

$$N_2 = \frac{D_1 N_1}{D_2} \tag{11}$$

$$N_1 = \frac{D_2 N_2}{D_1} \tag{12}$$

Where,

D_1 = Pitch diameter of the driven pulley

D_2 = Pitch diameter of the driver pulley

N_1 = Rotational Speed of the driven pulley

N_2 = Rotational Speed of the driver pulley

Schematic showing all the forces and reactions on the shaft is presented in Fig. 5.

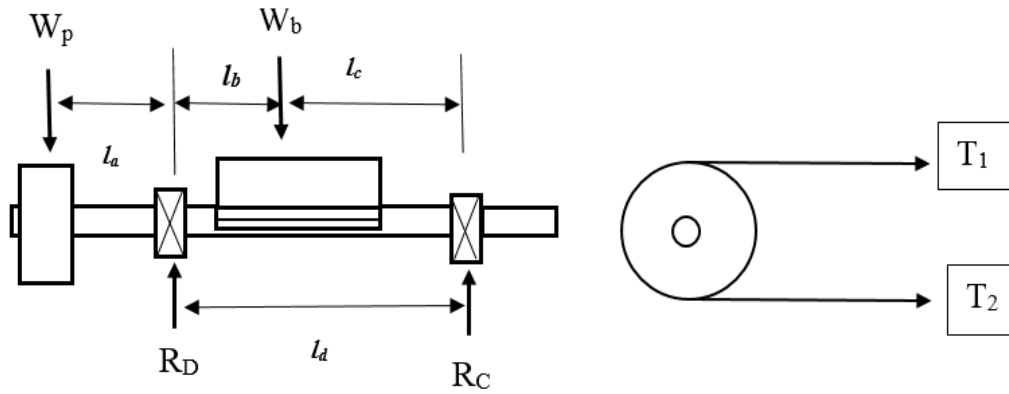


Fig. 5. Schematic Diagram of Weight and Bearing Reactions.

Where,

W_p = Measured weight of pulley

W_b = Measured weight of the blade

R_C = the reaction of bearing A

R_D = the reaction at B

T_1 = the tension in belt on the tight side

T_2 = the tension in the slack side

W_R = the sum of all the upward forces

Therefore,

$$W_R = W_b + W_p \tag{13}$$

$$W_b = 225N$$

$$W_p = 3672.17N$$

4. Results and Analysis

This section presents the results obtained from the different task mentioned in the Methodology (section 2 above).

4.1. Experimental Results for Shearing Force and power

An experiment to determine the shear force required to overcome the shear resistance of PET bottles was carried out using PET bottle samples with different strength requirements. A guillotine cutter was used to cut the flattened bottle under the influence of some desired dead weights. The experimental results are presented in Table 2. The results obtained for masses, crushing time and Machine Through put Capacity (MTC) of the PET bottles crushing Machine is tabulated in Table 3. Fig. 6 shows a graph of torque against effective force and crushing force, while Fig. 7 shows a graph of crushing power against crushing force.

Table 2. Results Obtained from Experimental Test

Mass (Kg)	Weight (N)	Effective Force F_{eff} (N)	Shear Stress(N/m ²)	Crushing Force F_c (N)	Torque (N/m)	Power (KW)	Power (Hp)
30	294.3	292.9623	2929623	219.7217	30.76103864	1.546234	2.0735
35	343.35	341.7893	3417893	256.342	35.88787841	1.80394	2.419084
40	441.45	390.6164	3906164	292.9623	41.01471818	2.061646	2.764667
45	490.5	439.4434	4394434	329.5826	46.14155795	2.319352	3.11025
50	539.55	488.2705	4882705	366.2028	51.26839773	2.577057	3.455834
55	588.6	537.0975	5370975	402.8231	56.3952375	2.834763	3.801417
60	637.65	585.9245	5859245	439.4434	61.52207727	3.092469	4.147001
65	686.7	634.7516	6347516	476.0637	66.64891705	3.350174	4.492584
70	735.75	683.5786	6835786	512.684	71.77575682	3.60788	4.838167
75	784.8	732.4057	7324057	549.3043	76.90259659	3.865586	5.183751
80	441.45	781.2327	7812327	585.9245	82.02943636	4.123292	5.529334

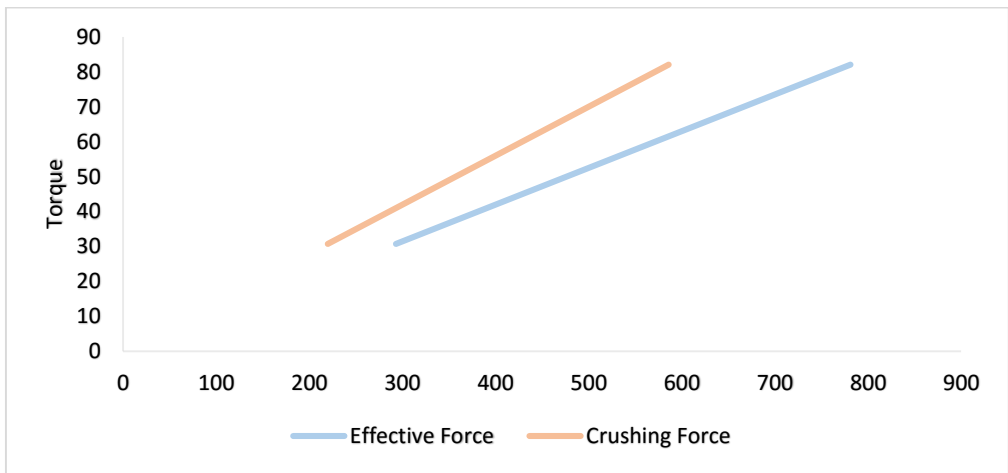


Fig. 6. Graph of Torque against Effective Force and Crushing force.

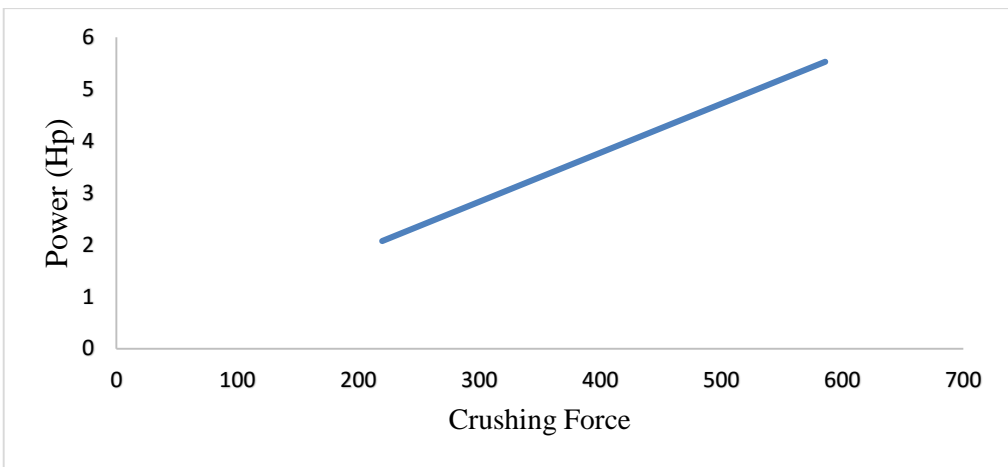


Fig. 7. Graph of Crushing Power against Crushing Force.

Table 3. Result for Masses, Crushing time and MTC of the Crushing Machine

S/N	Mass of PET Bottles fed into crushing machine M_1 (kg)	Mass of properly crushed PET Bottles M_2 (kg)	Crushing Time (s)	MTC (kg/s)
1	3.4	1.8	56	0.061
2	9.6	6.2	104	0.092
3	16.7	11.6	122	0.137
4	20.4	15.4	144	0.142
5	24.8	20.1	182	0.136
6	30.2	25.7	248	0.122
7	36.3	32.3	294	0.123
8	43.4	38.5	338	0.128
9	64.7	47.9	420	0.154
10	66.5	52.4	537	0.124
11	70.6	57.2	649	0.109
12	76.7	66.4	702	0.109
13	80.2	69.8	824	0.097
14	83.9	70.6	832	0.101
15	86.0	72.5	898	0.096
16	92.2	75.7	984	0.094
17	96.7	79.4	1010	0.096
18	104.6	84.8	1016	0.103
Σ	1006.9	828.3	9,360	2.024
Ave	56.0	46.02	520	0.112

The machine through put capacity is calculated from equation (14)

$$MTC = \frac{M_1}{T} \tag{14}$$

Where,

MTC = Machine through put capacity

M₁ = Mass of used PET bottle fed into the machine

M₂ = Mass of crush PET bottle plastic waste

T = Machine crushing time

The mass of PET Bottles fed into crushing machine M₁ (kg) was used for testing the crushing efficiency of the machine for each interval, and this was carried out for eighteen times during which the input (M₁) and the output (M₂) were recorded accordingly. Applying equation (15), the average of

used PET bottles fed into crushing machine and the output were determined, and these values were substituted into equation (16) to calculate the efficiency of the plastic crushing machine.

$$Ave. = \frac{\Sigma}{S/N} \tag{15}$$

$$C_{eff} = \frac{Output}{Input} * 100 = \frac{AveM_2}{AveM_1} * 100 \tag{16}$$

The output is the mass of empty PET bottles properly crushed while the input is the mass of empty PET bottles fed into the crushing the machine. These masses were substituted into equation (16) to determine the crushing efficiency of the machine as follows.

$$C_{eff} = \frac{46.02}{56.0} * 100 = 82.2\%$$

The results obtained indicated that the machine is 82.2% efficient. A graph of mass of properly crushed PET plastic waste bottle against crushing time is shown in Fig. 8.

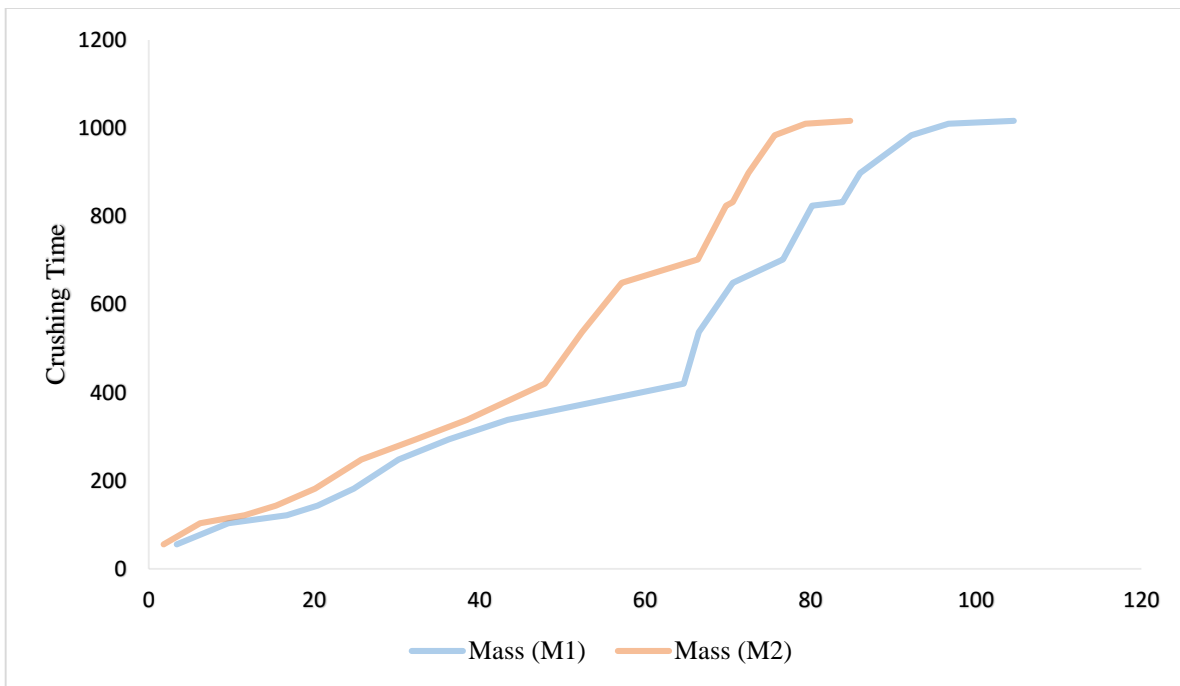


Fig. 8. Mass of properly crushed PET plastic waste bottle against crushing time.

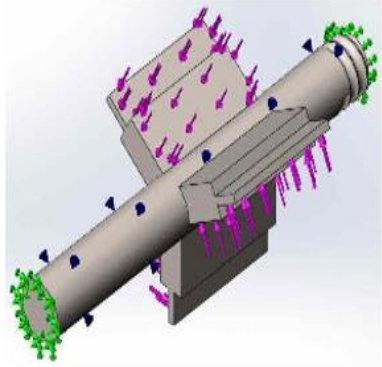

The crushing time is a function of properly crushed PET bottles. As shown in Fig. 8, as the mass of properly crushed plastic waste increases, the crushing time increase as well. This implies that there is a linear relationship between crushing time and masses of crushed PET bottles.

4.2. Computer Aided Design Analysis

The following analysis was carried out on the cutting blade using SOLIDWORKS to design and simulate the

stresses and also to examine the variations of stress distribution at different force applications. The factor of safety was maintained at 8. Static analysis was carried out by applying varying forces of 1000N-3000N to the cutting blade, and the stress variations resulting from the forces were recorded. Table 4 shows properties of the material used for the crushing blade design.

Table 4. Material Properties of the crushing blade

Solid Body 1 (Cut-Sweep Blade analysis)	Solid Mesh	Material Properties	
		Material	201 Annealed Stainless Steel (SS)
		Model type	Linear Elastic Isotropic
		Default failure criterion	Max von Mises Stress
		Yield strength	2.92e+008 N/m ²
		Tensile strength	6.85e+008 N/m ²
		Elastic modulus	2.07e+011 N/m ²
		Poisson's ratio	0.27
		Mass density	7860 kg/m ³
		Thermal expansion	1.7e-005 /Kelvin

This indicates the forces acting on the machine shaft due to the bearing connector. A bearing connector allows rotation in only one axis. During operation forces are set up which the

bearings must withstand from the shaft. Table 5 represents the axial, shear and reaction force components in the X, Y, and Z directions respectively.

Table 5. Bearing Connector Forces

Type	X-Component	Y-Component	Z-Component	Resultant
Axial Force (N)	0	0	-3.5353e-011	3.5353e-011
Shear Force (N)	1.9749e-009	-3.7355e-008	0	3.7407e-008
Reaction Force (N)	6.79065e-005	-2.55265e-005	2.51748e-007	7.25462e-005

4.3. Design Study

The following are results obtained when the blade was subjected to forces ranging from 1000N to 3000N using

Annealed stainless steel as material, and the maximum Von-mises stresses induced are tabulated in Table 6. Fig. 9 represents a graph of maximum Von-Mises stresses against applied force.

Table 6. Von Mises Stress Induced as a Result of Varying Force

Parameters	Units	Scenario 1	Scenario 2	Scenario 3	Scenario 4	Scenario 5
Force	N	1000	1500	2000	2500	3000
Material	N/A	201 Annealed Stainless Steel (SS)	201 Annealed Stainless Steel (SS)	201 Annealed Stainless Steel (SS)	201 Annealed Stainless Steel (SS)	201 Annealed Stainless Steel (SS)
Constraints	(N/m ²) ² /Hz	0.000000	0.000000	0.000000	0.000000	0.000000
Max Von Mises Stress	N/m ²	6.9646e+005	1.0447e+006	1.3929e+006	1.7412e+006	2.0894e+006

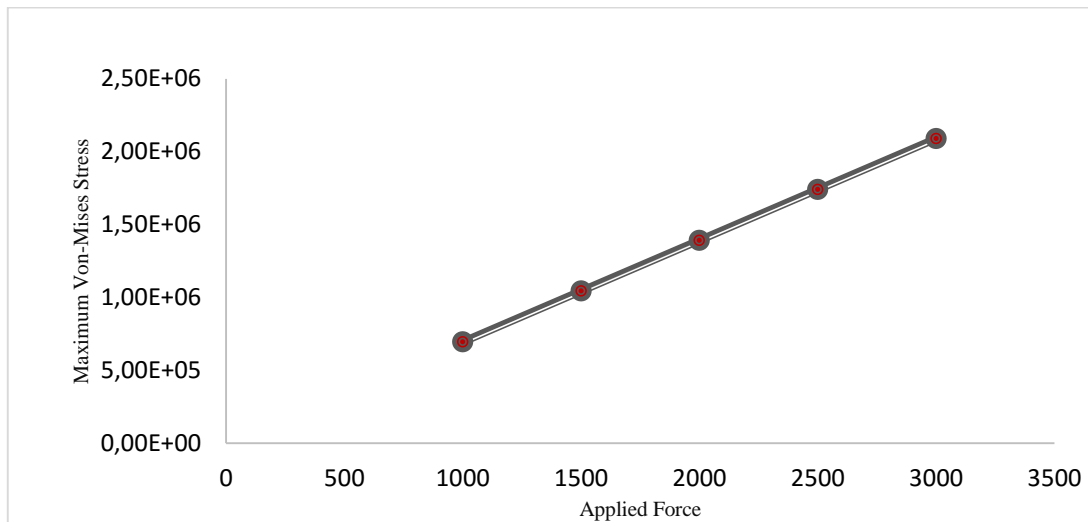


Fig. 9. Graph of Maximum Von Mises Stresses against Applied Force.

4.4. Static Stress Analysis

Using maximum force of 3000N to analyze the PET bottles crushing blade design model, the following Von-mises

stresses and displacement were obtained as shown in Fig 10 and 11 respectively.

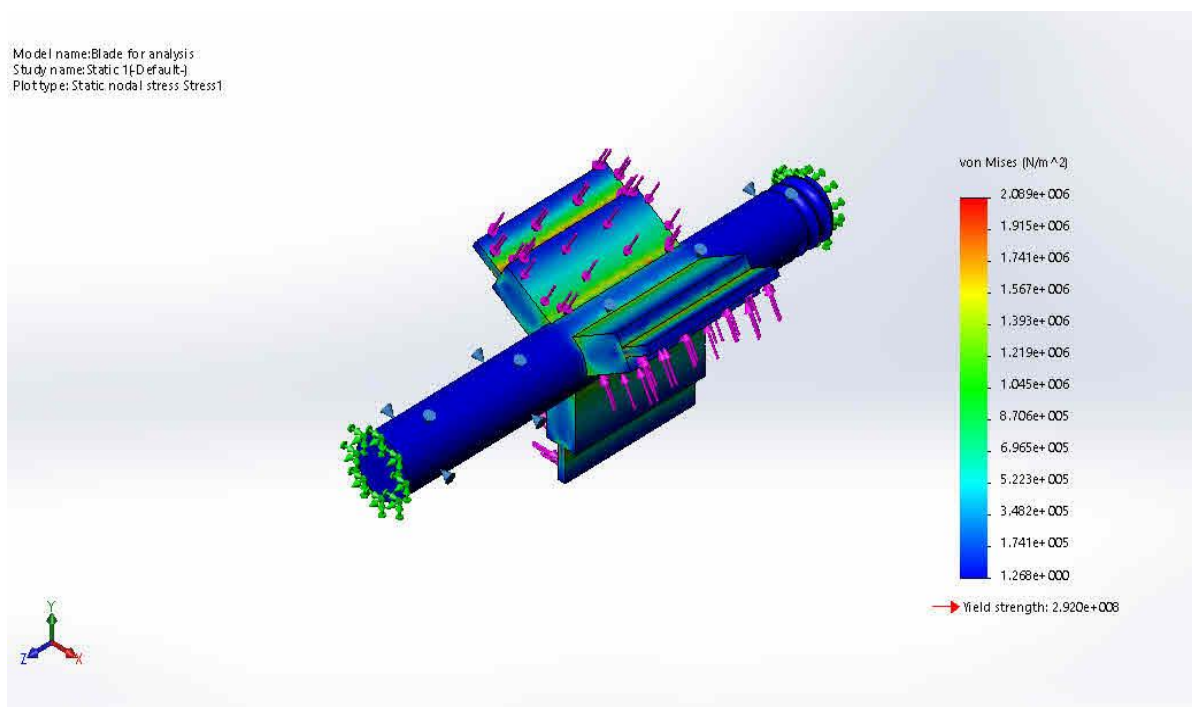


Fig. 10. Result of Von-mises Stress Obtained from the Crushing Blade Analysis.

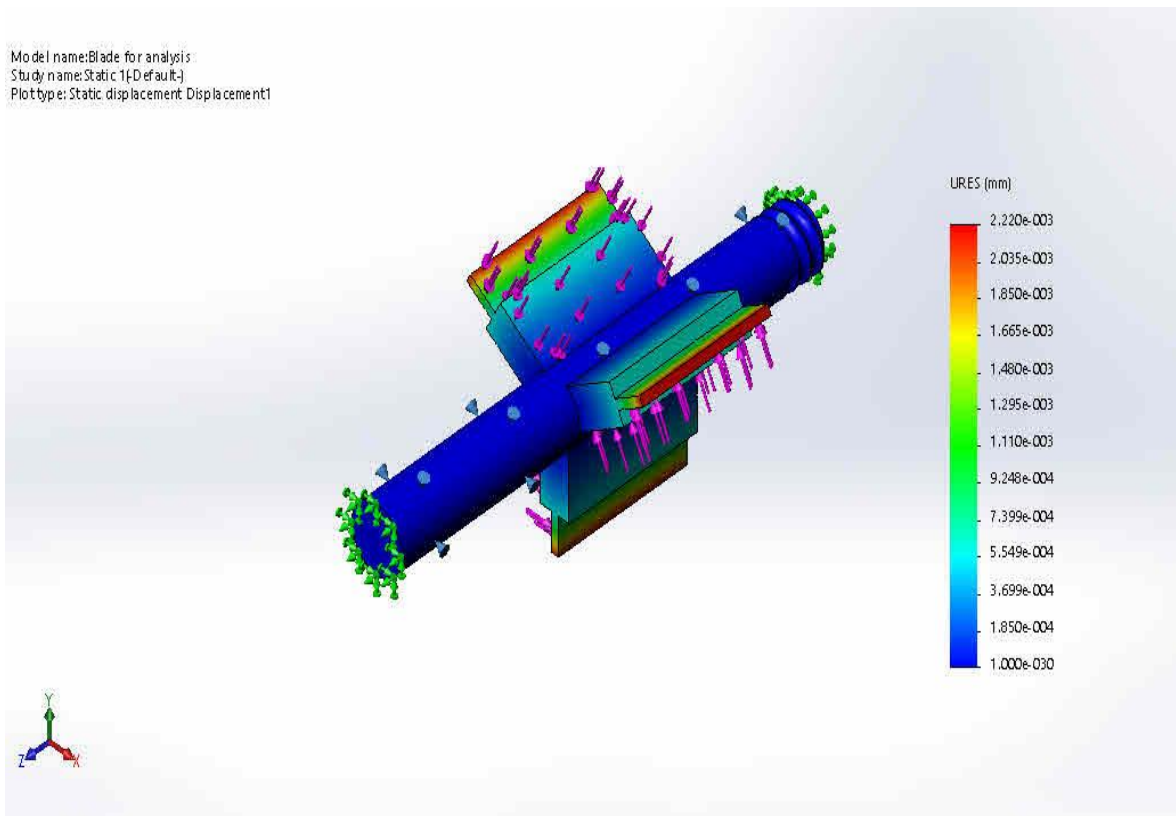


Fig. 11. Result of Displacement Obtained from the Crushing Blade Analysis.

It can be seen from the above that when a force of 3000N is applied on the cutting blade with all the conditions stated above taken into consideration, The maximum von Mises stress is $2.089e+006\text{N/m}^2$ at Node: 8523, and the minimum is $1.268e+000\text{N/m}^2$ at Node: 10247. The yield stress of the material was found to be $2.92e+008\text{N/m}^2$, and applying a force of 3000N on the cutting blade produced a maximum displacement of $2.220e-003\text{mm}$. This therefore implies that the material will not fail when subjected to a force or load equal to and below that value. The machine temperature during operation was 3K which is in the safe zone and will not result in any temperature deformation of the bottles.

5. Conclusion

PET bottles crushing machine was successfully designed in this study. The plastic bottle crushing machine was designed for PET bottles as well as plastic waste recycling mainly for commercial and industrial applications. Performance evaluation was carried out on the crushing machine and the results obtained indicated that the machine was efficient and could be used for reduction of PET bottle wastes littering our environment particularly in developing countries where there is insufficient technologies to handle this menace. The designed PET bottles crushing machine can be used to reduce the volume of PET bottle wastes dump indiscriminately, and this will ensure the wellbeing of the world's populace in a healthy environmental condition. Moreover, efficiency of 82.2% was recorded for the machine design which indicated that the machine can be used industrially in a small scale.

References

- [1] C. O. Aguoru and C. A. Alu, Studies on Solid Waste Disposal and Management Methods in Makurdy and its Environs North North Central Nigeria. Greener Journal of Environmental Management and Public Safety, Vol. 4, No. 2, pp. 019-027, 2015.
- [2] S. Ojoawo, O. Agbede and A. Sangodoyin, On the Physical Composition of Solid Wastes in Selected Dumpsites of Ogbomosoland, South Western Nigeria. Journal of Water Resource and Protection, Vol. 3, No. 9, 2011.
- [3] I. Igbinomwanhia, Status of Waste Management, Integrated Waste Management-Volume II, 11-34, ISBN: 978-953-307-447-4. Intech Europe, University Campus STeP Ri, Slavka Krautzeka 83/A. 51000 Rijeka, Croatia, 2011.
- [4] T. Al Seadi, Good practice in quality management of AD residues from biogas production. Report made for the International Energy Agency, Task 24- Energy from Biological Conversion of Organic Waste. IEA Bioenergy and AEA Technology Environment, Oxfordshire, United Kingdom, 2001.
- [5] A. Tukur, PET bottle use patterns and antimony migration into bottled water and soft drinks: the case of British and Nigerian bottles. Journal of Environmental Monitoring, Vol. 14, No. 4, pp. 1236-1246, 2012.
- [6] J. Hopewell, R. Dvorak, and E. Kosior, Plastics recycling: challenges and opportunities. Philosophical Transactions

- of the Royal Society B: Biological Sciences, Vol. 364, No. 1526, pp. 2115-2126, 2009.
- [7] B. Allen, Demand for PET Packaging Material to reach \$60 billion by 2019, Smithers Pira. [online] available at <http://www.smitherspira.com/news/2014/april/demand-for-pet-packaging-material-in-2019>, 2017.
- [8] K. W. Hayden, A. Jaimys, J. C. Russell, and P. I. Elena, Plastic Degradation and Its Environmental Implications with Special Reference to Poly (ethylene terephthalate) Polymers, Vol. 5, No 1, pp. 1-18, 2013.
- [9] E. Metin, A. Erozturk and C. Neyim, solid waste management practices and review of recovery and recycling operations in turkey. Waste management, Vol. 23, No. 5, pp. 425-432, 2003.
- [10] B. Oseni, Municipal Solid Waste Management in Developing Countries (Part II), Environment of Nigeria. [online] available at http://nigeriaenvironment.blogspot.com.ng/2012/12/municipal-solid-waste-management-in_11.html?m=1, 2012.
- [11] J. F. Tester, E. M. Drake, J. M. Driscoll, W. M. Golay, and A. W. Peters, Sustainable Energy-Choosing Among Option. PHI Learning Private Limited, New Delhi-110001, ISBN: 9788120329034, 2005.
- [12] A. Bruvoll, Factors influencing solid waste generation and management. Journal of solid waste technology and management, Vol. 27, No. 3/4, pp. 156-162, 2001.
- [13] European Commission, End-of-Waste Criteria for Waste Plastic for Conversion-Technical Proposals, Final Draft Report March 2013, IPTS Seville, Spain. Institute for Prospective Technological Studies, 2013.
- [14] C. A. Harper, E. M. Petrie, and E. Corporation, Plastics materials and processes, Wiley Online Library, 2003.
- [15] C. C. Ugoamadi and O. K. Ihesiulor, Optimization of the Development of a Plastic Recycling Machine. Nigerian Journal of Technology, Vol. 30, No 3, pp. 67-81, 2011.

Performance Evaluation and Modification of an Existing Rice Destoner

Mohammed Gana Yisa, Adeshina Fadeyibi[‡], Kamil Kayode Katibi, O. C. Ucheoma

Department of Food, Agricultural and Biological Engineering, College of Engineering and Technology, Kwara State University, Malete, P. M. B. 1530, Ilorin, Kwara State, Nigeria.

(mgyisa@gmail.com, adeshina.fadeyibi@kwasu.edu.ng, kamil.katibi@kwasu.edu.ng, gana.yisa@kwasu.edu.ng)

[‡] Corresponding Author; Dr. Adeshina Fadeyibi, P. M. B. 1530, Ilorin, Kwara State, Nigeria, Tel: +234 703 486 7681, Fax: +234 703 486 7681, adeshina.fadeyibi@kwasu.edu.ng

Received: 07.07.2017 Accepted: 22.09.2017

Abstract- Destoning is a processing technique for removing stones and broken grains from a batch of milled rice. This research was carried out to modify an existing rice destoner for the purpose of increasing its capacity and efficiency. Modification introduced addressed challenges associated with the existing machine, such as low stone removal efficiency and low air flow channel, which affects the aerodynamic lifting of the rice grains. Performance was evaluated for 3 kg of locally milled rice samples based on the design capacity of the machine, cleaning efficiency and degree of grain flow. The result showed that the design capacity (1.8 kg/h) of the modified destoner was higher than that of the existing (0.86 kg/h). Also, the modified machine has 40.8% destoning efficiency which is higher than that of existing machine (2.58%).

Keywords Cleaning efficiency, Design, Material flow efficiency, Rice destoner, Rice.

1. Introduction

Domestic processing of rice for local consumption and export is nowadays a serious business in Nigeria [1,2]. This is probably because of the renewed interest by government for the country to be self-sufficient in terms of food production rather than depending on importation of major agricultural commodities. Rice production is generally carried out by the local farmers who have little or no idea of modern technology as currently applied in agriculture [3]. Research efforts has shown that production and processing technologies have not been able to meet the increasing demand for rice [4]. This is true despite the huge production potential of the commodity in Nigeria judging from the vast arable and fertile land available for cultivation. Therefore, instead of spending billions of naira on importation, the commodity can be produced, processed and bagged for local consumption and export [5]. It is usually difficult to actualize this mandate without proper agricultural mechanization. Of course rice processing is not new to cultivators, but this is done locally and in the process impurities including stones introduced. The presence of

impurities inadvertently makes marketing tedious as consumers prefer clean quality rice product.

Prior to the conception of rice destoner, farmers make use of the traditional or manual method to separate impurities from rice. The manual method include handpicking which allows separation of stones from rice. But this is time consuming, tedious and contaminants such as stones, sticks, chaff and sand are not completely removed [6]. Another method is floatation which allows separation based on differences in density when a batch of unclean rice product is allowed to settle in bath of water. The heavier materials, which are stones, quickly settle to the bottom, and the clean rice at the top are carefully scooped. This, however, requires sufficient drying after separation and there is possibility of mold or fungi growth in storage when not properly dried [7]. Moreover, during rice processing, impurities may be purposely, accidentally, inevitably, or incidentally added. The level of impurities in rice, which are generally defined in relative terms, depends on the method of cleaning or separation used [8]. Standards have been established by various organizations that attempt to define the permitted levels of impurities in a manufactured product. Strictly speaking, the level of purity of the material can only be

stated as being more or less pure than some other material. Some of the factors that make the locally produced rice less acceptable are impurities like stones, dust and chaff, and these get into rice as a result of poor methods of harvesting and drying used by the farmers. As much as possible, therefore, the level of impurity in processed rice should be reduced so as to ensure quality of the final product.

Many researchers have developed machines for use in removing stones and other impurities from processed rice, so as to meet the demand for clean product by consumers [9-12, 8]. This has resulted to several breakthroughs in the innovation and method of separating impurities from rice. For instance, Adejuyigbe and Bolaji [12] developed a rice destoning machine using a vibrating sieve and reported a high destoning efficiency. Okunola *et al.* [8] developed a cereal cleaner which is particularly adoptable for use in cleaning impurities in processed rice. Henderson and Perry [9] designed a separator based on gravity and floating. The disadvantages of using separator however in rice cleaning are that sufficient drying is required after separation and there is possibility of mold or fungi growth in storage [7]. However, the technical requirements of the designs described are quite cumbersome and difficult to localize [6, 11-13]. This is probably the reason rice processing is still a major challenge in some instances despite the level of research achieved. Therefore, attempt to readdress the design concept and improve performance cannot be overlooked. At the moment, there is no reported attempt to modify the existing rice destoners in order to achieve this. Thus, the objective of this research was to evaluate the performance of an existing rice destoner and modify the machine in terms of destoning efficiency.

2. Materials and Methods

2.1. Materials

The materials used in the design of the modified rice destoner are local rice weighing balance, stop watch, electric motor and air flow meter. Mild steel material was used for the fabrication of the machine.

2.2 Performance and challenges of existing rice destoner

An existing rice destoner designed and fabricated by Nwoba [14] shown in Fig. 1 was evaluated for its performance. Three samples of *gwarri* rice variety (3 kg each and containing 0.5 kg of stones) were used to evaluate the performance of the destoning machine. As the machine operates, it vibrates the sieves and the grain mixture flows from the hopper through the vibrating sieves to the destoning section. In principle, the machine operates based on differences in terminal velocities of stone, rice and other impurities through aspiration. The machine was equipped with a blower (blast fan) which supplied air stream across the flowing grains. This caused the mixture of grains and stones to move at different velocities in different projectile directions. The machine was operated with a single phase 3hp (2.250 kW, 1440 rpm) electric motor and loaded. Cleaning efficiency of 73%, 2.58 % and 93% were reported

for chaff, stone and material flow, respectively. However, the stone cleaning efficiency of this design was extremely low, thereby causing both stones and chaffs to drop at the inlet of the flow channel. There were problems with the blower and obstruction caused by stone-chaffs mixtures in the stone tank. It was also reported that the airflow channel was not high enough to lift rice.

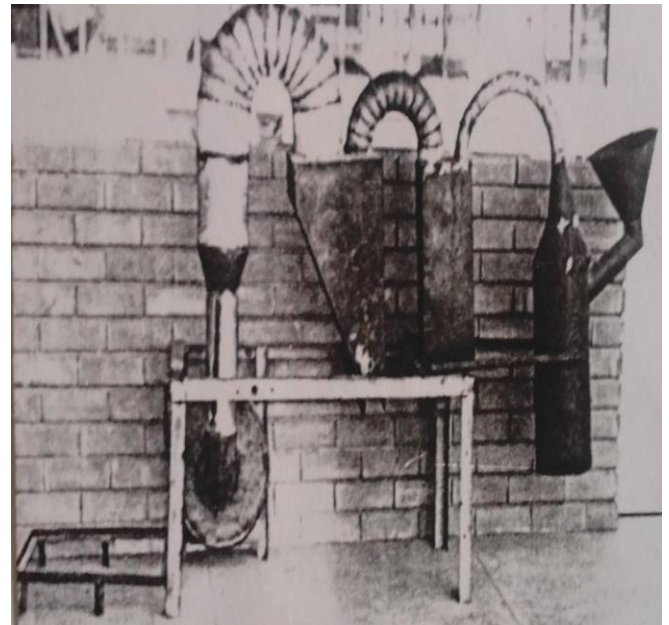


Fig. 1. Rice destoner constructed by Nwoba [14].

2.3 Design Concept for Modification

One of the problems associated with the rice destoner developed by Nwoba [14] was low stone cleaning efficiency. This problem appeared because the design did not take care of some factors influencing the performance of the various components of the cleaning systems, which are engineering properties of rice including physical, mechanical and aerodynamic properties. In this modification therefore, the aerodynamic characteristics of the rice grains, including density, terminal velocity, forces acting on the rice particles and the aerodynamic drag force, were determined according to the procedures described in Razavi *et al.* [15] and Tabatabaee-far [16]. Physical characteristics, including shape and size, were determined by the method described by Fadeyibi *et al.* [7]. Mechanical characteristics were the angle of repose of rice grains determined by the method described by Nwithiga and Moriasi [17].

2.3.1 Design Analysis

The design analysis was carried out with a view to evaluating the design parameters for selection of the machine parts, so as to minimize failure during the required working life of the machine.

1. Determination of hopper volume

Hopper was made of galvanized and iron sheet so as to prevent rusting and sagging due to the weight of rice grains

introduced. To achieve this requirement, a better hopper rigidity was analyzed and ensured as shown in Fig. 2. Thus, the volume of the hopper was calculated using the expression in Eq. (1).

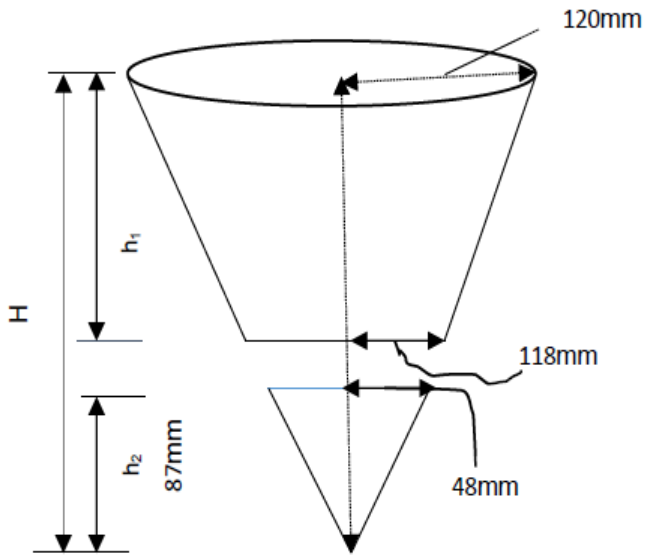


Fig. 2: Hopper analysis.

$$V = \frac{1}{3} \pi r^2 (H - h_2) \tag{1}$$

but, $H = h_1 + h_2$ or $h_1 = H - h_2$

By similar triangles the solution is:

$$\frac{R}{r_2} = \frac{h_1}{h_2}$$

where, R = base radius of the hopper, r_2 = truncated radius of the hopper, h_1 = hopper vertical height, h_2 = truncated vertical height.

Thus,

$$h_1 = \frac{R}{r_2} \times h_2 = \frac{118 \times 87}{48} = 214 \text{ mm}$$

Then the volume of the hopper was:

$$V = 1/3 \pi (120)^2 \times 214 = 3227462 \text{ mm}^3$$

Therefore, a total height $H = h_1 + h_2 = 310 \text{ mm}$ and the effective height of 220 mm with a volume of 3227462 mm^3 were used as hopper specification of the rice destoner.

II. Determination of volume of grain channel

Grain channel are perforations where the whole rice grains pass through without allowing impurities. In this design, the grain channel was made of galvanized iron because it is less vulnerable to rusting and available in

comparison to plain mild steel. The rusting effect of mild steel was also considered after which galvanized steel was chosen to avoid contamination due to rusting as the machine lasts in use. The grain channel is cuboidal in shape, as shown in Fig. 3. Assume a length of 40 mm, width of 36 mm and height of 40 mm, then the volume of the grain channel was calculated using Eq. (2).

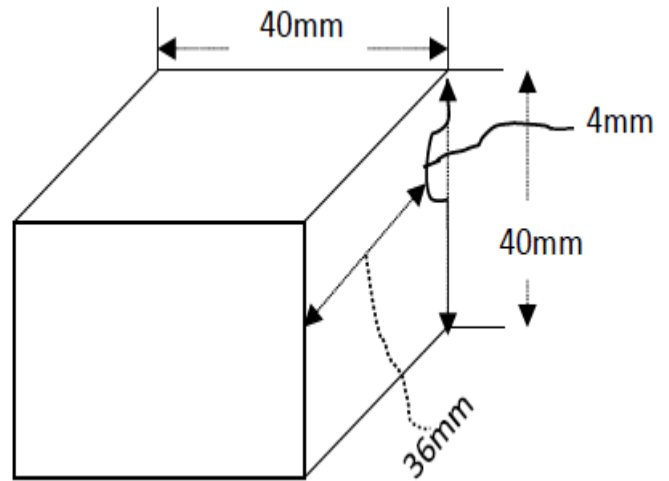


Fig. 3. Typical sketch of grain channel.

$$V_{gc} = lwh \tag{2}$$

where, V_{gc} = volume of grain channel (mm^3), l = length of channel (mm), w = width of channel (mm), h = height of channel (mm).

$$V_{gc} = 40 \times 36 \times 40 = 57600 \text{ mm}^3$$

III. Determination of blower discharge capacity

Blower was selected based on the volume of air required and its resistance in the system as shown in Fig. 4. Density of air at normal atmospheric pressure and temperature was used to determine air speed by the blower using Eq. (3).

$$Q = Q_1 \sqrt{\frac{\rho_{25^\circ\text{C}}}{\rho_{st}}} \tag{3}$$

where, Q_1 = discharge air speed by the blower (m^3), $\rho_{25^\circ\text{C}}$ = air density at 25°C (1.18 kg/m^3), ρ_{st} = air density at standard outdoor conditions (1.12 kg/m^3 for 40°C as obtained from specification of air conditioning and refrigeration table), Q = real discharge capacity of fan ($5,560 \text{ ft}^3/\text{min}$).

$$Q = 5560 \sqrt{\frac{1.18}{1.12}}$$

$$Q = 5707 \text{ ft}^3/\text{min} = 2.69 \text{ m}^3/\text{s of air.}$$

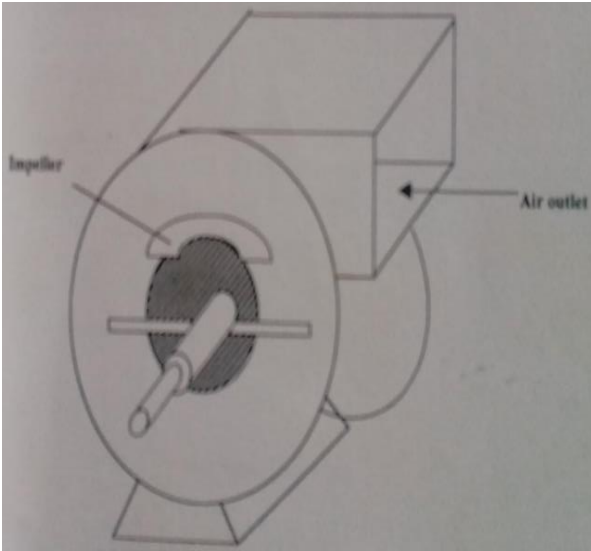


Fig. 4. A centrifugal fan.

Also, the power required to operate the centrifugal fan based on the amount of air stream flow rate (2.69 m³/s) was 1.54 HP (obtained from specification of air conditioning and refrigeration table). Thus, a 2HP electric motor was selected to provide the power required by the fan and to take care of the power loss in the system.

IV. Determination of angular velocity of sieves

The frequency of vibration of the sieves was determined based on whirling speed of the shaft, blades and pulley from Dunkerly's formula expressed in Equation (4). Also, the centripetal velocity was considered as the sieves rotate with the aid of blades attached to the fan shaft.

$$\bar{\omega}_s = \left(\frac{\pi^2}{l^2}\right) \sqrt{\frac{EI}{m}} \tag{4}$$

but since $m = \rho v$, then

$$\bar{\omega}_s = \left(\frac{\pi^2}{l^2}\right) \sqrt{\frac{EI}{\rho v}}$$

where, l = length of shaft (0.56 m), I = moment of inertia, m = mass of shaft (kg), v = volume of shaft (m³), ρ = 7,800 kg/m³, E = Elastic modulus (2×10^6 N/m²), $\bar{\omega}_s$ = whirling speed (rad/s).

$$I = \pi \times \frac{(0.0337)^2}{64} = 5.58 \text{ m}^4$$

$$v = \pi \frac{(0.0337)^2}{4} \times 0.56 = 0.0005 \text{ m}^3$$

$$m = 7800 \times 0.0005$$

$$\therefore m = 3.90 \text{ kg}$$

$$\bar{\omega}_s = \left(\frac{\pi^2}{0.56^2}\right) \sqrt{\frac{2 \times 10^6 \times 5.58}{3.90}}$$

$$\bar{\omega}_s = 31.5 \times 0.18 = 5.68 \text{ rad/s}$$

Thus, the angular velocity of sieves was 5.68 rad/s

V. Determination of column maximum deflection

The maximum column deflection of the shaft of the modified destoner was computed from Eq. (5).

$$Y_{max} = 5W L^4 / 384EI_{xx} \tag{5}$$

where, W = load per unit length (N/m); L = length of column (m); E = modulus of elasticity (kg/m²); I_{xx} = moment of inertia in the x- direction (m⁴); Y_{max} = vertical maximum deflection (m).

VI. Determination of safe load capacity

The load required to safely operate the machine without hindrance or failure was computed using Euler's equation for permissibility load as expressed in Equation (6).

$$P_c = \pi^2 \cdot E \cdot I_{xx} / L_e \tag{6}$$

where, P_c = crippling load; E = modulus of elasticity; I_{xx} = moment of inertia in the x- direction; L_e = effective length.

VII. Determination of strain energy

The strain energy from the column deflection on the rice destoner was computed using Eq. (7).

$$U = (P_e^2 / 2E) \times V \tag{7}$$

where, P_e = elastic stress constant; V = volume of material; E = modulus of elasticity; U = strain energy.

VIII. Determination of pressure distribution in the system

In order to determine the pressure distribution in the system the discharge velocity, continuity velocity and the density of air at room temperature, 24°C were considered as influencing factors. The pressure distribution in the system was therefore computed from Eq. (8).

$$\frac{p}{\rho_{25^\circ\text{C}}} + \frac{U_2}{2g} = \frac{P_1}{\rho_{25^\circ\text{C}}} + \frac{V^2}{2g} \tag{8}$$

where, P_1 = continuity pressure; $\rho_{24^\circ\text{C}}$ = density of air at 24°C; U_2 = discharge velocity/fan velocity, g = acceleration due to gravity (9.81 m/s²); V = velocity due to continuity (m/s).

IX. Determination of fan shaft diameter

The shaft diameter was determined using the expression in Eq. (9). According to Khurmi and Gupta [18], the diameter of a solid shaft with little or no axial load can be determined using:

$$d^3 = \frac{16}{\pi S_s} [(k_b m_b)^2 + (k_t m_t)^2]^{1/2} \tag{9}$$

where, k_b = combined shock and fatigue factor applied for bending moment = 1.5, k_t = combined shock and fatigue factor = 1; m_b = maximum bending moment, m_t = maximum torsional moment; S_s = allowable stress = 40MN/m² for shaft with keyway (machine design S series).

X. Bearing selection

Bearing selection was based on load requirement, speed of shaft, space limitation and desire for precise shaft positioning. Eq. (10) was used to compute the bearing rated life. For agricultural equipment, the design life L_{10} is between 3000-6000 [18]. This specification was used as guide for the bearing selection.

$$L_{10} = \left(\frac{C}{P}\right)^k \times \frac{10^6}{60n} \tag{10}$$

where, L_{10} = rated life, revolution; C = basic load rating = 1525.44 N; P= equivalent radial load, K= constant, 3 for single groove type, n = 2000 rpm (obtained from table of materials properties) [18].

However,

$$P = XVf_r + Yf_a$$

where, X = radial load factor (0.56) from table of materials properties, V = radial factor (1), f_r = radial load (120 N), $f_a = 0.7f_r = 0.7 \times 120 = 84$ N.

2.3.2 Drawing of modified rice destoner

Isomeric and orthographic projections of the modified rice destoner are shown in Fig. 5 and Fig. 6, respectively.

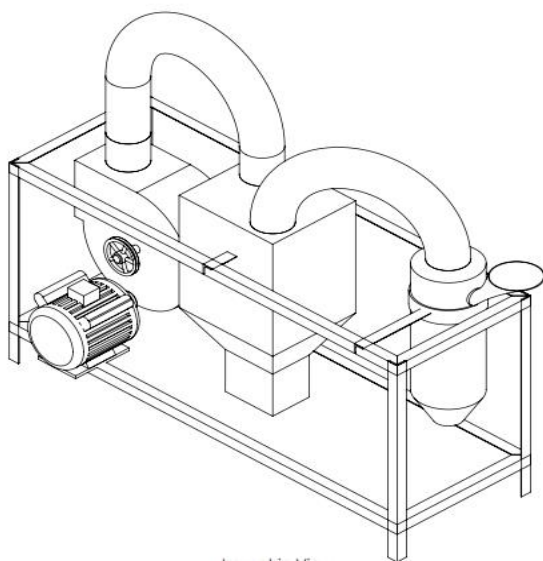


Fig. 5. Isometric view of rice destoner.

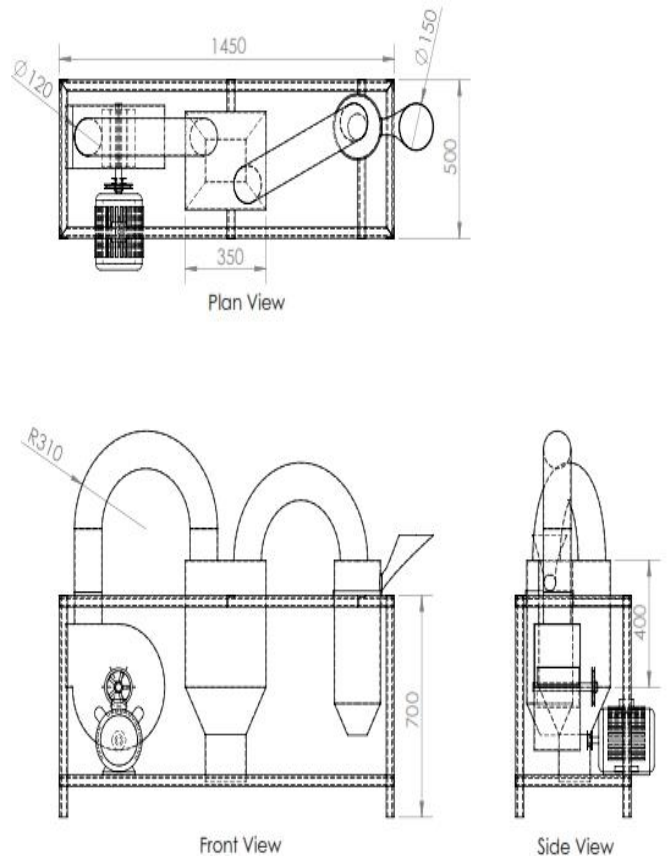


Fig. 6. Orthographic projection of rice destoner.

2.4 Principle of operation of modified rice destoner

The rice destoning machine was designed to achieve complete separation of stone from rice. The admixture (mixture of rice and stone) was fed through the hopper and into the vibrating sieve which allows stones smaller than the rice to pass through. Any stone that is larger than the diameter of the sieve size (≥ 2 mm) will fall along with the rice onto the vibrating sieve. The vibratory sieve transfers the stones in the opposite direction of the flow of clean rice so that the cleaned rice will not be mixed with separated stone. The clean rice was collected at the lower part of the inclined sieve.

2.5 Performance evaluation of modified rice destoner

Performance of the machine was evaluated to determine the ability of the material to flow freely through the sieves and the cleaning efficiencies of the machine with respect to impurity separation from rice.

2.5.1 Chaff Cleaning efficiency

This is the amount of chaff discharged through appropriate ducts to the total amount of the introduced into the hopper, expressed in percentage. It was computed using Eq. (11).

$$C_{eff} = \frac{M_c}{M_t} \times 100 \tag{11}$$

where C_{eff} = chaff cleaning efficiency (%), M_c = mass of chaff discharged through the appropriate chute (kg), M_t = total mass of chaff introduced into the grain (kg).

2.5.2 Stone Separation Efficiency

This is the mass of stone removed to total mass of stone introduced into the rice. It was computed using the expression in Eq. (12).

$$S_{eff} = \frac{M_s}{M_p} \times 100 \quad (12)$$

where, S_{eff} = stone separation efficiency; M_s = mass of discharged rice in stone tank, M_p = total mass of introduced into the hopper.

2.5.3 Free Flow of Material through the Hopper Efficiency

This is defined as the percentage of rice material introduced into the hopper and collected from the flow ducts when the machine is not at work. It was computed using Eq. (13).

$$M_e = \frac{M_1}{M_2} \times 100 \quad (13)$$

where, M_e = material flow efficiency (%); M_2 = mass of material introduced into the hopper (kg), M_1 = mass of material collected at the flow channel (kg).

3. Results and Discussion

Results of performance evaluation of the modified rice destoner is shown in Table 1. It can be seen that the modified rice destoner has the design capacity of 1,800 kg/h. This may be as a result of the larger space on the two flat sides of its fan housing (casing) to draw sufficient air for better efficiency of the fan. The top of its grain channel was made open to allow for free agitating of the grains. Metal arm was introduced to help move the reciprocating panel in order to make for the sieving action of the destoner. The lower sieve efficiency of the machine was higher than efficiency of upper sieve and this may be due to the presence of more broken rice grains at the lower end. With the introduction of L-shaped metal arm, it was observed that the destoner was able to give a destoning efficiency of 40.8 % higher than that of the existing machine. However, in contrast to this, Ogunlowo and Adesuyi [6], Simonyan *et al.* [11], Adejuyigbe and Bolaji [10] and Agidi *et al.* [13] reported higher destoning efficiency with lower machine capacity of rice destoner in their respective designs. It may be noted that this difference in efficiencies might be due to the differences in angle of inclination and the diameter of feed regulator opening of the machines. The present design presents an excellent machine capacity of 1800 kg/h compared to that reported by Olugboji and Yisa [19] and Adejuyigbe and Bolaji [10]. Thus, clearly one can see that the modified machine will be able to handle more tonnes of rice per hour than most machines reported.

Table 1. Performance of the modified rice destoner

s/n	Performance indices	Value	unit
1	Machine capacity	1.80	kg/h
2	Material flow efficiency:		
	lower sieve	97.0	%
	upper sieve	94.0	%
3	Cleaning efficiency:		
	Chaffs	85.0	%
	Stones	40.8	%

3. Conclusion

An existing rice de-stoning machine was tested, modified and its performance was evaluated. The performance evaluation carried out on the machine after modification showed that the chaff cleaning, stone separation and material flow efficiencies through lower and upper sieves were relatively higher than the existing rice destoner. Also, the modified machine has an impressive material flow efficiency through the lower and upper sieves. This work also revealed that the design capacity of the modified machine was found to be 1.80 kg/h which was higher than 0.86 kg/h obtained from the previous machine. The machine was able to improve the quality of rice by de-chaffing and separation of broken rice particles.

Acknowledgements

Authors thank Engr. Oyewale babatunde Joseph for assisting in preliminary investigation of rice destoning machine as reported by Nwoba [14].

References

- [1] O. Erenstein, F. Lançon, S.O. Akande, S.O. Titilola, G. Akpokodje, and O.O. Ogundele, "Rice production systems in Nigeria: A survey", WARDA, Abidjan, Cote d'Ivoire, 2003.
- [2] E. A. Echiego, "Essential Consideration in the Grading and Packaging of Nigerian Rice for Export", Paper presented by Hon. Commissioner for Ministry of Agriculture and Natural resources Abakaliki, Ebonyi state, at the south – East Regional Conference of the Nigerian Institute of Agricultural Engineers, held at Abakaliki, Ebonyi State, 16th – 18th of September, 2009.
- [3] J. O. Saka, and B. O. Lawal, "Determinants of adoption and productivity of improved rice varieties in south western Nigeria", African Journal of Biotechnology. Vol. 8 (19), pp. 4923 – 4932, 2009.
- [4] F.A.O, "Farming systems and poverty: improving farmers' livelihoods in a change world", Rome: Food and agricultural organization, 2001.
- [5] E. D. Imolehin, and A. C. Wada, "Meeting the Rice Production and Consumption demand of Nigeria with improved Technologies", National Cereal Research

- Institute, Badeggi, PMB 8, Niger State, Nigeria. pp1-11, 2000.
- [6] A. S. Ogunlowo, and A. S. Adesuyi, "A Low cost rice cleaning/destoning machine", Published by European Centre for Research Training and Development UK, Vol.2, No.2, pp. 33-43, 2014.
- [7] A. Fadeyibi, Z.D. Osunde, M.S. Ussaini, P.A. Idah, and A.A. Balami, "Evaluating Monolayer Moisture Content of Rubber Seed using BET and GAB Sorption Equations", International Journal of Farming and Allied Sciences, vol. 1(3), pp. 72-76. 2012.
- [8] A. A. Okunola, J. C. Igbeka, A. G. Arisoyin, "Development and evaluation of a cereal Cleaner", Journal of Multidisciplinary Engineering Science and Technology, vol 2 issue 6, pp. 14-19, 2015.
- [9] S.M. Henderson, and R.L. Perry, "Agricultural Process Engineering", 3rd Edition. The avi Publishing Company, Incorporated, West – port, Connecticut. Pp 170 – 189, 1976.
- [10] S.B. Adejuyigbe, and B.O. Bolaji, "Development and Performance Evaluation of A Rice Destoning Machine Using Vibrating Sieves", Journal of Natural Science, Engineering and Technology Agricultural Mechanization in Asia, Africa and Latin America, 30 (1): 20 -24, 2012.
- [11] K. S. Simonyan, I. S. Emordi, and J. C. Adama, "Development of A Locally Designed Rice Destoning Machine", Journal of Agricultural Engineering and Technology (JAET), vol. 18 (1), 2010.
- [12] I.K. Adegun, S.A. Adepoju, and J.A. Aweda, "A mini "Rice Processing Machine for Nigerian Farmers", Journal of Agricultural Technology, 8 (4): 1207-1216, 2012.
- [13] G. Agidi, B. Ndagi, A. M. Kuku, and L. Abdullahi, "Development and Testing of A Rice Destoning Machine", International Journal Engineering. Resources & Science & Technology, 2015. ISSN 2319-5991. www.ijerst.com 4(3), 2015.
- [14] Nwoba, "Design and Fabrication of Rice destoner" B.Eng. final year project in Agric. Engineering Department, Federal University of Technology, Minna of bean dehuller. Journal of Science and Technology, KNUST, Kumasi, Ghana, 25(1): 125-132, 1992.
- [15] S.M.A. Razavi, S. Yaganehzad, and A. Sadeghi, "Moisture Dependant Physical Properties of Canola Seeds", Journal of Agricultural Science and Technology, vol. 11, 309-322, 2009.
- [16] A. Tabatabee-far, "Moisture Dependant Physical Properties of Wheat", International Agrophysics, 17: 207-211, 2003.
- [17] R. S. Khurmi, and J. K. Gupta, "A textbook of machine design", Eurasia Publishing House (PVC) Ltd. Ram Nagar, New Delhi. pp 509-543, 686-960, 2007.
- [18] G. Nwithiga, L. Moriasi, "Study of Yield Characteristics during Mechanical Oil Extraction of Predicated and Ground Soybean", Journal of Applied Science Research, 3(10): 1146-1152, 2007.
- [19] O. A. Olugboji, and J. Y. Jiya, "Design and Fabrication of Rice Destoning Machine. Journal of Food Science and Technology", vol. 2 (1): pp. 1-5, 2014.

Evaporation Plant for Recycling of Caustic Soda

Emin Taner ELMAS*

*Department of Energy Systems Engineering, Faculty of Engineering And Natural Sciences,
İskenderun Technical University (İSTE) , Main Campus 31200 , İskenderun / Hatay – TURKEY

Tel: +90 (0) 543 733 64 21

(taner.elmas@iste.edu.tr)

Received: 28.07.2017 Accepted: 22.09.2017

Abstract- The most important problem that humanity is expected to face in the coming century shall be environmental pollution. On one hand, the population of human beings are using natural resources rapidly, on the other hand, they are adding hundreds of pollutants in the form of metals, acids, bases and etc. Thus, they have created an abnormal situation which has resulted in an imbalance in the natural systems.

As the industrialization improves, it creates pollution and also it creates jobs for the people. Especially in developed countries, for instance European countries and U.S.A. there are also many stringent restrictions for the environmental pollution, and there are many laws, political arrangements. Of course, a pollution free environment will require a high cost, often an expensive operation. However, it is much costlier trying to undo the damage done. On the basis of concept tried to mention above human beings have studied on the subjects related with environmental pollution. They have established waste water treatment plants, many kinds of recycling and recovery plants, and etc.

In this study, it has been tried to establish such an idea that a pollution free environment may be available if this technical process is used properly. So, the first goal of this study is to provide a concise statement of the requirements and opportunities for obtaining environmental benefits. The second objective will be to provide economical savings while providing the environmental benefits at the same time. To emphasize the great importance of above mentioned subjects the application of recycle technology for the sodium hydroxide (NaOH), which is named as caustic soda in industrial processes, realized by means of an evaporation plant is used. Caustic soda is used in textile industry for mercerizing process as it is used in many different processes. To give the cotton more strength and to obtain a smoother surface and an improved affinity the mercerizing is essential. After being finished the mercerizing operation, generally the process solution (containing caustic soda) is discharged to the environment, e.g., rivers, seas and sewage. In spite of the fact that this application is widely spread in use, it is forbidden in all developed countries to discharge the caustic soda solutions even at a 1% concentration since the caustic soda is highly basic (highly alkaline). For this reason, it is very harmful for the environment. It is possible to extract

the caustic soda from the caustic soda solutions before discharging it to the environment for preventing the harms of this material. The washing water containing NaOH will be concentrated by H₂O evaporation and shall be recycled in the mercerizing system. The concentration may take place in a single or multiple – stage (double–stage) installation under vacuum or atmospheric pressure.

The washing water to be concentrated is moved from the storage tank to the first evaporation stage and the thermal energy for evaporation operation is added by the steam. The vapor coming from the first evaporation stage is used for the next evaporation stage as the heating steam of this unit. The vapor from the last stage is condensed in a condenser. The condensed vapor can be safely discharged and the concentrated caustic soda can be reused for the subsequent mercerizing operation. So, both economical profits and environmental benefits can be provided by reusing the caustic soda for next processes, after it is recovered by the help of this way. Desalination unit in Jeddah which is the capital city of Saudi Arabia, is an example for this kind of operations. This plant was established 1970's and has been used as both a power station and a desalination unit. At this plant the exhaust steam coming from the steam turbines is used as the heating steam for evaporators of desalination unit. Unfortunately, in our country, even in İzmir, the waste water of textile industry is discharged to the environment. Because, the environmental laws are not adequate and the enterprisers think that a recycling plant is not an economical investment. However, it is stated in this study that such a concept is not right. It has been tried to show that such an investment, i.e., "An Evaporation Plant for Recycling of Caustic Soda" may be profitable if it is installed and operated properly, and also it has been tried to increase the attractively of these kinds of plants. It is hoped that, the laws and stringent restrictions related with environment shall be arranged, so that we shall live in a healthy world.

Keywords Evaporation, Recycling, Caustic soda, Sodium hydroxide, Vacuum, Steam

NOMENCLATURE

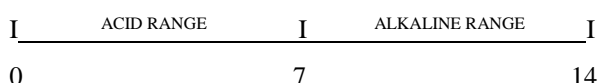
F	=Feed (NaOH Solution) Flow Rate, kg/h.
V ₀	=Mass Flow Rate for the Heating Steam, kg/h.
V ₁	=Mass Flow Rate of the Steam vaporized from NaOH Solution, kg/h.
L ₁	=Mass Flow Rate of the Product (Concentrated NaOH Solution), kg/h.
D	=Condensate, kg/h.
H	=Enthalpy Per Unit Mass of a Vapor Stream, kj/kg.
h	=Enthalpy Per Unit Mass of a Liquid Stream, kj/kg.
λ	=Latent Heat of Evaporation Per Unit Mass of Stream, kj/kg.
x'	=Mass Fraction of Solute in Stream, kg solute / kg of total stream.
U	=Over-all Heat Transfer Coefficient, kj/m ² hC°.
A	=Heating Surface Area, m ² .
ΔT	=Temperature Difference, C°.
T	=Temperature, C°.
q	=Heat flux, kj/h.
Q	=Heat amount, kj/h.
P	=Pressure, Bar(a) / Bar(g).

1. Introduction

This study describes the application of recycle technology for the sodium hydroxide (NaOH), which is named as caustic soda in industrial processes, realized by means of an evaporation plant and this study also emphasizes the great importance of water pollution problem caused by the wastewater that arise from mercerizing process of textile industry.

2. Caustic Soda (SODIUM HYDROXIDE - NaOH)

If we consider the pH scale;



It is possible to make such a comment that acid conditions increase as the pH values decrease and alkaline conditions increase as the pH values increase. The pH value of caustic soda is higher than 7 and furthermore it is a highly basic material, that is, a very strong alkaline. Because of this property caustic soda is very dangerous for the environment. As we mentioned above, caustic soda is used in textile industry for mercerizing as it is used in many different industries, however, especially in our country it is discharged to the environment, e.g., rivers, seas and sewage after the process has been completed. This event is very harmful. In all developed countries, for example in European countries and U.S.A. it is entirely forbidden to discharge the caustic soda even at a 1 % concentration. In all of these countries the caustic soda is recycled and reused for the subsequent process. So, both economic and environmental benefits can be provided by reusing the caustic soda for the next process, after it is recovered.

3. Recycling of Caustic Soda by Single-Effect Evaporation at Atmospheric Pressure

Recycling of caustic soda by evaporation is a special case of heat transfer to the boiling liquid which is NaOH solution. This particular heat transfer application, i.e. evaporation, is so common and important that it is treated as a separate unit operation of chemical engineering.

The main intent is to concentrate non-volatile solute (caustic soda) from the solvent, which is water. This is done by boiling of the solvent. Concentration by evaporation is normally stopped before the solute begins to precipitate.

The devices, used for evaporation operation are called as evaporators. The evaporators are classified by the number of effects. In a single - effect evaporator, steam provides energy for vaporization and the vapor product is condensed and removed from the system. In a double-effect evaporator, the vapor product of the first effect is used to provide energy for a second vaporization unit. This cascading of effect can continue for many stages. Double-effect evaporators can

remove much larger amounts of solvent than is possible in a single effect.

By considering the Figure 1 the related conditions shall be as follows:

The pressure in the evaporator tank shall be 1 Bar(a).

The Caustic Soda Solution shall be raised from 5% concentration to 20% concentration. For determining the boiling point of NaOH solution, Dühring Plot which is introduced in Figure 2 (Foust et al., 1959) should be used. Apart from that, for determining the enthalpy value of the NaOH solution the enthalpy-concentration diagram introduced in Figure 3 (Foust et al., 1959) should be used.

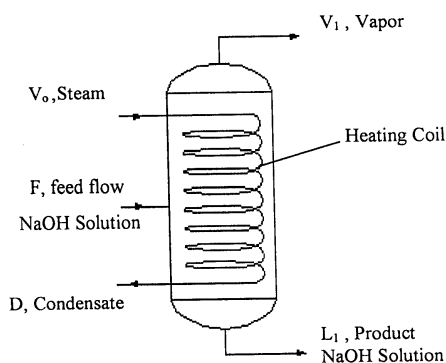


Figure 1. Recycling of caustic soda by single-effect evaporation unit.

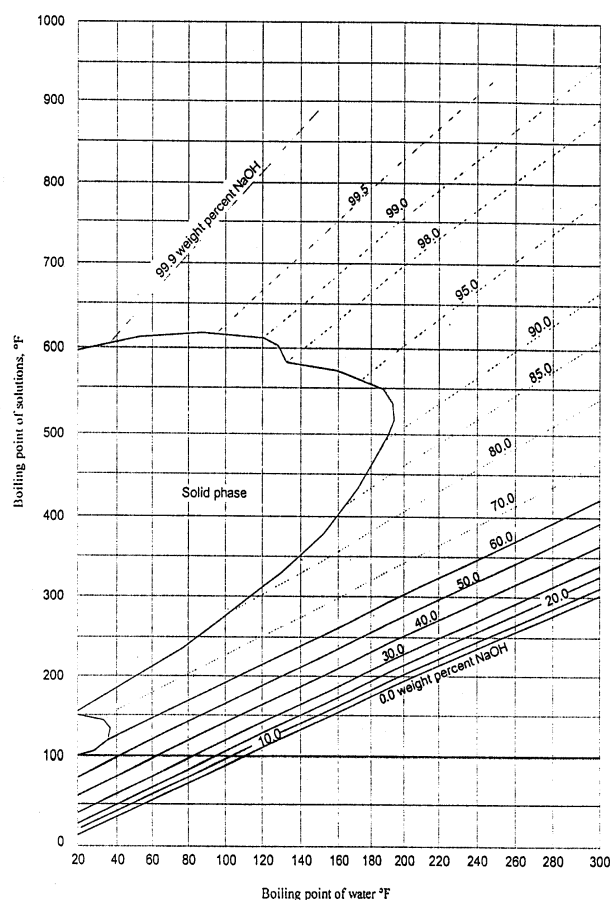


Figure 2. Dühring lines for the NaOH-H₂O system (Foust et al. 1959).

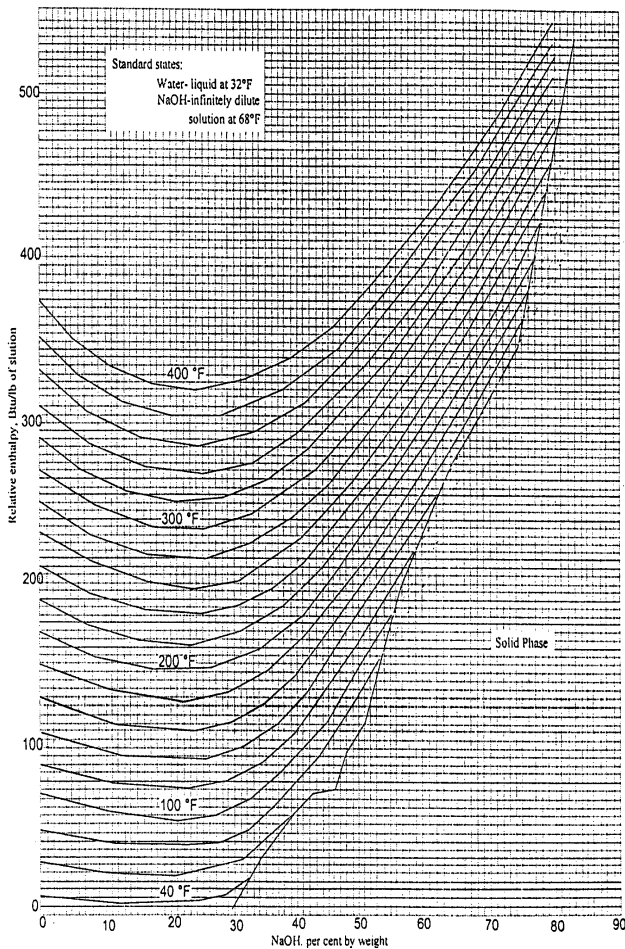


Figure 3. Enthalpy-Concentration diagram for aqueous solutions of NaOH under a total pressure of one atmosphere. The state for water is taken as liquid water at 32° F under its own vapor pressure (Foust et al.1959).

At a pressure of 1Bar(a), water boils at 100°C (212°F). From the Dühring Plot; the boiling point of a 20 per cent NaOH solution at a pressure such that water boils at 100°C is 110°C (230°F) which corresponds to a BPR (Boiling Point Rise) of 10°C (110°C - 100°C).

Through the use of the steam tables and enthalpy-concentration diagram H_1 and h_1 values can be determined readily as follows:

$$H_1=2696 \text{ kJ/kg.}$$

$$h_1=386 \text{ kJ/kg.}$$

By using the equations for heat balance and heat transfer the steam consumption for the heating steam and the required heating surface area can be determined. In industrial applications operating the system at the atmospheric pressure is not preferred because of the high costs of operation. Instead of this, operating at low pressures (under vacuum) is preferred since the operation costs decreases sharply.

4. Recycling of Caustic Soda by Single-effect Evaporation at Low Pressures

When the Figure 1 is considered again;

On such an evaporation unit it is possible to determine the real operational values which are calculated by using the variable data. For realizing this aim, the four equation bellow mentioned should be examined;

1-) Equation for material balance:

$$F + V_o = V_1 + L_1 + D \quad \text{note: } D = V_o \quad (1)$$

2-) Equation for NaOH solution:

$$F \cdot X_F = L_1 \cdot X_1 \quad (2)$$

3-) Equation for heat transfer:

$$V_o \cdot \lambda_{v_o} = U \cdot A \cdot (-\Delta T) \quad (3)$$

4-) Equation for heat balance:

$$V_o \cdot \lambda_{v_o} + F \cdot h_F = V_1 \cdot H_1 + L_1 \cdot h_1 \quad (4)$$

The wastewater of mercerising process generally includes the caustic soda (NaOH) at a concentration of 5% and it is possible to recycle this material by evaporating it.

After being evaporated the caustic soda solution, the concentration increases to a considerable rate.

The general operational data of an evaporation plant for recycling of caustic soda is as follows;

The percentage of feed flow = 5% NaOH solution

The temperature of feed flow = 50° C

The mass flow rate for feed = Variable between 250 kg/h and 1000 kg/h

Steam for heating the NaOH solution: saturated steam within a variable range from 4 Bar(a) to 10 Bar(a)

Product: 20% NaOH solution.

The evaporator tank is operated under low pressures for obtaining energy saving. If the NaOH solution kept under vacuum, the boiling point of the solution decreases depending upon the vacuum rate. Therefore, the energy that should be added to the NaOH solution for evaporation decreases. This event makes the system very economical.

Such a system mentioned here is generally operated within a vacuum range from 0,1 Bar(a) to 0,4 Bar(a). It is possible to operate the system under the atmospherically conditions, that is, at 1 Bar(a) pressure.

Within the scope of this study both the system operating under vacuum and under atmospheric conditions shall be regarded.

In accordance with the data above, it is possible to obtain much more specific information about the evaporation plant for recycling of caustic soda.

Conditions: $F \Rightarrow$ 250 kg/h - 1000 kg/h

50° C, 5% NaOH solution.

$V_o \Rightarrow$ 4 bar(a) - 10 bar(a).

Vacuum rate => 0,1 bar(a) - 0,4 bar(a).

L => 20% NaOH solution.

If the vacuum rate for the evaporator tank is 0,1 Bar(a);

At 0,1 bar(a), water boils at 45,81° C (114,5° F).

From the Dühring plot; the boiling point of a 20 Percent NaOH solution at a pressure such that water boils at 45,81°C is 57,22°C which corresponds to a BPR (Boiling Point Rise) of 11,41° C (57,42° C – 45,81° C).

Table 1. Mass flow rates of the heating steam for F = 250 kg/h

Steam pressure for	Pressure in the evaporator tank					
	Atmospheric			Below Atmospheric		
	V _o (Kg/h)	1 bar(a)	0,1 bar(a)	0,2 bar(a)	0,3 bar(a)	0,4 bar(a)
4 bar(a)		239	226	230	233	236
5 bar(a)		242	228	234	236	239
6 bar(a)		244	231	236	239	242
7 bar(a)		246	233	238	241	243
8 bar(a)		248	235	241	243	246
9 bar(a)		250,9	237	243	245	247
10 bar(a)		252,9	239	245	249	250

From the steam tables; for 0,1 bar(a) and 57,22° C, H₁ is determined as 2606,6 kJ/kg. (H₁ = 2606,6 kJ/kg).

From enthalpy – concentration diagram; for 20% NaOH solution and 57,22° C h₁ is determined as 80 Btu/lb. (h₁ = 186,08 kJ/kg).

The H₁ and h₁ values for the vacuum rates of 0,2 bar(a), 0,3 bar(a), and 0,4 bar(a) are determined through the use of same method mentioned above.

The enthalpy of the feed flow is determined by using enthalpy – concentration diagram.

For 5% NaOH solution and 50° C; the enthalpy of feed flow, h_F, is determined as 18648 kJ/kg. (h_F=186,48 kJ/kg).

With the help of the equation for heat balance;

$$\text{NaOH balance: } F \cdot X_F' = L_1 \cdot X_1'$$

The flow rate of product L₁ values are determined.

By using the equation for material balance;

$$F + V_o = V_1 + L_1 + D$$

Since D = V_o, the equation is re – arranged and then, F = V₁ + L₁.

The V₁ values can be determined by using the above equation.

By considering the equation for heat balance;

$$V_o \cdot \lambda_{vo} + F \cdot h_F = V_1 + H_1 + L_1 \cdot h_1$$

From beginning to now, h_F, V₁, H₁, L₁ and h₁ have been determined. The latent heat of vaporization λ_{vo} can also be determined readily from the steam tables. For instance, the latent heat of vaporization for steam at a pressure of 4 Bar(a) is 2134 kJ/kg (λ_{vo}=2134 kJ/kg). Since the pressure of steam for heating purpose varies from 4 Bar(a) to 10 bar(a), the λ_{vo} values can also be determined with the help of steam tables.

The only unknown in the equation for heat balance is V_o which represents the steam flow rate.

For F = 250 kg/h, 5% NaOH solution.

For L₁ = 62 kg/h, 20% NaOH solution.

The V_o values can be provided by using the equation for heat balance and can also be organized as indicated Table 1;

The required heat transfer area corresponding to the above V_o values can be calculated by the use of equation for heat transfer.

$$V_o \cdot \lambda_{vo} = U \cdot A \cdot (-\Delta T)$$

The only unknown in this equation is heat transfer area represented by A. However, one thing should be determined first. The total heat transfer coefficient, U should be determined. It is possible to use U = 2000 kJ/m²h°C (From Chemical engineering handbook, Robert H. Perry, Cecil H. Chilton. Mc – Graw – Hill Chemical Engineering series, 1969).

The heat transfer equation was;

$$V_o \cdot \lambda_{vo} = U \cdot A \cdot (-\Delta T)$$

By substituting the V_o values into the heat transfer equation the heat transfer area values can be obtained readily as indicated in Table 2.

For F = 250 kg/h, 5% NaOH solution

L₁ = 62 kg/h, 20% NaOH solution

The required mass flow rates for heating steam and the required heat transfer areas for the evaporation of caustic soda in the tank have been determined. All of the values in Table 1 and Table 2 are provided for a feed flow rate 250 kg/h, i.e., F = 250 kg/h. The results obtained by using the same equations for the other feed flow rates (400kg/h, 550 kg/h, 700kg/h, 850kg/h, 1000kg/h) may be provided by using the same calculation method.

If the data obtained from this method are organized as graphics the information at the proceeding pages are viewed.

By considering the Figure 4 and Figure 5 it is possible to observe the required mass flow rates of the heating steam for evaporating the caustic soda solution. In these two figures,

the mass flow rate of the caustic soda (feed flow) is varied from 250 kg/h to 1000 kg/h. The pressure of the heating steam changes from 4 bar to 10 bar. The calculations are realized for both the lower operating pressures and atmospheric conditions.

Table 2. Required heating surface area values for F = 250 kg/h

		Pressure in the evaporator tank →				
		Atmospheric		Below Atmospheric		
A (m ²)		1 bar(a)	0,1 bar(a)	0,2 bar(a)	0,3 bar(a)	0,4 bar(a)
Steam pressure for ↑	4 bar(a)	7,582	2,79	3,394	3,87	4,374
	5 bar(a)	6,1	2,545	3	3,436	3,828
	6 bar(a)	5,21	2,37	2,8	3,1424	3,45995
	7 bar(a)	4,63	2,23	2,62	2,9	3,1889
	8 bar(a)	4,217	2,127	2,48	2,7342	2,983
	9 bar(a)	3,897	2	2,361	2,5934	2,8167
	10 bar(a)	3,645	1,965	2,2699	2,476	2,6798

The lower pressures considered for the calculations are 0.1 bar, 0.2 bar, 0.3 bar and 0.4 bar. The atmospheric condition is represented as 1 bar tank pressure. For a given feed flow rate, heating steam pressure and tank pressure values it is possible to see the required mass flow rate of heating steam by using these figures. It can be clearly understood from these figures that, for a constant feed flow rate and heating steam pressure value; the required mass flow rate increases as the tank pressure approaches to atmospheric conditions. Similarly, it is possible to say that the required mass flow rate decreases as the tank pressure decreases.

The required heating surface area values for the evaporation of caustic soda are given from Figure 6 to Figure 11. The feed flow changes from 250 kg/h to 1000 kg/h. The steam pressure for heating changes from 4 bar to 10 bar and the tank pressure is also the same with mentioned at above paragraph. It can be clearly understood from these figures that, for a constant feed flow rate and heating steam pressure value; the required heating surface area value increases as the tank pressure approaches to atmospheric conditions. Similarly, it is possible to say that the required heating surface area value decreases as the tank pressure decreases.

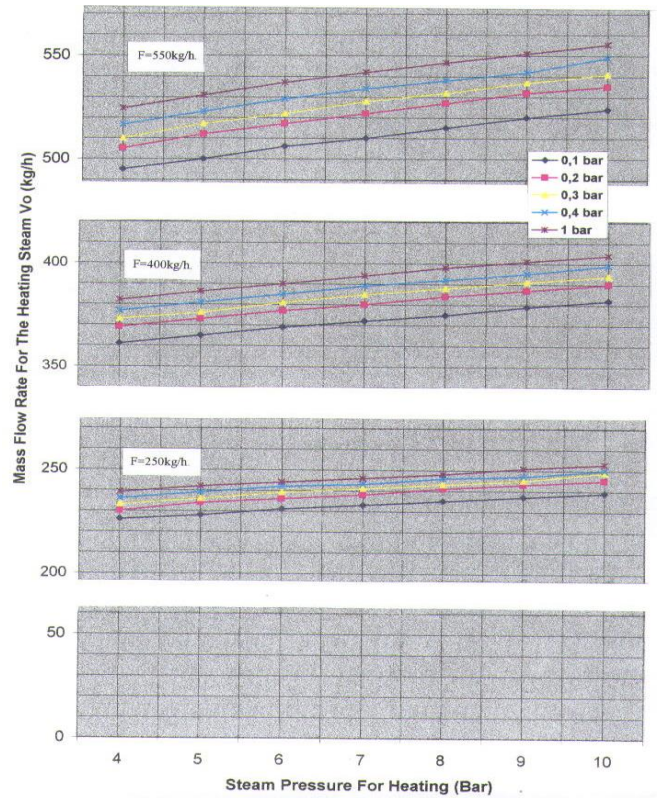


Figure 4. Mass flow rates of the heating steam for F-250, 400, 500 kg/h.

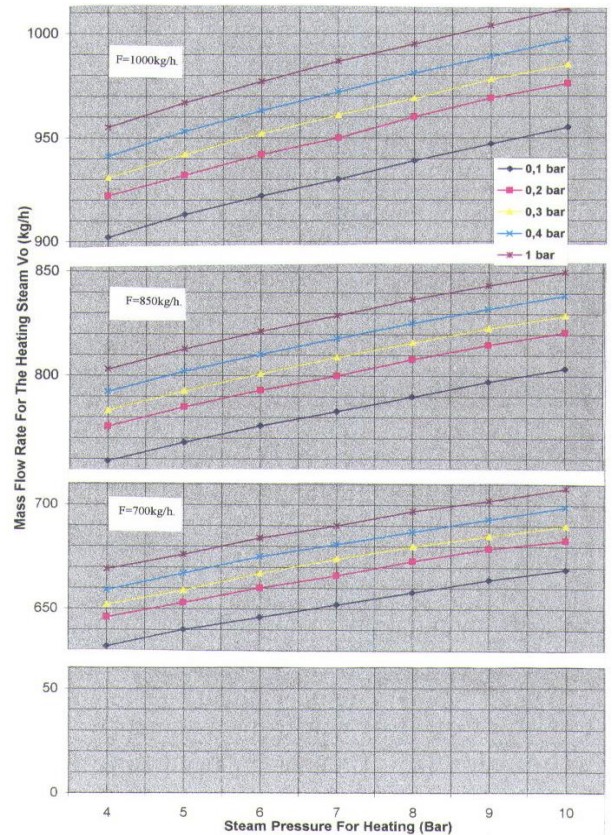


Figure 5. Mass flow rates of the heating steam for F-700, 850, 1000 kg/h.

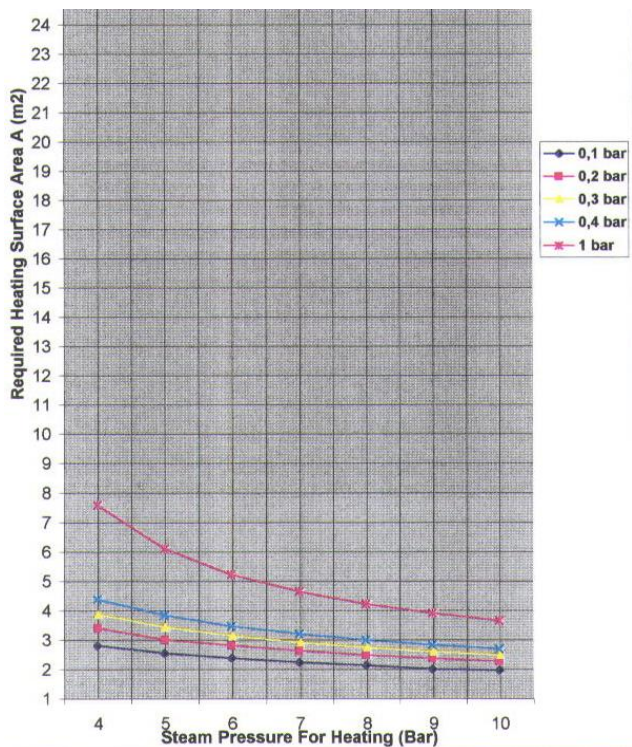


Figure 6. Required heating surface area values for F=250 kg/h.

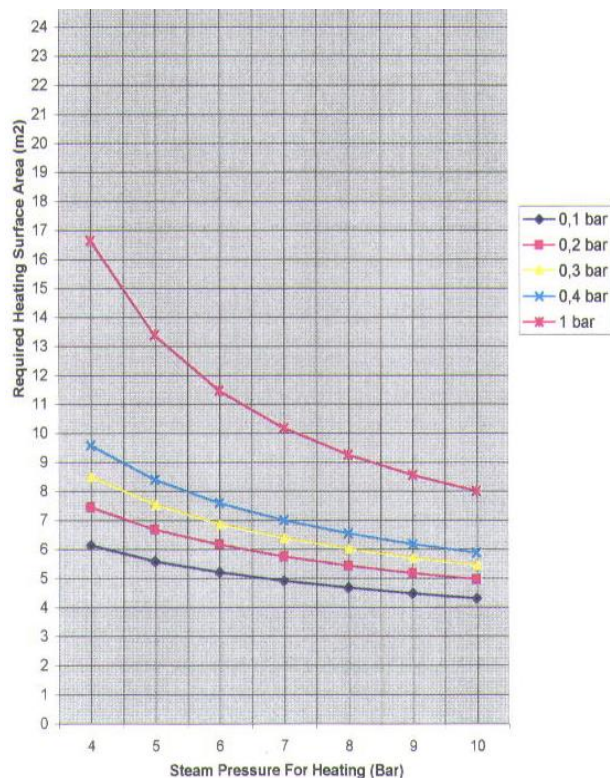


Figure 8. Required heating surface area values for F=550 kg/h.

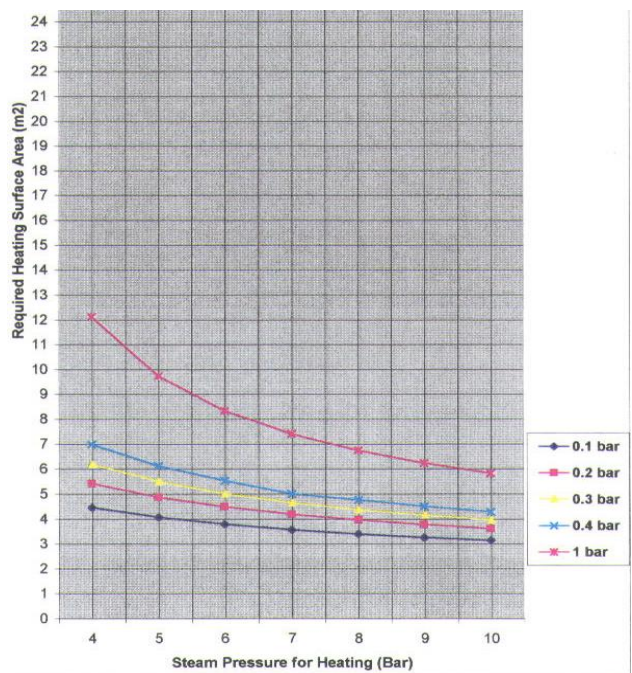


Figure 7. Required heating surface area values for F=400 kg/h.

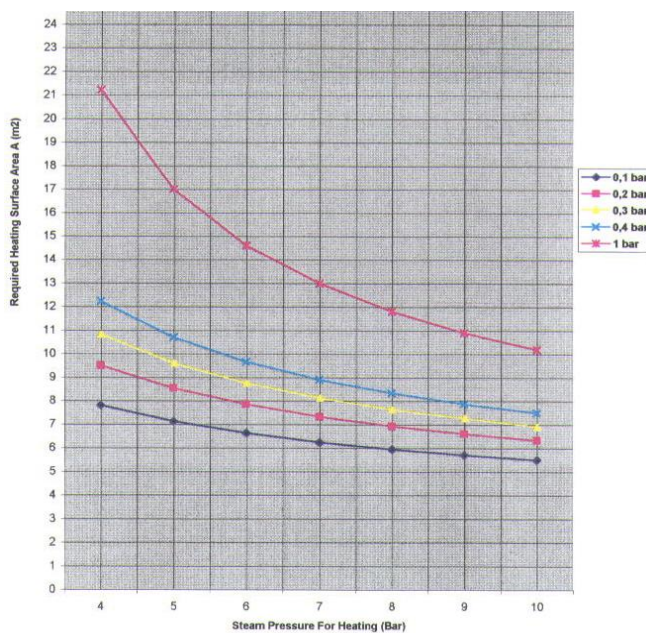


Figure 9. Required heating surface area values for F=700 kg/h.

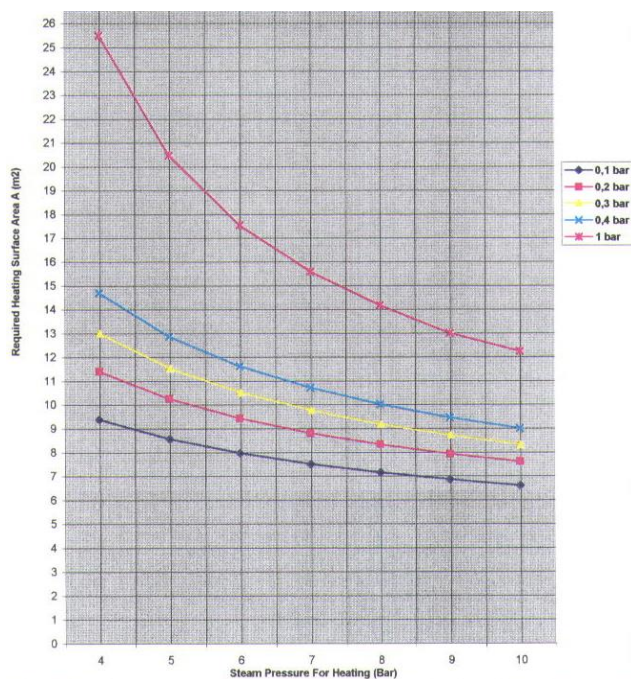


Figure 10. Required heating surface area values for F=850 kg/h.

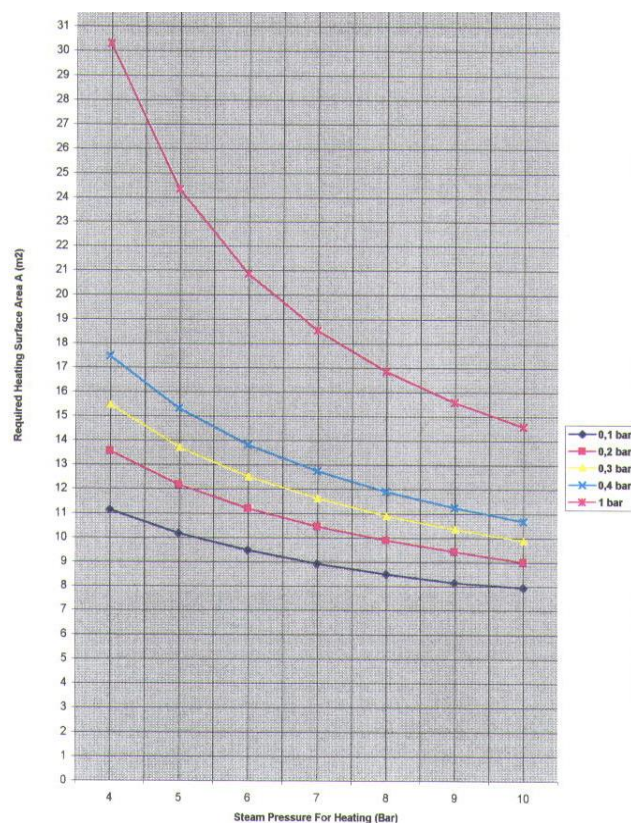


Figure 11. Required heating surface area values for F=1000 kg/h.

Up to now, single-effect evaporation model was considered. If double-effect evaporation is used, it is possible to decrease the steam consumption for heating, and also it is possible to increase the energy efficiency.

5. Recycling of Caustic Soda by Double-effect Evaporation at Atmospheric and Low Pressures

A similar calculation method is applied for the double-effect evaporation of caustic soda. The operational data for both single-effect and double-effect are identical. It should be noted that the calculations of the double-effect operation have been done for only a feed flow of 850 kg/h. The results can be observed on the graphics to have a much clearer idea. Figure 13 and Figure 14 explain the specific data. These figures can be used to make a comparison between the single-effect and double-effect evaporation. By using Figure 13, it is possible to say that; for a constant feed flow rate, heating steam pressure value and constant tank pressure double-effect evaporation decreases the required mass flow rate for the heating steam. Similar to the Figure 13, Figure 14 emphasizes that the double-effect evaporation decreases the heating surface area requirement.

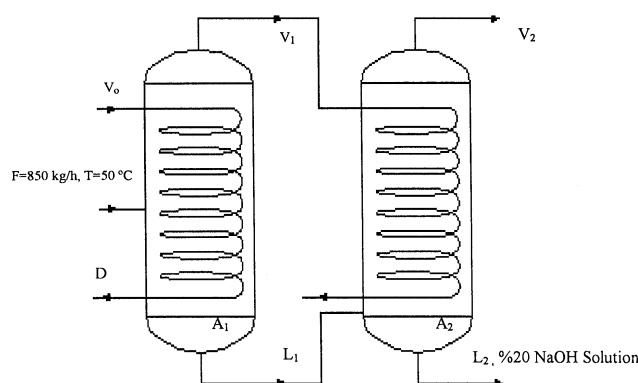


Figure 12. Recycling of caustic soda by double-effect evaporation.

6. Conclusion and Future Work

As it can be understood clearly from the previous explanation, two main concepts were tried to mention during this study. The first, requirements of protection of the environment from pollutants of textile industry. It is tried to explain the hazardous effects of the waste water (including caustic soda) of mercerizing which is an essential process for the textile industry.

On this basis, it has been tried to explain that caustic soda must not be discharged to the environment, e.g. to the rivers, sea and sewage even at a 1% concentration. The above concept has imposed on us to think a method that makes the recycling process of caustic soda possible. Thus, the evaporation process has been selected for recycling of caustic soda. However, the current plant system established on the evaporation operation might be required some review on. Since the system is very old, there are many energy losses on the plant.

For minimizing the energy loss and also to make such a recycling plant feasible it has been tried to operate the system under vacuum which provides energy saving and makes the plant much more economical. For this situation, an economic analysis from the aspect of energy consumption can be done.

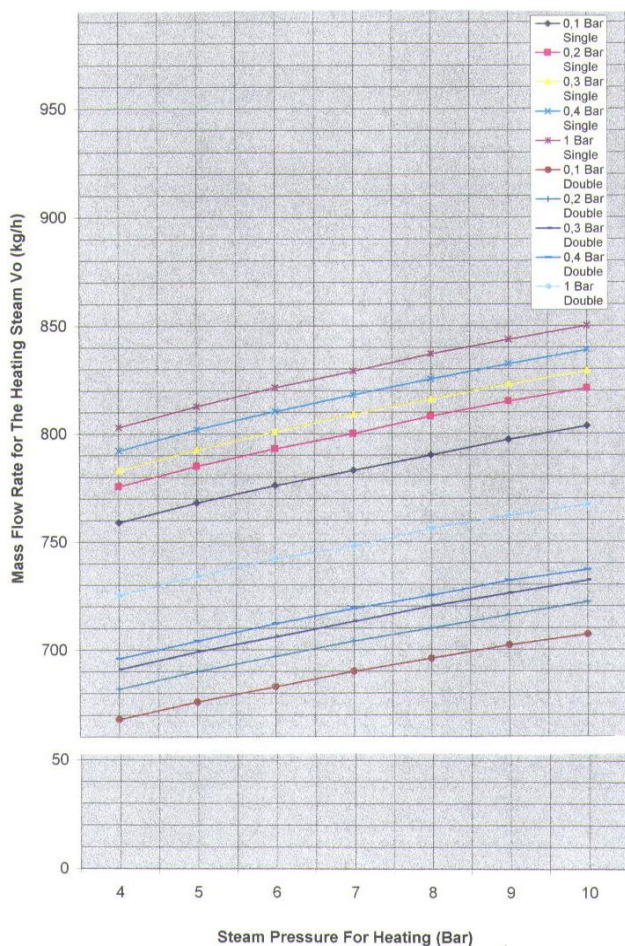


Figure 13. Mass flow rates of the heating steam for F=850 kg/h (comparison of single-effect and double-effect).

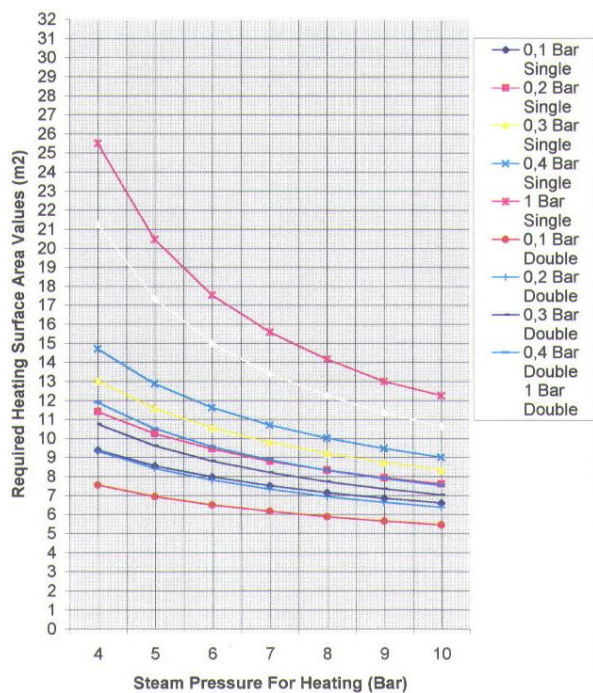


Figure 14. Comparison between the required heating surface (A1) values of double effect and the required heating area values of single effect for F=850 kg/h.

After this analysis has been realized, it is decided that an evaporation plant for recycling of caustic soda is a feasible investment. Because, after recycling the caustic soda by extracting it from the caustic soda – water solution with the help of evaporation operation, it can be used for the subsequent process. This event provides an economical profit, because caustic soda has an economical value. In addition, the environmental pollution arisen from discharging of the caustic soda solution can also be prevented.

To support these goals, the information in this study are tried to present through the use of simple graphics and figures which are available from Figure 1 to Figure 14. A thermodynamically analysis solution method is also tried to present.

To install double – effect evaporation plants instead of single – effect evaporation plants is another method for energy saving. The multiple – effect evaporation plants increases the capital cost of the system, however, since it is possible to use the vapor coming from the first stage for the subsequent stage as heating steam, this application is also a profitable method decreasing the operating costs. For both double - effect and single – effect evaporation, operating the recycling system under vacuum also increases the capital cost, furthermore this event causes and additional steam consumption for the steam – jet ejector which is used for obtaining vacuum. However, at the same time, related with this event, the boiling point of the caustic soda solution decreases considerably and the energy that must be added to the solution to be evaporated also decreases.

Here, the problem is the balance between the operating and capital costs. If it is achieved to install a balance between the capital and operating costs, it is possible to obtain much more energy efficient evaporation plants for recycling of caustic soda.

References

- [1] Elmas, Emin Taner, (1999) Evaporation Plant For Recycling of Caustic Soda, M.Sc. Thesis, İzmir. (Thesis)
- [2] Foust,A.S. , Wenzel,L.A. , Clump ,C.W. , Maus,L. , & Andersen,L.B. (1959). Principles of Unit Operations. Pennsylvania : John Wiley & Sons , Inc. (Book)
- [3] Özcan,Y. (1978). Tekstil Elyaf ve Boyama Tekniği. İstanbul. (Book)
- [4] Dokuz Eylül Üniv. Müh. - Mim. Fakültesi ve Ege Bölgesi Sanayi Odası. (18-19 Ekim 1983). Vakum Teknolojileri ve Vakum Metalurjisi Sempozyumu. İzmir. (Booklet)
- [5] Kern,D.Q. (1950). Process Heat Transfer. Tokyo: Kögakusha Company,Ltd. (Book)
- [6] Kirk - Othmer. (1970) Encyclopedia of Chemical Technology. 22.Vol. 2. ed. Water (Desalination) to Zone Refining . New York: John Wiley & Sons ,Inc. (Book - Encyclopedia)

- [7] Kirk - Othmer. (1967) Encyclopedia of Chemical Technology. 4.Vol. 2.ed. New York: John Wiley & Sons ,Inc. (Book - Encyclopedia)
- [8] Jeffries,M. , & Mills,D. (1994). Freshwater Ecology Principles and Applications. Chichester: John Wiley & Sons. (Book)
- [9] Henglein,F.A. (1969). Chemical Technology. Karlsruhe:Pergamon Press Ltd. & Headington Hill Hall,Oxford. (Book)
- [10]Perry,R.H., & Chilton,C.H. (1969). Chemical Engineers'Handbook.Tokyo:McGraw-Hill Kogakusha , Ltd. (Book)
- [11]Badger,W.L. , & Banchemo,J.T. (1955). Introduction to Chemical Engineering. : Kogakusha Company ,Ltd. ,McGraw-Hill Book Company ,Inc. (Book)
- [12]Mc.Cabe,W.L. , Smith, J.C. , & Harriott,P. (1967). Unit Operations of Chemical Engineering. New York: McGraw-Hill Book Company. (Book)

INTERNATIONAL JOURNAL OF ENGINEERING TECHNOLOGIES-IJET

Guide for Authors

The **International Journal of Engineering Technologies (IJET)** seeks to promote and disseminate knowledge of the various topics of engineering technologies. The journal aims to present to the international community important results of work in the fields of engineering such as imagining, researching, planning, creating, testing, improving, implementing, using and asking. The journal also aims to help researchers, scientists, manufacturers, institutions, world agencies, societies, etc. to keep up with new developments in theory and applications and to provide alternative engineering solutions to current.

The *International Journal of Engineering Technologies* is a quarterly published journal and operates an online submission and peer review system allowing authors to submit articles online and track their progress via its web interface. The journal aims for a publication speed of **60 days** from submission until final publication.

The coverage of IJET includes the following engineering areas, but not limited to:

All filed of engineering such as;

Chemical engineering

- Biomolecular engineering
- Materials engineering
- Molecular engineering
- Process engineering

Civil engineering

- Environmental engineering
- Geotechnical engineering
- Structural engineering
- Transport engineering
- Water resources engineering

Electrical engineering

- Computer engineering
- Electronic engineering
- Optical engineering
- Power engineering

Mechanical engineering

- Acoustical engineering
- Manufacturing engineering
- Thermal engineering
- Vehicle engineering

Systems (interdisciplinary) engineering

- Aerospace engineering
- Agricultural engineering
- Applied engineering
- Biological engineering
- Building services engineering
- Energy engineering
- Railway engineering
- Industrial engineering
- Mechatronics
- Military engineering
- Nano engineering
- Nuclear engineering
- Petroleum engineering

Types of Articles submitted should be original research papers, not previously published, in one of the following categories,

- Applicational and design studies.
- Technology development,
- Comparative case studies.
- Reviews of special topics.
- Reviews of work in progress and facilities development.
- Survey articles.
- Guest editorials for special issues.

Editor-in-Chief and Associate Editors

Editor-in-Chief:

Prof. Dr. Mustafa BAYRAM

Associate Editors:

Prof. Dr. A. Burak POLAT

Assoc. Prof. Dr. Baris SEVIM

Asst. Prof. Dr. Ahmet AKTAS

Asst. Prof. Dr. Yalcin CEKIC

Asst. Prof. Dr. Ali ETEMADI

Ethic Responsibilities

The publication of an article in peer-reviewed “*International Journal of Engineering Technologies*” is an essential building block in the development of a coherent and respected network of knowledge. It is a direct reflection of the quality of the work. Peer-reviewed articles support and embody the scientific method. It is therefore important to agree upon standards of expected ethical behavior for all parties involved in the act of publishing: the author, the journal editor, the peer reviewer, the publisher and the society of society-owned or sponsored journals.

All authors are requested to disclose any actual or potential conflict of interest including any financial, personal or other relationships with other people or organizations within three years of beginning the submitted work that could inappropriately influence, or be perceived to influence, their work.

Submission of an article implies that the work described has not been published previously that it is not under consideration for publication elsewhere. The submission should be approved by all authors and tacitly or explicitly by the responsible authorities where the work was carried out, and that, if accepted, it will not be published elsewhere in the same form, in English or in any other language, including electronically without the written consent of the copyright-holder.

Upon acceptance of an article, authors will be asked to complete a “Copyright Form”. Acceptance of the agreement will ensure the widest possible dissemination of information. An e-mail will be sent to the corresponding author confirming receipt of the manuscript together with a “Copyright Form” form or a link to the online version of this agreement.

Author Rights

As a journal author, you retain rights for a large number of author uses, including use by your employing institute or company. These rights are retained and permitted without the need to obtain specific permission from *IJET*. These include:

- ❖ The right to make copies (print or electronic) of the journal article for your own personal use, including for your own classroom teaching use;
- ❖ The right to make copies and distribute copies (including via e-mail) of the journal article to research colleagues, for personal use by such colleagues for scholarly purposes;
- ❖ The right to post a pre-print version of the journal article on internet web sites including electronic pre-print servers, and to retain indefinitely such version on such servers or sites for scholarly purposes
- ❖ the right to post a revised personal version of the text of the final journal article on your personal or institutional web site or server for scholarly purposes
- ❖ The right to use the journal article or any part thereof in a printed compilation of your works, such as collected writings or lecture notes.

Article Style

Authors must strictly follow the guide for authors, or their articles may be rejected without review. Editors reserve the right to adjust the style to certain standards of uniformity. Follow Title, Authors, Affiliations, Abstract, Keywords, Introduction, Materials and Methods, Theory/Calculation, Conclusions, Acknowledgements, References order when typing articles. The corresponding author should be identified with an asterisk and footnote. Collate acknowledgements in a separate section at the end of the article and do not include them on the title page, as a footnote to the title or otherwise.

Abstract and Keywords:

Enter an abstract of up to 250 words for all articles. This is a concise summary of the whole paper, not just the conclusions, and is understandable without reference to the rest of the paper. It should contain no citation to other published work. Include up to six keywords that describe your paper for indexing purposes.

Abbreviations and Acronyms:

Define abbreviations and acronyms the first time they are used in the text, even if they have been defined in the abstract. Abbreviations such as IEEE, SI, MKS, CGS, sc, dc, and rms do not have to be defined. Do not use abbreviations in the title unless they are unavoidable.

Text Layout for Peer Review:

Use single column layout, double spacing and wide (3 cm) margins on white paper at the peer review stage. Ensure that each new paragraph is clearly indicated. Present tables and figure legends in the text where they are related and cited. Number all pages consecutively; use 12 pt font size and standard fonts; Times New Roman, Helvetica, or Courier is preferred.

Research Papers should not exceed 12 printed pages in two-column publishing format, including figures and tables.

Technical Notes and Letters should not exceed 2,000 words.

Reviews should not exceed 20 printed pages in two-column publishing format, including figures and tables.

Equations:

Number equations consecutively with equation numbers in parentheses flush with the right margin, as in (1). To make equations more compact, you may use the solidus (/), the exp function, or appropriate exponents. Italicize Roman symbols for quantities and variables, but not Greek symbols. Use an dash (–) rather than a hyphen for a minus sign. Use parentheses to avoid ambiguities in denominators. Punctuate equations with commas or periods when they are part of a sentence, as in

$$C = a + b \tag{1}$$

Symbols in your equation should be defined before the equation appears or immediately following. Use “Eq. (1)” or “equation (1),” while citing.

Figures and Tables:

All illustrations must be supplied at the correct resolution:

- * Black and white and colour photos - 300 dpi
- * Graphs, drawings, etc - 800 dpi preferred; 600 dpi minimum
- * Combinations of photos and drawings (black and white and color) - 500 dpi

In addition to using figures in the text, upload each figure as a separate file in either .tiff or .eps format during submission, with the figure number.

Table captions should be written in the same format as figure captions; for example, “Table 1. Appearance styles.”. Tables should be referenced in the text unabbreviated as “Table 1.”

References:

Please ensure that every reference cited in the text is also present in the reference list (and viceversa). Any references cited in the abstract must be given in full. Unpublished results and personal communications are not recommended in the reference list, but may be mentioned in the text. Citation of a reference as “in press” implies that the item has been accepted for publication. Number citations consecutively in square brackets [1]. Punctuation follows the bracket [2]. Refer simply to the reference number, as in [3]. Use “Ref. [3]” or Reference [3]” at the beginning of a sentence: “Reference [3] was ...”. Give all authors’ names; use “et al.” if there are six authors or more. For papers published in translated journals, first give the English citation, then the original foreign-language citation.

Books

- [1] J. Clerk Maxwell, *A Treatise on Electricity and Magnetism*, 3rd ed., vol. 2. Oxford:Clarendon Press, 1892, pp.68-73.

Journals

- [2] Y. Yorozu, M. Hirano, K. Oka, and Y. Tagawa, “Electron spectroscopy studies on magneto-optical media and plastic substrate interface”, *IEEE Transl. J. Magn. Japan*, vol. 2, pp. 740-741, August 1987.

Conferences

- [3] Çolak I., Kabalci E., Bayindir R., and Sagiroglu S, “The design and analysis of a 5-level cascaded voltage source inverter with low THD”, *2nd PowerEng Conference*, Lisbon, pp. 575-580, 18-20 March 2009.

Reports

- [4] IEEE Standard 519-1992, Recommended practices and requirements for harmonic control in electrical power systems, *The Institute of Electrical and Electronics Engineers*, 1993.

Text Layout for Accepted Papers:

A4 page margins should be margins: top = 24 mm, bottom = 24 mm, side = 15 mm. Main text should be given in two column. The column width is 87mm (3.425 in). The space between the two columns is 6 mm (0.236 in). Paragraph indentation is 3.5 mm (0.137 in). Follow the type sizes specified in Table. Position figures and tables at the tops and bottoms of columns. Avoid placing them in the middle of columns. Large figures and tables may span across both columns. Figure captions should be centred below the figures; table captions should be centred above. Avoid placing figures and tables before their first mention in the text. Use the abbreviation “Fig. 1,” even at the beginning of a sentence.

Type size (pts.)	Appearance		
	Regular	Bold	<i>Italic</i>
10	Authors’ affiliations, Section titles, references, tables, table names, first letters in table captions, figure captions, footnotes, text subscripts, and superscripts	Abstract	
12	Main text, equations, Authors’ names, ^a		<i>Subheading (1.1.)</i>
24	Paper title		

Submission checklist:

It is hoped that this list will be useful during the final checking of an article prior to sending it to the journal's Editor for review. Please consult this Guide for Authors for further details of any item. Ensure that the following items are present:

- ❖ One Author designated as corresponding Author:
- E-mail address
- Full postal address
- Telephone and fax numbers

❖ All necessary files have been uploaded

- Keywords: a minimum of 4
- All figure captions (supplied in a separate document)
- All tables (including title, description, footnotes, supplied in a separate document)

❖ Further considerations

- Manuscript has been "spellchecked" and "grammar-checked"
- References are in the correct format for this journal
- All references mentioned in the Reference list are cited in the text, and vice versa
- Permission has been obtained for use of copyrighted material from other sources (including the Web)
- Color figures are clearly marked as being intended for color reproduction on the Web (free of charge) and in print or to be reproduced in color on the Web (free of charge) and in black-and-white in print.

Article Template Containing Author Guidelines for Peer-Review

First Author*, Second Author**‡, Third Author***

*Department of First Author, Faculty of First Author, Affiliation of First Author, Postal address

**Department of Second Author, Faculty of First Author, Affiliation of First Author, Postal address

***Department of Third Author, Faculty of First Author, Affiliation of First Author, Postal address

(First Author Mail Address, Second Author Mail Address, Third Author Mail Address)

‡Corresponding Author; Second Author, Postal address, Tel: +90 312 123 4567, Fax: +90 312 123 4567,corresponding@affl.edu

Received: xx.xx.xxxx Accepted:xx.xx.xxxx

Abstract- Enter an abstract of up to 250 words for all articles. This is a concise summary of the whole paper, not just the conclusions, and is understandable without reference to the rest of the paper. It should contain no citation to other published work. Include up to six keywords that describe your paper for indexing purposes. Define abbreviations and acronyms the first time they are used in the text, even if they have been defined in the abstract. Abbreviations such as IEEE, SI, MKS, CGS, sc, dc, and rms do not have to be defined. Do not use abbreviations in the title unless they are unavoidable.

Keywords- Keyword1; keyword2; keyword3; keyword4; keyword5.

2. Introduction

Authors should any word processing software that is capable to make corrections on misspelled words and grammar structure according to American or Native English. Authors may get help by from word

processor by making appeared the paragraph marks and other hidden formatting symbols. This sample article is prepared to assist authors preparing their articles to IJET.

Indent level of paragraphs should be 0.63 cm (0.24 in) in the text of article. Use single column layout, double-spacing and wide (3 cm) margins on white paper at the peer review stage. Ensure that each new paragraph is clearly indicated. Present tables and figure legends in the text where they are related and cited. Number all pages consecutively; use 12 pt font size and standard fonts; Times New Roman, Helvetica, or Courier is preferred. Indicate references by number(s) in square brackets in line with the text. The actual authors can be referred to, but the reference number(s) must always be given. Example: "..... as demonstrated [3, 6]. Barnaby and Jones [8] obtained a different result"

IJET accepts submissions in three styles that are defined as Research Papers, Technical Notes and Letter, and Review paper. The requirements of paper are as listed below:

- Research Papers should not exceed 12 printed pages in two-column publishing format, including figures and tables.
- Technical Notes and Letters should not exceed 2,000 words.
- Reviews should not exceed 20 printed pages in two-column publishing format, including figures and tables.

Authors are requested write equations using either any mathematical equation object inserted to word processor or using independent equation software. Symbols in your equation should be defined before the equation appears or immediately following. Use "Eq. (1)" or "equation (1)," while citing. Number equations consecutively with equation numbers in parentheses flush with the right margin, as in Eq. (1). To make equations more compact, you may use the solidus (/), the exp function, or appropriate exponents. Italicize Roman symbols for quantities and variables, but not Greek symbols. Use an dash (–) rather than a hyphen for a minus sign. Use parentheses to avoid ambiguities in denominators. Punctuate equations with commas or periods when they are part of a sentence, as in

$$C = a + b \tag{1}$$

Section titles should be written in bold style while sub section titles are italic.

3. Figures and Tables

3.1. Figure Properties

All illustrations must be supplied at the correct resolution:

- Black and white and colour photos - 300 dpi
- Graphs, drawings, etc - 800 dpi preferred; 600 dpi minimum
- Combinations of photos and drawings (black and white and colour) - 500 dpi

In addition to using figures in the text, Authors are requested to upload each figure as a separate file in either .tiff or .eps format during submission, with the figure number as Fig.1., Fig.2a and so on. Figures are cited as “Fig.1” in sentences or as “Figure 1” at the beginning of sentence and paragraphs. Explanations related to figures should be given before figure. Figures and tables should be located at the top or bottom side of paper as done in accepted article format.



Figure 1. Engineering technologies.

Table captions should be written in the same format as figure captions; for example, “Table 1. Appearance styles.”. Tables should be referenced in the text unabbreviated as “Table 1.”

Table 1. Appearance properties of accepted manuscripts

Type size (pts.)	Appearance		
	Regular	Bold	<i>Italic</i>
10	Authors’ affiliations, Abstract, keywords, references, tables, table names, figure captions, footnotes, text subscripts, and superscripts	Abstract	
12	Main text, equations, Authors’ names, Section titles		<i>Subheading (1.1.)</i>
24	Paper title		

4. Submission Process

The *International Journal of Engineering Technologies* operates an online submission and peer review system that allows authors to submit articles online and track their progress via a web interface. Articles that are prepared referring to this template should be controlled according to submission checklist given in “Guide f Authors”. Editor handles submitted articles to IJET primarily in order to control in terms of compatibility to aims and scope of Journal.

Articles passed this control are checked for grammatical and template structures. If article passes this control too, then reviewers are assigned to article and Editor gives a reference number to paper. Authors registered to online submission system can track all these phases.

Editor also informs authors about processes of submitted article by e-mail. Each author may also apply to Editor via online submission system to review papers related to their study areas. Peer review is a critical element of publication, and one of the major cornerstones of the scientific process. Peer Review serves two key functions:

- Acts as a filter: Ensures research is properly verified before being published
- Improves the quality of the research

5. Conclusion

The conclusion section should emphasize the main contribution of the article to literature. Authors may also explain why the work is important, what are the novelties or possible applications and extensions. Do not replicate the abstract or sentences given in main text as the conclusion.

Acknowledgements

Authors may acknowledge to any person, institution or department that supported to any part of study.

References

- [1] J. Clerk Maxwell, *A Treatise on Electricity and Magnetism*, 3rd ed., vol. 2. Oxford:Clarendon Press, 1892, pp.68-73.
(Book)
- [2] H. Poor, *An Introduction to Signal Detection and Estimation*, New York: Springer-Verlag, 1985, ch. 4. (Book Chapter)
- [3] Y. Yorozu, M. Hirano, K. Oka, and Y. Tagawa, "Electron spectroscopy studies on magneto-optical media and plastic substrate interface", *IEEE Transl. J. Magn. Japan*, vol. 2, pp. 740-741, August 1987. (Article)
- [4] E. Kabalcı, E. Irmak, I. Çolak, "Design of an AC-DC-AC converter for wind turbines", *International Journal of Energy Research*, Wiley Interscience, DOI: 10.1002/er.1770, Vol. 36, No. 2, pp. 169-175. (Article)
- [5] I. Çolak, E. Kabalci, R. Bayindir R., and S. Sagiroglu, "The design and analysis of a 5-level cascaded voltage source inverter with low THD", *2nd PowerEng Conference*, Lisbon, pp. 575-580, 18-20 March 2009. (Conference Paper)
- [6] IEEE Standard 519-1992, Recommended practices and requirements for harmonic control in electrical power systems, *The Institute of Electrical and Electronics Engineers*, 1993. (Standards and Reports)

Article Template Containing Author Guidelines for Accepted Papers

First Author*, Second Author**‡, Third Author***

*Department of First Author, Faculty of First Author, Affiliation of First Author, Postal address

**Department of Second Author, Faculty of First Author, Affiliation of First Author, Postal address

***Department of Third Author, Faculty of First Author, Affiliation of First Author, Postal address

(First Author Mail Address, Second Author Mail Address, Third Author Mail Address)

‡Corresponding Author; Second Author, Postal address, Tel: +90 312 123 4567,

Fax: +90 312 123 4567,corresponding@affl.edu

Received: xx.xx.xxxx Accepted:xx.xx.xxxx

Abstract- Enter an abstract of up to 250 words for all articles. This is a concise summary of the whole paper, not just the conclusions, and is understandable without reference to the rest of the paper. It should contain no citation to other published work. Include up to six keywords that describe your paper for indexing purposes. Define abbreviations and acronyms the first time they are used in the text, even if they have been defined in the abstract. Abbreviations such as IEEE, SI, MKS, CGS, sc, dc, and rms do not have to be defined. Do not use abbreviations in the title unless they are unavoidable.

Keywords Keyword1, keyword2, keyword3, keyword4, keyword5.

1. Introduction

Authors should use any word processing software that is capable of making corrections on misspelled words and grammar structure according to American or British English. Authors may get help from word processor by making visible the paragraph marks and other hidden formatting symbols. This sample article is prepared to assist authors preparing their articles to IJET.

Indent level of paragraphs should be 0.63 cm (0.24 in) in the text of article. Use single column layout, double-spacing and wide (3 cm) margins on white paper at the peer review stage. Ensure that each new paragraph is clearly indicated. Present tables and figure legends in the text where they are related and cited. Number all pages consecutively; use 12 pt font size and standard fonts; Times New Roman, Helvetica, or Courier is preferred. Indicate references by number(s) in square brackets in line with the text. The actual authors can be referred to, but the reference number(s) must always be

given. Example: "... as demonstrated [3,6]. Barnaby and Jones [8] obtained a different result"

IJET accepts submissions in three styles that are defined as Research Papers, Technical Notes and Letter, and Review paper. The requirements of paper are as listed below:

➤ Research Papers should not exceed 12 printed pages in two-column publishing format, including figures and tables.

➤ Technical Notes and Letters should not exceed 2,000 words.

➤ Reviews should not exceed 20 printed pages in two-column publishing format, including figures and tables.

Authors are requested write equations using either any mathematical equation object inserted to word processor or using independent equation software. Symbols in your equation should be defined before the equation appears or immediately following. Use "Eq. (1)" or "equation (1),"

while citing. Number equations consecutively with equation numbers in parentheses flush with the right margin, as in Eq. (1). To make equations more compact, you may use the solidus (/), the exp function, or appropriate exponents. Italicize Roman symbols for quantities and variables, but not Greek symbols. Use an dash (-) rather than a hyphen for a minus sign. Use parentheses to avoid ambiguities in denominators. Punctuate equations with commas or periods when they are part of a sentence, as in

$$C = a + b \quad (1)$$

Section titles should be written in bold style while sub section titles are italic.

6. Figures and Tables

6.1. Figure Properties

All illustrations must be supplied at the correct resolution:

- Black and white and colour photos - 300 dpi
- Graphs, drawings, etc - 800 dpi preferred; 600 dpi minimum
- Combinations of photos and drawings (black and white and colour) - 500 dpi

In addition to using figures in the text, Authors are requested to upload each figure as a separate file in either

Table 1. Appearance properties of accepted manuscripts

Type size (pts.)	Appearance		
	Regular	Bold	<i>Italic</i>
10	Main text, section titles, authors' affiliations, abstract, keywords, references, tables, table names, figure captions, equations, footnotes, text subscripts, and superscripts	Abstract-	<i>Subheading (1.1.)</i>
12	Authors' names,		
24	Paper title		

6.2. Text Layout for Accepted Papers

A4 page margins should be margins: top = 24 mm, bottom = 24 mm, side = 15 mm. The column width is 87mm (3.425 in). The space between the two columns is 6 mm (0.236 in). Paragraph indentation is 3.5 mm (0.137 in). Follow the type sizes specified in Table. Position figures and tables at the tops and bottoms of columns. Avoid placing them in the middle of columns. Large figures and tables may span across both columns. Figure captions should be centred below the figures; table captions should be centred above. Avoid placing figures and tables before their first mention in

.tiff or .eps format during submission, with the figure number as Fig.1., Fig.2a and so on. Figures are cited as "Fig.1" in sentences or as "Figure 1" at the beginning of sentence and paragraphs. Explanations related to figures should be given before figure.



Fig. 1. Engineering technologies.

Figures and tables should be located at the top or bottom side of paper as done in accepted article format. Table captions should be written in the same format as figure captions; for example, "Table 1. Appearance styles.". Tables should be referenced in the text unabbreviated as "Table 1."

the text. Use the abbreviation "Fig. 1," even at the beginning of a sentence.

7. Submission Process

The International Journal of Engineering Technologies operates an online submission and peer review system that allows authors to submit articles online and track their progress via a web interface. Articles that are prepared referring to this template should be controlled according to submission checklist given in "Guide f Authors". Editor handles submitted articles to IJET primarily in order to control in terms of compatibility to aims and scope of Journal. Articles passed this control are checked for

grammatical and template structures. If article passes this control too, then reviewers are assigned to article and Editor gives a reference number to paper. Authors registered to online submission system can track all these phases. Editor also informs authors about processes of submitted article by e-mail. Each author may also apply to Editor via online submission system to review papers related to their study areas. Peer review is a critical element of publication, and one of the major cornerstones of the scientific process. Peer Review serves two key functions:

- Acts as a filter: Ensures research is properly verified before being published
- Improves the quality of the research

8. Conclusion

The conclusion section should emphasize the main contribution of the article to literature. Authors may also explain why the work is important, what are the novelties or possible applications and extensions. Do not replicate the abstract or sentences given in main text as the conclusion.

Acknowledgements

Authors may acknowledge to any person, institution or department that supported to any part of study.

References

- [7] J. Clerk Maxwell, A Treatise on Electricity and Magnetism, 3rd ed., vol. 2. Oxford:Clarendon Press, 1892, pp.68-73. (Book)
- [8] H. Poor, An Introduction to Signal Detection and Estimation, New York: Springer-Verlag, 1985, ch. 4. (Book Chapter)
- [9] Y. Yorozu, M. Hirano, K. Oka, and Y. Tagawa, "Electron spectroscopy studies on magneto-optical media and plastic substrate interface", IEEE Transl. J. Magn. Japan, vol. 2, pp. 740-741, August 1987. (Article)
- [10] E. Kabalcı, E. Irmak, I. Çolak, "Design of an AC-DC-AC converter for wind turbines", International Journal of Energy Research, Wiley Interscience, DOI: 10.1002/er.1770, Vol. 36, No. 2, pp. 169-175. (Article)
- [11] I. Çolak, E. Kabalcı, R. Bayindir R., and S. Sagiroglu, "The design and analysis of a 5-level cascaded voltage source inverter with low THD", 2nd PowerEng Conference, Lisbon, pp. 575-580, 18-20 March 2009. (Conference Paper)
- [12] IEEE Standard 519-1992, Recommended practices and requirements for harmonic control in electrical power systems, The Institute of Electrical and Electronics Engineers, 1993. (Standards and Reports)

**INTERNATIONAL JOURNAL OF ENGINEERING TECHNOLOGIES (IJET)
COPYRIGHT AND CONSENT FORM**

This form is used for article accepted to be published by the IJET. Please read the form carefully and keep a copy for your files.

TITLE OF ARTICLE (hereinafter, "The Article"):

.....
.....
.....

LIST OF AUTHORS:

.....
.....
.....

CORRESPONDING AUTHOR'S ("The Author") NAME, ADDRESS, INSTITUTE AND EMAIL:

.....
.....
.....

COPYRIGHT TRANSFER

The undersigned hereby transfers the copyright of the submitted article to International Journal of Engineering Technologies (the "IJET"). The Author declares that the contribution and work is original, and he/she is authorized by all authors and/or grant-funding agency to sign the copyright form. Author hereby assigns all including but not limited to the rights to publish, distribute, reprints, translates, electronic and published derivatives in various arrangements or any other versions in full or abridged forms to IJET. IJET holds the copyright of Article in its own name.

Author(s) retain all rights to use author copy in his/her educational activities, own websites, institutional and/or funder's web sites by providing full citation to final version published in IJET. The full citation is provided including Authors list, title of the article, volume and issue number, and page number or using a link to the article in IJET web site. Author(s) have the right to transmit, print and share the first submitted copies with colleagues. Author(s) can use the final published article for his/her own professional positions, career or qualifications by citing to the IJET publication.

Once the copyright form is signed, any changes about the author names or order of the authors listed above are not accepted by IJET.

Authorized/Corresponding Author

Date/ Signature